MOLECULAR DISSECTION OF RANKL SIGNALING PATHWAYS IN OSTEOCLASTS

Cathy Ting-Peng Wang BSc (Hons)

This thesis is submitted to the
University of Western Australia
in fulfilment of the requirement for
the degree of

DOCTOR OF PHILOSOPHY

IN

MEDICAL SCIENCE

2007

The work presented in this thesis was performed at the University of Western Australia, School of Surgery and Pathology, Unit of Orthopaedics, Queen Elizabeth II Medical Centre, Nedlands, Perth, Western Australia.

TABLE OF CONTENTS

DECLARATION

This is to certify that all work contained herein was performed by myself, expect where indicated otherwise.

Cathy T. P. Wang

Professor Ming-Hao Zheng
(Supervisor)

Associate Prof Jiake Xu
(Supervisor)

ABSTRACT

Bone remodeling is intricately regulated by osteoclast-mediated bone resorption and osteoblast-mediated bone formation. The elevation in osteoclast number and/or activity is a major hallmark of several common pathological bone disorders including post-menopausal osteoporosis, osteoarthritis, Paget's disease, and tumour-mediated osteolysis. Receptor activator of nuclear factor kappa B ligand (RANKL) is a key cytokine for osteoclast differentiation and activation. The association of RANKL to its cognate receptor, RANK, which is expressed on osteoclast precursors and mature osteoclasts, is essential for osteoclast formation and activation. The intimate interaction between RANKL and RANK triggers the activation of a cascade of signal transduction pathways including NF-κB, NFAT, MAPK and PI3 kinase. Although osteoclast signaling pathways have been intensively studied, the precise molecules and signaling events which underlie osteoclast differentiation and function remain unclear. In order to dissect the molecular mechanism(s) regulating osteoclast differentiation and activity, this thesis herein explores the key RANKL/RANK-mediated signaling pathways.

Four truncation mutants within the TNF-like domain of RANKL [(aa160-302), (aa160-268), (aa239-318) and (aa246-318)] were generated to investigate their potential binding to RANK and the activation to RANK-signal transduction pathways. All were found to differentially impair osteoclastogenesis and bone resorption as compared to the wild-type RANKL. The impaired function of the truncation mutants of RANKL on osteoclast formation and function correlates with their reduced ability to activate crucial RANK signaling including NF-κB, IκBα, ERK and JNK. Further analysis revealed that the truncation mutants of RANKL exhibited differentially affinity to RANK as observed by *in vitro* pull-down assays. In addition, competition experiments demonstrated that RANKL mutants were capable of blocking the interaction of wild-type RANKL to RANK and also inhibit wild-type RANKL-induced osteoclastogenesis in a dose-dependent manner. Among the four truncation mutants of RANKL examined, mutant RANKL5 (aa246-318) displayed only minor effect on osteoclastogenesis, but exhibited the most potent inhibitory effect on wild-type RANKL-induced osteoclast formation and bone resorption. These data indicate that RANKL mutants might potentially serve as peptide mimic to inhibit RANKL-induced signaling, osteoclastogenesis and bone resorption.

Osteoclasts are exposed to high Ca^{2+} concentrations during bone resorption. Therefore, it is of interest to examine the potential role of RANKL in osteoclast tolerance to elevated extracellular Ca^{2+} and the effect of high extracellular Ca^{2+} on RANKL-induced signaling pathways. Interestingly, the results of this study demonstrate that RANKL enhances osteoclast tolerance to high extracellular Ca^{2+} by protecting cells from apoptosis dose-dependently. RANKL was found to attenuate high extracellular Ca^{2+}-induced intracellular Ca^{2+} influx. In addition, high extracellular Ca^{2+}-induced cell death could be partially inhibited by a caspase-3 inhibitor, suggesting that apoptosis might have occurred via the caspase-3-mediated pathway. Using complementary reporter gene assays and western blot analysis, high extracellular Ca^{2+} was shown to desensitize RANKL-induced activation of NF-κB and c-Jun N-terminal kinase (JNK), and inhibit constitutive and RANKL-stimulated ERK phosphorylation, indicating that a negative feedback mechanism existed via specific RANKL signaling pathways. This study documents evidence for a reciprocal regulation of the elevated extracellular Ca^{2+} and RANKL signaling pathways.

In an effort to establish a molecular link between Ca^{2+} and the regulation of osteoclast activity, the role of the Ca^{2+}-mediated signaling pathway, Protein Kinase C in osteoclastogenesis was examined using selective PKC modulators. For this purpose, a PKC activator named 12-*O*-tetradecanoylphorbol-13-acetate (TPA) was initially employed. Time course analysis showed that TPA inhibits osteoclastogenesis at the early stage of osteoclast differentiation. TPA was also found to suppress the RANKL-induced NF-κB activation. Given that NF-κB activation is obligatory for osteoclast differentiation, this study implied that the inhibition of osteoclastogenesis by TPA is, at least in part, caused by the suppression of RANKL-induced activation of NF-κB during the early stage of osteoclastogenesis

The selective modulation of RANKL signaling pathways by TPA prompted the further study of PKCs in osteoclastogenesis. Therefore, a conventional and a broad spectrum PKC inhibitor namely GÖ 6976 and GF 109203X were used, respectively. Both PKC inhibitors demonstrated an inhibitory effect on RANKL-induced osteoclastogenesis and bone resorption. In addition, both potently inhibited p65 translocation and its associated downstream signaling pathways such as NF-κB transcription but not upstream signaling pathways like IκBα degradation. Both GÖ 6976 and GF 109203X are selective inhibitors, but are not targeted to individual PKC isoenzymes. Thus, it is difficult to

ascertain the mechanisms for their inhibitory effect on osteoclastogenesis and bone resorption. Nonetheless, these results indicate that PKC plays an important role in osteoclast differentiation and activity.

To gain better insight into the role of PKC in RANKL-mediated osteoclast differentiation and activity, the individual isoenzyme, PKCδ was investigated using the selective PKCδ inhibitor and activator, Rottlerin and Bryostatin 1, respectively. Rottlerin was found to exert a potent inhibitory effect on RANKL-induced osteoclastogenesis and bone resorption. By comparison, the activation of PKCδ by Bryostatin 1 strikingly enhanced osteoclastogenesis. It is possible that Bryostatin 1 acts via upregulation of a fusion mechanism as the RANKL-induced OCLs are morphologically enlarged, exhibiting increased nuclei number expressing high level of DC-Stamp. Furthermore, Rottlerin was shown to inhibit NF-κB activity, whereas Bryostatin 1 showed the opposing effects. Both inhibitor and activator were also found to modulate other key osteoclastic signaling pathways including NFAT and total c-SRC. These findings implicate, for the first time, Protein Kinase C delta signaling pathways in the modulation of RANKL-induced osteoclast differentiation and activity.

Taken together, the studies presented in this thesis provide compelling molecular, biochemical and morphological evidence to suggest that: (1) RANKL mutants might potentially serve as peptide mimic to inhibit RANKL-induced signaling, osteoclastogenesis and bone resorption. (2) A cross talk mechanism between extracellular Ca2+ and RANKL exist to regulate on osteoclast survival. (3) TPA suppressed RANKL-induced osteoclastogenesis predominantly during the early stage of osteoclast differentiation via modulation of NF-κB. (4) Selective inhibition of Protein Kinase C signaling pathways involved in osteoclastogenesis might be a potential treatment method for osteoclast-related bone diseases. (5) Protein Kinase C delta signaling pathways play a key role in regulating osteoclast formation and function.

AWARDS

Awards arising from this work include:

1. **Christopher & Margie Nordin Young Investigator Poster Award (2005)**

   Abstract entitled: *"Truncation Mutants of RANKL inhibit RANKL-induced Osteocalst Differentiation and Activation"* **Wang, C**., Pavlos, N., Tan, W-Y., Li, J-M., Cornish, J., Zheng, M-H., Xu, J., Proceedings of the 15th Annual Scientific Meeting of the Australian and New Zealand Orthopaedic Research Society, Perth, Australia

2. **SCGH Science Week Young Investigator Award**,

   Abstract entitled: *"Truncation Mutants of RANKL inhibit RANKL-induced Osteocalst Differentiation and Activation"* **Wang, C**., Pavlos, N., Tan, W-Y., Li, J-M., Cornish, J., Zheng, M-H., Xu, J., Sir Charles Gardner Hospital Science Week, 2005, Perth

3. **ASMR Young Investigator Award (2006)**

   Abstract entitled: *"Truncation Mutants of RANKL inhibit RANKL-induced Osteocalst Differentiation and Activation"* **Wang, C**., Pavlos, N., Tan, W-Y., Li, J-M., Cornish, J., Zheng, M-H., Xu, J., Australian Symposium.Medical.Research Annual Meeting, June, 2006, Perth, Australia

LIST OF PUBLICATIONS

Publications arising from this work include:

Papers:

1. **Wang, C.**, J. H. Steer, et al. (2003). 12-O-tetradecanoylphorbol-13-acetate (TPA) inhibits osteoclastogenesis by suppressing RANKL-induced NF-kappaB activation. *Journal of Bone Mineral Research* 18(12): 2159-68.

2. Xu, J., Feng, H. T., **Wang, C.**, Yip, K. H., Pavlos, N., Papadimitriou, J. M., Wood, D., Zheng, M. H. (2003). Effects of Bafilomycin A1: An inhibitor of vacuolar H (+)-ATPases on endocytosis and apoptosis in RAW cells and RAW cell-derived osteoclasts. *Journal of Cellular Biochemistry* 88(6): 1256-64.

3. Xu, J., **Wang, C.**, Han, R., Pavlos, N., Phan, T., Steer, J. H., Bakker, A. J., Joyce, D. A., Zheng, M. H. (2005). "Evidence of reciprocal regulation between the high extracellular calcium and RANKL signal transduction pathways in RAW cell derived osteoclasts. *Journal of Cell Physiology* 202(2): 554-62.

4. Ang, E. S. M., Pavlos, N., **Wang, C.**, Scaife, R. M., Yip, K. M., Feng, H. T., Zheng, M. H., Xu, J. (2007). Paclitaxel inhibits osteoclast formation and bone resorption via influencing cytoskeletal structure, ERK and NF-kB pathways. *Revision*.

Abstracts:

1. **Wang, C.,,** Zheng, M-H., Tan, J.W-Y., Li, J-M., Cornish, G., Xu, J (2002) “Truncation mutants of RANKL inhibit RANKL-induced osteoclast differentiation and activation”, Proceedings of the 12th Annual Scientific Meeting of the Australian and New Zealand Bone and Mineral Society, Adelaide, Australia.

2. **Wang, C.,,** Zheng, M-H., Tan, J.W-Y., Li, J-M., Cornish, G., Xu, J (2002) “Truncation mutants of RANKL inhibit RANKL-induced osteoclast

differentiation and activation", Australian and New Zealand Orthopaedic Research Society, Melbourne, Australia.

3. **Wang, C.**, Zheng, M.H., Xu, J.(2004) "Protein Kinase C delta (PKC-δ) mediates Receptor Activator of NF-κB Ligand (RANKL)-induced signaling pathways required for osteoclastogenesis", Proceedings of the 14th Annual Scientific Meeting of the Australian and New Zealand Bone and Mineral Society, Sydney. Australia.

4. **Wang, C.**, Zheng, M.H., Xu, J. (2004) "Protein Kinase C delta (PKC-δ) mediates Receptor Activator of NF-κB Ligand (RANKL)-induced signaling pathways required for osteoclastogenesis", Australian Scientific Medical Research, Perth, Australia.

5. Xu, J., **Wang, C.,** Han, R., Pavlos, N., Phan, T., Steer, J.H., Bakkek, A.J., Joyce, D.A., Zheng, M.H. (2004) "Evidence of Reciprocal Regulation between the High Extracellular Calcium and RANKL Signal Transduction Pathways in RAW Cell Derived Osteoclasts" Proceedings of the 14th Annual Scientific Meeting of the Australian and New Zealand Bone and Mineral Society, Sydney. Australia.

6. Xu, J., **Wang, C.,** Han, R., Pavlos, N., Phan, T., Steer, J.H., Bakkek, A.J., Joyce, D.A., Zheng, M.H. (2004) "Evidence of Reciprocal Regulation between the High Extracellular Calcium and RANKL Signal Transduction Pathways in RAW Cell Derived Osteoclasts", The 26th Annual Meeting of the American Society for Bone and Mineral Research, Seattle USA.

7. **Wang, C**., Pavlos, N., Tan, W-Y., Li, J-M., Cornish, J., Zheng, M-H., Xu, J. (2005) "Truncation Mutants of RANKL inhibit RANKL-induced Osteocalst Differentiation and Activation", Australian Scientific Medical Research. Perth, Australia.

8. **Wang, C**., Pavlos, N., Tan, W-Y., Li, J-M., Cornish, J., Zheng, M-H., Xu, J. (2005) "Truncation Mutants of RANKL inhibit RANKL-induced Osteocalst Differentiation and Activation", Proceedings of the 15th Annual Scientific Meeting of the Australian and New Zealand Orthopaedic Research Society,

Perth, Australia.

9. **Wang, C**., Pavlos, N., Tan, W-Y., Li, J-M., Cornish, J., Zheng, M-H., Xu, J. (2005) "Truncation Mutants of RANKL inhibit RANKL-induced Osteocalst Differentiation and Activation", Sir Charles Hospital Medical Research Week. Perth, Australia.

10. **Wang, C**., Pavlos, N., Tan, W-Y., Li, J-M., Cornish, J., Zheng, M-H., Xu, J. (2005) "Truncation Mutants of RANKL inhibit RANKL-induced Osteocalst Differentiation and Activation", The 27th Annual Meeting of the American Society for Bone and Mineral Research, Nashville, Tennesse, USA.

11. **Wang, C.,** Tan, W-Y, Pavlos, N., Li, J-M., Cornish, J., Zheng, M-H., Xu, J. "Truncation Mutants of RANKL inhibit RANKL-induced Osteocalst Differentiation and Activation", Australian Scientific Medical Research. Perth, Australia.

ACKNOWLEDGEMENTS

This study was performed and accomplished in the Unit of Orthopaedics, School of Surgery and Pathology, University of Western Australia. I would like to extend my thanks and appreciation to Professor Ming-Hao Zheng for his endless support, guidance and encouragement throughout the course of my PhD, but most of all, for giving me opportunity to do PhD, to make my dream possible.

I wish to express my warmest thanks and appreciation to Associated Professor Jiake Xu, who has provided unconditional guidance throughout my PhD. His consistent motivation and enthusiasm in scientific research never fail to inspire me to learn and seek greater heights. Your encouragement and enlightenment give a great boost to my morale when I face difficulties in my research. Jiake's endless support and selfless acts often translate into a tremendous driving force for me to persevere and never to give up.

I would also like to acknowledge Dr. Nathan Pavlos for his valuable assistance and opinions during my study. Thank you for been a great listener when I faced obstacles. Your friendship and encouragement are really appreciated.

Special thanks to Mr. James Steer for his tireless technical support and wonderful advice. Appreciation to his kindness for correcting this thesis.

It is a pleasure to acknowledge my colleagues within the Unit of Orthopaedics. To Estabelle Ang, Jamie Tan and Tamara, for all the sentimental discussions, laughter and for sharing the gossip during our special coffee meetings. To Dr. Hao Tian Feng, Dr. Kirk Yip, Dr. Jim Chen, Tak Cheng, Jacky Chim and Craig Willers, Jane Lin, Norman, Rong, Charlene Li, Tracy Chai, Vincent Qian, Dr. Guan Feng Yao, Dr. Felix Yao, for their friendship, encouragement and enthusiasm throughout my PhD year. I will miss having lunch with you all. I also extend my appreciation to Lesley Gasmier for her continuous support, assistance as well as the decent talks throughout my study. Thanks you all for the good times.

My deepest thanks are reserved for Kenny Koh. Thank you for standing by my side through the good and bad times. Thank you for spending so much of your precious time for not just correcting my thesis, and also leading me to the right direction. You did add

value to my life. Your love, understanding and patient have made my tough time bearable. I cannot find enough words to express how I am truly grateful to have you by my side.

My PhD scholarship has been sponsored by Postgraduate Research scholarships from the National Health and Medical Research Council (NHMRC).

SPECIAL DEDICATION

This thesis is dedicated:

In loving memory of my father. Thanks you for your unconditional love and endless support to allow me to come this far. You have sacrificed and work hard in your entire life for providing me the best. I could not pursue my dream without your inspirational strength, guidance and encouragement. I love you and miss you everyday. You live forever in my heart.

&

To my mother, for her hard work, guidance and unconditional love throughout my life. Thank you for companying me in Perth throughout my study.

Without you, none of my work would have been possible.

LIST OF FIGURES

LIST OF TABLES

ABBREVATIONS

The following abbreviations are used throughout this thesis:

α-MEM	Alpha modified eagles medium
Amp	Ampicillin
ADP	Adenosine diphosphate
AMP	Ampicillin
AP-1	Adaptor protein complex-1
ATP	Adenosine triphosphate
ATPase	Adenosine triphosphate-binding protein
BMMs	Bone marrow monocytes
Bp	Base pairs
BRET	Bioluminescence resonance energy transfer
BSA	Bovine serum albumin
c-AMP	Cyclic adenosine monophosphate
CaR	Calcitonin receptor
Cath K	Cathepsin K
cDNA	Complementary deoxyribonucleic acid
CFU-GM	Granulocyte-macrophage colony-forming unit
CIAP	Calf intestinal alkaline phosphatase
Ca^{2+}	Calcium ions
CLSM	Confocal laser scanning microscopy
CMV	Cytomegalovirus
CO_2	Carbon dioxide
CTR	Calcitonin receptor
Cys	Cysteine
ddH_20	Double distilled water
DEPC	Diethyl pyrocarbonate
D-MEM	Dulbecco's modified eagles medium
DMSO	Dimethyl sulfoxide
DNA	Deoxyribonucleic acid
DNAse	Deoxyribonuclease
DTT	Dithiotheritol
E. Coli	*Escherichia Coli*
EDTA	Ethylene diamine tetra acetic acid
EGTA	Ethylene glycol bis-2-aminoethyl ether-N,N',N'',N'-tetraacetic acid
Erk	Extracellular signal-regulated kinase
EGFP	Enhanced green fluorescent protein
EYFP	Enhanced yellow fluorescent protein
FACS	Fluorescence-activated cell sorting
FCS	Foetal calf serum
FITC	Fluorescein isothiocyanate
GCT	Giant Cell Tumour
GFP	Green fluorescent protein
GST	Glutathione-S-Transferase
HCl	Hydrochloride acid
HEPES	N-2-Hydroxyethylpiperazine-N'-2-ethanesulfonic acid

His	Histidine
IL	Interleukin
IFN-γ	Interferon-gamma
ITPG	Isopropyl-β-thiogalactopyranoside
JNK	c-jun N-terminal kinase
KDa	Kilo Daltons
KO	Knockout
LAMP	Lysosome associated membrane protein
Luc	Luciferase
LPS	Lipopolysaccharide
MAP	Mitogen-activated protein
M-CFU	Macrophage-colony forming unit
M-CSF	Macrophage colony-stimulating factor
MMP	Matrix metalloproteinase
mRNA	Messenger ribonucleic acid
NFAT	
NF-κB	Nuclear factor kappa B
Noc	Nocodazole
Ob	Osteoblast
Oc	Osteoclast
OCIF	Osteoclastogenesis-inhibitory factor
ODF	Osteoclast differentiation factor
OLC	Osteoclast-like cell
OD	Optical density
Oligo	Oligonucleotide
OPG	Osteoprotegerin
OPGL	Osteoprotegerin ligand
OPN	Osteopontin
PAR	Parthenolide
PCR	Polymerase chain reaction
PBS	Phosphate buffered saline
PGE_2	Prostaglandin E_2
P I 3 kinase	Phosphatidylinositol 3-kinase
PKC	Protein Kinase C
PMSF	phenylmethylsulfonyl fluoride
PTH	Parathyroid hormone
PTHrP	PTH-related protein
RANK	Receptor Activator of Nuclear Factor kappa B
RANKL	RANK ligand
RGD	Arg-Gly-Asp
RNA	Ribonucleic acid
RNAse	Ribonuclease
RNAsin	Ribonuclease inhibitor
RT	Reverse transcriptase
SDS	Sodium dodecyl sulphate
SDS-PAGE	SDS-polyacrylamide gel electrophoresis
SEM	Scanning electron microscopy
Taq	*Thermus aquaticus*
TBS	Tris-buffered saline
TBST	TBS-tween

TG	Thapsigargin
TGF-β	Transforming growth factor beta
TNF-α/β	Tumour necrosis factor alpha/beta
TPA	12-0-tetradecanoyl phorbol-13-acetate
TRAFs	TNF receptor-associated factors
TRANCE	Tumour necrosis factor-related activation induced cytokine
TRACP	Tartrate-resistant acid phosphatise
UV	Ultra-violet
V-ATPase	Vacuolar-H^+ATPase
WT	Wild-type
X-Gal	5-Bromo-4-chloro-3-indolyl-β-D-galactopyranoside

CHAPTER 1

The Physiology

and

Biochemistry of the Osteoclast

CHAPTER 1– THE PHYSIOLOGY AND BIOCHEMISTRY OF THE OSTEOCLAST

1.1 INTRODUCTION

Bone is an essential tissue that provides a rigid framework known as the skeleton which supports and protects the soft organs of the body. It is a metabolically active form of connective tissue that exists naturally in the mechanical support system of all higher vertebrates. The bone is a unique living tissue that undergoes continual remodelling through the dynamic processes of formation and resorption to maintain skeletal growth, tooth eruption and serum calcium homeostasis (Vaananen et al., 2000). The mechanisms of bone turnover are highly regulated by osteotropic hormones which are determined by the degree of differentiation and functional states of the two principal resident bone cells called osteoblasts (OBs) and osteoclasts (OCs).

Osteoblasts are bone-lining cells derived from mesenchymal stem cells which orchestrate bone formation processes (Aubin, 2001; Ducy et al., 2000; Mackie, 2003). OBs actively produce extracellular bone matrix constituents including type I collagen, osteocalcin, osteopontin, bone sialoprotein and other ground substances (Mundlos and Olsen, 1997) which become incorporated into the sites of new bone synthesis. Osteoclasts are large terminally differentiated, multinucleated cells solely responsible for physiological bone resorption (Teitelbaum, 2000a; Vaananen et al., 2000; Zaidi et al., 2003). OCs are formed by the asynchronous fusion of mononuclear precursors derived from haematopoietic stem cells (Suda et al., 1999). They resorb actively and remove bone matrix in an effort to promote bone turnover throughout life.

Despite the vigorous regulation and control of bone remodelling, changes in equilibrium can still occur. Excessive osteoclastic bone resorption is the major hallmark of a number of common pathological bone disorders including post-menopausal osteoporosis, osteoarthritis, Paget’s disease, and tumour-mediated osteolysis (Haynes and Crotti, 2003). In the case of osteoporosis, it is endemic in western countries with an estimated 1 in 2 women and 1 in 3 men suffering from bone fractures during their lifetime (Osteoporosis Australia, 2003).

In Australia, the direct cost of treating osteoporotic fractures is estimated to be over $1.9 billion per annual (Osteoporosis Australia, 2003). The high treatment cost has

drawn/attracted great interest in the study of the cellular and molecular mechanisms underlying osteoclast formation and function for the provision of therapeautic intervention.

This chapter will focus on the current aspects of knowledge in osteoclast physiology and biology as the basis for the study of molecular mechanism governing its metabolic actions.

1.2 ONTOGENY OF OSTEOCLAST

Osteoclasts have been recognized as large multinucleated cells located in bone for more than a century. The term "osteoclast" has an interesting history. It was derived by putting osteo- (from the Greek osteon, bone) together with -clast (from the Greek klastos, broken). In 1873, Albert Kolliker, a Swiss physiologist and histologist, first described that osteoclasts were the “universal agents of bone resorption” and suggested that they secreted chemical substances capable of digesting ‘leimgebende’ or collagen and dissolving mineralised composition. Advances in cell biology, biochemistry and the advent of targeted gene disruption studies have allowed a much more detailed study of osteoclast physiology over the last decade. To date, the osteoclast is defined as a terminally differentiated, multinucleated cell of haematopoietic origin that possesses: 1) a ruffled border; 2) a sealing zone; 3) the presence of calcitonin receptors (CTR); 4) positivity for tartrate-resistant acid phosphatase (TRACP); and most importantly, 5) the ability to resorb mineralised matrix.

Although osteoclasts are initially believed to be native to the bone, a derivative of local osteoprogenitors or osteoblastic cells, it is now well established that osteoclasts are formed by the fusion of haematopoietic mononuclear progenitor cells derived from bone marrow and differentiation within the monocyte-macrophage lineage (Chambers, 2000; Roodman, 1999; Suda et al., 1999). Several landmark experiments conducted during the 1970’s have provided early insights into the ontogeny of osteoclasts and have tremendously influenced today’s bone biology investigation (Marks et al., 1984).

Using a parabiotic approach, Göthlin and Ericsson (1973) joined the circulations of two rats (Gothlin and Ericsson, 1973). Specifically, the haematopoietic progenitor cells of one rat were destroyed by irradiation, while the other’s blood cells were labelled with

[^{3}H] thymidine. They observed that both osteoclasts and macrophages were within the fractured callus of the irradiated rat contained [^{3}H] thymidine indicating that the osteoprogenitors were derived from the blood of its non-irradiated partner. Osteoblasts however, were not donor derived suggesting that they differ in the ontogeny of osteoclasts. Comparably, studies by Walker (1973) demonstrated that the osteopetrotic features of microphthalmic mi/mi mice could be rescued by parabiosis with normal littermates (Walker, 1973).

Further evidence in support of a haematopoietic origin was provided by experiments using chick-quail chimeras (Simmons and Kahn, 1979). In this study, quail osteoclast-free cartilaginous rudiments were grafted onto a chicken chorioallantoic membrane. Upon vascularization by the host circulation, the rudiments developed into bone that primarily contained osteoclasts of chick origin, demonstrating that they were haematopoietically derived. Moreover, subsequent studies by Walker (1975) demonstrated that the bone resorption capabilities of osteopetrotic grey-lethal (gl/gl) and microphthalmic (mi/mi) mice could be restored by the transplantation of spleen cells or bone marrow cells from normal donor mice (Walker, 1975). Collectively, these studies provided evidence that osteoclasts were formed by precursors circulating in the bloodstream.

1.2.1 Osteoclasts are derived from the fusion of mononuclear cells of the monocyte-macrophage linage

After establishing the haematopoietic origin of osteoclasts, many investigators focused their attention on identifying haematopoietic lineage cells that were capable of differentiating into functional osteoclasts. Among them, mononuclear monocytes/macrophages were favoured as osteoclastic precursors for several reasons.

First, early studies by Baron and co-workers (1986) using an *in vivo* model of osteoclastogenesis demonstrated that mononuclear cells with low nuclear-cytoplasmic ratio and an abundance of ribosomes invaded sites bone resorption (Baron et al., 1986b). These cells initially contained non-specific esterase (a marker enzyme of monocytes) and progressively became TRACP positive and non-specific esterase negative as they differentiated before eventually fusing to form multinucleated osteoclastic cells.

Second, several *in vitro* studies reported that osteoclast-like cells could be generated from both purified populations of the granulocyte-macrophage colony-forming unit (CFU-GM) and peripheral blood monocytes under adequate culture conditions (Burger et al., 1984; Kurihara et al., 1991; Matsuzaki et al., 1998).

Third, recent studies have shown that bone-resorbing osteoclasts can be generated from monocytes and macrophages that express the surface marker CD14 (Massey and Flanagan, 1999; Takeshita et al., 2000).

Finally, several established monocyte-macrophage cell lines have been shown to form osteoclast-like cells capable of bone resorption *in vitro* (Battaglino et al., 2002; Hayashi et al., 1998; Miyamoto et al., 1998). Having said that, osteoclast precursors can now be viewed as mononuclear cells derived from a pluripotent stem cell of M-CFUs/CFU-GM lineage that are CD14-positive, express MMP-9 and possess ambient levels of TRACP. These cells express high levels of pp60c-src, carbonic anhydrase II, cathepsin K (Cath K), TRACP, $\alpha_v\beta_3$, V-ATPase and calcitonin receptors as they differentiate and become committed towards the osteoclast lineage (Roodman, 1999).

1.3 MORPHOLOGY OF OSTEOCLASTS

Osteoclasts are highly specialized multinucleated cells localized to calcified bone surfaces like endosteum, periosteum and the haversian systems. They are often found residing within resorptive pits or “Howship’s lacunae” as a result of their own resorptive activity (Teitelbaum, 2000a).

Morphologically, the osteoclast can be distinguished by its size (50-100μm in average), its multinucleation (possesses between 2-20 nuclei) and the presence of a resorptive lacuna (~ 50μm deep). The nuclei are heterogeneous in size, shape and basophilia, reflecting the possible asynchronous fusion of mononuclear precursors (Nijweide et al., 1986). Each nucleus possesses 1-2 nucleoli. The nuclei are typically polarized away from the plasma membrane juxtaposed to bone in resorbing osteoclasts (Teitelbaum et al., 1997a).

In contrast, nuclei are organized either centrally or in a syncytium-like manner when cultured in glass surfaces. It has been suggested that the nuclear number may reflect the degree of osteoclast activity (Teitelbaum et al., 1997b). For example, the osteoclasts in Paget's disease, a disorder of accelerated resorption, are enormous, and often contain as many as 100 nuclei (Fallon and Schwamm, 1989). Being multinucleated, the osteoclasts possess extensive cytosol that is strongly basophilic, granular and highly vacuolated giving the cell a foam-like appearance.

Osteoclasts are readily identifiable by the expression of several distinguishing histochemical and cytochemical markers including TRACP, vacuolar-H^+ATPase (V-ATPase), carbonic anhydrase II, vitronection receptor ($\alpha_v\beta_3$), cathepsin K, and calcitonin receptor which is recognized as the most reliable marker of mature osteoclasts (Roodman, 1999). However, it should be noted that avian osteoclasts (chicken) lack demonstrable calcitonin receptors (Nicholson et al., 1987).

Perhaps the most prominent and characteristic morphological feature of the osteoclast is the numerous infolds and invaginations exhibited in the apical plasma membrane. This apical membrane abuts on the bone surface allowing intimate contact with the matrix and forms what is known as the "sealing zone" (Holtrop and King, 1977). The latter, also referred to as the "clear zone" as it is devoid of organelles, is a clearly demarcated structure that consists of a ruffled border (10-40μm) surrounded by a ring of contractile proteins (actin filaments) that attach the cell to the bone surface, subsequently sealing off the sub-osteoclastic cone resorbing compartment (King and Holtrop, 1975). The ruffle border is formed by rapid vectorial transport and insertion of highly acidified intracellular vesicles that fuse with the apical membrane domain (Baron et al., 1988). This appearance parallels the cells degradative activity (Fallon et al., 1983).

1.4 FUNCTIONAL ROLE OF OSTEOCLASTS

Osteoclasts are major cellular agents specialized in bone resorption, which is a process involving the removal of mineralised osseous tissue comprising an organic matrix. The latter consists of predominantly insoluble Type 1 collagen fibres (90%) embedded in a heavy deposit of solid calcium phosphate salt made up of mostly calcium hydroxyapatite (Teitelbaum, 2000a). Osteoclastic bone resorption occurs within the

isolated compartment of the bone and the cytoplasmic protrusions of osteoclasts' ruffled borders. This compartment, surrounded by the "sealing zone", provides the optimal microenvironment for osteoclastic bone resorption. The degree of resorption depends on the levels of acid and proteolytic lysosomal enzyme secretion.

The resorptive process can be characterized into four phases: (1) recognition and attachment of osteoclast to the bone surface; (2) osteoclastic membrane polarization; (3) degradation and resorption of the bone matrix; and (4) removal of degraded bone matrix constituents. This section focuses on the various aspects of the cellular and molecular mechanisms of the resorptive cycle.

1.4.1 Osteoclast attachment

The osteoclast is a highly motile cell. After resorption, the osteoclast detaches from its underlying lacuna and traverses on the bone surface to another site of resorption. As a prerequisite to initiating resorption, the osteoclast must recognise and attach itself to sites targeted for remodelling and subsequently generate a functionally polarized membrane interface. While the exact signal for osteoclastic migration remain rather obscure, the attachment of osteoclasts involves the specific interaction between adhesion molecules in the cell's membrane and specific proteins found in the bone matrix or on the bone surface. A number of putative surface markers have now been identified in both osteoclasts and their precursors. However, with the exception of integrins, few have been functionally involved in osteoclast attachment (Teitelbaum et al., 1997b).

Upon migration to bone surfaces, osteoclasts adhere strictly to the mineralised matrix through the formation of a specialized membrane domain known as the sealing zone. Essentially, this zone of adhesion serves as a "biological plug", sealing the resorptive site. Thus, it enables the generation of a highly acidified enzymatic microenvironment required for the dissolution of mineralised bone hydroxyapatite.

Ultrastructurally, the sealing zone is composed of a dense belt of filamentous actin bundles that lie perpendicular to the bone surface, and extend into short cellular processes that enter irregularities of the bone surface (Kanehisa et al., 1990; King and Holtrop, 1975; Zambonin-Zallone et al., 1988). These rings of punctate membrane

protrusions are collectively known as focal adhesions or podosomes and are thought to facilitate the anchoring of the sealing zone to the bone matrix (Lakkakorpi and Vaananen, 1991; Marchisio et al., 1984).

Podosomes contain a number of matrix-recognising integrins and proteins like fimbrin, α-actinin, gelastin, vinculin and talin that link these heterodimers to the underlying substratum (Zambonin Zallone et al., 1989). The podosomal/ F-actin ring is a hallmark of resorbing osteoclasts and disappears when the osteoclast detaches itself and becomes motile (Lakkakorpi and Vaananen, 1991; Vaananen and Horton, 1995). Systemic regulators of resorption like calcitonin and dbcAMP induce rapid destruction of the actin rings in osteoclasts undergoing bone resorption (Lakkakorpi and Vaananen, 1990).

Over the last decade, integrins have emerged as key regulators of osteoclast activity mediating matrix adhesion and cytoskeletal organization required for both cell migration and formation of the sealing zone and ruffled border (Duong et al., 2000). Integrins are heterodimeric transmembrane molecular assemblies consisting of α and β subunits with specific, receptor-like, extracellular binding sites that recognize defined sequences in matrix proteins. Osteoclasts express at least three integrins: $\alpha_v\beta_3$, a classic vitronectin receptor which is abundantly expressed in osteoclastic membranes (Duong et al., 2000); $\alpha_2\beta_1$ (collagen receptor); and $\alpha_v\beta_1$ (Horton et al., 1993). In particular, $\alpha_v\beta_3$ is pivotal to the resorptive process.

Within osteoclastic cells, the $\alpha_v\beta_3$ expression can be enhanced with oestrogen or retinoic acid administration (Chiba et al., 1996). Moreover, $\alpha_v\beta_3$ has been shown to differentially localize between the sealing zone and ruffled border during cycles of osteoclastic inactivation and activation (Faccio et al., 2002). During attachment, $\alpha_v\beta_3$ recognizes and binds to one or more bone matrix proteins containing Arg-Gly-Asp (RGD) motifs (Horton et al., 1991). The additions of RGD-containing peptides or blocking antibodies, which bind to $\alpha_v\beta_3$, have been shown to arrest osteoclast adhesion to bone, or cause retraction of attached osteoclasts (Horton et al., 1991).

Likewise, *in vivo* studies using dis-integrins (echistatin and kistrin) that contain RGD-sequence motifs have been shown to block PTH-stimulated bone resorption

(Fisher et al., 1993; Sato et al., 1990). Echistatin and synthetic RGD peptide treatment has also been shown to inhibit the formation of multinucleated, TRACP-positive osteoclasts from osteoclast precursors (van der Pluijm et al., 1994). Furthermore, echistatin co-localises with $\alpha_v\beta_3$ integrins in osteoclasts and inhibits bone loss in hypercalcemic mice maintained on a low calcium diet (Masarachia et al., 1998).

The infusion of anti-rat β_3 integrin subunit antibodies has also been shown to sufficiently block the effect of PTH on serum calcium in thyroparathyroidectomised rats and to inhibit bone resorption i*n vivo* (Crippes et al., 1996). In addition, studies have also shown that echistatin or RGD-peptidomimetics inhibit bone resorption in ovariectomised rodents *in vivo*, presumably by blocking $\alpha_v\beta_3$ integrin function (Engleman et al., 1997; Yamamoto et al., 1998). Recently, more compelling evidence has been provided by targeted gene disruption studies of $\alpha_v\beta_3$ (McHugh et al., 2000). β_3-defecient mice display dysfunctional osteoclasts and develop progressive osteosclerosis. Moreover, osteoclasts from these mice failed to spread, lacked distinctive F-actin rings and ruffled borders, and displayed abrogation in bone resorption activity *in vitro*. Full rescue of the osteoclast phenotype can be achieved by viral transduction with the β_3 subunit but not with mutated S(752)P-β_3 which is responsible for Glanzmann's thromboasthenia (Feng et al., 2001).

Although it has been illustrated that the ligands for $\alpha_v\beta_3$ contain RGD sequence, the precise bone matrix proteins recognised by the integrin, *in vivo*, have yet to be elucidated. To date, osteopontin (OPN), bone sialoprotein II (BSPII), thrombospondin, type I collagen, fibronectin, and possibly, vitronectin are the most likely candidates to play the role of integrin-binding proteins in bone (Helfrich et al., 1996; Holt and Marshall, 1998).

1.4.2 Osteoclastic membrane polarization

Following the attachment to the bone matrix, osteoclasts undergo a defined sequence of events, shifting from a non-polarized to a highly polarized resorbing state. Membrane polarization entails the simultaneous reorganization of the osteoclastic cytoskeleton and the coordinated targeting and fusion of intracellular vesicles with the plasma membrane. The rigorous plasmalemma expansion and reorganisation culminate in the segregation of the osteoclastic membrane into at least 3 functionally distinct membrane

domains: the ruffled border, a basolateral domain, and a sub-domain at the basolateral surface known as the functional secretory domain (FSD) (Nesbitt et al., 1993). Although little is known about the functions of the basolateral and functional secretory domains, the ruffled border has been well characterized morphologically.

The ruffled border is a highly specialized membrane that constitutes the apical surface of bone-resorbing osteoclasts (Stenbeck, 2002). Although initially thought to be continuous, recent studies have shown that it is spatially segregated into two distinctive functional sub-domains: (1) a peripheral secretory or vesicle fusion zone; and (2) a centralized matrix uptake or transcytotic domain (Mulari et al., 2003b). The ruffled border is formed by the rapid fusion of acidic intracellular vesicles with the bone-apposed plasma membrane, and serves as an exit site for protons and lysosomal proteases. Thus, it acts essentially as a giant “resorptive organelle” that shares analogies with both lysosomal and late endosomal membranes in other cell types (Baron et al., 1988; Mulari et al., 2003b).

During cellular polarization, in addition to vigorous organization of membrane domains and rapid intracellular vesicle trafficking, the cytoskeleton undergoes its own reorganisation. Here, actin microfilaments, intermediate filaments and microtubules undergo cytoskeletal changes, characteristic of the polarization of any cell type. *In vitro* studies on bone or dentine slices have revealed that both the intermediate filaments and the microtubules are radially organised in osteoclasts (Marchisio et al., 1984; Mulari et al., 2003b). In resorbing osteoclasts, microtubules form thick bundles in the middle of the cell, originating from the top of the cell and converging towards the ruffled border (Helfrich et al., 1996).

Surprisingly, the number of microtubule-organising centre (MTOC) was recently shown to differ significantly between avian and mammalian osteoclasts. Few MTOC were identifiable in rat, rabbit and human osteoclasts suggesting that they have different physiological requirements (Mulari et al., 2003b). Studies by Hunter et al (1989) and Baron et al (1990) demonstrated that the inhibition of microtubule assembly by calcitonin interferes with the cell’s functions. This is possibly because of the role played by microtubules in intracellular translocation of membrane vesicles between the plasma membrane and various intracellular compartments (Baron et al., 1990; Hunter et al., 1989). Moreover, other studies have demonstrated an association between

osteoclast microtubulin and $pp60^{c\text{-}src}$ (c-Src), a tyrosine kinase that is abundantly expressed in neural tissue, platelets and osteoclasts (Horne et al., 1992). They found that c-Src and tubulin (a microtubule protein) associate in avian osteoclast precursors in response to specific matrix components. Targeted disruption of *c-Src* in mice induced osteopetrosis, a family of sclerotic skeletal diseases caused by osteoclast dysfunction.

Like TRAF6-deficient mice, *c-Src* knockout mice contain abundant osteoclasts. However, they are incapable of bone resorption. These cells exhibit many features of normal osteoclasts such as tartrate acid-resistant acid phosphatase activity, but fail to form a polarized ruffled membrane (Boyce et al., 1992). The rescue of *c-Src*$^{-/-}$ mice by transgenic expression of *c-Src*-deficient in kinase activity restores the osteoclast's resorptive capacity, and endows it with the ability to develop a ruffled membrane (Schwartzberg et al., 1997). Collectively, these observations indicated that signalling mediated by c-*Src* is fundamentally involved in the polarization of osteoclasts.

1.4.3 Mechanisms of osteoclastic bone resorption

Early studies by Zambonin Zallone and colleagues (1984) established the first kinetics of bone resorption *in vitro*. They observed that when bone particles were added to osteoclast cultures, the osteoclasts progressively became polymorphic and adhered to the bone particles, subsequently resorbing the bone within one hour of attachment.

When the osteoclasts were plated on freshly prepared periosteum and endosteum-free vital bone, they adhered to the bone surface and began resorption. However, if the vital bone was pre-cultured for 24 hours before plating with osteoclasts, a newly formed multiple layer of lining cells completely enveloped the bone surfaces, preventing contact of the osteoclast with the bone substrate. These features, in some instances, were thought to reflect bone resorption *in vivo*.

In 1986, Blair and his co-workers developed the first biochemical model for osteoclastic bone resorption. In their assay, osteoclasts were cultured on bone fragments that have been pre-labelled with either ^{45}Ca or ^{3}H-proline. The measurement of radioactive ^{45}Ca or ^{3}H-proline released into the culture media was found to be directly proportional to the rate of mineral matrix dissolution (Blair et al., 1986).

1.4.4 Inorganic matrix degradation

It is now well established that the dissolution of the inorganic bone matrix precedes that of the protein. The degradation of crystalline hydroxyapatite is known as demineralisation and requires the acidification of resorptive lacuna. The importance of acidification in bone resorption was first demonstrated using microelectrode-based pH measurements at the osteoclastic ruffled border of osteoclasts (Fallon, 1984). Subsequently, several studies incorporating the use of vital-dyes have revealed the presence of a low pH (3-4.8) extracellular micro-compartment beneath the resorbing cells as well as a high density of acidic vesicles within the cytoplasm of non-resorbing osteoclasts (Baron et al., 1985; Inoue et al., 1999).

The acidification of extracellular resorptive space is achieved through the action of ATP-consuming vacuolar H^+ ATPase pumps (V-ATPase) concentrated at the ruffled border membrane (Blair et al., 1989; Laitala and Vaananen, 1994; Laitala and Vaananen, 1993; Laitala-Leinonen et al., 1996; Vaananen et al., 1990). These vacuolar proton pumps share close similarities with the multi-enzyme complex ATPase in the intercalated cells of kidney, and actively transport H^+ protons across the ruffled border to the underlying bone matrix (Wang et al., 1992a).

V-ATPases are considered to be the critical moiety in osteoclast acidification for two main reasons. First, numerous independent studies have shown that osteoclastic bone resorption can be effectively blocked by fungal, metabolite bafilomycin A, a potent and specific inhibitor of all V-ATPases both *in vitro* (Mattsson et al., 1991; Sundquist et al., 1990) and *in vivo* (Sundquist and Marks, 1994). Bafilomycin has also been shown to induce apoptosis and disrupt endocytosis indicating the importance of V-ATPases in osteoclastic intracellular acidification (Xu et al., 2003).

Second, targeted disruption of the *Atp6i* gene in mice resulted in a severe osteopetrotic phenotype due to the loss of osteoclast-mediated extracellular acidification (Li et al., 1999). Finally, the importance of V-ATPases in osteoclast-mediated bone resorption is further supported by recent findings that mutations in the *OC116* gene that encodes the α3 subunit of the vacuolar H^+-ATPase complex cause infantile malignant osteopetrosis, a rare autosomal recessive genetic disease that manifests itself during the first months of life (Kornak et al., 2000).

Protons are supplied to the proton pumps by the action of carbonic anhydrase type II, a cytoplasmic enzyme in osteoclasts, in a reaction encompassing CO_2 within the mitochondria (Dulce et al., 1960). Carbonic anhydrase is an essential isoenzyme of active human osteoclasts (Sly and Hu, 1995). A disruption or deficiency in carbonic anhydrase II results in an unusual form of inherited osteopetrosis in children (Sly et al., 1983). During bone resorption, osteoclasts maintain electroneutrality by the efflux of chloride anions (Cl^-) that simultaneously balances the continual pumping of protons through the ruffled border.

The presence of a high number of chloride channels has been identified in the ruffled border of osteoclasts (Blair and Schlesinger, 1990). Among them, the C1C-7 chloride channel has recently been shown to be highly expressed in osteoclasts, and vital to the maintenance of the ruffled border and resorption. The knockout of C1C-7 results in severe osteopetrosis in mice while CLCN7 mutations have been linked with human infantile malignant osteopetrosis (Kornak et al., 2001). The outflow of Cl^- through to the ruffled border is compensated by the presence of HCO_3^-/Cl^- ion exchangers that are studded within the osteoclastic basolateral domain (Teti et al., 1989). In addition, the basolateral domain possesses a number of ion pumps and channels including, a Na^+/H^+ anti-porter (Hall et al., 1992), a Na^+/K^+-ATPase (Baron et al., 1986a), a Ca^{2+}-ATPase (Akisaka et al., 1988) and a Na^+/Ca^{2+}exchanger (Moonga et al., 2001), all operating to preserve cellular hemostasis.

1.4.5 Organic matrix degradation

Following the dissolution of the mineral phase, the organic matrix undergoes proteolytic degradation. The acidic resorptive microenvironment provides the optimal conditions for the activation of a mélange of proteolytic enzymes involved in the degradative process. Several lysosomal enzymes (i.e. lysosomal acid phosphatase (LAP), TRACP, β-gylcerophosphotases, arylsulfate, β-glucuronidase and cysteine-proteinases), Non-lysosomal enzymes (i.e. matrix metalloproteinases (MMPs), tissue plasminogen activator and lysozyme), matrix proteins and free oxygen radicals have been identified in the resorptive lacunae, all potentially involved in the degradation of the extracellular matrix (Delaisse et al., 1993; Key et al., 1994; Silverton, 1994). Of these secretory products, lysosomal cysteine proteinases and MMPs have been extensively characterised.

Lysosomal cysteine proteinases are proteolytic enzymes released by osteoclasts during bone resorption. Lysosomal hydrolases are capable of degrading type-I collagen and other matrix constituents under an acidic environment like the one encountered in the resorbing compartment. Several lysosomal cysteine proteinases including cathepsins B, D, L, H, K, O and S have been detected by a combination of *in situ* hybridisation and/or immunochemical methods and implied in osteoclastic bone resorption (Delaisse et al., 1991; Goto et al., 1994; Hill et al., 1994a; Kakegawa et al., 1993; Ohsawa et al., 1993).

Among them, cathepsin K is now recognised as the predominant osteoclast protease responsible for active collagen digestion (Bossard et al., 1996; Drake et al., 1996). Deficiency in cathepsin K results in impaired bone resorption and osteopetrosis in mice (Saftig et al., 1998). The importance of cathepsin K is further strengthened by the fact that patients who exhibit mutations in the gene that encodes cathepsin K display pyknodysostosis (a rarely inherited osteochondrodysplasia characterised by osteosclerosis), short stature, and acroosteolysis of the distal phalanges (Motyckova and Fisher, 2002).

In addition to cysteine proteases, neutral collagenases and MMPs have been implicated in organic bone matrix degradation. MMPs can be classified into three distinct subclasses: interstitial collagenases, gelatinases and stromolysins. Several collagenases have been identified in osteoclasts including MMP-1, MMP-9 (type-IV collagenase/gelatinase) and MT1-MMP (Delaisse et al., 2003). Despite a number of independent *in vitro* studies verifying the existence of MMPs within the ruffled border and implicating them in collagen matrix dissolution (Everts et al., 1992; Okada et al., 1995), osteoclasts derived from MMP-9 and MT1-MMP null mice display only transient disturbances in resorptive activity suggesting that they are not obligatory for bone resorption processes (Vu et al., 1998). Whether these mild phenotypes may reflect compensational redundancy from other MMPs remains to be clarified.

1.4.6 The fate of degraded bone substrates

After matrix degradation, bone products (Ca^{2+} and collagen fragments) must be efficiently removed from the resorption lacunae in order for continuous resorption to occur. Theoretically, there are two different routes for resorption by-products: (1)

they can either diffuse continuously from the resorption lacunae beneath the sealing zone; or (2) they can be transported through the resorbing cell via transcytotic carriers. While the precise fate of degraded matrix constituents remains controversial, to date there is little experimental evidence for the leakage beneath the sealing zone. However, a recent study by Stenbeck and Horton (2000) demonstrated that the sealing zone is permeable to negatively charged molecules with *Mr* less than 10,000 (Stenbeck and Horton, 2000), raising the possibility of passive diffusion of resorption by-products through the sealing zone.

There is growing evidence supporting the transcytotic route of bone matrix disposal as vesicular transcytosis of labeled bone products from the ruffled border to a central area of the basal membrane have been observed by several independent groups (Mulari et al., 2003a; Nesbitt et al., 1993; Salo et al., 1997). Although the composition of these transcytotic carriers is yet to be characterized, they are thought to mimic transcytotic vesicles such as those observed in polarized epithelial cells and thus, may share functionally conserved molecular machinery (Mostov and Werb, 1997).

The key stages of osteoclastic bone resorption can be summarised in Figure 1.1.

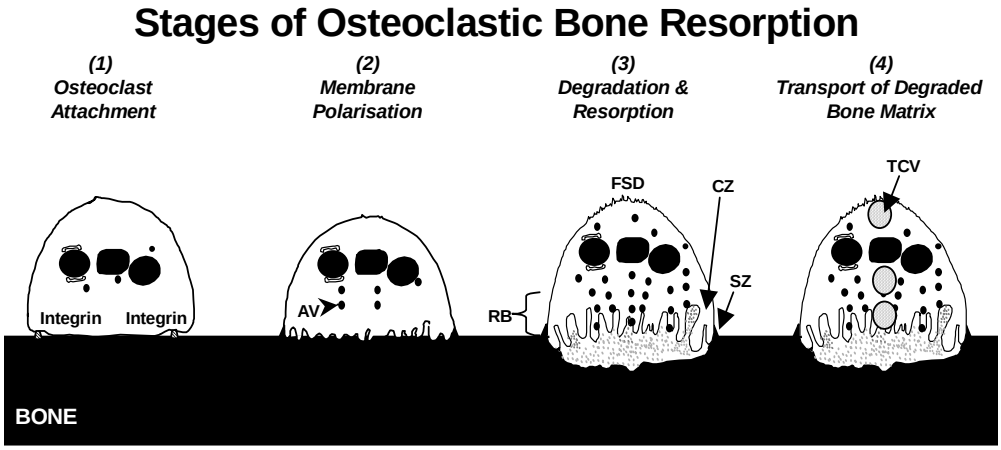

Figure 1.1 Stages of osteoclastic bone resorption: (1) The osteoclast initiates resorption through attachment to calcified bone surfaces via actin microfilaments and integrins, specific for bone matrix proteins possessing RGD sequences. **(2)** Upon attachment, osteoclasts undergo membrane polarisation through the formation of intracellular acidified vesicles (AV), which rapidly fuse to the bone-facing surface to create a ruffled membrane domain. The ruffled border (RB) is essentially, the "resorbing organ". **(3)** During bone degradation and resorption, a sealing zone (SZ) seals off the acidic microenvironment generated and electrochemical homeostasis is maintained through the basolateral domain. **(4)** Degraded bone matrix products are then endocytosed and transported via transcytotic carrier vesicles (TCV) from the ruffled border to the functional secretory domain (FSD) and released into the extracellular environment. CZ, clear zone.

1.5 KEY CYTOKINES FOR OSTEOCLAST DIFFERENTICATION AND ACTIVATION

The differentiation and activation of mononuclear precursors into functionally mature osteoclasts have long been known to be dependent on their interaction with osteoblastic/stromal cells residing within the bone microenvironment (Rodan and Martin, 1981; Udagawa et al., 1989). In 1982, Burger et al demonstrated that culturing haematopoietic precursors in contact with foetal bone rudiments generated bone-resorbing osteoclasts (Burger et al., 1982). The studies performed by Udagawa et al 1989, using co-cultures of spleen cells and osteoblastic/stromal cells in the presence of 1,25$(OH)_2$ vitamin $D_{3,}$ demonstrated that cell-to-cell contact between osteoclastic progenitors and osteoblasts was an essential requirement for osteoclast development. Similarly, osteoblasts were also shown to play an important role in osteoclast activation and potentiate bone resorption *in vitro* (Katoh et al., 1995).

Even though osteoclast formation was known to be largely reliant on interactions between haematopoietic precursors and osteoblasts/stromal cells, the identity and nature of the key factor(s) underlying osteoclastogenesis remained somewhat enigmatic. To date, at least two osteoblastic/stromal cell factors are essential and sufficient for osteoclast formation and activation. They are Macrophage Colony-Stimulating Factor (M-CSF) and Receptor Activator of Nuclear Factor kappa B (RANK) ligand or RANKL.

1.5.1 Macrophage colony-stimulating factor (M-CSF)

M-CSF is an important factor for both the proliferation and differentiation of osteoclast progenitors (Biskobing et al., 1995). The crystal structure revealed that M-CSF is a member of a family of molecules related by having a distinctive four-helical-bundle structural core. As illustrated by site-directed mutagenesis, residues in or near helix A and helix C are involved in receptor binding, reflected by decreased bioactivity and receptor binding of certain mutants.

There are multiple mRNA spliced variants of human M-CSF that give rise to distinct protein products, all of which are initially membrane bound at their C-terminus and are released by proteolysis (Koths, 1997). All the spliced variants conserve the N-terminal

receptor binding domain as well as the C-terminal transmembrane domain, but have variable-size inserts between these domains. Other variations in naturally occurring M-CSF include difference in glycosylation and glycosaminoglycan additions (Shadle et al., 1989). Both membrane-bound and secreted forms of M-CSF are biologically active and bind a single, high affinity transmembrane receptor, a product of the c-fms proto-oncogene (Coussens et al., 1986). Through its interaction with the receptor *c-fms*, M-CSF promotes maturation and survival of early but committed macrophage progenitor cells (Fuller et al., 1993). Perhaps the significance of M-CSF in bone remodelling is best demonstrated by the *op/op* mice. The latter possess a point mutation in the *M-CSF* gene and exhibit severe osteopetrosis (Yoshida et al., 1990). Osteoblasts derived from the *op/op* mice fail to support osteoclast formation *in vitro* (Felix et al., 1990; Takahashi et al., 1991).

Surprisingly, *op/op* mice possess normal osteoclasts but in reduced numbers, and osteopetrosis resolves after several weeks, a process which can be accelerated by the transgenic overexpression of anti-apoptotic Bcl-2 (Lagasse and Weissman, 1997). In addition, the *op/op* phenotype can be partially rescued by the administration of recombinant human M-CSF (Sundquist et al., 1995). Furthermore, M-CSF has been shown to stimulate osteoclast-like cell formation in human marrow cultures and prolong mature osteoclast survival (Fuller et al., 1993; Sarma and Flanagan, 1996). However, M-CSF alone is not sufficient for osteoclast formation *in vitro* and *in vivo (Kodama et al., 1991)* as the formation requires the presence of receptor activator of nuclear factor kappa B ligand (RANKL).

1.5.2 Receptor activator of nuclear factor kappa B ligand (RANKL)

One of the most significant discoveries in osteoclast biology so far was the identification of a novel “osteoclast differentiation factor”, better known as RANKL, by groups at Snow Brand and Amgen (Lacey et al., 1998a; Yasuda et al., 1998a). RANKL/ODF/TRANCE/OPGL is a ~35 kDa, membrane-bound signal transducer of the TNF superfamily responsible for the formation, differentiation and maintenance of osteoclasts (Kong et al., 1999a; Lacey et al., 1998a). The knockout of the RANKL gene results in severe osteopetrosis with complete absence of osteoclasts and failed tooth eruption (Kong et al., 1999a).

Similarly, the over-expression of RANKL in transgenic mice induces pronounced osteoporosis (Mizuno et al., 2002). RANKL is abundantly expressed in osteoblasts, stromal cells, activated T lymphocytes and mammary tissue where it mediates an essential signal for osteoclastogenesis through specific cell-cell interactions with its receptor, Receptor Activator of NFκB receptor (RANK), that is localised to the surface of osteoclasts and their progenitors (Hsu et al., 1999a) (Refer to Figure 1.2). The details of RANKL will be fully discussed later in this chapter.

Osteoclastogenic factors including PTH, 1,25$(OH)_2$ vitamin D_3, PGE_2, IL-1 and TNF-α have demonstrated their capability to up-regulate RANKL expression (Hofbauer, 1999; Lacey et al., 1998a). In addition, soluble recombinant RANKL is sufficient to induce the osteoclast formation of myeloid cell lines (Battaglino et al., 2002; Hotokezaka et al., 2002a), purified macrophage and spleen cell populations in the presence of M-CSF (Quinn et al., 1998), thus replacing the needs for osteoblast/stromal cell co-culture systems, and that have facilitated and eased the study of osteoclast biology in many ways. Besides, TNF-α has also been shown to act synergistically with RANKL in inducing osteoclastogenesis *in vitro* (Lam et al., 2000). Furthermore, mice injected with recombinant RANKL developed hypercalcemia and increased osteoclast activation and differentiation *in vivo* (Lacey et al., 1998a).

1.5.3 Receptor activator of nuclear factor kappa B (RANK)

The expression of RANK/TRANCER on osteoclasts and their precursors is essential for osteoclast formation and activation (Fuller et al., 1998; Hsu et al., 1999a). Similar to its ligand, mice with RANK target disrupted develop severe osteopetrosis (Li et al., 2000). On the other hand, RANK expression is markedly enhanced in the presence of M-CSF (Arai et al., 1999). RANK belongs to the TNF-receptor family and is expressed on dendritic cells, T cells and haematopoietic cells. It has been identified as the receptor for RANKL (Anderson et al., 1997a; Lacey et al., 1998a).

RANKL interacts with RANK and triggers the activation of downstream signalling cascades. In brief, activation induces RANK recruitment of TNF receptor-associated factors (TRAFs) 1,2,3,5 and 6 (Kim et al., 2002) that function as TNF signal transducers, and upon binding to the intracellular domain of RANK activate a cascade of signalling pathways including NF-κB; mitogen-activated protein (MAP) kinases, i.e.

extracellular signal-regulated kinase (ERK); c-jun N-terminal kinase (JNK) and p38; and Akt (Theill et al., 2002) pathways. Mice lacking TRAF6 gene exhibit osteopetrosis phenotype in which osteoclast numbers are normal but lack polarization and resorptive activity (Lomaga et al., 1999a). Later in this chapter, the mechanism underlying the RANKL-inducing NF-κB signalling pathway activation, as well as the major components involved will be discussed in detail.

1.5.4 Osteoprotegerin (OPG)

The dimeric secretory protein osteoprotegerin (OPG) is a soluble "decoy" receptor that competes with RANK for RANKL. Moreover, OPG also in part regulates the level of RANKL expression (Lacey et al., 1998a). OPG, although widely expressed, exhibits strong expression in osteoblasts (Bucay et al., 1998). OPG-deficient mice developed severe osteoporosis (Bucay et al., 1998; Mizuno et al., 1998) whereas transgenic over-expression of OPG inhibits osteoclast formation causing osteopetrosis (Hofbauer, 1999). Recently, Capparelli et al (2003) demonstrated that a single intravenous injection of recombinant human OPG (rhOPG) with a sustained serum half-life was sufficient to suppress osteoclastic bone resorption and increase bone density in developing rats (Capparelli et al., 2003).

In addition, several studies have demonstrated that OPG might have wide therapeutic applications, as recombinant OPG has been shown to suppress IL-1, TNF-α, PTH, PTHrP, 1,25$(OH)_2$ vitamin D_3 induce hypercalcemia and suppress bone destruction in adjuvant arthritis (Kong et al., 1999a; Kong et al., 1999b). Moreover, in several osteolytic diseases including rheumatoid arthritis (Haynes et al., 2001), peri-implant loosening (Crotti et al., 2003; Haynes et al., 2001), giant cell tumours of bone (GCT) (Huang et al., 2000) and periodontitis (Liu et al., 2003), the ratio of RANKL/OPG expression is significantly elevated, suggesting that an intricate balance between the levels of RANKL and OPG must be sustained in order to maintain physiological bone resorption (Haynes and Crotti, 2003).

1.5.5 Local and systemic modulators of osteoclast formation and activation

Stimulatory factors including parathyroid hormone (PTH), PTH-related protein (PTHrP), 1,25$(OH)_2$ vitamin D_3, interleukin-1 (IL-1), IL-6, IL-11, IL-17 TGF-α,

TNF-α and TNF-β have all been shown to potentiate the proliferation of osteoclast progenitors, and enhance osteoclast differentiation and activation either directly or indirectly through osteoblasts and stomal cells. In contrast, TGF-β, IFN-γ, IL-4, IL-10, IL-12, IL-13, IL-18, nitric oxide, oestrogen and calcitonin exert inhibitory effects on osteoclastogenesis and osteoclast activity either by blocking the proliferation and differentiation of mononuclear precursors, or by directly impeding their resorptive activity.

Even though all these local and systemic osteotropic hormones and soluble growth factors have been identified and have demonstrated their importance in the modulation of osteoclast formation, development and activation *in-vivo*, M-CSF, RANKL and OPG are still by far the most recognised and significant cytokines in osteoclast physiology (Chambers, 2000; Heymann et al., 1998; Suda et al., 1999). (see Table 1.1 for summary of the modulators effect).

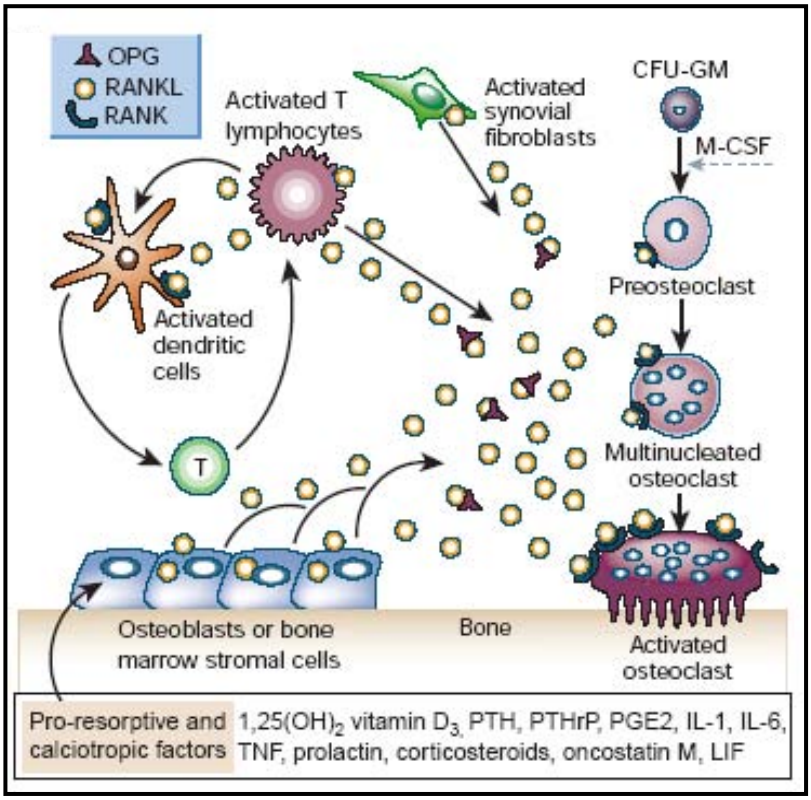

Figure 1.2 Schematic representation of the mechanism by which osteoblasts /stromal cells regulate osteoclastogenesis. RANKL expression is induced in osteoblasts, activated T cells, synovial fibroblasts and bone marrow stromal cells by pro-resorptive and calcitropic factors, and subsequently binds to its specific membrane-bound receptor RANK, thereby triggering a network of TRAF-mediated kinase cascades that promote osteoclast differentiation, activation and survival. Conversely, OPG expression is induced by factors that block bone catabolism (refer to Section 2.3.5) and promote anabolic effects. OPG binds and neutralizes RANKL, leading to a block in osteoclastogenesis and decreased survival of pre-existing osteoclasts. *Figure taken from (Boyle et al., 2003).*

Table 1.1: Local and systemic modulators of osteoclast formation and activation

Modulators	Effect on Osteoclast Formation/Activity
Parathyroid hormone (PTH)	Positive
PTH-related protein (PTHrP)	Positive
$1,25(OH)_2$ vitamin D_3	Positive
Interleukins: IL-1, IL-6, IL-11, IL-17	Positive
TGF-α	Positive
TNF-α and β	Positive
MCSF	Positive
RANKL	Positive
TGF-β	Negative
IFN-γ,	Negative
Interleukins : IL-4, IL-10, IL-12, IL-13, IL-18,	Negative
Nitric oxide,	Negative
Oestrogen	Negative
Calcitonin	Negative
OPG	Negative

1.6 RANKL BIOLOGICAL FUNCTION

Soon after OPG has been characterized, it is highly possible that it might be the key to identify the osteoclast differentiation factor, which is important for the osteoclast development. Both Lacey *et al* and Yasuda *et al* used expression cloning with OPG as a probe and have identified its ligand, termed OPGL or ODF. It was then found to be identical with two previously known members of TNF ligand family called TNF-related activation-induced cytokine (TRANCE) and RANKL.

1.6.1 Structure characteristics of RANKL

Human RANKL is a 317-amino acid peptide. It is approximately 87% identical to the murine RANKL, indicating that this protein is highly conserved during evolution (Lacey et al., 1998a). It also has approximately 30% homology to the TNF-related apoptosis-inducing ligand and to CD40, and approximately 20% homology to Fas ligand (Anderson et al., 1997a; Lacey et al., 1998a; Wong et al., 1997b; Yasuda et al., 1998a). Our group has cloned the rat rRANKL in year 2000, and found that rRANKL has 84% homology to human RANKL and 96% homology to mouse RANKL (Xu et al., 2000b).

The RANKL amino acid sequence contains a probable hydrophobic transmembrane domain between residues 49 and 69 (Lacey et al., 1998a). It is a type II transmembrane protein, in which the C-terminal extracellular domain shows homology to other TNF family members. It consists of a short N-terminal intracellular domain and a long C-terminal extracellular domain. The C-terminal region consists of two domains: a stalk region extending from leucine 70 to glycine 157, and an active ligand moiety extending from lysine 158 to the C terminus (Lacey et al., 1998a).

All TNF cytokines share a common structural core, a scaffold of ten hydrogen-bonded strands in two sheets that has a characteristic jellyroll β-sandwich fold (Lam et al., 2001a). Even the locations and general nature of the TNF-ligand and receptor contact surfaces are similar among the characterized family members. On the other hand, the specific sequences and conformations of the receptor and ligand loops that mediate the interactions are largely different. These specific sequences are thought to be accounting for the specificity of the receptor-ligand interactions (Aoki et al., 2006).

All known TNF cytokine family members self-assemble into noncovalently associated trimers. The core β-strand topology underlies the intrinsic nature of these monomers to oligomerize around an axis of three-fold rorational symmetry. While initially tethered to the membrane, ciologically active trimers exist as both member-bound and soluble cleaved forms (Aoki et al., 2006). Both membrane-bound and soluble forms of RANKL are able to induce osteoclast formation *in vitro* (Lacey et al., 1998a; Yasuda et al., 1998a). Both the rat and the mouse RANKLs appear to have a consensus TNF-α convertase TACE cleavage site (VGPQR/FSG) (Lum et al., 1999). Like TNF-α, RANKL can be cleaved by TACE at the stalk region resulting in the release of the soluble form of RANKL into circulation.

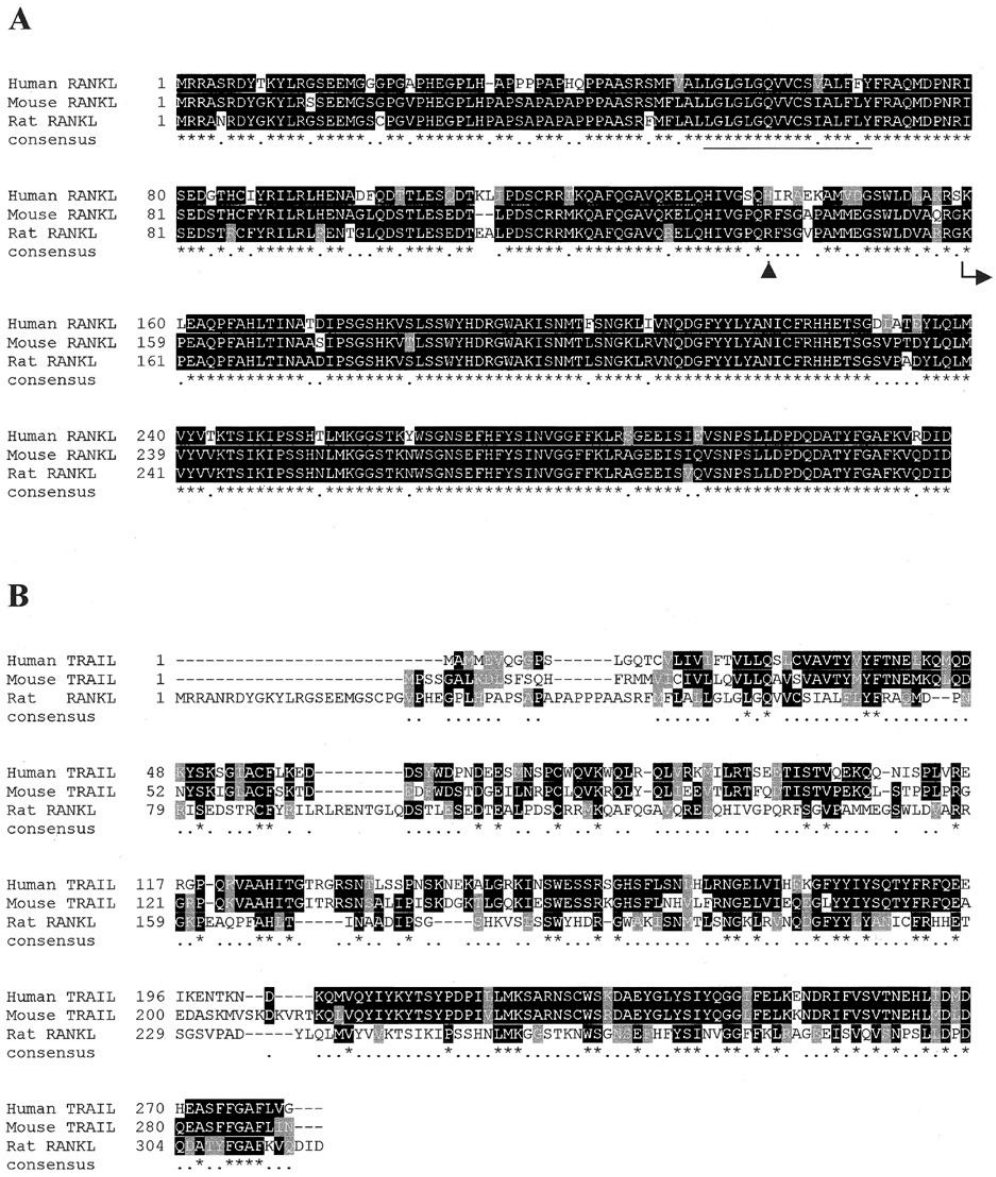

Figure 1.3 Sequence homology of the predicted amino acid sequences of human, mouse and rat RANKL. (A) Alignment of the predicted amino acid sequences of rRANKL with those of human and mouse RANKL. The predicted transmembrane regions are underlined. The metalloprotease disintegrin TACE cleavage site is marked by an arrow head. Right arrow marks the beginning of the TNF-like core domain within the extracellular region extending to the C terminus. (B) Alignment of the amino acid sequences of the rRANKL with those of human and mouse TRAIL. Identical amino acids are marked with black block and asteroids on the consensus lines. Similar amino acids are indicated with gray color and dots on the consensus lines. *Figure taken from Xu et al., 2000.*

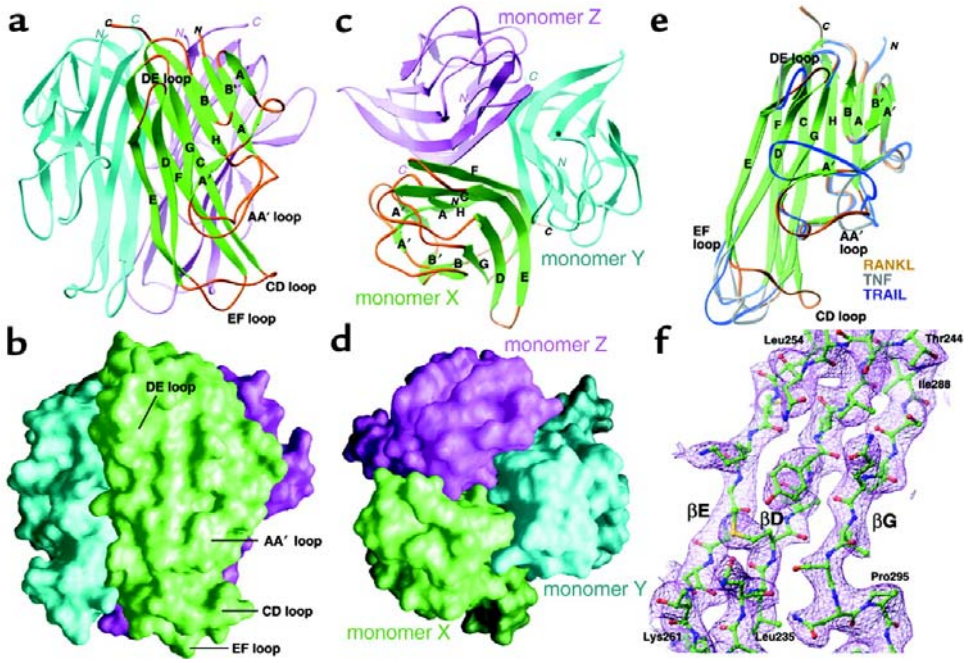

Figure 1.4 Crystal structure of RANKL. (**a**) Ribbon diagram of the RANKL trimer, shown with the ß-strands (green) and connecting loops (orange) of one RANKL monomer labeled according to standard TNF-ß–sandwich nomenclature. The other two RANKL monomers are cyan and magenta, respectively. (**b**) In this view, oriented identically to **a**, the RANKL transmembrane stalk projects to the top of the image, while the membrane-distal region is toward the bottom. The homotrimer exhibits the shape of a truncated pyramid, being slightly wider at the membrane-proximal end. (**c**) Ribbon diagram of the RANKL trimer viewed down the axis of threefold symmetry, oriented with the membrane-distal face forward. The secondary structure of monomer X is labeled as in **a**. (**d**) The RANKL trimer, shown with the molecular surfaces of monomers X, Y, and Z colored in green, cyan, and magenta, respectively. The orientation of the molecule is identical to that in **c**. (**e**) Comparison of a single RANKL monomer with those of TNF and TRAIL. The ß-strands of all three structures are colored green, while the connecting loops are colored orange for RANKL, gray for TNF (PDB code 1tnr), and blue for TRAIL (PDB code 1d4v). When the structures of these proteins are superimposed, it is apparent that the ß-strands of RANKL superimpose almost identically with those of TNF and TRAIL. In contrast, the AA", CD, EF, and DE loops of RANKL exhibit unique topology when compared with those of other TNF family cytokines. (**f**) Electron density of the E-D-G ß-strands. The structure is viewed from the solvent-accessible surface of the RANKL monomer, with an orientation similar to (**e**). Displayed in magenta is a 2.6-Å composite omit map (contoured at 1.2 ς) with the RANKL structure depicted in green (carbon), red (oxygen), blue (nitrogen), and yellow (sulfur). *Figure taken from* (Lam et al., 2001b)

1.6.2 RANKL Function and Tissue Distribution

The TNF-family molecule RANKL has been identified as a key osteoclast differentiation factor and regulator of interactions between T cells and dendritic cells *in vitro* (Anderson et al., 1997b).

Kong et al showed that RANKL $^{-/-}$ mice exhibited severe osteopetrosis. The long bones were shortened and had a distinct broadening of the ends of the bones due to a bone-remodeling defect. They also have a defect in tooth eruption as none of these mice have incisor or molar teeth erupted into the oral cavity. This is a typical finding of osteopetrosis since bone resorption is required to open an avenue through the bone of jaw for eruption of teeth. The lack of osteoclasts in RANKL knock out mice is due to the inability of osteoblasts or stromal cells to support osteoclastogenesis, and not an intrinsic block in osteoclast development. The mice lacking RANKL or its receptor RANK also failed to form lobulo-alveolar mammary structures during pregnancy, resulting in death of new born (Fata et al., 2000).

The analysis of tissue distribution of the transcribed RANKL gene was strongly expressed in trabecular bone, thymus, and lungs, and weakly expressed in spleen and bone marrow (Yasuda et al., 1998a). Our group has also shown that the expression of RANKL mRNA in OVX rat was most abundant in the thymus, followed by tibia, vertebrae, rib crest, and spleen, and much lower levels in the lung, with just traces of expression in the liver and kidney. The RANKL transcripts were undetectable in the brain and heart (Xu et al., 2000b).

1.6.2.1 Lymph-node organogenesis

RANKL is an important factor for osteoclast maturation. Interestingly, the same molecule that regulates osteoclastogenesis is also a key factor for early differentiation of thymocytes and B-cells precursors (Kong et al., 1999d).

Studies in mice deficient in lymphotoxin-α (De Togni et al., 1994; Rennert et al., 1998), lymphotoxinβ (Alimzhanov et al., 1997; Koni et al., 1997), TNFR1 (TNFRp55) (Alimzhanov et al., 1997), TNF-α (Pasparakis et al., 1996), or the lymphotoxin-β receptor have revealed important roles of each of these molecules in the development and organization of secondary lymphoid tissues. Mice with disrupted LTα, LTβ, or the

LTβR genes lack lymph nodes, Peyer's patches and follicular dendritic cells and exhibit altered aplenic architecture. The RANKL$^{-/-}$/*opgl*$^{-/-}$ mice completely lack of lymph nodes but exhibit intact splenic architecture and develop Peyer's patches, indicating that RANKL has a specific and essential role in lymph node development (Kong et al., 1999d). The defect is not due to a homing effect of lymphcytes into nodes.

RANKL probably acts as a growth and survival factor on a lymph-node-organizing cell during embryonic development since the normal bone-marrow cells cannot rescue the lymph-node defect in *rankl*$^{-/-}$ mice in chimaeric transfer experiment carried out by Kong *et al.*, 1999. RANKL expression is also required for T- and B-cell maturation. It was found to regulate early B cell differentiation from the B220^{+}CD43^{+}CD25^{-} pro-B cell to the B220^{+}CD43^{-}CD25^{+} pre-B cell stage of development (Kong et al., 1999d). This indicates that the TNF-family cytokine RANKL is a novel regulator of early B lymphocyte development.

1.6.2.2 Mammary gland development

Another role for RANKL has been revealed from the RANKL and RANK null mice. In addition to having osteoporosis due to the failure of osteoclast development, the mice fail to lactate because of the lack of development of lobulo-alveolar structures during pregnancy. In mammals, mammary gland morphogenesis and the formation of a lactating mammary gland are controlled by sex and pregnancy hormones. Mammary branching commences during puberty and leads to the infiltration of the epithelial duct tree into the mammary fat pad.

During pregnancy, branching increases and the lubolo-alveolar structure is developed owing to the expansion and proliferation of ductal and alveolar epithelium (Fata et al., 2000). Fata et al, 2000, reported that pregnancy hormones induced RANKL expression in mammary epithelial cells. The mutations of *RANKL* or *RANK* genes resulted in the total inhibition of lobulo-alveolar epithelial development, and a complete block in the formation of a lactating mammary gland, leading to the death of newborn pups.

Most importantly, the implantation of RANKL into the mammary tissue of pregnant RANKL$^{-/-}$ mice restored lobulo-alveolar differentiation and milk production (Fata et al., 2000). The link between local events in the breast and bone is already substantial.

However, there are many other factors acting directly and indirectly on lobulo-alveolar differentiation in mammary gland, including prolactin, cyclinD1 and ErbB2 (Martin and Gillespie, 2001). The studies of Fata *et al*. also found that PTHrP enhances the *RANKL* mRNA production. The *Pth1r* expression has been located only in stromal cells of breast tissue. The effect of PTHrP on RANKL production might be indirect, depending first on PTHrP action upon the stromal cells, which in turn influence epithelial production of RANKL (Martin and Gillespie, 2001).

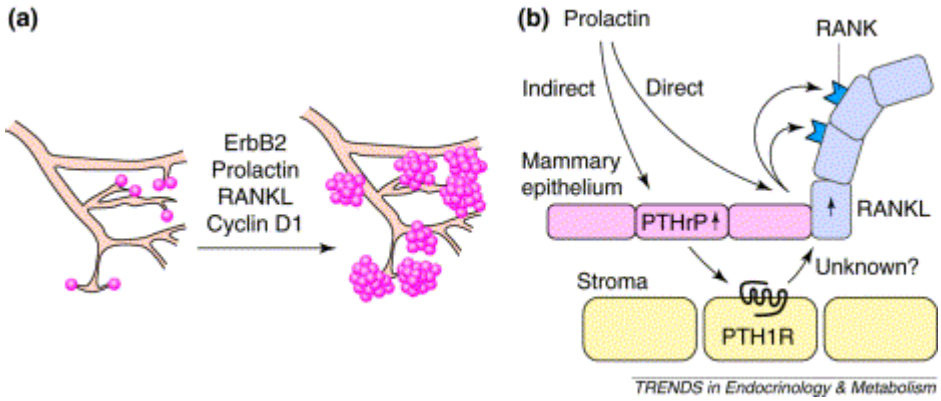

Figure 1.5 RANKL: another link between breast and and bone. (a) Lobulo-alveolar differentiation in mammary gland. Cyclin D_1, ErbB2, prolactin and RANKL do not affect ductal branching morphogenesis, but affect the terminal differentiation of lobulo-alveoli into acini. However,under- or overexpression of the gene encoding PTHrP (*Pthrp*) impedes ductal branching. (b) Possible mechanism of RANKL-induced differentiation of mammary epithelial cells into acini. Both PTHrP and prolactin induce expression of the gene encoding RANKL (*Rankl*) by mammary epithelial cells resulting in lobulo-alveolar development: epithelial cells of acini (blue) express elevated levels of *Rankl*. Prolactin might act directly to enhance expression of *Rankl* by epithelial cells, which, in turn, stimulates differentiation of epithelial cells following signalling through the cognate receptor RANK expressed on epithelial cells. Alternatively, prolactin might act indirectly through PTHrP. For such an interaction to take place, epithelial–mesenchymal–epithelial signalling would be required to elicit RANKL actions, as *Pthrp* is expressed by epithelial cells, and the gene encoding PTHrP receptor (PTH1R: *Pth1r*) is expressed by mesenchymal cells. Abbreviations: PTHrP, parathyroid hormone-related protein; PTH1R, PTHrP receptor; RANK, receptor activator of nuclear factor κB; RANKL, RANK ligand. *Figure taken from* (Martin and Gillespie, 2001)

1.7 RANK SIGNALLING PATHWAYS IN OSTEOCLASTS

Differentiation and the activation of bone resorption by osteoclasts are complicated processes that involve precise temporal and spatial activation and regulation of cellular events at different levels. A plethora of reports has been published documenting the indispensable role of RANK signalling pathways in the regulation of osteoclasts (Dougall et al., 1999; Teitelbaum, 2000a; Zaidi et al., 2003). The activation of RANK by its ligand, RANKL, triggers the activation of downstream signalling cascades that subsequently leads to the expression of osteoclast specific genes during differentiation, which is the activation of resorption by mature osteoclasts, and their survival and participation in new rounds of bone degradation at neighbouring sites.

The major signal transduction cascades of RANKL have been reported to be crucial for osteoclasts activation and functions. They include the signalling pathways of nuclear factor-kappa B (NF-κB) (Galibert et al., 1998), mitogen-activated protein kinases (MAPKs) (Lee et al., 2002), serine/threonine kinase Akt (Wong et al., 1999a) and nuclear factor of activated T cell (NFAT) (Takayanagi et al., 2002). See Figure 1.5 to view the RANK signaling network in osteoclast.

1.7.1 RANK signalling via NF-κB pathways

RANK mediated NF-κB signalling pathway activity appears to be central for osteoclast differentiation. NF-κB is activated by RANKL both in $RAW_{264.7}$ cells and in monocytes (Hsu et al., 1999a; Jimi et al., 1999a; Lacey et al., 1998a; Wong et al., 1997a), and is required *in vivo* for osteoclast formation (Franzoso et al., 1997a). The importance of NF-κB was demonstrated by the block in osteoclastogenesis in mice deficient in NF-κB proteins p50 and p52 (Iotsova et al., 1997a). In addition, more recent studies indicated that NF-κB p50 and p52 expression are essential for the RANK-expressing osteoclast precursors to differentiate into TRACP+ osteoclasts in response to RANKL and other osteoclastogenic cytokines (Xing et al., 2002).

NF-κB proteins are present in the cytoplasm in association with inhibitory proteins that are known as inhibitors of NF-κB (IκBs). After activation by a large number of inducers, the IκB proteins become phosphorylated and ubiquitinated, and are subsequently degraded by the proteasome. The degradation of IκB allows NF-κB

proteins to translocate to the nucleus and bind their cognate DNA binding sites to regulate the transcription of a large number of down stream target genes (Dixit and Mak, 2002; Mercurio and Manning, 1999).

Over the past decade or so, intensive studies have provided many new insights into the signaling pathways linking ligand/receptor family with NF-κB activation. At the molecular level, the structure and components of NF-κB are highly complex. The core components of NF-κB comprise five mammalian reticuloendotheliosis family (Rel)/nuclear factor κB (NF-κB) proteins that belong to two groups (Joyce et al., 2001; May and Ghosh, 1997). The first group consists of Rel-A (also known as p65), C-Rel and Rel-B, which do not do require proteolytic processing. The second group includes NF-κB_1 (also known as p105) and NF-κB_2 (also known as p100), which are processed to produce the mature p50 and p52 proteins, respectively. These two groups form dimmers.

The most commonly detected NF-κB dimer is p50-Rel-A. Due to the presence of a strong transcriptional activation domain, Rel-A (p65) is responsible for most of NF-κB transcriptional activity. p50-C-Rel dimers are less abundant and seem to be activated with slower kinetics. Both p50-p65 and p50-C-Rel dimers are regulated by interactions with “Inhibitor of NF-κB” (IκB) proteins, which cause their cytoplasmic retention. Rel-B, by contrast, mostly associates with p100 (Solan et al., 2002). The p100-Rel-B dimers are exclusively cytoplasmic. The proteolytic processing of p100 results in the release of p52-Rel-B dimers, which translocate to the nucleus (Solan et al., 2002). Rel-B, unlike p65 and C-Rel, can have both activating and repressing functions (Dixit and Mak, 2002; Mercurio and Manning, 1999).

All NF-κB proteins contain a REL homology domain (RHD) which mediates their dimerization and binding to DNA. The RHD also contains, at its C-terminus, a nuclear localization signal (NLS) and is recognized by the IκB proteins, the binding of which to the RHD interferes with the function of the NLS (Joyce et al., 2001; May and Ghosh, 1997). The IκB proteins include IκBα, IκBβ and IκBε, which TRACP NF-κB dimers in the cytoplasm, and BCL3, which acts as a transcriptional co-activator for p50 and p52 homodimers (May and Ghosh, 1999).

All IκB’s contain 6-7 ankyrin repeats which mediate their binding to RHDs. IκBα,

IκBβ and IκBε each contains an N-terminal regulatory domain, within which there are two conserved serines (SS). The phosphorylation at this site targets the IκB's to ubiquitin-dependent degradation. Lysine residues, is present within the N-terminal regulatory domain. The C-terminal halves of p105 and p100 are similar in sequence, structure and function to the IκB's. Like the latter, the C-terminal portions of p105 and p100 prevent nuclear entry, and are removed by ubiquitin-dependent degradation. While the processing of p105 is constitutive, that of p100 is regulated (Ghosh and Karin, 2002).

The inhibitor of κB (IκB) kinase (IKK) complex is composed of two catalytic subunits, IKKα and IKKβ, and one regulatory subunit, NEMO (IKKγ) (Tegethoff et al., 2003). In response to stimuli such as tumor-necrosis factor-α (TNF-α), interleukin-1 (IL-1) or lipopolysaccharide (LPS), the IKKβ subunit is activated, and phosphorylates the IκB proteins (bound to the NF-κB heterodimers) at two conserved serines. This phosphorylation event triggers the ubiquitin-dependent degradation of IκB by the 26S proteasome, resulting in the nuclear translocation of Rel-A-p50 (or C-Rel-p50) heterodimers and transcriptional activation of target genes. This pathway is designated as the "classical" NF-κB signalling pathway with a bias towards inflammation through NF-κB_1 (Giuliani et al., 2001; Whiteside and Israel, 1997).

In response to the other stimuli, such as the TNF family members, CD40L, lymphotoxin B (LTβ) and BAFF, IKKα is activated to induce the phosphorylation of p100 (bound to Rel-B) at two serine residues at its C-terminus. This phosphorylation event triggers the ubiquitin-dependent degradation of the C-terminal half of p100, releasing its N-terminal half, and the p52 polypeptide, which together with its heterodimer partner, Rel-B, translocates to the nucleus to activate transcription. This pathway has been called "alternative" NF-κB signaling pathway with a bias towards differentiation, architecture and proliferation within the B cell compartment acting mainly through NF-κB_2 (Giuliani et al., 2001; Magnani et al., 2000).

1.7.2 RANK signaling via MAPK pathways

The MAPK pathway is mainly activated by environmental stress and inflammatory cytokines. Its vital roles include cell survival, apoptosis and inflammation (Troen, 2003). Up to date, three major MAPKs have been identified: 1) extracellular signal

regulated kinases (ERK); 2) Jun N-terminal kinases (JNKs); and 3) p38 MAP kinases (Lee and Kim, 2003). The MAP kinase becomes activated through the phosphorylation of threonine and tyrosine residues in response to external stimuli, such as cellular stress, mitogens, reactive oxygen species and cytokines (Abbas et al., 2003; Givant-Horwitz et al., 2003). This is also followed by the translocation of the phosphorylated threonine and tyrosine residues to the nucleus where they activate a large number of transcription factors such as, Activator Protein-1 (AP-1), p53, EIK-1, Ets-1, c-Myc and STATs. These processes result in several biological effects (Liu et al., 2001; Yoshizumi et al., 2004).

The members of all three MAPK families have been well illustrated as activated by RANK in osteoclasts or osteoclast precursors (Lee et al., 2002; Li et al., 2002; Wong et al., 1997a). The involvement of p38 MAPK in osteoclastogenesis was corroborated by studies using p38 inhibitors (Lee et al., 2002; Li et al., 2002). On the other hand, some studies have suggested the critical role of TRAF6 for RANK signalling via the MAPKs, as spleen cells derived from TRAF6-deficient mice failed to activate JNK and p38 in response to RANKL (Kobayashi et al., 2001). In differentiated osteoclasts, the correlation of ERK1/2 activity with cell survival, but not with resorption function, has been reported (Miyazaki et al., 2000).

The JNK1 and JNK2 knockout mice are embryonic lethal due to failure of the closure of the neural tube, and mice are also immunodeficient owing to a defect in T-cell function (David et al., 2002b). JNK has also been reported critical in mediating cell apoptosis (Wong et al., 1997b). A recent study has suggested that JNK1, but not JNK2, is most likely the predominant isoform for efficient osteoclast differentiation. As a target gene disruption study has showed that when osteoclast progenitor cells are derived from $jnk1^{-/-}$, but not from $jnk2^{-/-}$, mice have a reduced potential for RANKL-stimulated osteoclastogenesis (David et al., 2002b).

More lines of evidence are available to establish MKK6 and MKK7 as the upstream targets of JNK in RANK signalling as independent studies have reported that the dominant-negative form of MKK6 and MKK7 suppressed p38 activation and RANKL-dependent osteoclast formation from RAW 264.7 cells respectively (Matsumoto et al., 2000a; Yamamoto et al., 2002). Along the ERK signalling pathway, Raf has been implicated in the activation of the kinase activity with the involvement of

CD40, a TNFR family receptor that shares similar signaling characteristics as RANK (Kashiwada et al., 1998). Moreover, the RANKL induced recruitment of linker molecules TAK1/TAB2 to their upstream partner TRAF6 and the formation of complex between them, is required for JNK and p38 activation (Mizukami et al., 2002).

The downstream targets of ERKs and JNKs include the AP-1 transcription factor, a dimer composed of a Fos family (c-Fos, FosB, Fra-1, and Fra-2) and a Jun family (c-Jun, JunB, and JunD) protein. ERK can induce and activate c-Fos, while JNK can increase AP-1 transcriptional activity through the phosphorylation of c-Jun (Cano and Mahadevan, 1995). The fundamental role of AP-1 in osteoclast development was underscored by the study that showed mice deficient in c-fos developed osteopetrosis due to the failure to commit to osteoclast lineage (Grigoriadis et al., 1994). A study using MITF antibody directed against conserved residue Ser(307), a potential mitogen-activated protein kinase (MAPK) site, has demonstrated that MITF was rapidly and persistently phosphorylated upon the stimulation of primary osteoclasts with RANKL, osteoclast specific gene expression and activation of p38 MAPK, corroborating the transcription factor MITF to be a target of p38 in the RANK signalling pathway in osteoclasts (Mansky et al., 2002).

1.7.3 RANK signalling via PI3K/Akt pathways

In osteoclasts, the RANK mediated activation of PI3K/Akt signaling pathways have been linked with the regulation of cell survival through the activation of multiple targets with anti-apoptotic functions. For instance, RANK induced the activation of Akt which was blocked by the PI3K inhibitor LY294002 and thus, reduced the RANK-mediated survival response of osteoclasts (Lee et al., 2002; Wong et al., 1999a). In addition, the PI3K inhibitor also displayed a potent inhibitory effect on osteoclast differentiation (Lee et al., 2002) which may have resulted from a reduced survival of osteoclast precursor cells during differentiation.

Although the explicit evidence for RANK activation of PI3K is limited, it has been shown in osteoclasts that RANK elevates Src kinase activity and the RANK activation of Akt is blocked by a Src family kinase inhibitor or the genetic deletion of c-Src (Wong et al., 1999a). Thus, the potential regulatory role of Src for the RANK to PI3K/Akt signal has been proposed. Furthermore, PYK2 and c-Cbl, two of the down

stream targets of Src, have also been implicated in osteoclast adhesion signaling and bone resorption function (Duong et al., 1998; Tanaka et al., 1996).

Additionally, the involvement of RANK mediated PI3K/Akt pathways in cytoskeletal organization and the actin filament formation in osteoclasts was suggested from the observation that actin-binding protein gelsolin associated with PI3K (Chellaiah et al., 1998). It is possible that Src and PI3K may function at the point where RANK and adhesion signals converge, transmitting the signals for proper actin cytoskeletal organization that facilitates the resorption activity of osteoclasts.

1.7.4 RANK signalling via calcium signaling pathway

1.7.4.1 NFAT and calcineurin pathways

There is accumulating evidence suggesting that the NFAT signalling transduction cascade is one of the key-regulatory pathways involved in osteoclast differentiation. The transcription factors of the NFAT family, originally discovered in the context of the activation of the immune system (Shaw et al., 1988), are also involved in the function and development of diverse cells in other biological systems, including cardiovascular and musculoskeletal systems in vertebrates, where they are under the control of Ca^{2+}-regulated phosphatase, calcineurin (Berridge et al., 2000).

Recently, NFAT was found to be induced and activated by RANKL during osteoclastogenesis in a TRAF6, c-Fos and calcineurin dependent manner. Surprisingly, the over-expression of NFAT isoforms, NFAT1 or 2 promoted the differentiation of osteoclast precursor cells into multinucleated osteoclast-like cells even in the absence of RANKL (Ikeda et al., 2004). This suggested that the NFAT mediated signal transduction might represent an unconventional signalling pathway that functions in a RANK signalling independent manner in order to regulate osteoclast differentiation. However, further investigations are necessary to clarify the role and importance of this transcriptional factor family in osteoclast physiology.

Calcineurin is well known for its ability to regulate the activity of NFAT family of transcriptional factors. It couples stimulation of the T cell antigen-receptor to changes in the expression of cytokines and other important immunoregulatory genes (Hirotani et al., 2004). Calcineurin in T cells is activated in response to the T cell

receptor-induced increase in the intracellular calcium concentration. Studies have found that calcineurin inhibitors inhibited the RANKL-induced osteoclast formation, thus defining calcineurin as important downstream effector of the RANKL-induced signaling pathway (Hirotani et al., 2004).

1.7.4.2 Calmodulin

Ionic calcium (Ca^{2+}) is a highly versatile intracellular signal that operates to regulate proliferation, differentiation and death in different cell types (Orrenius et al., 2003). In osteoclast lineage cells, cytosolic Ca^{2+} regulates cell adhesion, bone resorptive activity and the organization of the cytoskeleton of osteoclasts (Zaidi et al., 1999a). The extent of cross-talk between Ca^{2+} and receptor activator of NF-κB (RANKL)-mediated intracellular signaling pathways appear to be important in regulating apoptosis or the differentiation of osteoclast lineage cells (Yip et al., 2005).

Calmodulin is a highly conserved 17 kDa protein found ubiquitously throughout animals, plants, fungi and protozoa. It is concentrated at the ruffled border of osteoclast and its expression increases during bone resorption (Seales et al., 2006). Studies have demonstrated that the activation of Ca^{2+}/calmoduline-dependent protein kinase II (CaMKII) is required for calmodulin regulates acid transport in mature osteoclast (Seales et al., 2006).

CamKII is activated in the presence of Ca^{2+} and Calmodulin, resulting in autophosphorylation and subsequently, the generation of a Ca^{2+} / CaM-independent form of the enzyme (Schworer et al., 1986). It is a complex Ca^{2+}/Calmodulin-activated serine/threonine kinase. In addition, it is also well known for its regulation of neural and cardiac development and function (Seales et al., 2006). CaMKII is encoded by four genes (α, β, γ and δ) which can be modified into numerous subunits isoforms by alternate splicing. In particular, the CaMKII-α mutant mice have shown a reduced number of TRACP+ osteoclast in both the tibia and femur. CaMKII was also recently established to be involved in the differentiation of both the osteoclast and osteoblast (Zayzafoon et al., 2005).

Upon Ca^{2+}/calmodulin stimulation, calcineurin dephosphorylates cytoplasmic NFATs, subsequently allowing their translocation and transcriptional activity (Hogan et al.,

2003). The activation of CaMKII leads to the autophophorylation of threonine 286. The phosphorylated CaMKII then modulates the activity of several transcription factors including CREB, ATF, CAAT-enhancer-binding protein β and serum response factor (Zayzafoon et al., 2005). Eventually, the activation of CaMKII and its subsequent downstream signaling cascade is involved in the regulation of a wide range of cellular events which includes proliferation, differentiation and apoptosis.

1.7.5 Protein Kinase C

In the last few decades, protein phosphorylation was widely used for the regulation of cellular processes. It is now clear that kinases and phosphatases are involved in the transmission of signals generated at the cell membrane. Both kinases and phosphatases are also involved in cell morphology and motility, the control of cell cycle as well as many other processes. Based on the amino acid sequence of the kinase domain of protein kinases, the kinase super families are categorized into five large groups. Three of them contain families of kinases that phosporylate substrates on serine or threonine residues. The fourth group contains kinase families that phosphrylate substrates on tyrosine residues and these kinases can be either membrane-spanning or non-membrane-spanning. The last group consists of kinases that are not easy to classify.

Protein Kinase C (PKC) was first identified by Nishzuka and colleagues (Nishizuka, 1984), based upon the ability of cellular Ca^{2+}-activated neutral proteases to cleave the inactive holo-enzyme *in vitro* and hence, derived a catalytically active fragment often referred to as PKM. However, as a physiological means of control, this proteolysis remains a controversial issue. Various laboratories have identified numerous mammalian and non-mammalian PKC groups, giving rise to a large family of polypeptides.

On the basis of overall amino acid sequence similarity, the PKC family has been divided into subfamilies. The first subfamily is usually referred to as the classical PKCs or conventional PKCs (cPKCs) which consists of PKC-α, β1, β2 and γ. The second subfamily is called the novel PKCs (nPKCs) comprising PKC-δ, ε, η, and θ. Finally, the atypical PKCs (aPKCs) consist of PKC-ι, λ and ζ. PKC-related kinases (PRK-1 (PKN) and PRK-2), PKC-μ and dictyostileum discoideum PKC are more distantly

related to the other members of the PKC family.

More specifically, the PKCs isoenzymes are classified according to their activator/cofactor requirements. The conventional PKCs require both Ca^{2+} and diacylglycerol or phorbol esters such as phorbol 12-myristate 13-acetate (PMA) as cofactor. The novel PKCs can be stimulated by diacylglycerol or PMA alone, independent of Ca^{2+}. While the atypical PKCs are independent of both stimuli, the PKC related kinases are structurally different.

1.7.5.1 Domain structure and assembly

The alignment of the various PKC isotypes allows the identification of several highly conserved regions. All PKCs contain a C-terminal catalytic domain and an N-terminal regulatory domain. The catalytic domains show a high degree of homology whereas the regulatory domains are more diverse, providing the basis for the subdivision of the PKC family in the subgroups mentioned earlier. The regulatory domains of the classical PKCs contain two conserved regions, C1 and C2.

The C1 region is identified as the functional site, containing two zinc finger cystein-rich regions, and also the diacylglycerol and phorbol esters binding site. The C2 region contains a calcium-binding sequence which is responsible for the Ca^{2+}-dependent activity in this group. The C1 and C2 regions are also present in nPKCs but the C2 region is located towards the N-terminus. Although the nPKCs has the overall structure of a C2 barrel, it is significantly different from the cPKCs. They lack the Ca^{2+}-binding C2 domain and do not coordinate Ca^{2+}, reflecting its Ca independent property. The aPKCs differ fundamentally from the classical and novel PKCs as they contain neither recognizable C2 region nor C1 region which is structurally different from the typical C1 region as described in classical and novel PKCs. Finally, a catalytic region (C3 and C4 domains), a Ser/Thr-specific protein kinase that binds ATP and pseudosubstrate, is present in all PKCs.

1.7.5.2 Functions of PKCs and its signaling pathways

Protein kinase C has been involved in a wide variety of intracellular signal transduction pathways that regulate cell growth, differentiation, secretion, apoptosis, tumour development as well as in the rearrangement of the sytoskeleton and migration. The

functions of PKC isotypes differ in individual cell types. As the members of the PKC family, the phenotypic characterization of PKC isotype-deficient mice revealed that isotypes may play a role in cellular processes (see Table 1.2).

PKCs reside in the cytosol in an inactive conformation and translocate to the membrane (or other subcellular sites) upon activation where they modify various cellular functions through phosphorylation of target substrate (Brandt et al., 2002). We have first demonstrated that PKCs play a very important role in the modulation of NF-κB pathways which results in the abnormal activation of osteoclast formation (Wang et al., 2003b). To date, the role of individual PKC isoforms in RANKL-induced NF-κB has yet to be determined. Studies have reported that PMA activates several PKC's of the classical and novel subfamilies, and has effects on macrophage differentiation in THP1 cells (Joyce and Steer, 1992).

Table 1.2 Processes in which PKC isotypes have been implicated based upon analysis of PKC-deficient mice.

Isotype	**Function**
PKCα	Insulin receptor feedback
PKCβ	B-cell receptor signalling, feedback regulation
	Mast cell activation
	Neutrophil NADPH oxidase activation
	Glucose transport
	Transcription factor activation in hypoxia
	Fear conditioning
PKCγ	Hippocampal LTP
	Learning, addition, anxiety
	Neuropathic pain
PKCδ	Smooth muscle cell homeostasis/apoptosis
	B-cell tolerance
PKCε	Acute Pain
	Alcohol addiction
	Macrophage actication, host defense
PKCη	
PKCθ	T-cell activation
PKCζ	NF-κB activation
	B-cell recptor signaling
PKCι	

Refer to Dekker, L.V., 2004

1.7.5.2.1 cPKCs and osteoclast differentiation and function

To date, only one group, Rucci *et al*., 2005, has reported the functions of PKCα in osteoclasts and in Chinese hamster ovary (CHO) cells. The integrin $\alpha_v\beta_3$ in osteoclasts recognizes specific bone matrix proteins (i.e. osteopontin and bone sialoprotein II) and is activated by these ligands to provide adhesion, cytoskeletal re-organization and intracellular signaling mandatory for cell survival and cone resorbing activity (Nakamura et al., 1999; Ross et al., 1993). The PKCα isoenzyme is recruited by αvβ3 upon the activation of the signal transduction pathway that is associated with αvβ3, and contributes to the adhesion-dependent ERK 1/2 activation. It does so with a novel mechanism but the only recognized direct ERK1/2 activator, and MAP/ERK Kinase (MEK) 1/2 (Rucci et al., 2005).

The PKCβ generates two isoforms (PKCβI and βII) through alternative splicing of pre-mRNA where the two isoforms are different only in their C-terminal 50 and 52 amino acids, respectively. It has been reported that its functions differ in various cell types. They include: 1) the involvement of PKCβ in cell cycle regulation of vascular smooth muscle cells and insulin-stimulated glucose transport (Chalfant et al., 1996; Yamamoto et al., 2000); 2) mediated phorbol 12-myristate 13-acetate (PMA)-induced interleukin-2 (IL-2) secretion; and 3) lymphocyte function – associated antigen 1-dependent cell movement (Long et al., 2001; Volkov et al., 2001). Furthermore, the disruption of the PKCβ gene led to defects in B-cell responses and consequently, humoral immunity (Leitges et al., 1996).

The cDNA microarray performed by Lee et al., 2003 has shown that the PKCβ gene expression is upregulated during osteoclastogenesis (Lee et al., 2003). This group is the first to report that PKCβ has a functional role in osteoclast differentiation, fusion and resorption activity. They have also stated that PKCβ exert its effects through the regulation of ERK, and not NF-κB signaling pathway.

1.7.5.2.2 nPKCs functions

The different tissue distribution of PKC isoforms combined with the finding that more than one isoform are expressed in a single cell type suggest that each isoform perform a distinct cellular function. Among the PKCs, nPKCs (PKCδ and ε) are most abundantly expressed in R6 rat embryo fibroblasts (Borner et al., 1992). It has also been reported

that the PKCε and PKCδ are highly membrane bounded in R6 rat fibroblasts. Studies by Meldrum *et al*., have shown that nPKCs regulate TNF-αproduction in alveolar macrophages and IL-1 production in both alveolar and peritoneal macrophages (Meldrum et al., 1998).

Other studies have shown that the nPKCs are important regulators of human involucrin (hINV) gene expression during keratinocyte differentiation (Efimova and Eckert, 2000). Involucrin is a precursor of the keratinocyte-cornified envelope and a marker of early keratinocyte differentiation. Recent studies by the same group have discovered that the nPKCs regulate human keratinocyte differentiation by activating a p38δMAP kinase cascade which targets C/enhancer-binding protein α to increase hINV gene expression (Efimova et al., 2002). To date, there have been few reports on the function and mechanism of nPKC in different cell types. Their functions have yet to be discovered in bone biology. Further investigations are required to unveil the distinctive role of novel PKCs.

1.7.5.2.3 aPKCs and its functions in osteoclastogenesis

In the TNFα signaling pathway, it has been reported that the atypical PKCs phosphorylate and activate IKKβ *in vitro* and *in vivo* (Lallena et al., 1999). The blockage of aPKCs by using micro injected pseudosubstrate peptide inhibitors, antisense oligonucleotides or the transfection of kinase-dead dominant-negative mutants of ζPKC or λ/ιPKC dramatically impairs NF-κB activation (Sanz et al., 1999). Collectively, these results reinforce the notion that the aPKCs are important components of the TNFα signaling pathway that controls NF-κB activation, and that the aPKCs are linked to this activation through the interaction of p62 with RIP (Sanz et al., 1999).

Duran et al., 2004 reported that the basal association of an aPKC with p62 in unstimulated RAW cells is dramatically induced upon the addition of RANKL. They have also showed that the RANK pathways promote the formation of TRAF2-p62-aPKCs complex required for NF-κB activation, NFATc1 synthesis and osteoclast differentiation. Since it was suggested that the atypical PKC-interacting protein p62 is an important mediator of RANK-activated osteoclastogenesis, it might be involved in imbalanced pathological bone resorption such as Paget's diease of the

bone (PDB). To date, there have been only few studies on the role/involvement of aPKCs in osteoclast biology. Further investigations and direct approaches are required to ascertain the mechanisms of aPKCs in osteoclastogenesis.

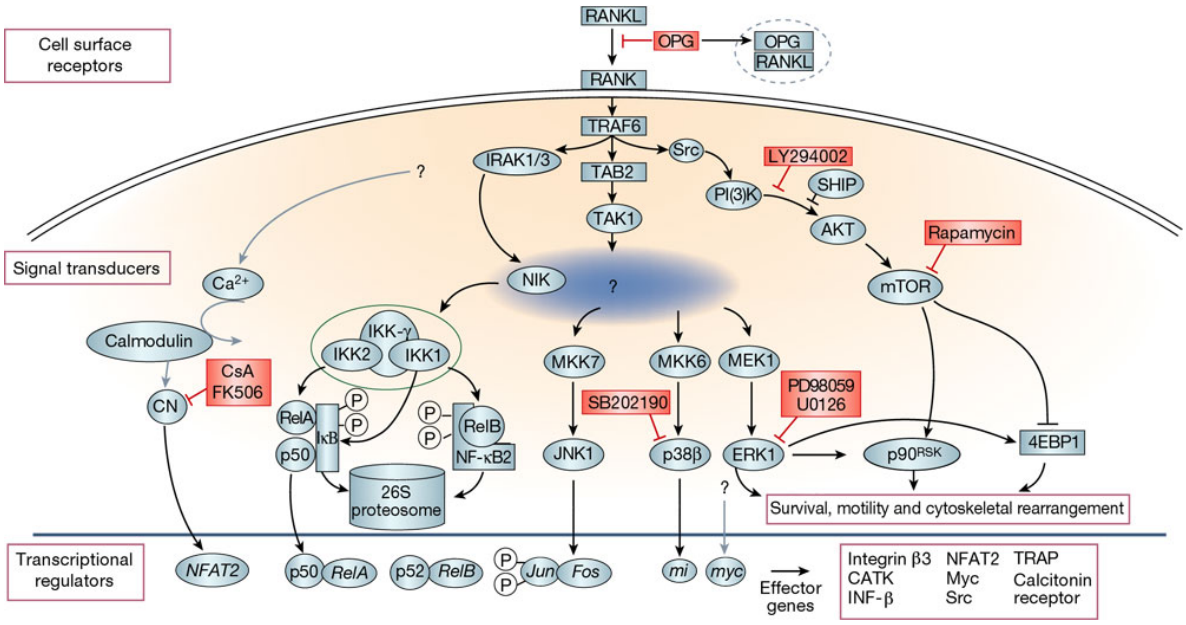

Figure 1.6 RANK signaling network in osteoclast. Proteins with validated effects involved in RANK signal transduction during osteoclast development and activation, arranged in a signalling cascade from the cytoplasmic membrane to nuclear effectors. RANK and OPG are TNFR receptor-related proteins, and RANKL is a TNF-related cytokine that interacts specifically with either RANK or OPG. Protein nodes are shown in representations of their functional annotation, and are connected by edges (arrows or lines) that denote functional associations depicted in the literature. Red bars indicate target of known small-molecule inhibitors. *Figure taken from Boyle et al., 2003.* (Boyle et al., 2003)

1.8 PHARMACOLOGIC AGENTS AND NATURAL INHIBITORS ON OSTEOCLAST FORMATION AND ACTIVATION

A number of pharmacologic agents have been used as inhibitors of bone resorption. They are effective therapies for patients with osteoclast related diseases. These agents inhibit osteoclastic bone resorption, differentiation, activation as well as induce the cells to undergo apoptosis by acting on their respective specific targets. Having said that, some of their mechanisms of action are still remain controversial.

1.8.1 Bisphosphonates (BPs)

Among these agents, bisphosphonate derivatives are one of the most important and commonly used inhibitors of osteoclastic bone resorption *in vivo* that have achieved increasing use in diseases associated with increased bone resorption, particularly osteoporosis, hypercalcemia of malignancy, Paget's disease of bone, prevention of bone metastasis and cancer-induced osteolytic bone disease (Barrett et al., 2004; Dando and Wiseman, 2004).

There are three main groups of BPs: 1) the first-generation compounds (such as clodronate and etidronate) which have been in clinical use for more than 30 years, possess simple substituents attached to the central carbon and exert comparatively weak actions on bone resorption (Rogers et al., 2000); 2) the more potent second-generation BPs (for example, pamidronate, alendronate and ibandronate) which are characterized by an aliphatic side chain containing a single nitrogen atom (N–BPs); (iii) the third-generation N–BPs which are characterized by a heterocyclic substituent, containing one nitrogen atom in a pyridyl ring (risedronate) or two nitrogen atoms in an imidazole ring (zoledronic acid). These are the most potent BPs that are currently available. Together with a recently developed third-generation bisphosphonate, named YH529 or YM529 {1-hydroxy-2-[imidazo (1,2-a) pyridin-3-yl] ethylidene}, they exhibit the strongest bone-resorption-inhibiting action among the currently known BPs (Perry and Figgitt, 2004; Sasaki et al., 1998).

The pharmacokinetic and drug actions of bisphosphonates on osteoclastic bone resorption and apoptosis have been well documented. Unlike their first-generation predecessors which are metabolized into cytotoxic analogues of ATP, N–BPs inhibit the

activity of farnesyl diphosphate (FPP) and geranylgeranyl diphosphate (GGPP) synthases. FPP and GGPP are two key enzymes that are involved in the mevalonate pathway. As both enzymes are required for the post-translational lipid modification (prenylation) of small guanine triphosphatases, such as Ras, Rho and Rac (Gibbs and Oliff, 1997), inhibiting the prenylation of these small intracellular GTPases could account for most, if not all, of the various effects on osteoclast function including 1) the loss of the ruffled border and disruption of the actin cytoskeleton; 2) altered trafficking of membranes and intracellular proteins, such as the osteoclast proton ATPase; 3i) the disruption of integrin-induced intracellular signalling; and 4) the induction of osteoclast apoptosis (Coxon et al., 2000; Rogers et al., 2000).

1.8.2 Antagonist to cytokines and growth factors

In recent years, a number of studies have been performed in search of novel agents for the control of osteoclast formation and activity. They can be categorized into different subclasses according to their specific targets in osteoclasts. To begin with, there are inhibitors that are designed to antagonize the effects of osteoclastogenic cytokines and factors. Inhibitors in this class include recombinant osteoprotegerin (Fc.OPG) and monoclonal antibodies against RANK and RANKL. They neutralize the effect of RANKL and prevent the activation of RANKL-induced signalling pathways.

Studies have shown that RANKL blockade (using OPG or RANK fusion proteins or RANKL antibodies) prevents bone loss caused by osteoporosis, chronic inflammatory disorders and malignant tumours in animal models. For instance, a high-affinity and specific fully human monoclonal antibody to RANKL or AM162, in postmenopausal women with low lumbar spine BMW, significantly increased these women’s lumbar spine BMD within one month of treatment (McClung et al., 2004). This suggests the possibility of the use of these inhibitors as a therapy in humans based on studies in postmenopausal osteoporosis, myeloma bone disease and osteolytic metastases (Croucher et al., 2003; Hofbauer and Schoppet, 2004; Romas et al., 2002). In addition, some studies have also demonstrated the therapeutic potential of using IL-1 receptors antagonists in the treatment of osteoporosis, debris-induced osteolysis and rheumatoid arthritis (Abramson and Pecht, 2002; Yang et al., 2004).

1.8.3 Inhibitors of signalling transduction of osteoclast

There has been more evidence demonstrating the significant role of NF-κB signalling pathway in osteoclast differentiation and functions (Andela et al., 2003; Clohisy et al., 2004; Teitelbaum, 2000a). Many of the synthetic and natural NF-κB inhibitors have been reported which target different molecular targets along the NF-κB signalling pathway, for instance, synthetic cell-permeable peptide inhibitor of the Iκ-B kinase complex, a crucial component of signal transduction pathways to NF-κB inhibited RANKL-stimulated NF-κB activation and osteoclastogenesis both *in vitro* and *in vivo* (Jimi et al., 2004). On the other hand, a number of natural compounds including curcumin (diferuloylmethane), a pigment derived from turmeric (Bharti et al., 2004); flavonoids; micronutrients widely present in food of plant origin (Wattel et al., 2004); as well as parthenolide, a major constituent of the medicinal plant feverfew (Yip et al., 2004), have recently been found to be capable of inhibiting NF-κB activation, osteoclast function and formation. Thus, these findings suggest that the blockage of NF-κB signalling pathways offers an effective treatment approach for osteoclast related bone disorders.

The NFAT signal transduction pathways have recently attracted much attention owing to its role in osteoclast differentiation. Yoneda T. et al recent findings on NFAT have manifested the significance of this transcriptional factor in osteoclast. They reported that the over-expression of NFAT1 (NFATc2/NFATp) or NFAT2 (NFATc1/NFATc) promoted the differentiation of osteoclast precursor cells into tartrate-resistant acid phosphatase-positive (TRACP-positive) multinucleated osteoclast-like cells even in the absence of RANKL (Ikeda et al., 2004). While calcineurin is the key meditator of NFAT signalling pathways, both cyclosporine A and FK506 are known to suppress the activity of calcineurin. The selective inhibition of calcineurin by cyclosporine A and FK506 has been linked to the inhibition of bone marrow derived osteoclast formation through the induction of apoptosis (Igarashi et al., 2004).

A similar result has been reported in other culture systems as RANKL-induced differentiation of RAW264.7 to multinucleated osteoclasts was significantly affected by cyclosporine A and FK506 treatment (Hirotani et al., 2004). For instance, c-Src, a proto-oncogen, plays an important role in the signal transduction pathway for the activation of quiescent osteoclasts to become bone-resorbing osteoclasts. As for

animals lacking c-Src gene, the osteoclast formation is normal. However, they develop osteopetrosis because the c-Src -/- osteoclasts are unable to form ruffled borders (Boyce et al., 1992) and resorb bone (Soriano et al., 1991). In addition, it has been suggested that c-Src might act as an adaptor molecule, recruiting other proteins that are necessary for the modulation of integrin-cytoskeletal links, cell attachment and migration in osteoclast (Miyazaki et al., 2004). These animals can be rescued by the transplantation of normal hematopoietic precursors from animals expressing c-Src (Lowe et al., 1993).

Recent studies have demonstrated that selective c-Src inhibitors, including herbimycin A, USC15A, AP-22408 and AP23236, potently inhibit osteoclast bone resorption activity. Despite all these inhibitors' functions to inhibit osteoclastic bone resorption, different molecular mechanisms for their actions have been suggested. First, herbimycin A inhibits c-src tyrosine kinase activity by destabilizing src through interference with Hsp90 (Yoneda et al., 1993). Second, UCS15A does not inhibit Src tyrosine kinase activity. Instead, it disrupts the interaction of proteins associated with Src, hence modulating downstream events in the Src signal transduction pathway (Sharma et al., 2001). Third, AP-22408 and AP-23236 do so by virtue of blocking Src-dependent non-catalytic or catalytic activities in osteoclasts (Shakespeare et al., 2003). Collectively, the pharmacological intervention using selective c-Src inhibitors has been shown to be an effective approach to inhibit osteoclast function.

The other major class of inhibitors are those primarily functioning to inhibit osteoclastic bone resorption. First of all, alpha(v)beta(3) integrin is abundantly expressed in osteoclasts and has been implicated in playing a role in regulating the two processes required for effective osteoclastic bone resorption: cell migration and maintenance of the sealing zone in a RGD-dependent manner (Nakamura et al., 1999). Inhibitors such as echistatin have been shown to inhibit osteoclastic bone resorption potently. The RGD-containing disintegrin echistatin, a snake venom peptide of 49 amino acids isolated from the saw-scaled viper Echis carinatus, was previously reported to inhibit bone resorption *in vitro* (Sato et al., 1990) and *in vivo* (Fisher et al., 1993). Moreover, echistatin has recently been found to inhibit bone resorption *in vivo* in estrogen-deficient mice and rats (Yamamoto et al., 1998), and in mice with secondary hyperparathyroidism (Masarachia et al., 1998).

In addition, echistatin has also been suggested to inhibit the migration of multinucleated osteoclast by antagonizing the function of alpha(v)beta(3) (Carron et al., 2000). Furthermore, an orally bioavailable, nonpeptide RGD mimetic alpha(v)beta(3) antagonist, SB 265123, has been shown to prevent bone loss *in vivo* when dosed by oral administration (Lark et al., 1999).

1.8.4 Proton pump inhibitors

There are other subclasses of inhibitors that suppress osteoclastic bone resorption via targeting the vacuolar ATPases (V-ATPases) of osteoclast. V-ATPases are ATP-dependent proton pumps which are highly expressed in the ruffled border membranes. Their function is to acidify the resorption lacunae (Blair et al., 1989). Thus, the plasma membrane V-ATPase of osteoclasts (osteoclast V-ATPase) is thought to be a good molecular target for reducing osteoclast activity. A number of inhibitors targeting the osteoclasts V-ATPase have been proposed, including bafilomycin A1 (Xu et al., 2003) and its derivative SB242784 (Farina and Gagliardi, 2002), as well as recently identified inhibitor FR167356 which is available for oral administration (Niikura et al., 2004).

All of them have showed inhibitory effects on bone resorption. V-ATPase is not only localized in the plasma membranes of osteoclasts but also the plasma membranes of renal intercalated cells and macrophages. Moreover, V-ATPases are also present on ubiquitous intracellular acidic compartment such as lysosomes, endosomes, the Golgi apparatus and secretory vesicles, and are responsible for their acidification (Nishi and Forgac, 2002). Even though bafilomycin A1 significantly suppressed the osteoclastic bone resorption in-vitro, the former equally inhibits all these V-ATPase activities leading to systemically undesirable alteration of cellular physiology when administered to animals. The characteristics of bafilomycin A1 suggested/showed that it is not suitable for therapeutic application.

Recently, FR167356 was synthesized through random screening using/with osteoclast microsomes. It exerted higher selective action on osteoclast-V-ATPase among the same class of inhibitors. Furthermore, it inhibited not only H^+ transport activity of osteoclast V-ATPase but also H^+ extrusion from cytoplasm of osteoclasts which depends on the V-ATPase activity. FR167356 also showed inhibitory effects on other V-ATPases like

renal brush border V-ATPase, macrophage microsome V-ATPase and lysosomal V-ATPase. Particularly, its inhibiting effect was approximately seven-fold less potent in lysosomal V-ATPase compared to osteoclast V-ATPase.

In addition, the LDL metabolism in cells, which depends on the acidification of lysosome, was blocked merely at higher concentration than bone resorption. This suggested that FR167356 inhibits V-ATPase of osteoclast ruffled border membrane still more selectively than lysosome at the cellular level (Niikura et al., 2004). The selective inhibition characteristic of osteoclast V-ATPase might indicate an effective approach for the control of osteoclast activity. Having said that, more clinical trials might demonstrate whether they have significant advantages over other inhibitors of bone resorption for the treatment of osteoclast related diseases.

1.8.5 Antagonist of bone resorbing enzymes

There are the other types of agents that target to interfere with the osteoclast bone matrix degradation process. The cysteine protease, cathepsin K, which has high proteolytic activity and localizes primarily in osteoclasts, has been demonstrated to take part in the degradation of organic bone matrix in osteoclasts (Troen, 2004). It has been shown that the Cathepsin K inhibitors potently suppressed osteoclastic bone resorption *in-vitro* and *in-vivo*.

For instance, SB331750 prevented bone resorption *in vivo* and this inhibition resulted in the prevention of ovariectomy-induced loss in trabecular structure (Lark et al., 2002). In addition, agents including 1-Cyanopyrrolidine (Falgueyret et al., 2001), azepanone-based cathepsin K inhibitor (Marquis et al., 2001) and SB357114 (Stroup et al., 2001) with their selective cathepsin K inhibitory actions, suppressed osteoclastic bone resorption.

Finally but not least, another factor involved in tissue destruction is matrix metalloproteinase 9 (MMP-9), a member of the MMP gene family. It is produced by osteoclasts in human bone tissues and has been suggested as being capable of degrading bone collagens in concert with MMP-1 and cysteine proteinases in the subosteoclastic microenvironment (Okada et al., 1995). Agents such as CT435 (Hill et al., 1994b), function/act to diminish the effect of MMPs and have been shown to

effectively inhibit bone resorption. Collectively, these studies suggesting/exhibiting the inhibition of osteoclast bone matrix degradation process may prove to be a viable approach to the treatment of bone diseases.

CHAPTER 2

Hypothesis and Statement of Aims

CHAPTER 2– HYPOTHESIS AND STATEMENT OF AIMS

2.1 RATIONALE

Bone remodeling is strictly regulated by osteoclast-mediated bone resorption and osteoblast-mediated bone formation. The excessive formation and activity of osteoclasts are the hallmark of common bone lytic disorders like osteoporosis, Paget's disease, osteoarthritis and tumour-mediated osteolysis. The osteoclast-mediated bone resorption is highly regulated by multi-faceted processes that include rapid biosynthesis, hormonal and cytokine-induced activation of signaling pathways, rapid trafficking of proteolytic enzymes as well as the transportation of degraded bone substances to and away from the resorptive sites. All processes involved in osteoclastogenesis as well as survival and activities of osteoclast are crucial for their physiology. Receptor Activator of NF-κB Ligand (RANKL) is the key cytokine for osteoclastogenesis and osteoclast activity. It requires interaction with its cognate receptor called Receptor Activator of NF-κB (RANK) for functional binding and biological pathways activation. Although the crystal structures of RANKL (Lam et al., 2001b) have been proposed, the functional binding sites for the biological pathways activation still remain unclear. The interaction of RANKL and RANK triggers the activation of many major signaling pathways like the NF-κB, NFAT, MAPK and PI3 kinase signal transduction pathways. Even though osteoclast signaling pathways have been studied extensively, the signaling cascades and molecules involved in the osteoclast differentiation and function are yet to be elucidated.

In order to study the functional binding of RANKL to RANK for osteoclast differentiation and function and their biological pathway activations, the extracellular and intracellular mechanisms were investigated sequentially. The inhibition of extracellular and intracellular mechanisms is the explicit approach for determining the mechanisms involved in RANKL-induced osteoclastogenesis. It is believed that a better understanding of the RANKL-RANK interaction and their signaling pathways will provide a new therapeutic development for the treatment of osteoclast-related diseases.

2.2 HYPOTHESIS AND AIMS

First of all, four truncation mutants of RANKL were generated in this study. Their bindings to RANK and modulations to RANK-signal transduction pathways were to be determined. The identification of inhibitors to RANKL and its signaling pathways might facilitate the design of strategies to treat a wide range of debilitating clinical bone disorders. The hypothesis testing and the aims of the study are as follow:

Hypothesis 1

"RANKL mutants act as antagonists which would bind to RANK and inhibit osteoclast formation and bone resorption. These may be of potential therapeutic value for the treatment of bone lytic disorders."

Aims

To examine:

1) the effect(s) of RANKL mutants on osteoclast formation and bone resorption.
2) the capacity of RANKL mutants to interact with their cognate receptor RANK.
3) whether RANKL mutants act as competitive inhibitors of wild type RANKL.
4) the effect(s) of RANKL mutants on the activation of crucial osteoclast signaling pathways (such as NF-κB, JNK and ERK).

Secondly, to continue studying the regulation of osteoclasts, the response of osteoclast to the extracellular calcium level became one of our interests as osteoclasts are exposed to high Ca^{2+} concentrations during bone resorption. Moreover, the role of RANKL in osteoclast tolerance to elevated extracellular Ca^{2+} and the effect of high extracellular Ca^{2+} on RANKL-induced signaling pathways have, however, not been determined.

Hypothesis 2

"RANKL enhances osteoclast tolerance to high extracellular Ca^{2+} by protecting cells from cell death. The cross-talk mechanism of extracellular Ca^{2+} on osteoclast survival is through the regulation of RANKL."

Aims

1) To examine the relationship between RANKL and high extracellular Ca^{2+} in the regulation of osteoclast survival.
2) To examine the effect of high extracellular Ca^{2+} on RANKL-induced major signaling pathways like the NF-κB, JNK and ERK signalings.

The establishment of a link between Ca^{2+} and regulation of osteoclast in our lab has promoted us to examine the role of PKC, a Ca^{2+}-mediated signaling pathways in osteoclastogenesis. In this study, we have employed several PKC mediators to study the RANKL-induced osteoclastogenesis, osteoclast activities and their signaling pathways. The compounds used in this study include a protein kinase C (PKC) activator named **12-*O*-tetradecanoylphorbol-13-acetate (TPA)**, two general PKC inhibitors named **GÖ 6976** and **GF 109203X**, and selective PKCδ inhibitor and activator called **Rottlerin** and **Bryostatin 1,** respectively.

Hypothesis 3

"12-O-tetradecanoylphorbol-13-acetate (TPA) inhibits osteoclastogenesis by suppressing the RANKL-induced activation of major signaling pathways."

Aims

1) To investigate the effects of TPA on RANKL-induced osteoclastogenesis.
2) To examine the effect of TPA on RANKL-induced NF-κB, JNK, p38 and ERK activation and therefore, determine the inhibitory mechanisms of TPA in relation to these major signaling pathways.

Hypothesis 4

"The selective inhibition of Protein kinase C (PKC) by GÖ 6976 and GF 109203X suppresses osteoclast differentiation and bone resorption, and induces apoptotic cell death via the modulation of RANKL signaling pathways."

Aims

1) To investigate the effects of GÖ 6976 and GF 109203X on RANKL-induced osteoclastogenesis.
2) To examine the effects of GÖ 6976 and GF 109203X on mature osteoclasts and bone resorption by $RAW_{264.7}$ cells and giant cell tumour-derived osteoclast-like cells.
3) To investigate the effects of GÖ 6976 and GF 109203X on RANKL-induced signaling pathways like NF-κB, ERK, and NFAT.

Hypothesis 5

"The selective PKC δ inhibitor and activator, Rottlerin and Bryostatin 1 respectively, modulate osteoclast differentiation and bone resorption via the regulation of major RANKL-induced signaling pathways."

Aims

1) To determine the effects of Rottlerin and Bryostatin 1 on RANKL-induced osteoclast differentiation and LPS-induced osteolysis model.
2) To investigate the effects of Rottlerin and Bryostatin 1 on bone resorption mediated $RAW_{264.7}$ cells and giant cell tumour-derived osteoclast-like cells.
3) To examine the effects of Rottlerin and Bryostatin 1 on RANKL-induced signaling pathways activation

CHAPTER 3

Materials and Methods

CHAPTER 3– MATERIALS AND METHODS

3.1 MATERIALS

3.1.1 Cell lines

CELL LINE	*DESCRIPTION*	*SUPPLIER*
• RAW 264.7 (Subclone C4)	*Mouse myeloid/monocytes*	*Kindly provided by Dr A.I. Cassady, Centre for Molecular and Cellular Biology, Department of Biochemistry, University of Queensland.*
• *COS-7*	*African green monkey kidney, Simian CV-1 fibroblast-like cells*	*Gift from Dr Karen Kroeger, West Australian Institute for Medical Research, Western Australia*

3.1.2 Bacterial and yeast strains

STRAIN	GENOTYPE / DESCRIPTION	SUPPLIER
• DH5 α		
• *E. coli* XL-1 BLUE	*SupE44hsdRI7recA1, endA1 gyrA46thire 1A11ac^{-}F, [proAB^{+} lacIq1acZΔ M15Tn10(tet^{r})]* cDNA insert cloning host, propagation of plasmid DNA	Dr DJ Chang, Department of Microbiology, The University of Western Australia
• *E. coli* BL21 (DE3)	*F^{-}, omp T, hsdS$_B$, (r$_B^{-}$, m$_B^{-}$), dcm, gal, λ (DE3)* Prokaryotic expression host for recombinant polypeptides	EMD Biosciences, Inc. (Novagen), San Diego, CA, USA

3.1.3 General reagents and biochemicals

All chemical reagents used in the experiments outlined in this thesis were of analytical (Anala®) or biochemical grade, unless otherwise indicated and were purchased from following manufacturers:

DESCRIPTION	SUPPLIER
• Acrylamide (99.9%)	Bio-Rad Laboratories, Hercules, CA., USA
• Agarose	Promega Corp., Madison, Wi., USA
• Agar powder	BDH Laboratory Supplies, Poole, Dorset, England
• Amino Acids (L-Arginine, L-Aspartic acid, L-adenine hemi-sulphate salt, L-Isoleucine, L-Histidine HCl monohydrate, L-Leucine, L-Lysine, L-Methionine, L-phenyl-alanine, L-Proline, L-Threonine, L-Tryptophan, L-Tyrosine, L-Uracil, L-Valine)	Sigma Chemical Co., St Louis, Mo., USA
• 3-aminopropyltriethoxy-saline	Sigma Chemical Co., St Louis, Mo., USA
• Ammonium persulfate	Bio-Rad Laboratories, Hercules, CA., USA
• Ampicillin	Sigma Chemical Co., St Louis, Mo., USA
• Adenosine triphosphate (ATP)	Sigma Chemical Co., St Louis, Mo., USA
• Bacto yeast extract	Difco Laboratories, Detroit, Michigan, USA
• Bacto peptone tryptone	Difco Laboratories, Detroit, Michigan, USA
• Bafilomycin A	Sigma Chemical Co., St Louis, Mo., USA
• Bis (N, N', Methylene-bis-acrylamide)	Bio-Rad Laboratories, Hercules, CA., USA
• Bovine serum albumin (BSA)	Sigma Chemical Co., St Louis, Mo., USA
• Bradford reagent	Bio-Rad Laboratories, Hercules, CA., USA
• Brefeldin A	Sigma Chemical Co., St Louis, Mo., USA
• Bromophenol blue	Sigma Chemical Co., St Louis, Mo., USA
• Calcium chloride ($CaCl_2$)	Sigma Chemical Co., St Louis, Mo., USA
• Cell Dissociation Buffer	Sigma Chemical Co., St Louis, Mo., USA
• Chlorobutanol (1,1,1-trichlroro-2-methyl-2-propanol)	Sigma Chemical Co., St Louis, Mo., USA
• Chloroform	BDH Laboratory Supplies, Poole, Dorset, England
• Coelenterazine H	Sigma Chemical Co., St Louis, Mo., USA
• Coomassie® brilliant Blue R-250	Bio-Rad Laboratories, Hercules, CA., USA
• Cytochalasin D	Sigma Chemical Co., St Louis, Mo., USA
• Cycloheximide	Sigma Chemical Co., St Louis, Mo., USA
• dATP, dCTP, dGTP, dTTP nucleotides	Promega Corp., Madison, Wi., USA
• DePeX mounting medium	BDH Laboratory Supplies, Poole, Dorset, England
• Diethyl pyrocarbonate (DEPC)	Sigma Chemical Co., St Louis, Mo., USA
• Dimethyl sulphoxide (DMSO)	BDH Laboratory Supplies, Poole, Dorset, England
• Dithiothreitol (DTT)	Sigma Chemical Co., St Louis, Mo., USA
• Ethanol (100%)	BDH Laboratory Supplies, Poole, Dorset, England
• Ethidium bromide (2,7-diamino-10-ethyl-ni9-phenylphenanthridium bromide; homidium bromide)	Sigma Chemical Co., St Louis, Mo., USA

• Ethylene tetra-acetic acid (EDTA) Disodium	Boehringer Mannheim Corp., Indpl, IN, USA
• Glacial acetic acid	BDH Laboratory Supplies, Poole, Dorset, England
• Glutaraldehyde	Merck, Darmstadt, Germany
• Glycerol	BDH Laboratory Supplies, Poole, Dorset, England
• Glycine	BDH Laboratory Supplies, Poole, Dorset, England
• Glutathione Sepharose™ 4B	Amersham Life Science, Amersham Place, Little Chalfont, Buckinghamshire, UK
• Guanosine diphosphate (GDP)	Sigma Chemical Co., St Louis, Mo., USA
• HEPES	Sigma Chemical Co., St Louis, Mo., USA
• Hydrochloric acid (HCl)	BDH Laboratory Supplies, Poole, Dorset, England
• Isopropanol (Propan-2-ol)	BDH Laboratory Supplies, Poole, Dorset, England
• ITPG, dioxane-free (isopropyl-β-thiogalactopyranoside)	Promega Corp., Madison, Wi., USA
• Lithium acetate	BDH Laboratory Supplies, Poole, Dorset, England
• β-Mercaptoethanol	Sigma Chemical Co., St Louis, Mo., USA
• Methanol	BDH Laboratory Supplies, Poole, Dorset, England
• Monensin sodium	Sigma Chemical Co., St Louis, Mo., USA
• Nitro-blue tetrazolium (NBT)/ 5-bromo-4-chloro-3-indolyl-phosphate (BCIP)	Boehringer Mannheim, Germany
• Nonidet® P 40 Substitute (Nonylphenylpolyethylene glycol) NP-40	Fluka Chemie AG., Sigma Chemical Co., St Louis, Mo., USA
• Nocodazole	Sigma Chemical Co., St Louis, Mo., USA
• Paraformaldehyde	Merck, Darmstadt, Germany
• Phenol red	Sigma Chemical Co., St Louis, Mo., USA
• Phosphoric acid	BDH Laboratory Supplies, Poole, Dorset, England
• PMSF (Phenylmethylsulfonyl fluoride)	Boehringer Mannheim Corp., Indpl, IN, USA
• Polyethylene glycol (PEG)	Sigma Chemical Co., St Louis, Mo., USA
• Poly-L-lysine	Sigma Chemical Co., St Louis, Mo., USA
• Polyvinyl alcohol (PVA)	Sigma Chemical Co., St Louis, Mo., USA
• Rapid-hyb buffer	Amersham Life Science, Amersham Place, Little Chalfont, Buckinghamshire, UK
• RNA sample loading buffer	Sigma Chemical Co., St Louis, Mo., USA
• RNAzol^{TM} (B)	Tel-Test Inc., Friendswood, TX., USA
• Salmon sperm DNA	Sigma Chemical Co., St Louis, Mo., USA
• Sodium acetate	BDH Laboratory Supplies, Poole, Dorset, England
• Sodium azide	BDH Laboratory Supplies, Poole, Dorset, England
• Sodium bicarbonate	Sigma Chemical Co., St Louis, Mo., USA
• Sodium cadcolyate	SPI Supplies, West Chester, PA, USA
• Sodium carbonate	Sigma Chemical Co., St Louis, Mo., USA
• Sodium chloride (NaCl)	BDH Laboratory Supplies, Poole, Dorset, England
• Sodium citrate	Sigma Chemical Co., St Louis, Mo., USA

• Sodium deoxycholate	BDH Laboratory Supplies, Poole, Dorset, England
• Sodium diphosphate	BDH Laboratory Supplies, Poole, Dorset, England
• Sodium dodecyl sulphate (SDS)	BDH Laboratory Supplies, Poole, Dorset, England
• Sodium hydroxide (NaOH)	BDH Laboratory Supplies, Poole, Dorset, England
• Sodium phosphate, dibasic, anhydrous (Na_2HPO_4)	Sigma Chemical Co., St Louis, Mo., USA
• Sodium phosphate, monobasic, anhydrous (NaH_2PO_4)	Sigma Chemical Co., St Louis, Mo., USA
• TEMED (N, N, N`, N`-Tetra-methyl-ethylenediamine)	Bio-Rad Laboratories, Hercules, CA., USA
• Thiamine hydrochloride	Sigma Chemical Co., St Louis, Mo., USA
• Tris (Tris (hydroxymethyl) aminomethane)	Boehringer Mannheim Corp., Indpl, IN, USA
• Tris (hydroxymethyl) methane	BDH Laboratory Supplies, Poole, Dorset, England
• Tri-sodium citrate	BDH Laboratory Supplies, Poole, Dorset, England
• Triton X-100 (Iso-octylphenoxypolyethoxyethanol)	Packard Instrument International, SA., Zurich, Switzerland
• Triton X-114	Sigma Chemical Co., St Louis, Mo., USA
• Tween-20	Sigma Chemical Co., St Louis, Mo., USA
• X-Gal	Sigma Chemical Co., St Louis, Mo., USA
• Xylene cyanol	Sigma Chemical Co., St Louis, Mo., USA

3.1.4 Tissue Culture Reagents

DESCRIPTION	SUPPLIER
• α-MEM (alpha-Modification of Eagles Medium)	TRACE, Sydney, Australia
• D-MEM (Diubcos-Modification of Eagles Medium)	TRACE, Sydney, Australia
• Foetal calf serum (FCS)	TRACE, Sydney, Australia
• Foetal horse serum (FHS)	TRACE, Sydney, Australia
• Ficoll-Paque Plus	Amersham Life Science, Amersham Place, Little Chalfont, Buckinghamshire, UK
• Geneticin (G418)	Gibco BRL, Life Technologies, Melbourne, Australia
• L-Glutamine	Gibco BRL, Life Technologies, Melbourne, Australia
• Penicillin-Streptomycin	Gibco BRL, Life Technologies, Melbourne, Australia
• Trypsin-EDTA (pH 7)	Gibco BRL, Life Technologies, Melbourne, Australia

3.1.5 Enzymes

DESCRIPTION	SUPPLIER
• Calf Intestinal Alkaline Phosphatase (CIAP)	Promega Corp., Madison, Wi., USA
• Moloney Murine Leukaemia Virus (MMLV) reverse transcriptase	Promega Corp., Madison, Wi., USA
• Pepstatin A (Isovalery-Val-Val-Sta-Ala-Sta)	Sigma Chemical Co., St Louis, Mo., USA
• Proteinase K	Promega Corp., Madison, Wi., USA
• Restriction Enzymes (Bam H1, Bgl II, EcoR1, Hind III, PstI, Sal I, Xba I and Xho I)	Promega Corp., Madison, Wi., USA
• RNAse H	Promega Corp., Madison, Wi., USA
• RNAsin	Promega Corp., Madison, Wi., USA
• *Taq* DNA Polymerase	Promega Corp., Madison, Wi., USA

3.1.6 Cytokines and Steroids

DESCRIPTION	SUPPLIER
• Vitamin D_3 [1,25$(OH)_2D_3$]	Calbiochem-Novabiochem, Alexandria, Australia
• Dexamethasone	Sigma Chemical Co., St Louis, Mo., USA
• Recombinant human M-CSF	R&D systems, Minneapolis, USA
• Recombinant GST-rat RANKL	Readily available in our Laboratory (Xu et al., 2000c)
• Recombinant GST-mouse RANKL	Generous gift from A/Prof F.P. Ross, Department of Pathology, Washington University School of Medicine, St. Louis, Missouri, USA (Lam et al., 2000)

3.1.7 Antibodies

DESCRIPTION	SUPPLIER
• BD Living Colours A.V. Peptide Antibody (GFP-antibody), (Rabbit)	Clontech, Laboratories Inc.
• Polyclonal anti-EEA-1 (Rabbit)	Santa Cruz Biotechnology Inc.
• Monoclonal anti-pERK	Santa Cruz Biotechnology Inc.
• Polyclonal anti-IκBα (Rabbit)	Santa Cruz Biotechnology Inc.
• Monoclonal anti-NFATc1 (mouse)	Santa Cruz Biotechnology Inc.
• Anti-p38	Cell Signaling
• Monoclonal anti-c-Src (mouse)	Santa Cruz Biotechnology Inc.
• Monoclonal anti-β-Tubulin	Sigma Chemical Co., St Louis, Mo., USA
• Polyclonal anti-β-Tubulin (Sheep)	Sigma Chemical Co., St Louis, Mo., USA
• Monoclonal anti-FLAG® (M2)	Sigma Chemical Co., St Louis, Mo., USA
• Monoclonal anti-p58K	Sigma Chemical Co., St Louis, Mo., USA
• Alexa Fluor® 488 goat anti-Chicken IgG	Molecular Probes, Inc, Eugene
• Alexa Fluor® 488 goat anti-Rabbit IgG	Molecular Probes, Inc, Eugene
• Polyclonal HRP-conjugated anti-mouse IgG (Goat)	Amersham Life Science, Amersham Place, Little Chalfont, Buckinghamshire, UK
• Polyclonal HRP-conjugated anti-Rabbit IgG (Goat)	Amersham Life Science, Amersham Place, Little Chalfont, Buckinghamshire, UK
• Polyclonal Rhodamine-conjugated anti-Phalloidin	Molecular probes, Eugene, Oregon, USA

3.1.8 Pharmacological compounds

DESCRIPTION	SUPPLIER
• Bryostatin 1	Sigma Chemical Co., St Louis, Mo., USA
• Rottlerin	Sigma Chemical Co., St Louis, Mo., USA
• GF 109203X	Sigma Chemical Co., St Louis, Mo., USA
• Gö 6976	Sigma Chemical Co., St Louis, Mo., USA
• TPA (12-0-tetradecanoyl phorbol-13-acetate)	Sigma Chemical Co., St Louis, Mo., USA

3.1.9 Vectors

DESCRIPTION	SUPPLIER
• p3kB-Luc	Clontech, Laboratories Inc
• pNFAT-Luc	Clontech, Laboratories Inc
• pFlag-RANK	Generated in our laboratory

3.1.10 Fluorescent probes

DESCRIPTION	SUPPLIER
• Transferrin, Alexa Fluor® 546 conjugate	Molecular Probes, Inc, Eugene
• Alexa Fluor® 488 conjugate	Molecular Probes, Inc, Eugene
• Dextran, Rhodamine-B, 10,000 MW	Molecular Probes, Inc, Eugene
• Hoechst dye	Molecular Probes, Inc, Eugene

3.1.11 Radioisotopes

DESCRIPTION	SUPPLIER
• [γ^{36}P] ATP (3000 Ci/mmol)	Amersham Life Science, Amersham Place, Little Chalfont, Buckinghamshire, UK

3.1.12 Commercially purchased kits and systems

DESCRIPTION	SUPPLIER
• Qiagen™ Gel Extraction Kit	GeneWorks Pty Ltd, Australia
• Digoxigenin (DIG) RNA Labelling Kit	Boehringer Mannheim, Germany
• DYNABEADS® mRNA purification kit	DYNAL® Inc., USA

• ECL+Plus Lumigen™ PS – 3 Detection Reagent	Amersham Life Science, Australia
• Gel Drying Kit	Promega Corp., Madison, Wi., USA
• TOPO® TA Cloning® Kit	Invitrogen, Australia
• PGEM-T Cloning Kit	Promega Corp., Madison, Wi, USA
• RETROscript™ first strand synthesis kit	Ambion INC, USA
• One Shot™ TOP10 F' Competent Cells	Invitrogen, Australia
• Taq DNA polymerase kit	Promega Corp., Madison, Wi, USA
• Terminal Transferase kit	Boehringer Mannheim, Germany
• Leukocyte Acid Phosphatase (TRACP) Kit	Sigma Chemical Co., St Louis, Mo., USA
• Wizard® Plus SV Minipreps DNA Purification System	Promega Corp., Madison, Wi, USA
• Wizard® Plus SV Midipreps DNA Purification System	Promega Corp., Madison, Wi, USA
• PolyFect® Transfection Reagent	QIAGEN, Aus

3.1.13 Oligonucleotide Primers

Oligonucleotide primers for use in PCR and sequencing reactions were purchased from the following manufacturers: Bresatec Ltd, Pacific oligos (Australia) and Geneworks, Australia. Upon receipt of lyophilised oligos, they were resuspended in Baxter ddH_20 accordingly and stored at –20°C in a constant temperature freezer.

3.1.14 Other Materials

DESCRIPTION	SUPPLIER
• 100 bp DNA Ladder (250 µl)	Promega Corp., Madison, Wi., USA
• 1 kb DNA Ladder (250 µl)	Promega Corp., Madison, Wi., USA
• Baxter ddH_20	Baxter, Sydney,Australia
• BigDye™ reaction mix	Promega Corp., Madison, Wi., USA
• Black and white film (667) (Polaroid)	Polapan, Perth Professional Sales, Australia
• Carbon Dioxide (CO_2) gas, food grade	Aligal® 2, Air Liquid, WA, Australia
• Cell culture flasks: T-25; T-75	Life Technologies, Australia
• Cell culture plates: 6 -, 24- & 96-wells	Life Technologies, Australia
• Cell Scraper	Sarstedt, Germany
• Centrifuge tubes: 10 ml, 50 ml	Sarstedt, Germany
• Cling Film	Glad, Australia

• Cover slips (22 mm x 22 mm)	Knittel Glaser, Germany
• Cryogenic vials (sterile)	Corning Glassworks, USA
• Cuvette (4 mm gap, sterile)	Invitrogen, Australia
• Filter paper	Whatmans International, England
• Filter units (Bottle-top) (0.45 μm)	Whatmans International, England
• Gel drying Kit	Bio-Rad Laboratories, Hercules, CA., USA
• Gene Pulser II system	Bio-Rad Laboratories, USA
• Glass Slides	Knittel Glaser, Germany
• Hybond™-C Nitrocellulose membranes (0.45μm)	Amersham Life Science, Amersham Place, Little Chalfont, Buckinghamshire, UK
• Hybond™ N^+ membranes	Amersham Life Science, Amersham Place, Little Chalfont, Buckinghamshire, UK
• Liquid Nitrogen (N_2)	Air Liquid, WA, Australia
• Microcentrifuge tubes: 1.5 ml	Sarstedt, Germany
• Microcentrifuge tubes: 0.5 ml, 2.0 ml	TRACE Bioscience, Australia
• Micropore filters (0.2, 0.45 & 0.8 μm)	Crown Scientific, Australia
• Nail Polish	Satin, Australia
• Nalgene® centrifuge tubes: 30 ml, 250 ml	Nalgene Labware, Selby Biolab, Australia
• Parafilm Laboratory film	American National Can™, Menasha, Wi, USA
• PCR 0.2 ml thin-walled tubes	Unimed Australia Pty Ltd, Australia
• Petri dishes (90mm)	Sarstedt, Germany
• Pre-stained SDS-PAGE standards, low range, 250 μl	Bio-Rad Laboratories, Hercules, CA., USA
• RNasezap™	Ambion, USA
• Serological pipettes: 5 ml, 10 ml	Life Technologies, Australia
• Skim milk powder	Diploma, Melbourne, Australia
• Transfer pipette, 1 ml	Sarstedt, Germany
• X-Omat Blue XB-1 films	Kodak, USA

3.1.15 Equipments and Software

DESCRIPTION	SUPPLIER
• Adobe® Photoshop® version 5.0	Adobe Systems Inc., USA
• Agarose gel comb	Bio-rad, Hercules, CA., USA
• Auto Vortex Mixer, CSV90	Crown Scientific Pty Ltd, WA, Australia
• Biofuge A microcentrifuge	Heraeus Sepatech, Germany
• BIOHIT Proline single channel pipettes, ranges: 0.1-2µL, 0.5-10µL, 10-100µL, 50-200µL, 200-1000µL	BIOHIT OY PROLINE Pipettes, Finland
• Centra-M2 centrifuge	International Equipment Company, USA
• Clemco fumehood	Oliphant Pty Ltd, Sydney, Australia
• Confocal Assistant, version 4.02.	Bio-Rad Laboratories Ltd, Hemel Hempstead Hertfordshire, UK
• Confocal Microscopy Operating System (COMOS), Coherent® Enterprise	Bio-Rad Laboratories Ltd, Hemel Hempstead Hertfordshire, UK
• Cryo 1°C Freezing Container	Nalgene Labware, Selby Biolab, Australia
• Fisher & Paykel freezer (-20°C)	Fisher & Paykel Ltd, Auckland, New Zealand
• Gene Amp PCR system (2400)	Perkins-Elmer, Norwalk, USA
• Gene Cross-linker	Bio-Rad Laboratories Ltd, Hemel Hempstead Hertfordshire, UK
• Grant W14 water bath	Selby Scientific and Medical, USA
• Hettich Universal 2S Centrifuges	Hettich Zentrifugen, Germany
• Hybridisation Oven	Hybaid Ltd, Teddington, Middlesex, England
• J2-MI Series High Speed Centrifuges	Beckman Instruments, Inc., USA
• Kelvinator, no frost 400 Impression Series N400V fridge (4°C)	Kelvinator, Australia
• Land Camera CU-5 (Polaroid)	Polapan, Perth Professional Sales, Australia
• Magnetic Stirrer/Heat Block, model 209-1	IEC Australia Industrial Equipment & Control Pty Ltd, Australia
• Microsoft Office® 2000 Professional	Microsoft Corporation, USA
• Mini SUB^{TM} DNA Cell	Bio-Rad Laboratories, Hercules, CA., USA
• Model 200/2.0 Power Supply	Bio-Rad Laboratories, Hercules, CA., USA
• Nikon, Phase contrast inverted microscope, ELWD 0.3	Nikon, Japan
• Nikon View 2, version 21	Nikon, Japan
• Orbital mixing incubator	RATEK Instruments, Australia
• pH-2 Scan pH meter	Whatmans International, England
• PolarStar Optima	BMG Labtechnologies, Offenburg, Germany
• PowerPac 300 Power Supply	Bio-Rad Laboratories, Hercules, CA., USA
• Powerpette	Jencons Scientific Ltd, Lab-Supply, Australia

• QC 1 – R/T Processor, Film processor	Du Pont Medical Products, NSW, Australia
• Quick Shooter, model QSP Gel Electrophoresis PHOTOSYSTEM	IBI, International Biotechnologies Inc., New Haven, Connecticut, USA
• REVCO –80°C Freezer	Legaci Refrigeration System, Asheville, North Carolina, USA
• Rocking platform mixer	RATEK Instruments, Australia
• Sartorius research P1210 weighing balance	Mettler, Zurich, Switzerland
• Scion Image Beta 4.0.2	Scion Corporation, USA
• Simpson microwave oven	Simpson Ltd, Korea
• Swiss-Pdb Viewer v3.7b2	Glaxo Welcome Experimental Research, Switzerland
• TPS Digital pH Meter, model 1852-mV	TPS Pty Ltd, Brisbane, Australia
• Ulead iPhoto Express	Ulead Systems, Inc., USA
• UV Microscope, Laborlux S	Leitz Wetzlar, Germany
• Ultraviolet Transilluminator (UVT)	IBI, International Biotechnologies Inc., New Haven, Connecticut, USA
• UV transparent gel tray (10 x 15 cm & 7x 10cm)	Bio-rad, Hercules, CA., USA
• Varian DMS 70 UV Visible Spectrophotometer	Varian Techtron Pty Ltd, Victoria, Australia
• Water Jacketed Incubator	Forma Scientific, Ohio, USA
• Wide Mini SUB^{TM} Cell	Bio-Rad Laboratories, Hercules, CA., USA

3.1.16 Centrifugation

All micro-centrifugation (0.2 ml, 0.5 ml, 1.5 ml and 2.0 ml) procedures at room temperature were performed using the Biofuge A microcentrifuge. Micro-centrifugation at 4°C was carried out in a Centra-M2 centrifuge. Centrifugation of solutions in 10 and 50 ml centrifuge tubes were performed using a Hettich Universal 2S centrifuge. All high speed and large volume (250 ml and 500 ml) centrifugation procedures were performed in the J-2 Series High Speed Centrifuges (Beckman Instruments) at 4°C unless otherwise specified.

3.2 BUFFERS AND SOLUTIONS

Solutions and buffers were prepared using highly purified Milli-que (milli-Q) double distilled water (ddH_20) and, where appropriate, were sterilised by autoclaving and stored at room temperature unless otherwise stated. All chemicals were weighed using a Mettler P1210 balance. Adjustments of pH were made using a pH-2 Scan pH meter, calibrated with appropriate pH standards (pH 4.0 or 7.0).

3.2.1 General solutions

SOLUTIONS	COMPOSITION AND PREPARATION
• 30% Acrylamide	29 g of acrylamide and 1 g of bisacrylamide were dissolved in a total volume of 60 ml of ddH_2O with mild heating at 37°C to acid solubility. Volume adjusted to 100 ml with ddH_2O, then filtered through two sheets of Whatman # 1 filter paper. Stored at 4°C in the dark.
• Ampicillin	100mg/ml stock prepared in ddH_2O and stored in 1ml aliquots at -20°C
• Aprotinin	10mg/ml stock dissolved in ddH_2O. dispensed into small aliquots and stored at -20°C
• Bafilomycin A (Baf A)	100 μM stock dissolved in DMSO and stored at -20°C
• BSA/PBS	0.2% stock. Dissolved in 1 x PBS, sterilized by filtration and stored at 4°C.
• Bromophenol blue	1% stock, prepared using sterile ddH_2O. Swirled before use to suspend sediment.
• Calcium chloride	100 mM stock prepared from solid $CaCl_2$. $2H_2O$. Stored at 4°C.
• d.A.G.T.p	100 mM stock of dATP, dGTP and dTTP diluted to 5 mM in Baxter ultrapure ddH_2O.
• Decalcifying solution (14% EDTA)	14g of EDTA dissolved in 100ml of ddH_2O, pH was adjusted to pH7.4 with 1M NaOH
• Denaturing Buffer	0.25 M HCl stock prepared in ddH_2O. Stored at room temperature.
• DEPC water	2 ml of DEPC in 18 ml of ethanol (100%) diluted in ddH_2O to a final volume of 2 L. Solution was left to stand overnight for DEPC treatment prior to autoclaving.
• dNTPs	100 mM stock solution made up of each dNTP constituent (dATP, dTTP, dCTP and dGTP). An equal volume of these components mixed together produced a 25 mM combined stock of dNTPs, which was diluted to 5 mM with ddH_2O and stored as 200 µl aliquots at –20°C.
• Dithiothreitol (DTT)	Prepared at a concentration of 1M and stored at –20° C in 1 ml aliquots. Not sterilized.
• 6 X DNA Sample Buffer	Composition: 0.25% xylene cyanol, 0.25%

	bromophenol blue, 30% glycerol. Stored at room temperature.
• EDTA	0.5 M stock, brought to pH 8.0 with NaOH and stored at room temperature.
• Ethidium bromide	Prepared as 10 mg/ml stock with sterile ddH_2O. Stored in the dark at 4°C.
• Geneticin (G418)	50 mg/ml stock dissolved in PBS, filter sterilised and stored at 4°C.
• IPTG,	Prepared at a concentration of 100mM, filtered, and stored in 1ml aliquots at -20°C
• Kanamycin sulphate	50mg/ml stock solution, made up in ddH_2O. stored as small aliquots at -20°C.
• Low Fade Mounting Medium	5ml of Tris-$P0_4$ buffer, 10µl of phenol red (1%), 20g of PVA dissolved in 75ml of ddH_2O. Mixture was dissolved in a water bath for 2-3 h at 60°C before 30 ml of glycerol and 100 mg of chlorobutanol was added. PH was adjusted to 8.2 with Tris-PO_4 buffer. 20 ml aliquots were stored at –20°C. Working aliquot stored in the dark at 4°C.
• Lysosome	10mg/ml stock solution made up fresh when required in the appropriate buffer. Not sterilized.
• Paraformaldehyde (4%)	10% stock prepared by dissolving 5g of paraformaldehyde in 50ml ddH_2O. Solution was warmed to 60°C and pH adjust to 7.4 with 1M NaOH. Stored as 1ml aliquots at -20°C
• Phosphate buffered saline (PBS)	20X stock prepared from the following components: 10g NaH_2PO_4, 203.6g Na_2HPO_4, 170g NaCl in ddH_2O. pH was equilibrated to 7.4 with HCl.
• PBS	1X pH7.4 solution was prepared by diluting 100ml of stock solution in 1L ddH_2O. Solution was filtered-sterilized and stored at room temperature.
• PBS-T	1X stock solution was prepared from the following components: 8g NaCl, 0.2g KH_2PO_4, 1.44g Na_2HPO_4, 0.2g KCl and 0.5ml Tween 20. Stored at room temperature.
• Pepstatin A	1.0mg/ml stock prepared in methanol. Stored as small aliquots at -20°C.
• Phenylmethylsulfonyl fluoride (PMSF)	100mM stock solution prepared fresh in ethanol when required
• RipaRipa Lysis Buffer	50mM Tris pH7.5, 150mM NaCl, 1% Nonidet P-40, 0.1% SDS, 1% Sodium deoxycholate. Sterilized by autoclaving and stored at 4°C.
• Sodium acetate	Prepared at 3M sodium ion concentration by dissolving 24.6g of powder form in 100ml of ddH_2O, adjusting the pH with glacial acetic acid to 5.2, and making up any remaining volume requirement with ddH_2O. Sterilized by autoclaving and stored at room temperature.
• Sodium chloride	5M stock solution prepared in ddH_2O, autoclaved and stored at room temperature.
• di-sodium hydrogen orthophosphate	1M stock solution prepared form powdered anhydrous form. Autoclaved and stored at 4°C.
• SDS	Prepared as an unsterilized, 10% (w/v) solution, stored at room temperature.
• SDS-PAGE Gel Destaining	20% methanol, 5% glacial acetic acid (v/v) in ddH_2O

Solution	
• SDS-PAGE Gel Staining Solution	Coomassie Brilliant Blue R (final concentration 0.5% (w/v)) was dissolved in a 1:6:3 mixture of glacial acetic acid, ddH_2O and methanol. Filtered before use through two pieces of Whatman #1 filter paper.
• SDS-PAGE Running Buffer (10X)	30.2g of Tris (hydroxymethyl) methane, 188g of glycine, 100ml of 10% SDS to 1L ddH_2O: pH8.3 (without adjustment).
• SDS-PAGE Sample Buffer	2X stock solution composed of 20mM Tris, 2mM EDTA, 40% glycerol and 2% SDS, 0.01% bromophenol blue. Prepared from stock solutions of the respective components. pH adjusted to 6.8 before addition of SDS. Prior to use add 5% β -mercaptoethanol.
• SDS-PAGE Stacking Gel Buffer	0.5M Tris, 0.4% SDS. Prepared in ddH_2O from powdered components. pH adjusted to 6.8 before addition of SDS. Stored at 4^oC.
• SDS-PAGE Resolving Gel Buffere	1.5M Tris, 0.4% SDS. Prepared in ddH_2O from powdered components. pH adjusted to 8.8 prior to addition of SDS. Stored at 4^oC.
• TAE	50X stock solution prepared by mixing 242g Trizma base, 57.1 ml glacial acetic acid and 100ml of 0.5M EDTA pH8.0, and diluting to 1L with ddH_2O. Stored at room temperature.
• Tris-HCL buffers	1M Tris stock solutions were prepared at various pHs between 7.3 and 8.0. adjustment of the pH to the desired value was achieved by adding appropriate amounts of concentrated HCL after dissolving the Tris powder in a volume of ddH_2O 80% the amount of the total volume. The final volume was then made up with more ddH_2O. Autoclaved and stored either at room temperature or 4^oC.
• Tris-buffered saline (TBS)	15ml of 5M NaCl, 25ml of 1M Tris-HCl (pH7.4) in 500ml ddH_2O.
• TBS-Tween (0.2%) (TBST)	TBS containing 0.2% Tween-20 detergent.
• Triton X-100/ PBS	0.1% stock solution made up by dissolving 50 μl of (100%) Triton X-100 in 50ml PBS. Filter-sterilized and Stored at room temperature.
• Western Transfer Buffer	25mM Tris, 192mM glycine, 20% methanol; pH 8.3 (without adjustment). Stored at 4^oC.
• X-Gal	50mg/ml stock solution prepared by dissolving X-Gal powder in N,N-dimethyl formamide. Wrapped in aluminium foil to prevent damage by light. Stored at -20^oC without sterilization.

3.2.2 Media and Agar

MEDIA	COMPOSITION AND PREPARATION
• Luria Bertani (LB)[a]	1% (w/v) bactotryptone, 0.5% (w/v) bactoyeast extract, 1% (w/v) NaCl. Sterilized by autoclaving.
• LB-Amp_{50}	Stock LB supplemented with 50 μg/ml Ampicillin.

[*] 15 g/L of bacto-agar, Amp to a final concentration of 50 μg/ml, ITPG (0.012%) and X-Gal to 40 μg/ml was added to the liquid medium just before autoclaving to prepare solid agar plates.

3.3 GENERAL METHODS

3.3.1 Animal Procedures

3.3.1.1 Animal Housing and Handling

Animals were housed in plastic cages with hay shaving as bedding in an air-conditioned room (22^{o}C) under regulated lighting conditions (12h light: 12h dark). Food and water were provided ad libitum. All anumal handling procedures were carried out in accordance with the protocols approved by the University of Western Australia Animal Ethics Committee.

3.3.1.2 Necropsy of Mice and Tissue Collection

All mice were anaesthetized and sacrificed in accordance with the University of Western Australia Animal Ethics Committee standards. Tissues harvested for RNA/DNA/protein analysis were excised using RNAse-treated sterile scalpels and snap frozen in cryovials in liquid nitrogen and stored at -80^{o}C. Adult mouse bone tissues (6-12 weeks of age) were collected and bone marrow cells were extracted for use in primary cell cultural which will be discussed later in detail.

3.3.2 Cell Culture Procedure

3.3.2.1 Cell Lines

a) COS-7 cells culture

The monkey kidney epithelial cell line, COS-7 cells, were cultured in Dulbecco's Modified Eagle medium (DMEM) supplemented with 10% heat inactivated FBS, 2mM of L-glutamine, 100U/ml penicillin and 100μg/ml streptomycin (Gibco BRL) in T-75 culture flasks (Life Technologies) in a humidified atmosphere of 5% CO_2 (Aligal® 2) and 95% air at 37°C in a Water-Jacketed incubator (Forma Scientific).

b) HEK293 cells culture

The Human Embryonic Kidney cell line, 293 cells were cultured in Dulbecco's Modified Eagle medium (DMEM) (TRACE) supplemented with 10% heat inactivated FBS, 2mM of L-glutamine, 100U/ml penicillin and 100μg/ml streptomycin (Gibco BRL) in T-75 culture flasks (Life Technologies) in a humidified atmosphere of 5% CO_2

(Aligal® 2) and 95% air at 37°C in a Water-Jacketed incubator (Forma Scientific).

c) RAW264.7 cells culture

The mouse macrophage RAW264.7 cells were cultured in alpha-Modified Eagle Medium (α-MEM) (TRACE) supplemented with 10% heat inactivated FBS, 2mM of L-glutamine, 100U/ml penicillin and 100μg/ml streptomycin (Gibco BRL) in T-75 culture flasks (Life Technologies) in a humidified atmosphere of 5% CO_2 (Aligal® 2) and 95% air at 37°C in a Water-Jacketed incubator (Forma Scientific).

For all cell cultures, FBS was heat-inactivated before adding to the media by incubating the chock serum at 55^{o}C for 30 minutes. The culture media was replenished every two to three days with fresh complete media and the cells were passaged upon reaching appropriate confluence.

3.3.2.2 Cryopreservation of Cell Lines

For long-term storage, the cell lines were trypsinised, centrifuged and resuspended in an appropriate medium supplemented with 8 % DMSO and 92 % FBS. The cell solutions were aliquotted into sterile 2 ml cryogenic vials and stored overnight at -70°C in an ethanol-equilibrated Cryo-freezing container before being transferred to liquid nitrogen for long-term preservation.

3.3.2.3 Generation of Osteoclasts

Two systems were used in this study to isolate and culture mouse osteoclasts *in vitro:*

a) Bone Marrow Cell Culture

Primary mouse or rat bone marrow monocytes (BMMs) were isolated from the long bones of C57/Black Mice or Winstar female Ex-breeder rat as described previously (Udagawa et al., 1989) but with minor modification. Briefly, BMMs were isolated and pooled from whole bone marrow and incubated in T-75 flasks at 37^{o}C in 5% CO_2, in the presence of complete α-MEM (10% FBS) containing 10ng/ml recombinant human M-CSF.

After 48 hours of culture, the adherent cells were collected and then plated in complete α-MEM (10% FBS), at 37^{o}C in 5% CO_2 in the presence of recombinant hM-CSF (10ng/ml) and RANKL (100ng/ml), and plated according to each experimental condition. The cultured cells were supplemented with fresh media and RANKL (100ng/ml) on the fourth day of culture. A typical monolayer of multinucleated OCLs was obtained during day 7 to 10 of culture. In some cases, the multinucleated OCLs were detached from the wells using Cell Dissociation Buffer, pelleted, and reseeded onto devitalized bovine bone for bone resorption assay.

b) RAW 264.7 Cell- RANKL System

Osteoclasts (OCs) were generated using the highly osteoclastogenic RAW 264.7 cells, subclone C4; (Cassady et al., 2003) cultured in T-25 culture flasks at a density of 1 x 10^5 cells/flask, 6-well plates at a density of 2-2.5 x 10^4cells/well, 1-1.5 x 10^3cells/well in 96-well plates or on glass coverslips in 24-well plates at a density of 1 x 10^4 cells/well in α-MEM containing recombinant GST-rat RANKL (Xu et al., 2000) at a concentration level of 100 ng/ml. The culture medium containing RANKL was replaced every two to three days.

OCLs were evident after 5-7 days of culture. The cells were subsequently harvested and processed for total RNA extraction, Western Blot analysis, or/and immunohistochemistry. In some instances, osteoclasts were detached from the wells using Cell Dissociation Buffer and gentle scraping, pelleted and reseeded onto the devitalised bovine bone or whale dentine slices (100-150 μm thick) before being processed for scanning electromagnetic microscopy.

3.4 RNA EXTRACTION AND QUANTITATION METHODS

3.4.1 General handling procedures

Buffers, ultrapure water, microfuge tubes, micropipette tips, and any implements that were in contact with RNA, were sterilized by autoclaving or filtration before use. General aseptic techniques were employed when working with RNAs, which were stored in sterile TE buffer pH 8.0, Baxter ultrapure water or DEPEC-treatment ultrapure water at either -80°C or – 20°C. When removed from the freezer, RNAs were thawed and kept on ice.

3.4.2 Extraction of total RNA

The total cellular RNA was isolated from various mouse tissues or cultured cells using RNeasy Mini Kit in accordance with the manufacturer's protocol (QIAGEN). Cells grown as monolayers in 6-well culture plates (approximately 10^6 cells) were lysed directly by the addition of 350 μl of Buffer RLT to disrupt the cells. The cell suspensions were carefully pipetted until they were evenly dispersed, and samples were transferred to the 1.5 ml Eppendorf tubes. One volume (350 µl) of 70% ethanol was subsequently added to each tube and the samples were mixed by pipetting. The samples (700µl) were then transferred to an RNeasy mini column placed in a 2 ml collection tube and then centrifuged at 10,000 rpm for 15 seconds at room temperature.

Discarded the flow-through and added 700µl Buffer RW1 to the RNeasy column. Thereafter, the samples were centrifuged at 10,000 rpm for 15 seconds. The flow-through was removed and the RNeasy column was transferred into a new 2ml collection tube. The RNeasy columns were washed twice with 500 µl Buffer RPE and centrifuged for 2 min at 10,000 rpm to dry the RNeasy silica-gel membrane. RNA was eluted with 30-50µl RNase-free water and collected in a new 1.5 ml collection tube (supplied) by centrifuge at 10,000 rpm for 1 min at room temperature. The RNA samples were ready to use or stored at -80°C.

3.4.3 Quantitation of RNA

The concentration and purity of RNA in each sample was determined spectrophotometrically using a Beckman DU650 spectrophotometer according to Sambrook et al (1989). The samples were diluted at 1:100 in Baxter ddH_2O and the OD_{260} and OD_{280} measured against a Baxter ddH_2O blank. An OD_{260} of 1 is equivalent to 40 µg/ml of single stranded DNA or RNA (Sambrook et al., 1989). The OD_{260}/OD_{280} ratio was calculated to determine the purity of each RNA sample. The pure RNA has an OD_{260}/OD_{280} ratio between 1.5 and 2.0 (Sambrook et al., 1989). All samples typically exhibited ratios higher than 1.8.

3.5 REVERSE TRANSCRIPTION-POLYMERASE CHAIN REACTION

3.5.1 Reverse transcription of mRNA

The reverse transcription of mRNA was performed using the conventional method. Generally, 2 µl (~1 µg) of template mRNA, 2 µl of dNTP mix (20 mM), 0.25 µl of oligo (dT) first strand primers and 9.75 µl of Baxter ddH_2O were added on ice to thin walled, RNAse-treated, PCR tubes. The reaction mixtures were then combined, centrifuged, and heated in a thermal cycler at 75^{o}C for 3 minutes to disrupt secondary structures.

Subsequently, the reaction mixes were returned to ice to promote primer annealing and 4 µl of 5X RT-PCR buffer (Promega), 1 µl of placental RNAse inhibitor (Promega) and 1 µl of Molney Leukaemia Virus (M-MLV) Reverse Transcriptase (Promega) were added to yield final reaction volumes of 20 µl. The samples were mixed briefly and centrifuged before being incubated for 1 hour at 42^{o}C in the thermal cycler. Finally, the tubes were heated to 92°C for 10 minutes to inactivate the reverse transcriptase. The reactions lacking M-MLV reverse transcriptase were used as negative controls in order to check for genomic DNA contamination. All cDNA samples were stored at –20°C.

3.5.2 Polymerase chain reaction (PCR)

The polymerase chain reaction (PCR) is a powerful *in vitro* technique for the enrichment of specific target DNA sequences. It utilizes two primers complementary to the ends of a target sequence and by repeated cycles of annealing, synthesis, and denaturation in the presence of a thermostable DNA polymerase i.e. *Thermus aquaticus* DNA polymerase (*Taq* polymerase), sequences bounded by a pair of short, sequence specific primers can be amplified more than a million-fold.

In general, for PCR amplification, the reaction mixtures contained 400 µM each of dATP, dCTP, dGTP and dTTP; 1 U of *Taq* polymerase; as well as 0.1 µM of forward and reverse primers (Refer to Table 3.1) in a final concentration of 1.5 mM $MgCl_2$, 50 mM KCl, 10 mM Tris-HCl pH 8.3 (10x reaction buffer from the *Taq* DNA polymerase kit) and approximately 100 ng of target cDNA in a final reaction volume of 50 µl. Each reaction was mixed and centrifuged before being placed into a thermal cycler. The standard PCR cycling profiles comprised initial denaturation of 94°C for 5 minutes, 94°C for 40 seconds, an annealing temperature (varied with each primer, ~50-62°C) as

well as an extension of 72°C for 40 seconds with 20-35 repeated cycles. The reaction mixtures were subjected to a final extension step of 10 minutes at 72°C. Primer annealing and the cycling conditions are summarised in Table 3.1.

Table 3.1 Primers and cycling parameters.

NAME	PRIMER FORWARD SEQUENCE (5'-3')	PCR CONDITIONS (ANNEALING)
36B4	TCA TTG TGG GAG CAG ACA	54°C 40 sec, 25 cycles
Calcitonin R.	TGG TTG AGG TTG TGC CCA	62°C 45 sec, 30 cycles
Cathepsin K	GGG AGA AAA ACC TGA AGC	55°C 45 sec, 30 cycles
RANK	GGA AGA TCT TTC CAT GCA CCC AGG AGA G	60°C 40 sec, 30 cycles
Calcitonin R.	CTC GTG GGT TTG CCT CAT C	62°C 45 sec, 30 cycles
Cathepsin K	ATT CTG GGG ACT CAG AGC	55°C 45 sec, 30 cycles

For semi-quantitative RT-PCR, 10μl of each PCR products were electrophoresed on 1 X TAE agarose gels with concentration levels ranging from 1-2 % depending on the predicted PCR product size. The relative mRNA ratios between samples were normalised to 36B4.

3.5.3 Quantitation of DNA

The spectrophotometric measurement of the amount of ultraviolet irradiation absorbed by nucleic acid bases provides a simple but accurate method of determining the concentration levels of pure oligonucleotide and plasmid DNA samples. After being diluted 100-200-fold in sterile Baxter ddH_2O, the DNA samples were placed in 1 ml quartz cuvettes, exclusively used for UV spectroscopy, and the absorbance was read at a wavelength of 260 nm. The concentration level of nucleic acid in the sample was calculated on the basis that an Optical Density (OD) of 1 corresponds to approximately 50 μg/ml for double-stranded DNA, and 33 μg/ml for single-stranded synthetic oligonucleotide DNA. In order to assess the purity of the DNA samples, OD readings were also taken at a wavelength of 280 nm. Pure preparations of DNA have OD_{260}/OD_{280} value of 1.8.

3.6 RAPID AMPLIFICATION OF 3' AND 5' CDNA ENDS (RACE)

The 3' and 5' sequences of unknown Rab3 clones 11 and 25 were determined by RACE, adopted from the protocol outlined in Frohman et al (1988), using RNA isolated from osteoclasts/ST2-cell co-cultures.

3.6.1 Reverse transcription of RNA

mRNA isolated from mouse osteoclast-ST2 cell co-cultures (Section 4.4.3) was treated with DNAse and then reverse transcribed with RETROscript™ M-MLV reverse transcriptase as essentially described in Section 4.5.1 with the following minor modifications. For 3'end RACE, RT-PCR was performed in the presence of an oligo$(dT)_{17}$ primer containing an adapter sequence (Table 4.1). For 5'end RACE, RT-PCR reactions were carried out in the presence of gene-specific primers (0.1 μg) based on the 3'ends of either Rab3B (Rab3B-3', M2) or Rab3C (Rab3C-3').

3.6.2 Oligo-dA tailing of cDNA

For 5' RACE, cDNAs generated in Section 4.6.1 were purified using QuickSpin Columns as described in Section 4.5.2. Oligo–dA tails were then added to the 5' ends of purified Rab3B and Rab3C cDNAs using terminal deoxynucleotidyl-transferase (TdT). To thin walled PCR tubes, the following components were added: 4 μl 5 x tailing buffer, 10 μl purified cDNA, 1.6 μl dATP (10 mM) and 3.4 μl Baxter ddH_2O. The tubes were incubated for 2 min at 94°C in a thermal cycler, chilled on ice for 1 min and briefly centrifuged. One μl TdT was added to each tube, the tubes incubated at 37°C for 60 min and then heated to 70°C for 10 min to inactivate the TdT. The tubes were briefly centrifuged and placed on ice.

3.6.3 PCR amplification

3' RACE was performed using an adaptor primer together with one of two gene-specific primers based on internal sequences from Rab3 clones 11 (M3) and 25 (M1). PCR reactions were prepared in thin walled PCR tubes, each containing 12.4 μl Baxter ultrapure ddH_2O, 2 μl 10 x reaction buffer, 1.5 μl 25 mM $MgCl_2$, 0.5 μl dNTP mix, 70 ng primers, 1 U *Taq* DNA polymerase and 2 μl cDNA. The final volume of each reaction was 20 μl. Reactions were placed into a lid thermal cycler and were cycled at

94°C for 5 min (1 cycle), [94°C for 30 sec, 54°C for 45 sec, 72°C for 2 min] (35 cycles) and 72°C for 10 mins (1 cycle). PCR products were stored at -20°C.

Gene-specific primers were also designed to PCR amplify 5' fragments of Rab3B and Rab3C cDNAs using a nested-PCR based approach. For the primary PCR, reaction products were prepared in thin walled PCR tubes, each containing 12.4 µl Baxter ultrapure ddH_2O, 2 µl 10 x reaction buffer, 1.5 µl 25 mM $MgCl_2$, 0.5 µl dNTP mix, 70 ng primers: $(dT)_{17}$-adaptor and internal designed gene-specific primers (Rab3B 5' PCR or Rab3C 5' PCR), 1 U *Taq* DNA polymerase and 2 µl cDNA. The final volume of each reaction was 20 µl. Reactions were placed into a lid thermal cycler and were cycled at 94°C for 5 min (1 cycle), [94°C for 30 sec, 54°C for 45 sec, 72°C for 2 min] (35 cycles) and 72°C for 10 mins (1 cycle). PCR products were stored at -20°C.

Secondary PCR reactions were prepared in thin walled PCR tubes, each containing 13.4 µl Baxter ddH_2O, 2 µl 10 x reaction buffer, 1.5 µl 25 mM $MgCl_2$, 0.5 µl dNTP mix, 70 ng primers: adaptor and gene-specific primers Rab3B (M4) or Rab3C (M2), 1 U *Taq* DNA polymerase and 1 µl of primary PCR products diluted 1:100 in sterile ddH_2O. The final volume of each reaction was 20 µl. Reactions were placed into a thermal cycler and were cycled at 94°C for 5 min (1 cycle), [94°C for 30 sec, 54°C for 45 sec, 72°C for 2 min] (25 cycles) and 72°C for 10 mins (1 cycle). PCR products were electrophoresed on 1.2% agarose gels and either transferred for Southern Blotting or readied for DNA extraction.

3.7 RESTRICTION ENZYME DIGESTION OF DNA

Restriction enzymes bind and cleave double stranded DNA at specific sites known as recognition sites, which are specific sequences of bases. Restriction enzyme digestion is a useful method for the digestion of plasmid DNA with known restriction sites to release plasmid DNA inserts for either DNA assessment, for further ligation with other vectors, or DNA sequencing analysis.

For plasmid digests, the digestion mixtures generally contained the following components:

Plasmid (Mini-prep isolation)	5 µl
10 X Restriction Enzyme Buffer	3 µl
Baxter ddH_2O	21 µl
Restriction Enzyme	1 µL
Total Volume	**30µL**

The reaction mixtures were incubated at 37°C for one night. Upon digestion, 5 µl of each reaction mix were electrophoresed against DNA standards and visualized on a UV transilluminator. The gels were examined for plasmid DNA inserts corresponding to predicted sizes. The remaining digest products were stored at -20°C until required.

In some cases where single restriction cuts were introduced, plasmids were dephosphorylated to prevent re-ligation using calf intestinal alkaline phosphatase (CIAP). Typical reaction mixes included:

Digested plasmid DNA-restriction enzyme solution	50 µl
CIAP	1 µl
10x CIAP buffer	10 µl
Baxter ddH_2O	39 µl
Total Volume	**100µl**

The mixtures were incubated at 37°C for 1 hour before deactivating the CIAP at 75°C for 15 minutes. The samples were stored at -20°C until required.

3.8 DNA AGAROSE GEL ELECTOPHORESIS

DNA samples to be electrophoresed were combined with 1/5th volume of 6 x Loading Dye. The samples were loaded into 1-2% agarose gels depending on the size of DNA fragments to be separated, each containing ethidium bromide (0.5 μg/ml) and electrophoresed in a Bio-Rad mini-or wide mini-sub-cell apparatus in 1 X TAE buffer at 60-150 V. Four μl (520 ng) of a 100 bp DNA ladder or 1 kb DNA ladder (400 ng) were electrophoresed in each gel to estimate fragment sizes. DNA bands were visualized by UV trans-illumination of gels using an IBI (Kodak) transilluminator, and photographed with a Polaroid CU-5 land camera with 667 black and white Polaroid film or Nikon digital camera.

3.9 DNA EXTRACTION FROM AGAROSE GEL

The extraction of DNA from agarose gel was performed by using QIAEX II Agarose Gel Extraction Kit (QIAEX) in accordance with the manufacturer's protocol with minor modifications. First of all, the DNA band of interest was excised from the agarose gel with a clean, sharp scalpel and placed into a clean 1.5ml microfuge tube. The DNA gel band was weighed and added with three volumes of Buffer QX1 to 1 volume of the gel weight (for example, add 300μl of Buffer to 100mg of gel). Next, QIAEX II was resuspended by vortexing for 30 seconds, and 5μl of the resuspended aliquot was added to the DNA sample. The sample was then incubated at 50°C for 10 minutes to allow the gel to solubilize and DNA/QIAEX II binding.

During the incubation, the sample was mixed by vortexing every two minutes to keep QIAEX II in suspension. After the incubation, the sample was spun at 13,000 rpm for 30 seconds, and the supernatant was carefully discarded with a pipette. The pellet was washed once with 500μl of Buffer QX I, then twice with 500μl of Buffer PE, and air-dried for 10 minutes at room temperature. The DNA was eluted from the bead by resuspending the pellet with 10μl of autoclaved ddH_2O. The sample was incubated at 50°C for 5 minutes. It was then centrifuged at 13,000 rpm for 30 seconds and the purified DNA was collected from the supernatant. The resulting elutant contained the DNA and was either used immediately or stored at -20^{o}C.

3.10 CLONING METHODS

PCR products were cloned into the pGEM®-T Easy Vector (Figure 3.1) using the pGEM®-T TA Cloning® Kit.

3.10.1 T/A Cloning

T/A cloning was achieved using pGEM®-T Easy Vector Easy System I. In brief, the purified DNA obtained from agarose gel extraction was cloned into pGEM®-T Easy Vector by ligating the 3'-A overhang on each end of the PCR product to a linearized cloning vector with single, 3'-T overhangs. The ligation reaction was carried out in a 1.5ml microfuge tube as follows:

Gene clean product	7µl
pGEM®-T Easy Vector	1µl
10 × Ligation Buffer	1µl
T4 DNA Ligase	1µl
Total Volume	**10µl**

The ligation mixture was mixed by gently flicking the tube, then centrifuged briefly and incubated at 14°C overnight. After incubation, the ligation product was either stored at -20°C for future use or transformed directly into competent cells.

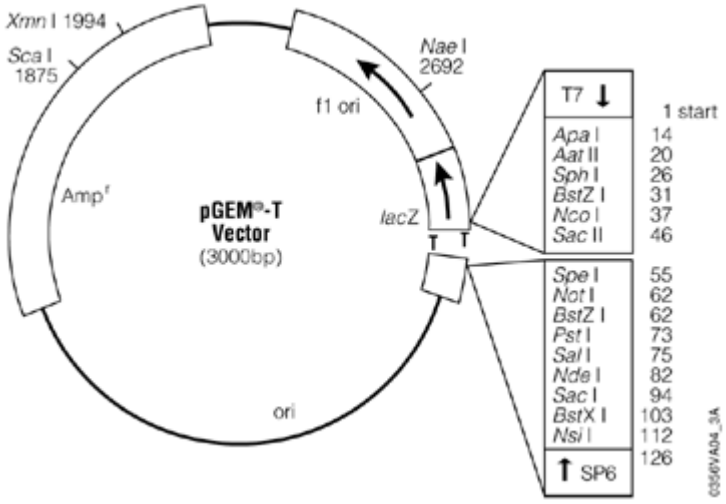

Figure 3.1 pGEM®-T Easy Vector. Map of the cloning vectors showing the restriction enzymes sites and positions of primers and promoters in the vector.

3.10.2 Transformation and plating of cells

1-2μg of DNA plasmid was added to 200μl of DH5α competent cells. Pipette up and down gently to mix DNA thoroughly with cells in a microfuge tube. The mixture was then incubated on ice for 30 minutes. Following the incubation, the sample was heat shocked at 42°C on a heating block (BioRad) for 90 seconds and immediately placed on ice for an additional 2 minutes. The DNA/cell mixture was added to 1ml of LB medium and incubated at 37°C with vigorous shaking at 225 rpm in an orbital mixer incubator (RATEK) for 1 hour. The transformed cells were then plated out onto LB plates containing 100μg/ml of ampicillin, and incubated at 37°C overnight. In order to transform the plasmid obtained from T/A cloning, the LB-ampilcillin plates were spread over the surface with 100μl of 100mM IPTG and 20μl of 50mg/ml X-gal, to allow absorption for 30 minutes prior to plating out of transformed cells.

3.10.3 Bacterial culture and maintenance

Single white colonies were picked from plates with sterile yellow tips and inoculated into 4 ml aliquots of LB-Amp_{50} broth. The cultures were incubated at 37°C for 16-20 hours with vigorous shaking (225 rpm). For long-term storage, both recombinant and non-recombinant bacterial cells were resuspended in LB medium supplemented with 15% glycerol, aliquotted out into sterile 1.5 ml microfuge or 2 ml cryotubes, snap-frozen in liquid nitrogen, and stored at -80°C. In order to obtain cells from a frozen stock, an aliquot was slightly thawed at the surface and impregnated either with a sterile loop or micropipette tip to remove a sample of semi-solid material, which was then streaked onto an LB agar plate or inoculated into fresh culture medium. The stock is refrozen and stored away at - 80°C. After storing for 2 months at 4°C, the agar plate cultures were discarded.

3.11 ISOLATION AND PURIFICATION OF PLASMID DNA

The small-scale plasmid DNA isolation and purification were carried out as follow. A single colony was picked up/selected and inoculated into 4ml of LB medium containing 4μl of 100μg/ml ampecillin (1/1000) and grown overnight at 37°C shaking at 225 rpm in an orbital mixer incubator (RATEK). Plasmid DNA was extracted and purified using the Wizard® Plus SV Minipreps DNA purification System (Promega) in accordance

with the manufacturer's guidelines. The plasmid was eluted with 50µl of autoclaved ddH_2O and stored at -20°C until use.

3.12 DNA SEQUENCING AND ANALYSIS

The DNA sequences were determined using ABI Prism® Big Dye™ sequencing mix and an ABI Prism® 377 automated sequencer.

3.12.1 DNA sequencing reactions

The sequencing reactions were prepared in thin-walled PCR tubes. Each tube contained 4 µl Big Dye terminator premix Version 3, 2 µM GFPseq 25 ng M13 forward or reverse primer (Table 4.1), ~ 50 ng DNA template and the volume adjusted to 10 µl using Baxter ddH_2O. The reactions were placed into a thermal cycler (Perkin-Elmer) and were cycled at 94°C for 40 seconds (1 cycle) and subsequently, 50°C for 30 seconds and 60°C for 4 minutes (25 cycles).

3.12.2 Purification of sequencing reactions

For DNA sequence analysis, the PCR products were ethanol precipitated. After the completion of DNA sequencing reactions, the PCR products were transferred to 0.5 ml Eppendorf tubes and the volume adjusted to 20 µl by the addition of Baxter ddH_2O. In order to precipitate DNA, 0.1 volumes 3 M sodium acetate and 2.5 volumes of 100% ethanol were added to each tube. The solutions were mixed by shaking and the tubes were incubated at room temperature for 15 minutes. The tubes were centrifuged at 14,000 rpm for 20 minutes at room temperature resulting in a small DNA pellet.

The supernatants were removed using a pipette and the pellets were washed with 250 µl 70% ethanol. The tubes were centrifuged at 14,000 rpm at 4°C for 5 minutes. The supernatants were removed and the pellets were air-dried for 5 minutes. Sequencing was performed at the Australian Neuromuscular Research Institute (QEII Medical Centre). The pellets were resuspended in 5 µl sequencing loading buffer, vortexed and centrifuged at 5,000 rpm for 10 seconds. The samples were denatured by incubation at 90°C for 2 minutes and placed on ice prior to loading onto the ABI Prism® 377 sequencer for automated DNA sequence analysis.

3.13 PROTEIN ISOLATION AND WESTERN BLOTTING

3.13.1 Protein extraction from tissues and cultured cells

For protein extraction from cultured cells, cells grown as monolayers were lysed directly in 6-well plates with 2-3ml/T-75 flask or well of 6-well plate with 200-300µl/ RipaRipa lysis buffer containing a cocktail of protease inhibitors (aprotinin, 1 µg/ml; sodium orthovanadate ; PMSF 50 µg/ml) on ice for 20 minutes. Following lysis, the cells were vigorously removed from the culture flask/wells using plastic cell scrapers, and the resulting suspensions were transferred to the Eppendorf tubes.

For the detection of IκB-α degradation, NFATc1 synthesis and pERK activation, stable transfected RAW 264.7 cell lines were seeded at a density of 1 x 10^5 cells/well in 6-well plates prior to stimulation with either vehicle (PBS) or 100 ng/ml recombinant GST-mouse RANKL for designated periods before being lysed with RipaRipa lysis buffer containing a cocktail of protease inhibitors (aprotinin, 1 µg/ml; leupeptin 1 µg/ml; pepstatin A, 1 µg/ml; PMSF 50 µg/ml).

All protein lysates were centrifuged for 20 minutes at 12,000 rpm (4°C) to pellet cell nuclei and unlysed cells. The cleared post-nuclear supernatants (PNS) were aspirated, placed into fresh Eppendorf tubes and the samples were stored at -80°C until required.

3.13.2 Quantification of protein concentration

The protein concentration was determined spectrophotometrically at A_{595} for protein using Bradford Assay. The values were obtained by extrapolation from a Bovine Serum Albumin (BSA) standard curve

3.14 SDS-PAGE PROTEIN ANALYSIS AND WESTERN BLOTTING

3.14.1 Polyacrylamide gel electrophoresis

Proteins were separated by electrophoresis on discontinuous SDS polyacrylamide slab gels, prepared and run using the mini-PROTEAN® III Cell casting apparatus as specified in the manufacturer's instructions. Briefly, a 10% separating gel solution was pipetted into the gel space to 0.5 cm below the level of the gel comb. The surface of the

gel was overlayed with 20% ethanol in ddH_2O to reduce shrinkage and aid polymerisation, and it was left to solidify at room temperature for approximately 25 minutes. Following polymerization, the ethanol was removed from the surface of the separating gel and the remaining gel space was rinsed with ddH_2O.

The remaining gel space was then filled with 4% stacking gel solution and the well-forming combs were inserted. Once the 4% stacking gel has polymerised, the combs were removed and wells were rinsed with ddH_2O to remove unpolymerised acrylamide. The Western gel apparatus was assembled and filled with 1 X SDS-PAGE Running Buffer. 10-25 µl of each protein sample (50-200 µg/well) was combined with 10-25 µl of 2X SDS-PAGE Sample Loading Buffer. The samples were denatured by boiling (100°C, 5 minutes), briefly centrifuged and loaded into wells. 5 µl of prestained protein molecular weight markers (150 µg/ml of each protein) was run in parallel for molecular weight analysis. All the samples were electrophoresed at 160V at room temperature.

3.14.2 Protein transfer

Following electrophoresis, the Western gel apparatus was rinsed in ddH_2O and disassembled. The gels were incubated in the ice-cold transfer buffer for 10 minutes to remove excess SDS. The Mini Trans-Blot Electrophoretic Transfer Cell was assembled according to the manufacturer's guidelines (Bio-Rad). Briefly, scotch pads and Whatman 3 MM paper were pre-soaked in the ice-cold transfer buffer. A scotch pad was placed onto the black (negative) side of the apparatus followed by 3 pieces of Whatman 3 MM paper cut slightly larger than the gel.

The gel was placed on top of the Whatman 3 MM paper, followed by an equilibrated piece of nitrocellulose membrane (Hybond-C) of the same size as the gel. The membranes were equilibrated by soaking in methanol for 10 seconds, rinsing in ddH_2O, and then placing in ice-cold transfer buffer for 10 minutes. All air bubbles between the gel and membrane were removed to facilitate even transfer of proteins. Next, 3 pieces of Whatman 3 MM paper followed by a second scotch pad were placed on top. The apparatus was closed and placed in the Western transfer tank in ice-cold transfer buffer together with an ice block. The proteins were transferred at a constant current of 30mAmp overnight.

3.14.3 Western blotting

Following the transfer of proteins to nitrocellulose membranes, the transfer apparatus was disassembled and the membranes briefly rinsed in TBS. In order to reduce non-specific binding, the membranes were blocked with TBS-Tween (TBST) containing 5% non-fat skim milk for 1 hour at room temperature on a rocking platform mixer (RATEK). After blocking, the membranes were washed twice in TBST for 5 minutes each at room temperature. The proteins were detected using either a primary rabbit polyclonal and mouse monoclonal antibodies (diluted in 1% skim milk/TBST) against NFATc1 (7A6) (1:1000), IκB-α (1:1000), pERK (1:1000), or β-tubulin (1:2000) and incubated for 2 hour at room temperature. The membranes were then washed 1 x 15 minutes and 2 x 5 minutes in TBST and incubated with a secondary HRP-conjugated anti-rabbit or anti-mouse antibody at a 1:5000 dilution for 45 minutes at room temperature.

After the removal of excess secondary antibody, the membranes were washed in TBST for 2 x 5 min and 2 x 5 min with TBS. The visualization of immunoreactivity was achieved using the ECL™-Plus detection system. Solutions A and B were pre-warmed to room temperature, combined in a 40:1 ratio and incubated with washed membranes for 5 minutes at room temperature. The excess detection reagent was drained from the membranes. The latter was wrapped in plastic wrap and transferred to a Cronex Quanta II intensifying screen cassette where they were exposed to X-Omat Blue XB-1 film. The films were developed for 2 minutes in the developer, 1 minute in the water to rinse off the developer and finally 2 minutes in the fixer.

3.15 NUCLEAR EXTRACT PREPARATION AND ELECTROPHORETIC MOBILITY SHIFT ASSAY (EMSA)

3.15.1 Nuclear extract preparation

RAW cells at the density of 2.5×10^6 were harvested from the 50ml Polypropylene tube by centrifugation at ~1,000rpm for 5minutes. The supernatant was removed and the cell pellets were resuspend in 1ml cold DPBS and then transferred to the 750µl eppendorf microfuge tube. The cells were spun at 14,000 rpm for 1 minute and upon centrifugation, the supernatant was discarded. 300ul of ice-cold buffer A was used to resuspend the cell pellet, and the cells were subjected to an additional spin at 14,000 rpm for 1 minute at

4°C. The supernatant was discarded, and the cell pellet was lysed in 600µl of buffer A* (10mM HEPS, 1.5mM $MgCl_2$, 10mM KCl and 0.5mM DTT) passing suspension through a 27gauge needle 8-10 times on ice. The nuclei were collected by spinning for 8 seconds in a microfuge at 14,000 rpm at 4°C.

Next, the supernatant was discarded and the crude nuclei were extracted with 70µl of ice-cold buffer C* (20mM HEPES, 1.5mM $MgCl_2$, 420mM KCl, 25% (v/v) sterile glycerol, 0.5mM DTT and 0.2mM EDTA) for 25-30 minutes on ice. 50µl of buffer D* (20mM HEPES, 20% (v/v) sterile glycerol, 0.5mM DTT and 0.2mM EDTA) were added to the extract and the sample was centrifuged at 14,000 rpm for 10 minutes at 4°C. The supernatant was then transferred into fresh tubes in 20 µl aliquots to reduce freeze thawing, snap freeze using liquid nitrogen, and stored at -70°C.

** 0.5mM PMSF, 2 µg/ml pepstatin A and 2µg/ml leupeptin were added just before use*

3.15.2 Electrophoretic mobility shift assay

4µg of nuclear proteins were pre-incubated for 10 minutes at room temperature with 0.5µg of poly (dI-dC) (Amersham Pharmacia Biotech) in a binding buffer (4% Ficoll, 20mM HEPES (pH 7.9), 1mM EDTA, 1mM dithiothreitol, 50mM KCl, 0.05% IGEPAL CA-630) to obtain a final reaction volume of 10µl. A double stranded NF-κB consensus oligonucleotide probe 5'-GGGCATGGGAATTTCCAACTC-3' (0.25 pmol) with overhanging 5' G which had been fill-in labeled with [α-32P]dCTP (Amersham Pharmacia Biotech) using Klenow fragment of E. coli DNA polymerase I (Promega) was added subsequently.

In competition experiments, unlabelled oligonucleotide probes (incorporating either a consensus NF-κB-binding sequence, a non-binding mutant NF-κB sequence, GCAGAAGTAACTTTCCGAGAGG) (Steer et al., 2000) were added at 100-fold molar excess. After ten minutes of incubation, the samples were loaded onto a 4% polyacrylamide gel, containing 0.25 x Tris-Borate-EDTA buffer which had been pre-run for 2 hours in the same buffer. The gels were then exposed to Kodak X-ray film using a single intensifying screen.

3.16 PROTEIN PURIFICATION

3.16.1 Expression of GST-fusion proteins

GST-fusion protein plasmids were transformed into BL-21 cells and the transformed cells were grown in 20mL of LB overnight. The bacterial culture can be kept as glycerol stock (20% glycerol) and ready for use for further inoculation for the fusion protein production. 20mL bacterial culture was inoculated into 500ml of LB medium with a final concentration of 50ug/mL Ampicillin. The culture was grown at 37^{o}C with vigorous shaking at 225rpm in an orbital mixer incubator for 4 hours or until an OD_{600} reading reached 0.4-0.5. IPTG with a final concentration of 0.05mM was then added to the culture for protein induction. The cultures were allowed to continue growing for another 2 hours at a lower temperature of 30^{o}C with vigorous shaking at 225rpm. The cultures were collected separately by centrifugation at 4,000rpm for 30minutes at 4^{o}C in a 500mL centrifuge bottle. The supernatant was then decanted and the cell pellets were stored at -80^{o}C overnight.

3.16.2 Extraction of GST-fusion proteins from cell cultures

Subsequently, the cell pellets were taken out from -80^{o}C freezer and allowed to thaw at room temperature. The pellets were then resuspended in 20mL Lysis buffer containing 50ul of neat Triton X-100 and transferred into a new 50mL tube. In order to prevent protein degradation, supplements were added to the Lysis buffer including Lysozyme and PMSF. DNase was also added to the suspension to breakdown the DNAs thus, preventing stickiness. The suspension was incubated on ice for 20 minutes with occasional agitation.

The lysed cell suspensions were then sonicated at low sonication (Pulsor at 30-40%) for no more than 1 minute each time in a Sonicator XL2020 Ultrasonic Processor or until the cultures showed no viscosity. The cell debris was then removed by centrifugation at 15,000 rpm at 4^{o}C for 30 minutes.

3.16.3 Affinity purification of soluble GST-fusion proteins

The supernatant containing the soluble GST-fusion proteins was then transferred to a new 50mL tube. 0.5mL of rinsed Glutathione Sepharose^{TM} 4B beads was added. The beads-supernatant mixtures were incubated at 4^{o}C on the rotating wheels overnight.

They were then transferred to a column and the supernatants were flowed through the column and discarded. After the supernatants were removed, the beads were subjected to at least 3 washes with 10mL of washing buffer with 1% Triton X-100, followed by 2 washes with 20mL of washing buffer without Triton X-100. This procedure washes the unbounded (undesirable) proteins away.

The GST-fusion proteins were eluted from the beads by adding 1ml of Elution buffer containing 10mM reduced Glutathione (at pH 7.8) and incubated for 10 minutes at room temperature with occasional agitations. Next, the eluted protein was collected by filtering them through the column. This process was repeated 2-3 times or until no more protein could be eluted. The presence of protein can be monitored by using the BIORAD Bradford protein assay. The proteins turned the brown colored BIORAD solution into blue. As the presence of protein will change the BIORAD solution from brown to blue, the protein concentration can be estimated by the intensity of the blue colour. Dark blue would mean a higher protein concentration level while light blue would mean a lower protein concentration level. This step gave a rough idea of the protein concentration. The elution procedure was stopped and finalized when no colour changes can be detected.

3.16.4 Concentrating of purified GST-fusion proteins

The elutates were pooled together, desalted and concentrated using the ULTRAFREE-0.5 Centrifugal Filter Device. A 0.5mL elutate was transferred to the centrifugal filter device and centrifuged up to 12,000 x g for 10 minutes. The filtrate was discarded and the sample was reconstituted back to 0.5ml by adding 1XPBS. The sample was again concentrated to 0.02mL. This desalting and buffer exchange process was repeated at least 3 times until the concentration of the contaminating solutes was reduced. A 0.5mL soluble fusion-protein was concentrated down to 20uL.

3.16.5 Concentration of determination of the concentrated and purified GST-fusion proteins

In order to determine the concentration of purified fusion-proteins, the BIORAD Bradford protein assay was used. A set of concentrations of BSA was used as a standard with the most appropriate reference proteins being applied here. The concentration

range was between 0.05mg/mL to 0.5mg/mL and 5 different concentrations were set between this range (0.05, 0.1, 0.2, 0.4 and 0.5mg/mL). 200uL of the dye reagent provided by the protein assay kit were added into each well of 96-well plate. 10uL of the standard proteins or the proteins with unknown concentration were then added to the well. All the proteins were measured in triplicates. They were mixed and the resultant mixtures were incubated at room temperature for 5 minutes before the absorbance were measured at 595nm. The dye reagent was used as blank to zero the spectrophotometer (BIORAD plate reader). The concentrations of the unknown proteins were calculated according to the concentration of the reference protein (standard).

3.16.6 Bioinformatics analysis of GST-RANKL mutants

The crystal structure of RANKL mutants were generated based on the sequence and crystal structure of full-length RANKL. The sequence of full-length RANKL was incorporated into a pdb file. This file was then exported and visualized as a ribbon crystal structure using the Swiss-PdbViewer V3.762 program (http://www.expasy.ch/spdbv/mainpage.htm). From this crystal structure, specific amino acids were selected to encompass the peptide sequences.

3.17 CELL BIOLOGY METHODS

3.17.1 Transfection

3.17.1.1 Electroporation mediated transfection

RAW 264.7 cells were transiently transfected by electroporation essentially as described [Stacey, 1993 #13143] except that 20 μg of plasmid DNA were used for the transfection. Briefly, RAW 264.7 cells, grown to ~50% confluence in T-75 flasks, were split one day prior to transfection. The cells were counted and then resuspended at a concentration of 2×10^7 cells/ml in a complete medium. 20 μg of plasmid DNA were added to 250 μl of the cell suspension (i.e. 5×10^6 cells/transfection) in a 1.5 ml Eppendorf tube. The mixture was carefully inverted several times to redissolve the DNA.

This mixture was then placed into a 4 mm gap sterile cuvette and the cells were electroporated using the Gene Pulser II system at 280 V, 960 μFaradays. Following electroporation, the cells were immediately resuspended in 10 ml complete α-MEM and

then seeded at the required density onto the 24 well, 6 well, 25cm^2 or 75cm^2 flasks. The cells were left to recover for at least 24 hours before further experimentation. In some instances, sodium butyrate (2 mM; in complete growth medium) was added to the transfected cells for 16-20 hours prior to fixation, to transiently enhance CMV promotor expression.

3.17.1.2 Dextran mediated transfection

5μg of plasmid were mixed thoroughly with 4μl of DEAD dextran in a microfuge tube and topped up to a final volume of 250μl with RPMI/HEPES buffer. The mixture was then incubated at room temperature for 30 minutes to allow the formation of the transfection complex. For each transfection, 1-1.5×10^7 cells were used. The cells were trypsinized, harvested and spun at 2,500 rpm for 5 minutes. Trypsin was discarded and the pelleted cells were resuspended with 10ml of RPMI/HEPES. Prior to transfection, the cells were washed with 20ml of RPMI/HEPES in a 50ml centrifuge tube.

Subsequently, the cells were pelleted down at 2,500 rpm for 5 minutes and RPMI/HEPES buffer was carefully aspirated without disrupting the cell pellet. The washed cells were resuspended in 750μl of RPMI/HEPES and added to the DNA mixture in a microfuge tube. The cells/DNA mixture was mixed thoroughly and incubated in a 37°C incubator for 30 minutes. In order to avoid precipitation of the cells, the tube was inverted up and down at the 10th and 20th minute during the incubation. After 30 minutes, the cells were spun at 2,500 rpm for 5 minutes. The buffer was aspirated and the pelleted cells were washed with 1 ml of RPMR/HEPES for three times. After three consecutive washes, the transfected cells were resuspended in the α-MEM serum supplemented media, aliquoted into the 24-well plate and kept in the cell culture incubator at 37°C.

3.17.1.3 Polyfect mediated transfection

The Polyfect mediated transfection was performed by using the Polyfect® Transfection kit (Qiagen) in accordance with the manufacturer's instruction. In brief, for transient transfecting HEK 293 cells in 6-well plate, 6×10^5 cells per well were seeded in 3ml of serum supplemented medium the day before transfection, to allow cells to reach 60-70% confluent on the day of transfection. For single plasmid transfection, 2μg of plasmid

were diluted to a final volume of 100µl with serum-free media. 10µl of PolyFect Trasnfection Reagent were added to the DNA solution, and the mixture was mixed thoroughly by pipetting up and down five times. The DNA mixture was incubated at room temperature for 8-10 minutes for the formation of transfection complex.

During incubation, the cells were gently washed once with serum-free media. The media were removed and replaced with 1,500µl of serum-supplemented media. After incubation, 600µl of serum-supplemented media were added to the DNA/PolyFect solution. The solution was mixed immediately by pipetting up and down twice and transferred to the cells drop-by-drop from the edge of the well. The plate was swirled gently during the addition of the DNA/Polyfect complex to ensure even distribution of the complexes. The transfected cells were kept at 37°C and with 5%CO_2 to allow gene expression. The cells were washed once with serum-free media and replaced with fresh serum-supplemented media 20-24 hours after transfection, to avoid transfection reagent-induced cytotoxic effect on the cells.

For the transient transfection of HEK293 cells and COS-7 in different formats, see table 3.2 and 3.3.

Table 3.2 Parameters for transient transfection of HEK293 cells in different formats

Culture format	Number of cells to seed a day prior to transfection	Volume of medium (µl)	DNA (µg)	Final volume of diluted DNA (µl)	Volume of PolyFect Reagent (µl)	Volume of medium to add to cells prior to addition of complexes (µl)	*Volume of medium to add to complexes (µl)
24-well plate	1.5×10^5	1,000	1.5	50	5	750	300
96-well plate	4×10^4	150	1	50	5	150	300

* When working with 96-well plate, transfers 60µl aliquot of the final complex solution to cells

Table 3.3 Parameters for transient transfection of COS-7 cells in different formats

Culture format	Number of cells to seed a day prior to transfection	Volume of medium (μl)	DNA (μg)	Final volume of diluted DNA (μl)	Volume of PolyFect Reagent (μl)	Volume of medium to add to cells prior to addition of complexes (μl)	*Volume of medium to add to complexes (μl)
6-well plate	4×10^5	3,000	2	100	10	1500	600
24-well plate	8×10^4	1,000	1.5	50	5	750	300
96-well plate	1.5×10^4	150	1	50	5	150	300

* When working with 96-well plate, transfers 60μl aliquot of the final complex solution to cells

3.17.2 Antibiotic (G418) selection of transfected cells

For the generation of stable cell lines, the transiently transfected RAW 264.7 cells were cultured in selective media containing 500 μg/ml Geneticin (G418) for at least 2 weeks. Clones found to be antibiotic resistant were selected and expanded further. The transgene expression levels and transfection efficiency were assessed routinely using a combination of Western blotting, fluorescence-activated cell sorting (FACS) analysis and confocal microscopy. For FACS, the cells were briefly washed with PBS, trypsinised, pelleted and resuspended in complete α-MEM medium (20% FBS), and sorted by a Facstar Plus cytometer (Becton Dickinson). The cell lines were frequently re-sorted to maintain homogeneity of the populations.

3.17.3 Immunofluorescence

Cells grown as monolayers on glass coverslips, or on bone and dentine slices were washed twice with PBS, fixed with 4% paraformaldehyde in PBS, pH 7.4, for 15 minutes at room temperature, and washed three times for 30 seconds each in PBS. Subsequently, the cells were incubated for 5 minutes in 0.1% Triton X-100 in PBS. Following permeablization, the cells were washed twice in PBS containing 0.2% Bovine Serum Albumin (BSA) and labeled with primary antibodies (diluted in 0.2% BSA-PBS) (polyclonal rabbit anti-TRAF6 at 1/500, polyclonal rabbit anti-Ub (FL-76) at 1/500) for 45 minutes at room temperature. After extensive washing (4 x with 0.2% BSA-PBS, 4 x with PBS, 2 x with 0.2% BSA-PBS), the cells were incubated with

secondary antibodies (Alexa Fluor® 546 goat anti-Rabbit IgG at 1/500) for 1 hour at room temperature. After incubation, the cells were washed in 0.2% BSA-PBS and PBS as described above, before being mounted onto slides in Low Fade Mounting Medium.

For the detection of F-actin microfilaments, cells were fixed and permeablized as described above and incubated with Rhodamine-conjugated Phalloidin (1:100) for 2 hours at room temperature. Cell nuclei were visualized by counter-staining with Hoechst 33258 (1:10,000; 3 minutes at room temperature). In some other cells, for the detection of cellular acidic compartments, the cells were treated with acidotropic probe Lysotracker Red DND-99 (100 nM) for 30 minutes in complete MEM before being fixed and permeablized.

3.17.4 TRACP cytochemical staining

Cells grown as monolayers or on devitalized bone and dentine slices (150 μm) were stained for tartrate-resistant acid phosphatase (TRACP) using a commercially available kit (387-A; Sigma). In brief, the cells were washed twice with PBS and fixed for 15 minutes in 4% paraformaldehyde. The fixed cells were then washed three times in PBS and incubated for 30 minutes at 37°C in the staining solution. After staining, the cells were rinsed with PBS, photographed and quantified under a light microscope.

3.17.5 Resorption assay

In order to study the ability of osteoclasts to form resorption pits on bone and dentine, osteoclasts were generated either by direct seeding RAW 264.7 cells onto 150 μm thick bone slices and cultured for 9 days in the presence of soluble rat GST-RANKL (100 ng/ml), or by harvesting the pre-cultured osteoclasts, and seeded onto bone slices. The osteoclasts on the bone slices were subsequently fixed (4% paraformaldehyde; 15 minutes) and stained for TRACP activity as described above.

The dentine slices were then incubated in 2M NaOH (2 hours) and the adhered cells were removed by gentle brushing and sonication (Branson Sonifier Cell Disruptor Model B15). Resorption lacunae were processed and visualized with scanning electron microscopy (SEM).

3.18 MICROSCOPY METHODS

3.18.1 Confocal microscopy and, time-lapse live-cell imaging

The detection of fluorochromes was carried out using a confocal laser-scanning microscope (CLSM) (MRC-1000, Bio-Rad) equipped with a krypton-argon laser or a Helium/Neon laser coupled with an epifluorescence Nikon Diaphot 300 inverted microscope. For the detection of immunofluorescent staining and EYFP-signal, a 60X oil immersion objective lens (NIKON, NA= 1.6), 40X UV oil immersion objective lens (NIKON, NA=1.2) and 10X dry lens (NIKON, NA=0.7) were used. 40 serial optical sections (z= 0.1 μm) were acquired satisfying the Nyquist criteria for sampling. The images were recorded in a 512 x 512 pixel format. The confocal images were collected as Bio-Rad PIC files and were analysed by Confocal Assistant 4.02, Adobe PhotoShop® 5.0, COMOS, Scion Image Beta 4.0.2 as well as Ulead iPhoto Express.

3.18.2 Electron Microcopy

For scanning electron microscopy (SEM), the osteoclasts cultured on bone slices were fixed with 4% paraformaldehyde in PBS. Depending on the experiment, the osteoclasts were either left attached to the bone slices or mechanically removed to expose the underlying resorptive lacunae. The bone slices were then washed extensively with PBS and dehydrated in varying grades of ethanol. Following overnight drying at room temperature, the bone slices were subjected to critical point drying before being carbon-coated using the sputter coater. The samples were visualized using an Olympus Scanning electron microscope, and the images were collected as TFF formats and processed using Abode® Photoshop® 5.0.

3.19 STATISTICS AND DATA PRESENTATION

The statistical analysis was performed using paired or unpaired Students' *t*-test with significance taken at $p<0.05$ in Microsoft Office Excel 2003. At lease three independent experiments were conducted. A set of data was then randomly selected from one of the experiments.

CHAPTER 4

Truncation Mutants of RANKL Inhibit RANKL-induced Osteoclast Differentiation and Activation

Key message:

RANKL mutants might potentially serve as peptide mimic to inhibit RANKL-induced signaling, osteoclastogenesis and bone resorption.

CHAPTER 4– TRUNCATION MUTANTS OF RANKL INHIBIT RANKL-INDUCED OSTEOCLAST DIFFERENTIATION AND ACTIVATION

4.1 INTRODUCTION

Osteoclasts are multinucleated giant cells that are exclusively responsible for the degradation of bone matrix. They are formed by the fusion of precursor cells which are derived from the monocyte-macrophage lineage (Teitelbaum, 2000a). Overproduction or activation of osteoclasts occurs in many bone lytic disorders such as osteoporosis, Paget's disease, bone metastatic diseases, arthritis, aseptic bone loosening and non-union of fractures. The receptor activator of NF-κB ligand (RANKL) (Anderson et al., 1997a), also known as osteoprotegerin ligand (OPGL) (Lacey et al., 1998a), TNF-related activation-induced cytokine (TRANCE) (Wong et al., 1997a) as well as osteoclast differentiation factor (ODF) (Yasuda et al., 1998a) is essential for osteoclastogenesis and bone resorption. Mice deficient in *rankl* gene exhibit severe osteopetrosis, defective in tooth eruption, and completely lack osteoclasts as a result of the failure of osteoblasts to support osteoclastogenesis (Kong et al., 1999a). Furthermore, RANKL has been shown to play a role in dendritic cells (Anderson et al., 1997a; Wong et al., 1999b; Wong et al., 1997b), mammary gland development (Fata et al., 2000), lymph-node organogenesis and lymphocyte development (Kong et al., 1999d). RANK, the receptor activator of NF-κB, is the cell surface receptor of RANKL (Hsu et al., 1999a). Like RANKL, RANK knockout mice lack osteoclasts. They have a profound defect in bone resorption and remodeling as well as in the development of cartilaginous growth plates of endochondral bone (Li et al., 2000). Transgenic mice expressing a soluble RANK-Fc fusion protein display osteopetrosis, and have a defect of osteoclast activity (Hsu et al., 1999a). In addition to their role in osteoclast physiology, recent studies have shown that RANKL is involved in cell migration and the metastatic behaviour of cancer cells (Jones et al., 2006). Enhanced expression of RANKL and RANK has been found in a number of pathological bone lytic diseases such as giant cell tumor of bone (Huang et al., 2000), periodontal disease (Liu et al., 2003), and multiple myeloma (Roux et al., 2002). Thus, it is clear that the modulation of RANKL and RANK function is critical for the regulation of osteoclastogenesis and bone resorption.

RANKL is a type II transmembrane protein that consists of a short N-terminal

cytoplasmic domain and a conserved extracellular, a receptor binding domain that defines this molecule as a member of the TNF family (Lacey et al., 1998a; Xu et al., 2000b; Yasuda et al., 1998a). The receptor-binding domain consists of antiparallel b sheet that assembles into a trimer required for receptor activation (Ito et al., 2002; Lam et al., 2001a). RANK, the functional receptor of RANKL, is a type I transmembrane protein with a single transmembrane domain that separates the molecule into an extracellular and intracellular domain (Anderson et al., 1997a). The extracellular domain shares sequence homology with those of the TNF receptor (TNFR) family members, and which is the domain responsible for binding to its active ligand RANKL. The intracellular domain contains binding sites for TNFR-associated factors (TRAFs) which is important for the initiation of a receptor-mediated signal transduction cascade and the activation of NF-κB, c-Jun N-terminal kinase (JNK) and ERK (Anderson et al., 1997a; Galibert et al., 1998, Li, 2000 #46; Wang et al., 2003b}). In the present study, it is aimed to investigate whether truncation mutants of RANKL within the TNF-like core domain alter the biological activities, their binding to receptor RANK, and the activation of signaling pathways. More importantly, also it was evaluated whether RANKL mutants might potentially serve as peptide mimic to inhibit RANKL-induced signaling, osteoclastogenesis and bone resorption.

4.2 RESULTS

4.2.1 Truncation mutants of RANKL impair osteoclastogenesis

Previous mutagenesis and structural analysis have revealed that the TNF-like core domain of RANKL is essential for its signaling during osteoclastogenesis and bone resorption (Lacey et al., 1998a; Xu et al., 2000b) (Figure 4.1A). Therefore, in an effort to dissect the minimal structural domain or amino acid required for RANKL signaling, a mutagenesis approach was employed by truncating the domains for RANKL. A total of 5 truncation mutants (aa160-302), (aa160-268), (aa239-318) and (aa246-318) were constructed and all were expressed as GST fusion proteins (Figure 4.1B). As shown in Figure 4.1B and C, RANKL mutant (aa160-300) carried a deletion of bH strand on the C-terminal of the TNF-like core domain. Mutant (aa160-268) carried a deletion of bF, bG and bH strands, also on the C-terminal of the TNF-like core domain. Mutant (aa239-318) had a deletion of bA, AA' loop, bB, bC and CD loop, whereas mutant (aa246-318) had a deletion of bA, AA' loop, bB, bC, CD loop and bD. Both deletions are on the N-terminal end of the TNF-like core domain. The GST fusion proteins of various RANKL mutants were stably expressed in bacteria and soluble forms of recombinant. All RANKL mutants were affinity-purified to greater than 95% purity as determined by SDS-PAGE (Figure 4.2A). Furthermore, western blot analysis using a specific monoclonal antibody to RANKL was performed and the results confirmed the identity of the GST-RANKL recombinant proteins (Figure 4.2B).

4.2.2 Predicted structure of RANKL mutants and their binding to receptor RANK

As a first step towards validating the biology activity of GST-RANKL mutants, their ability to associate with their cognate receptor RANK was examined using *in vitro* GST-pull down assays. Based on the crystal structure of wild type RANKL (Ito et al., 2002; Lam et al., 2001a), the proposed structure of RANKL mutants was generated (Figure 4.3). As expected, each RANKL mutant protein showed structure characteristics of its own due to the various truncation mutations on the TNF-like core domain. Next, it was aimed to examine how each RANKL mutant interacts with the receptor RANK using a GST pull down assay as described in materials and method. COS-1 cells were transfected with an expression construct pFlag-RANK (aa34-616) and an equal amount of cell lysates was applied to 5 mg of GST-RANKL mutants (aa160-302), (aa160-268),

Figure 4.1

Figure 4.2

(aa239-318) and (aa246-318) which were previously immobilized to agarose beads. The interaction complexes were separated by SDS-PAGE and analyzed by Western blot using the anti-Flag monoclonal antibody. The results showed all RANKL mutants (aa160-302), (aa160-268), (aa239-318) and (aa246-318) were capable of binding to the receptor RANK differentially, whereas GST alone did not have any binding ability (Figure 4.4). However, compared with full length RANKL (aa160-318), RANKL mutants (aa160-302), (aa160-268), (aa239-318) and (aa246-318) showed various levels of binding affinity to Flag-RANK (aa34-616). Truncation mutants of RANKL exhibited differential affinity to RANK and impair osteoclastogenesis *in vitro*.

4.2.3 The effect of RANKL mutants on osteoclastogenesis

Having validated their biological interaction, it was aimed to explain their ability to induced osteoclast formation *in vitro*. For this purpose, RAW264.7 cells were stimulated with either full length (aa160-318) or truncation mutants. After 5 days, cells were fixed and stained with TRACP to assess potential osteoclastogenesis. As shown in Figure 4.5A and B, RANKL mutants (aa160-302), (aa160-268), (aa239-318) and (aa246-318) induced lower levels of OCL cell formation compared with full length RANKL (aa160-318). The treatment with GST alone showed no TRACP-positive cells. In addition, the TRACP-positive multinucleated cells induced by RANKL mutants were smaller and have less multinucleation when compared to well-spread osteoclasts induced by the full length RANKL (Figure 4.5A). In order to confirm the reduced inductive effects of RANKL mutants on osteoclastogenesis, the gene expression of calcitonin receptor and cathepsin K, the specific marker genes for osteoclast differentiation was examined. The total RNA was isolated from RAW264.7 cells treated with RANKL mutants, and semi-quantitative RT-PCR was performed. The results demonstrated that RANKL mutants were exhibiting reduced gene expression of cathepsin K and calcitonin receptor compared with full length of RANKL (Figure 4.5 C).

4.2.4 The effect of RANKL mutants on osteoclast maturation and bone resorption

The previous experiments clearly demonstrate that RANKL mutants exhibited dramatic reduction on OCLs formation. However, it is not conclusive that OCLs induced by RANKL mutants are functional osteoclasts. To address this question, RAW264.7 cells

Figure 4.3

Figure 4.4

Figure 4.5A and B

Figure 4.5C

were directly cultured on bone slices in the presence of RANKL mutants and examined the formation of F-actin ring and bone pits. At this stage, RAW264.7 cells were seeded on bone slices and treated with each RANKL mutants subsequently. After 15 days, bone slices were fixed with paraformadelhyde and stained with antibody to F-actin. The formation of the F-acting rings was examined by confocal microscopy. As shown in Figure 4.6A, OCLs from the RANKL mutant treatment groups did not form F-actin ring structure, where as RANKL wild type formed typical F-actin ring, a maker for actively resorbing osteoclasts. Using scanning electron microscopy, it was confirmed that OCLs induced by RANKL mutants did not exhibit any bone pits as compared with wild type RANKL-treated OCLs which showed significant numbers of bone pits (Figure 4.6B). Collectively, these results indicated that RANKL mutants have impaired ability to generate functional osteoclasts.

4.2.5 The effect of RANKL mutants on the induction of key RANKL signaling pathways: NF-κB, IκBα, ERK and JNK

It is well established that RANK is able to recruit members of the TRAF adapter proteins including TRAF6 and TRAF2 for the activation of NF-κB, ERK and JNK (Darnay et al., 1998; Galibert et al., 1998; Wang et al., 2003b; Zhang et al., 2001). In order to investigate the effects of RANKL mutants on major signal transduction pathways involved in osteoclastogenesis, NF-κB, ERK, JNK activity and IkBα degradation were examined. In the study of NF-κB activation by RANKL mutants, a stable RAW264.7 cell line transfected with a *3κB-Luc-SV40* expression construct was employed. The transfected RAW264.7 cells were then treated with 200 ng/ml of RANKL mutants (aa160-302), (aa160-268), (aa239-318) and (aa246-318), and harvested at 1 hour and 24 hour time points. The NF-κB activation was measured by the NF-κB reporter construct for luciferase activity. The results showed that after 24 hours of stimulation, RANKL mutants (aa160-302), (aa160-268), (aa239-318) and (aa246-318) were able to induce the activation of NF-κB, but significantly reduced the NF-κB activity compared with full length RANKL (aa160-318). GST protein alone had no significant effect on NF-κB activity (Figure 4.7A). To exclude the possibility that the reduced effect of RANKL mutants on NF-κB activation was due to endotoxin contamination, an endotoxin assay was also performed. The results show that all RANKL mutants and GST have comparable levels of endotoxin activities ranging from 24-86 pg/ml in stock which was diluted at least 1/100 dilution for a final working

Figure 4.6A

Figure 4.6B

concentration. It is important to note that, at these levels, GST alone did not induce the activation of NF-κB in RAW264.7 cells (Figure 4.7A) indicating that the activation of NF-κB induced by RANKL mutants was not due to endotoxin contamination.

The activation of ERK and IκBα degradation by RANKL mutants were also examined by immunoblotting. RAW264.7 cells were treated with RANKL mutants (aa160-302), (aa160-268), (aa239-318) and (aa246-318), wild type RANKL (aa160-318) or GST for 30 mins and then harvested. The results demonstrated that RANKL mutants (aa160-302), (aa160-268), (aa239-318) and (aa246-318) have attenuated effects on ERK phosphorylation and IκBα degradation compared with wild type RANKL (aa160-318) (Figure 4.7B). It appeared that mutant (aa246-318) has the least effect on IκBα degradation but has the greatest effect on the induction of ERK phosphorylation (Figure 4.8A). These results suggested that the mutant (246-318) might alter the NF-κB but ERK signaling pathway independently. Thus, the truncated domain of the mutant might be important for NF-κB signaling pathway.

Finally, the effect of RANKL mutant on JNK activation was examined using c-Jun kinase assay. RAW264.7 cells were treated with RANKL mutants (aa160-302), (aa160-268), (aa239-318) and (aa246-318), full length RANKL (aa160-318) or GST for 15 mins and harvested. The c-Jun kinase assay was performed and the results demonstrate that RANKL mutants (aa160-302), (aa160-268), (aa239-318) and (aa246-318) significantly reduce JNK activation as compared with full length RANKL (aa16-318) (Figure 4.8B).

4.2.6 RANKL mutants competitively inhibit RANKL-induced osteoclastogenesis and bone resorption

Although RANKL mutants were able to bind to RANK and had reduced osteoclast formation and signaling, the OCLs generated failed to resorb bone. Therefore, it was reasoned that RANKL mutants might act as competitive inhibitors effect with the wild type RANKL. To examine this possibility, the effect of RANKL mutants on RANKL-induced osteoclastogenesis was tested using RAW264.7 cells culture. At this stage, RAW264.7 cells were pretreated with various concentration of RANKL mutants (aa160-302), (aa160-268), (aa239-318) and (aa246-318) for 1 hour before 100 ng/ml of full length RANKL (aa160-318) was added during osteoclastogenesis. After 5 days of

Figure 4.7

Figure 4.8

culture, TRACP staining was performed and TRACP-positive OCLs were counted. As shown in Figure 4.9, RAW264.7 cells pretreated with RANKL mutants have significantly fewer OLCs compared to RAW264.7 cells treated with wild type RANKL alone, or pretreated with GST control. Among the mutants tested, mutant (aa246-318) exhibited the most potent inhibitory effects on RANKL-induced osteoclastogenesis. In addition to using a 1:1 ratio of RANKL mutants and full length RANKL, the effect of RANKL mutants on RANKL-induced osteoclastogenesis was also examined using a ratio of 1:2 (50 ng/ml of RANKL mutants and 100 ng/ml of wild type RANKL). The results demonstrated a similar trend of inhibitory effects. Furthermore, morphologically, the TRACP-positive cells induced by the pretreatment of RANKL mutants were smaller and had less cell fusion compared to the multinucleated, well-spread osteoclasts that were induced by full length RANKL alone or with GST control. These results indicate that RANKL mutants act as competitive inhibitors against RANKL-induced osteoclastogenesis.

Having established that RANKL mutants inhibit wild type RANKL-induced osteoclastogenesis, next the combined effect of RANKL mutants on RANKL-induced osteoclastic bone resorption was examined. Given RANKL mutant (aa246-318) has the least ability to induce the formation of TRACP cells but the most potent inhibitory effect on RANKL-induced osteoclastogenesis, this mutant was further tested on RANKL-induced osteoclast bone resorption. Isolated rat osteoclasts were cultured on bone slices in the presence of full length RANKL (aa160-318), RANKL mutant (aa246-318) or in combination. The resorption pits were counted and the results showed that RANKL mutant (aa246-318) significantly impaired the number of resorption pits per osteoclasts induced by wild type RANKL (aa160-318) (Figure 4.10).

Finally, rRANKL5 (aa246-318) was examined to determine whether it competes with full-length RANKL to bind to the RANK receptor. To this end, the full-length rRANKL (aa160-318) was labelled with Alexa Fluor 488. RAW264.7 cells were seeded on the glass overnight and then simulated with labelled RANKL-Alexa 488 for 5 to 45 minutes following a temperature shift (37^{o}C). The internalization of Alexa Fluor 488-labelled GST-rRANKL in RAW264.7 cells were analysed using confocal microscopy. The results showed that Alexa Fluor 488-labelled GST-rRANKL was first appeared on the cell surface and internalized overtime time from 15 to 45 minutes (Figure 4.11A). Next, the competition binding of mutants and full-length rRANKL to the receptor

RANK was examined by FACS analysis. RAW264.7 cells were separately pre-treated with GST (10ug) and rRANKL5 (aa246-318) (10 and 20ug) for 1 hour at 4^{o}C. OPG (1ug) was mixed with rRANKL (500ng) for 1 hour prior adding to the cells suspension. The cells were separately treated with a labelled RANKL-Alexa 488 and, a mixture of OPG and labelled rRANKL-Alexa 488 for 1 hour at 4^{o}C and 30 minutes at 37^{o}C. The cells were then fixed with 4% paraformaldehyde and analysed by using FACS calibur to detect the fluorescence of the Alexa Fluor 488. The results were shown in graphs which represent the negative (no labelled RANKL-Alexa 488 were added) and positive (labelled rRANKL-Alexa 488 were added) controls (Figure 4.11B). Overall, it showed that rRANKL5 (aa246-318) at 20 ug decreased 23% of labelled rRANKL-Alexa 488 signal. OPG, as a positive control caused 80% reduction of labelled rRANKL-Alexa 488 signal (Figure 4.11C).

Figure 4.9

Figure 4.10

Figure 4.11

4.3 DISCUSSION

Increasing evidence has indicated that peptide sequences (mimotopes), which mimic conformational epitopes of ligand-receptor interactions, are able to block the biological activities of cytokines (Partidos et al., 1997; Partidos and Steward, 2002). Recently, a TNF receptor loop peptide mimic was found to be capable of blocking bone resorption by interfering with the recruitment and activation of osteoclasts by both RANKL and TNF (Aoki et al., 2006). Given the essential role of RANKL in osteoclast formation and activation, the characterization of the structural and functional relationship of RANKL and its biological function might allow the development of small molecule mimetics for the specific inhibition of RANKL action on its active targets. In this study, it was documented, for the first time, that the truncation mutants of RANKL within the TNF-like core domain showed impaired osteoclastogenesis and bone resorption compared with the wild type RANKL. The impaired function of RANKL mutants correlated well with their reduced effect on RANK signaling including NF-κB, IκBα, ERK and JNK. Interestingly, these truncation mutants are able to bind to RANK. Thus, although RANKL mutants are capable of binding and activating RANK signaling at various degrees, they are insufficient for the complete induction of osteoclastogenesis and bone resorption. These observations suggested that RANKL mutants might serve to mimic binding to RANK and act as competitive inhibitory peptides with wild type RANKL.

In supporting of this notion, it was found that RANKL mutants were capable of effectively blocking wild type RANKL-induced osteoclast formation. Among the four RANKL mutants examined, mutant RANKL5 (aa246-318), which displayed the least effect on osteoclastogenesis, exhibited the most potent inhibitory action on wild type RANKL-induced osteoclast formation. RANKL5 was also found to inhibit the wild type RANKL-induced bone resorption. Thus, these data suggested that RANKL mutants could act as inhibitory peptides for RANKL-induced osteoclast formation and function. these findings are consistent with previous studies which showed that naturally occurring shorter isoforms of RANKL have no effect on the formation of preosteoclasts or osteoclasts, but significantly inhibit fusion of preosteoclasts when co-expressed with full length RANKL (Ikeda et al., 2003).

Structural studies on the mouse RANKL extracellular domain have revealed that

RANKL exists as a trimer. Each subunit has a beta-strand jellyroll topology resembling other members of the TNF family (Ito and Hata, 2004). The nature of the binding of RANKL to RANK has not been determined but is likely to resemble the interaction of TNF and TNF receptor. The crystal structure of soluble TNF 55-kDa receptor with TNF-ß revealed that the binding of cytokine to its receptor occurs over large surface areas of both ligand and receptor, notwithstanding that certain amino acid residues were believed to be more important for the ligand-receptor interaction (Banner et al., 1993). Recently, the crystallization of the ectodomain of murine RANKL revealed that RANKL self-associates as a homotrimer with four unique surface loops that distinguish it from other TNF family cytokines as well as having conserved features of RANKL in the TNF superfamily (Ito et al., 2002; Lam et al., 2001a). Structural analysis has predicted that several residues in RANKL are likely to be important for the ligand-receptor interaction. These residues include Ile-248 in the DE loop for a conserved interaction, Gln-236 in the N-terminal region of the D strand, and Lys-180 in the AA" loop for the specific interaction. All three of these residues are conserved in mouse, human and rat RANKL (Ito et al., 2002). The rat RANKL mutants (aa239-318) and (aa246-318) contain the deletion of both AA’ loop and CD loop, and the deletion of residues Lys-180 and Gln-236. The RANKL mutant (aa160-302) carried a deletion of bH whereas the RANKL mutant (aa160-268) has a deletion of bF, bG and bH. Under normal conditions, RANKL self-associates as a homotrimer with four unique surface loops. It has been speculated that the disruption of any of these loops could affect the trimeric formation of RANKL and their biological function. The functional analyses on the RANKL mutants are consistent with previous reports which showed that mutations in the DE loop, AA" loop of RANKL failed to induce differentiation of osteoclast precursors *in vitro* (Lam et al., 2001a). Thus, it is possible that the binding of RANKL mutants to RANK might interfere with the complete assembly of the trimeric structure of RANKL/RANK interaction. Further studies on the crystal structure of RANKL mutants and RANKL/RANK interaction will be an important tool in elucidating the structural and functional relationship.

RANKL/RANK/OPG has been a major axis in osteoclast formation and activation. The truncation and point mutation of OPG have been shown to impair both the secretion and activity of OPG associated with the increased osteoclastogenesis and high bone turnover observed in juvenile Paget's disease (Janssens et al., 2005; Middleton-Hardie et al., 2006). The deletion mutants of RANK have been used to identify motifs that play a

crucial role in osteoclast differentiation and function (Xu et al., 2006).

In conclusion, this study highlights the potential of RANKL mutant molecules in blocking the deleterious biological effects of RANKL-induced osteoclastogenesis and bone resorption. Studies on the structural determinants of RANKL-RANK interaction could facilitate the pharmacological design of small molecule mimetic to block RANKL activity and hence, alleviate osteoporotic disorders of bone.

CHAPTER 5

Evidence of Reciprocal Regulation Between the High Extracellular Calcium and RANKL Signal Transduction Pathways in RAW264.7 Cell Derived Osteoclasts

Key message:

A cross talk mechanism between extracellular Ca2+ and RANKL exist to regulate on osteoclast survival.

CHAPTER 5– EVIDENCE OF RECIPROCAL REGULATION BETWEEN THE HIGH EXTRACELLULAR CALCIUM AND RANKL SIGNAL TRANSDUCTION PATHWAYS IN RAW264.7 CELL DERIVED OSTEOCLASTS

5.1 INTRODUCTION

Osteoclasts are derived from the cells of monocyte-macrophage lineage and as bone-resorbing cells, they play a critical role in bone morphogenesis and remodeling (Teitelbaum, 2000b). During osteoclastic bone resorption, crystal hydroxyapatite is dissolved into free Ca^{2+} ions in the resorptive hemivacuole where it can reach concentration levels as high as 40mM (Silver et al., 1988a). High extracellular Ca^{2+} has been shown to trigger an increase in cytosolic Ca^{2+} through Ca^{2+} release from internal stores and/or Ca^{2+} influx, and this results in the inhibition of bone resorption (Zaidi et al., 1999b; Zaidi et al., 1999c) and induction of osteoclast apoptosis (Lorget et al., 2000).

As osteoclasts are able to migrate to new sites on the bone surface after the completion of bone resorption, it is reasonable to speculate that regulatory mechanisms do exist enabling osteoclasts to tolerate high levels of Ca^{2+} in their immediate microenvironment. Indeed, it has been reported that high Ca^{2+} enhances IL-6 secretion which, via autocrine and paracrine loops, attenuates Ca^{2+} sensing and thus reverses the inhibition of bone resorption (Adebanjo et al., 1998).

Receptor activator of NF-kappa B ligand (RANKL), a membrane-bound TNF-like ligand expressed by osteoblasts, is required for the differentiation and maintenance of osteoclasts (Burgess et al., 1999b; Kong et al., 1999c; Lacey et al., 1998b; Yasuda et al., 1998b). In addition, RANKL has been found to be an important regulator of Ca^{2+} homeostasis (Burgess et al., 1999b; Xu et al., 2000a). Recent studies have demonstrated that high extracellular Ca^{2+} increased the expression of RANKL mRNA in osteoblasts (Takami et al., 2000a), providing evidence for a paracrine regulation of RANKL by elevated extracellular Ca^{2+} and hence, also osteoclast function and survival. However, the role of RANKL in osteoclast tolerance to elevated extracellular Ca^{2+} and the effect of high extracellular Ca^{2+} on RANKL-induced signaling pathways have yet to be examined.

In this study it was demonstrated that RANKL attenuates high Ca^{2+}-induced cytosolic Ca^{2+} elevation and, in a dose-dependent manner, protects osteoclasts from high extracellular Ca^{2+}-induced cell loss. High extracellular Ca^{2+} suppressed RANKL-induced NF-κB, Jun amino-terminal kinase (JNK) and ERK signaling. This study thus provides evidence for a reciprocal regulation of the elevated extracellular Ca^{2+} and RANKL signaling pathways.

5.2 RESULTS

5.2.1 RANKL protects osteoclasts from high extracellular Ca2+-induced cell death

In the present study, RAW264.7 cells were cultured in the presence RANKL to generate OCLs. As shown in Figure 5.1A and B, the RAW264.7 cell derived OCL exhibited multinucleated TRACP positive staining as well as expressed both calcitonin receptor mRNA as shown by RT-PCR, and calcitonin receptor protein as detected by immuno-localization (Figure 5.1C and D). When cultured on the bovine bone slices in the presence of RANKL for 7 days, the RAW264.7 cells derived OCLs showed strong TRACP positive staining (Figure 5.1E) and were capable of forming bone resorbing pits (Figure 5.1F). Quantitative analyses showed that the average pit number per OCL was 0.75±0.25 based on six separate experiments, suggesting that a significant portion of the multinucleated TRACP positive cells were capable of resorbing bone.

In order to examine the inter-relationship between RANKL and high extracellular Ca^{2+} in the regulation of osteoclast survival, the RAW264.7 cell-derived OCLs were harvested and exposed to a range of Ca^{2+} concentration levels (1.8, 6.8, 11.8 and 21.8 mM) in the presence or absence of 100 ng/ml of RANKL, fixed and stained for TRACP activity after 24 hours of treatment (Figure 5.2). The exposure of RAW264.7 cells to elevated extracellular Ca^{2+} led to a dose-dependent loss of TRACP positive OCLs as a result of the cell detachment and/or cell death (Figure 5.2A). RANKL was found to have a dose-dependent, protective effect against the loss of these TRACP positive cells induced by the exposure to 11.8 and 21.8 mM extracellular Ca^{2+} (Figure 5.2B).

In determining whether the loss of OCLs by elevated extracellular Ca^{2+} was due to apoptosis, the RAW264.7 cell derived OCLs were exposed to 11.8 and 21.8 mM of Ca^{2+} in the presence or absence of a caspase 3/7 inhibitor called Ac-DEVD-CHO (100 μM) for 24 hours. The treated cells were fixed and stained for TRACP activity. The caspase 3/7 inhibitor reduced Ca^{2+}-induced cell death (Figure 5.3), indicating that Ca^{2+}-induced osteoclast death was mediated at least in part by an apoptotic pathway.

Figure 5.1

Figure 5.2

Figure 5.3

5.2.2 RANKL attenuates high extracellular Ca^{2+}-induced cytosolic Ca^{2+} elevation

In investigating the mechanism in which RANKL protects osteoclasts from elevated extra cellular Ca^{2+}-induced death, single cell cytoplasmic Ca^{2+} flux experiments were performed. The application of 20 mM Ca^{2+} to OCLs elicited a fast elevation of intracellular Ca^{2+} in all the cells that were tested. This Ca^{2+} response was sensitive to the phospholipase C inhibitor U73122 (data not shown), as previously reported (Bennett et al., 2001). The extracellular Ca^{2+}-induced intracellular Ca^{2+} response was repeatable and no significant change in the amplitude of the responses was observed in the subsequent trials after a 10-min wash (ratio of 2^{nd} trial to 1^{st} trial and 3^{rd} trial to 1^{st} trial was 0.95 ± 0.15 and 0.97 ± 0.23, respectively; n=5; p=0.42).

Hence, the effect of RANKL on extracellular Ca^{2+}-elicited cytosolic Ca^{2+} elevation was examined in OCLs by pre-treatment of the OCLs with RANKL (100 ng/ml) for 5 minutes before the 2^{nd} trial. In 7 out of 15 OCLs tested, RANKL (100 ng/ml) almost completely suppressed 20 mM Ca^{2+}-induced Ca^{2+} elevation (ratio of 2^{nd} trial to mean of the 1^{st} and 3^{rd} trials: 0.03 ± 0.11, $p<0.0001$) (Figure 5.4A). In two other cells, RANKL partially inhibited the Ca^{2+}-induced intracellular Ca^{2+} responses (ratio of 2^{nd} trial to mean of the 1^{st} and 3^{rd} trials: 0.28 ± 0.14) (Figure 5.4B). And in the remaining six cells, RANKL had no significant inhibitory effect on these Ca^{2+} responses (ratio of 2^{nd} trial to mean of the 1^{st} and 3^{rd} trials: 0.98 ± 0.09, p=0.17) (Data not shown). These results suggested that RANKL was capable of markedly attenuating Ca^{2+}-induced intracellular Ca^{2+} elevation in a significant proportion of RAW264.7 cell derived OCLs.

5.2.3 High extracellular Ca2+ inhibits RANKL-induced activation of NF-κB

The activation of the RANK signaling pathway leads to the NF-κB dependent formation and activation of osteoclasts, which in turn results in increased bone resorption and the production of high extracellular Ca^{2+} in the local environment. In order to determine whether high extracellular Ca^{2+} might negatively regulate the RANKL-induced NF-κB signaling pathway, the osteoclast precursor RAW264.7 cells were transiently transfected with a NF-κB luciferase reporter gene, and treated with various doses of Ca^{2+} in the

Figure 5.4

presence or absence of different concentrations of RANKL. At the physiological concentration level of Ca^{2+} (1.8 mM), RANKL dose dependently induced NF-κB activation (Figure 5.5, first bar of each group of bars). At the physiological concentration level of Ca^{2+} (1.8 mM), the extent to which RANKL induced NF-κB activation depends on its dosage. Extracellular Ca^{2+} had no significant effect on the constitutive NF-κB activity (Figure 5.5, first group of bars). However, the extent to which it inhibited RANKL-induced NF-κB transcriptional activity is dose-dependent (Figure 5.5).

5.2.4 High extracellular Ca2+ inhibits RANKL-induced JNK signaling and ERK signaling

The RANK/TRAF6/JNK/AP-1/c-Fos cascade is an important signaling pathway in RANKL-mediated osteoclast formation and survival (David et al., 2002a; Johnson et al., 1992a; Kim et al., 1999b; Lomaga et al., 1999b; Wang et al., 1992b). In examining the effect of extracellular Ca^{2+} on JNK activation induced by RANKL, the osteoclast precursor RAW264.7 cells were transiently transfected with an AP-1 driven luciferase reporter gene construct, and then treated separately with RANKL, Ca^{2+} or RANKL plus Ca^{2+}. At the physiological concentration level of Ca^{2+} (1.8 mM, as a control), RANKL doses-dependently, induced AP-1 transcriptional activity (Figure 5.6B, second bar of each group of bars). Figure 5.6A and B show that increasing concentrations of Ca^{2+} reduced both constitutive and RANKL-activated AP-1 activity.

The activation of ERK is one of the signaling events induced by the interaction between RANKL and RANK. In order to examine the effect of Ca^{2+} on RANKL-induced ERK activation, the osteoclast precursor RAW264.7 cells were treated separately with RANKL, Ca^{2+} or RANKL plus Ca^{2+} for 0-30 minutes. Western blot analysis using an antibody to phosphorylated ERK showed that 11.8mM Ca^{2+} inhibited basal levels of ERK phosphorylation (Figure 5.7A, lanes 2-3) as well as RANKL-induced activation of ERK (Figure 5.7A lanes 4-5). These results indicated that high extracellular Ca^{2+} has a negatively regulatory effect on the basal levels and RANKL-stimulated ERK pathway (Figure 5.7).

Figure 5.5

Figure 5.6

Figure 5.7

5.3 DISCUSSION

During bone resorption, the dissolution of crystalline hydroxyapatite by osteoclasts results in an accumulation of extracellular Ca^{2+} (up to 40 mM) within the isolated resorbing compartment (Silver et al., 1988a). High extracellular Ca^{2+}, when added to osteoclast culture, leads to a rapid rise in cytosolic Ca^{2+} levels which in turn induces cell retraction and apoptosis as well as suppresses bone resorption (Lorget et al., 2000; Zaidi et al., 1999b; Zaidi et al., 1999c). In addition, high extracellular Ca^{2+} inhibits osteoclast formation by directly acting on the Ca^{2+}-sensing receptor of osteoclast precursor cells (Kanatani et al., 1999).

In response to high Ca^{2+}, it has been shown that osteoclasts enhance the production and secretion of IL-6 to overcome the inhibitory effects, via autocrine and paracrine loops during bone resorption (Adebanjo et al., 1998). Furthermore, recent studies have demonstrated that high extracellular Ca^{2+} enhanced the expression of RANKL mRNA in osteoblasts (Takami et al., 2000a). This study confirmed that high extracellular Ca^{2+} induced loss of OCLs is at least in part due to the apoptosis (Lorget et al., 2000). It was demonstrated that RANKL protects against high extracellular Ca^{2+}-induced loss of OCLs, indicating a paracrine action of RANKL on combating the deleterious effects of elevated extracellular Ca^{2+} on osteoclasts.

RAW264.7 cells are a convenient model system to study osteoclast biology and have been widely used to investigate osteoclastogenesis, signaling transduction pathways and bone resorption (Hotokezaka et al., 2002b; Hsu et al., 1999c; Matsumoto et al., 2000b; Wang et al., 2003a). RAW264.7 cell derived multinucleated TRACP positive cells have many characteristics of osteoclasts, but OCLs might not apply equally to authentic osteoclasts under physiological conditions.—Therefore, this system has its own limitation. *In vivo* it appears that osteoclasts are exposed to high extracellular Ca^{2+} generated due to hydroxyapatite dissolution at the ruffled border, whereas the experimentally added extracellular Ca^{2+} is spread out around the apical surface of osteoclasts. Notably, osteoclasts are motile cells *in vivo*. Upon the completion of bone resorption, osteoclasts migrate to other bone surfaces, and the resorptive compartment is opened up to the bone marrow microenvironment. Thus, Ca^{2+} is released locally to generate high extracellular Ca^{2+} gradients which can affect the neighboring osteoclasts. The experimentally added extracellular Ca^{2+} therefore might mimic these temporal

events during osteoclast function.

The mechanism in which high extracellular Ca^{2+} induces the elevation of intracellular Ca^{2+} is complex and involves both Ca^{2+} influx through Ca^{2+} capacitive entry as well as Ca^{2+} release from internal stores. Several pathways have been shown to be involved in the capacitative Ca^{2+} influx in osteoclasts, including a ryanodine receptor-like protein (Zaidi et al., 1995), receptor operated channels (Bennett et al., 2001) and the Ca^{2+}-sensing receptor (CaR) (Kameda et al., 1998; Kanatani et al., 1999). It is well established that elevations in extracellular Ca^{2+} induce intracellular Ca^{2+} signals through interactions between CaR and phospholipase C (PLC), which is mediated by heterotrimeric G proteins (Kifor et al., 1997). The activation of CaR recruits G_{qa} and leads to the hydrolysis of PtdIns $(4,5)P_2$ by PLC to form inositol-1,4,5-trisphosphate and diacylglycerol ($Ins(1,4,5)P_3$) (Hofer and Brown, 2003).

In addition, CaR interacts with G_{ia}, which resulting in the inhibition of adenylate cyclase and a reduction in the cellular cyclic AMP levels (De Jesus Ferreira and Bailly, 1998; de Jesus Ferreira et al., 1998). Furthermore, the interaction between CaR and G_{qa} has been shown to activate MAPK signaling pathways including ERK and JNK (Arthur et al., 2000; Hobson et al., 2003; McNeil et al., 1998). In this study, it was observed that high extracellular Ca^{2+} had a dramatic effect on the induction of calcium elevation in RAW264.7 cell-derived OCLs (Figure 5.4) but had weak to marginal negative effects on the basal levels of NF-κB, JNK and ERK in these cells (Figure5.5-7).

RANKL, a key cytokine for osteoclast formation and activation, is expressed by osteoblasts and stromal cells, and plays a role in increased bone resorption and Ca^{2+} homeostasis (Burgess et al., 1999b; Xu et al., 2000a). The NF-κB activation by RANKL is required for osteoclast formation and survival (Boyce et al., 1999a; Franzoso et al., 1997c; Hsu et al., 1999c; Iotsova et al., 1997b; Jimi et al., 1999c; Lacey et al., 1998b). The signaling pathways mediated by RANK/TRAF6/JNK/AP-1 are also known to have a critical role in osteoclast function as both TRAF6 and *c-fos*-deficient mice develop osteopetrosis (David et al., 2002a; Johnson et al., 1992a; Kim et al., 1999b; Lomaga et al., 1999b; Wang et al., 1992b).

These studies have shown that high extracellular Ca^{2+} inhibited both RANKL-induced activation of NF-κB and AP-1, thus acting as a negative feedback mechanism. However,

it is not known which pathway is employed by RANKL to attenuate the Ca^{2+}-induced Ca^{2+} elevation. Recent studies reported that RANKL elevated cytosolic Ca^{2+} by releasing it from intracellular stores via a PLC pathway, resulting in increased NF-κB nuclear translocation and transcription which in turn promoted osteoclast survival under normal Ca^{2+} concentration (Komarova et al., 2003). Similarly, it was found that RANKL activated NF-κB, JNK and ERK signaling and increased the survival rate of RAW264.7 cell-derived OCLs.

Surprisingly, significant changes in cytosolic Ca^{2+} in response to RANKL was not observed under the physiological concentration level (1.8 mM) of Ca^{2+} using RAW264.7 cells or RAW264.7 cell-derived OCLs. This indicated that RANKL-induced NF-κB activation in RAW-derived OCLs was independent of the elevation of cytosolic Ca^{2+}.

In fact, only partial inhibitory effects on NF-κB activation and on osteoclast survival were seen when calcium blockers were used (Komarova et al., 2003). These studies suggested that OCLs derived from RAW264.7 cells may behave differently with respect to RANKL-induced calcium elevation compared to the isolated rat osteoclasts used by Komarova et al (Komarova et al., 2003). A possibility made more likely considering that RAW264.7 cells originate from an immortalized cell line.

In summary, this study highlighted the reciprocal regulation of high extracellular Ca^{2+} and RANKL signaling pathways. While RANKL protected osteoclasts from high Ca^{2+}-induced cell death, RANKL also increased osteoclast mediated bone resorption. This resulted in increased extracellular Ca^{2+} which in turn suppressed the NF-κB and JNK signaling pathways as well as triggered osteoclast apoptosis. Thus, the cross-talk between extracellular Ca^{2+} and RANKL signaling pathways plays an important role in the regulation of osteoclast function.

CHAPTER 6

12-O-Tetradecanoylphorbol-Acetate (TPA) Inhibits Osteoclastogenesis by Suppressing RANKL-induced NF-κB Activation

Key message:

TPA suppressed RANKL-induced osteoclastogenesis predominantly during the early stage of osteoclast differentiation via modulation of NF-κB.

CHAPTER 6– 12-O-TETRADECANOYLPHORBOL-ACETATE (TPA) INHIBITS OSTEOCLASTOGENESIS BY SUPPRESSING RANKL-INDUCED NF-KB ACTIVATION

6.1 INTRODUCTION

Osteoclasts are multinucleated giant cells that resorb bone and are derived from monocyte-macrophage lineage cells (Teitelbaum, 2000a). The protein kinase C (PKC) pathway has been suggested to be an important regulator of osteoclastic bone resorption (Su et al., 1992). 12-0-tetradecanoyl phorbol-13-acetate (TPA), an activator of PKC, decreased osteoclastic bone-resorbing activity (Mano et al., 2000). A synthetic peptide fragment called PKC (530-558) activates PKC and significantly inhibits osteoclastic bone resorption. However, this effect is negated in the presence of another synthetic peptide fragment named PKC (19-36). The latter inhibits PKC, suggesting an important physiological role for the PKC pathway in osteoclast function (Moonga and Dempster, 1998). More evidence was provided by synthetic diacylglycerols through its inhibition of bone resorption. The former are analogues of the physiological activators of PKC (Moonga et al., 1996). Nevertheless, to date, the mechanisms of PKC activation in the signaling pathways during osteoclastogenesis are not well established.

The receptor activator of NF-κB ligand (RANKL/OPGL/ODF/TRANCE), a member of the tumor necrosis factor (TNF) receptor-ligand family, is directly involved in the differentiation of monocyte-macrophages into osteoclasts (Lacey et al., 1998a; Teitelbaum, 2000a; Yasuda et al., 1998a). Mice with a disrupted RANKL gene show a deficiency in osteoclasts, severe osteopetrosis and a defect in tooth eruption, indicating that RANKL is an essential for osteoclast differentiation (Kong et al., 1999d). In addition, RANKL was able to induce mature osteoclast activation *in vitro* (Burgess et al., 1999a), osteoclast polarization and hypercalcemia *in vivo* (Burgess et al., 1999a; Xu et al., 2000b). RANKL-induced osteoclastogenesis is mediated through its receptor, RANK.

The interaction between RANKL and RANK leads to the recruitment of members of TNF receptor associated factor (TRAF) adapter proteins as well as the activation the NF-κB and c-Jun N-terminal kinase (JNK) signaling pathways (Darnay et al., 1998; Galibert et al., 1998; Hsu et al., 1999a; Zhang et al., 2001). In addition, MEK/ERK and

p38 MAP kinase pathways have been shown to play important roles in RANKL-induced osteoclastogenesis (Hotokezaka et al., 2002a; Matsumoto et al., 2000c). The selective modulation of RANKL signaling pathways may have important therapeutic implications for the treatment of bone diseases associated with enhanced bone resorption such as osteoporosis, osteoarthritis and cancer-induced bone loss.

In the present study, we examined the effects of TPA on RANKL-induced osteoclastogenesis and potential mechanisms in which TPA interfered with RANKL-activated signaling pathways. We showed that TPA inhibited RANKL-induced RAW264.7 cell differentiation into osteoclasts and the expression of osteoclast specific genes. We also demonstrated that TPA suppressed the RANKL-induced NF-κB activation and nuclear translocation of DNA binding-competent NF-κB complexes. However, it had little effect on the RANKL-induced activation of JNK. It also prevented the RANKL-induced activation of ERK but had little effect on p38 activation. Given NF-κB's essential role in osteoclast differentiation (Boyce et al., 1999b; Franzoso et al., 1997a; Iotsova et al., 1997a), our studies implied that the inhibition of osteoclastogenesis by TPA is, to a certain extent, due to the suppression of RANKL-induced activation of NF-κB.

6.2 RESULTS

6.2.1 TPA inhibits differentiation of RAW264.7 cells into osteoclast like cells

RANKL is a key cytokine for the induction of osteoclastogenesis. While the differentiation of bone marrow cells or spleen cells into osteoclasts requires M-CSF and RANKL, that of RAW264.7 cells requires only RANKL to form *bona fide* bone resorbing osteoclasts (Hsu et al., 1999a; Xu et al., 2000b). Therefore, RAW264.7 cells were used to study the explicit effect of TPA on RANKL-induced osteoclast formation and the relevant signaling pathways. The former was treated for 5 days with different concentrations of TPA in the presence and absence of RANKL. When RAW264.7 cells were treated with RANKL alone, they formed osteoclast-like cells which displayed TRACP activity. They also expressed calcitonin receptor mRNA and are capable of bone resorption.

In contrast, when RAW264.7 cells were treated with TPA alone, TRACP activity, calcitonin receptor mRNA and bone resorption were not observed. Although RANKL was capable of inducing osteoclastogenesis in the presence of TPA, the latter decreased RANKL-induced osteoclastogenesis as evidenced by TRACP activity in the culture. The effect of TPA on RANKL-induced osteoclastogenesis was in a dose-dependent manner (Figure 6.1). Interestingly, it appeared that the TRACP positive mutinucleated osteoclast-like cells induced by RANKL in the presence of TPA (Figure 6.1C-D) exhibited smaller sizes compared with those in the absence of TPA (Figure 6.1E). Collectively, these results indicated that TPA inhibited RANKL-induced osteoclastogenesis.

Next, we examined whether the inhibitory effect on RANKL-induced osteoclastogenesis caused by TPA occurs at the early stage of osteoclast differentiation. To begin with, RAW264.7 cells were pretreated with TPA under three groups: 1) 24 hours before the addition of RANKL; 2) at the early time (at days 1-2); and 3) late time course (at days 3-4) and in the presence of RANKL.

The degree of osteoclast formation was examined by TRACP staining after 5 days of culture. The results showed that a dose of 10 ng/ml of TPA inhibited osteoclastogenesis

Figure 6.1

induced by RANKL in the pretreatment, early and late treatment groups. The greatest reduction was evidenced in the early treatment group (Figure 6.2). At a lower dose of 1 ng/ml, TPA inhibited osteoclastogenesis in the early treatment group but had minimum effects on the pretreatment and late groups. Thus, these data demonstrated that the inhibitory effect of TPA occurred predominantly, but not exclusively, during the early stage of RANKL-induced osteoclastogenesis.

To further investigate the inhibitory effects of TPA on RANKL-induced osteoclastognesis, RAW264.7 cells were treated with RANKL in the absence and presence of TPA at varying doses, and the total RNA was isolated. Semiquantitative RT-PCR was performed using primers for calcitonin receptors and cathepsin K, both markers of osteoclast differentiation. The results showed that TPA reduced the gene expression of calcitonin receptors and cathepsin K during RANKL-induced osteoclastogenesis, and the reduction amount was dependent on the dosage of TPA (Figure 6.3).

6.2.2 TPA suppresses the RANKL-induced activation of NF-κB

The RANKL-induced osteoclast differentiation involves the activation of two major signaling pathways, JNK and NF-κB pathways (Darnay et al., 1998; Galibert et al., 1998; Hsu et al., 1999a; Zhang et al., 2001). The activation of PKC by TPA has also been shown to involve the JNK and NF-κB pathways in several cell types (Ariga et al., 2002; Engedal et al., 2002; Lin et al., 2002; Mauro et al., 2002; Nomura et al., 2000; Zhou et al., 2000). In order to examine the effect of TPA on the RANKL-induced activation of NF-κB, RAW264.7 cells were transiently transfected with a NF-κB-driven luciferase reporter gene construct called 3κB-Luc-SV40, and subsequently treated separately with just RANKL, TPA as well as RANKL together with TPA. The treated cells were harvested at various time points and the luciferase activities were measured. It was found that RANKL alone induced NF-κB activation (21.5 ±0.55 fold at 6 hr, Figure 6.4A). In comparison, the treatment of TPA alone resulted in a low level of NF-κB activation in RAW264.7 cells (1.86 ±0.12 fold after 6hr). TPA also decreased the RANKL-induced NF-κB activation at every time point.

In order to examine the dose-dependence of the inhibitory effect of TPA on NF-κB activation by RANKL, a stable RAW264.7 cell line transfected with 3κB-Luc-SV40

Figure 6.2

Figure 6.3

expression construct was established. The transfected RAW264.7 cells were then treated with RANKL in the presence of varying doses of TPA - 1, 10 and 50 ng/ml. It was found that TPA suppressed the NF-κB activation by RANKL in a dose-dependent fashion (Figure 6.4B). In our bid to examine if TPA also inhibited the activation of NF-κB induced by stimuli other than RANKL in RAW264.7 cells, we tested the effect of TPA on LPS, TNF-α and IL-1β-induced luciferase activity in RAW264.7 cells, stably expressing the 3kB-Luc-SV40 reporter gene. The results demonstrated that TPA suppressed the induction of NF-κB mediated transcription by LPS, TNF-α and IL-1 at different degrees when compared with the control groups (Figure 6.4C).

For further verification of the effect of TPA on RANKL-induced NF-κB activation, the nuclear translocation of DNA binding capability of NF-κB was examined by EMSA as described in materials and methods chapter. First, RAW264.7 cells were treated separately with RANKL, TPA as well as RANKL plus TPA during various time periods. Next, the nuclear extracts were prepared and incubated with [γ-32P] labeled oligonucleotide containing a concensus NF-κB binding site. As shown in Figure 6.5A, TPA decreased the abundance of DNA-binding NF-κB complexes in nuclei of RANKL-stimulated RAW264.7 cells. This implied that such inhibition occurred before the DNA binding of the NF-κB complexes.

In order to determine the subunits present in the RANKL-activated NF-κB complexes, an EMSA was performed using anti-NF-κB1 (p50), Rel-A (p65), c-Rel, and B-Rel antibodies. Supershift bands of the specific DNA-bound proteins were detected (Figure 6.5B) in the presence of anti-NF-κB1 (p50), Rel-A (p65) and c-Rel. In contrast, no supershift signal was detected when B-Rel antibody was added. These results suggested that the RANKL-induced DNA binding of NF-κB complexes in RAW264.7 cells consisted of NF-κB1 (p50), Rel-A (p65) and c-Rel, but not B-Rel.

To confirm that the suppression of RANKL-induced NF-κB activity induced by TPA was due to the activation of a PKC isoform, we tested the effect of the PKC inhibitors, Gö 9676, GF109203X and rottlerin. As shown in Figure 6.6 Gö 9676 (5μM), an inhibitor of conventional PKC isoforms, prevented the suppressive effect of TPA on RANKL-induced NF-κB transcriptional activation. On the other hand, the PKC delta specific inhibitor named rottlerin (5μM) had no effect on NF-κB mediated transcriptional activity while the broad spectrum PKC inhibitor GF109203X (5μM)

Figure 6.4

Figure 6.5

partially prevented TPA's suppression of RANKL-induced NF-κB transcriptional activity (data not shown). These results indicated that the TPA-induced activation of conventional PKC isoforms was involved in the inhibition of RANKL-induced NF-κB activation.

6.2.3 TPA has no effect on RANKL-induced activation of JNK

The activation of JNK is one of the major signaling events induced by the interaction between RANKL and RANK (Hsu et al., 1999a). In order to examine the effect of TPA on JNK activation induced by RANKL, RAW264.7 cells were treated separately with RANKL, TPA as well as RANKL plus TPA at various time points 30 min. The c-Jun kinase assay was performed using recombinant GST-c-Jun protein and [γ-^{32}P] ATP. The phosphorylated GST-c-Jun proteins were separated by SDS-PAGE and visualized by autoradiography. The result showed that both RANKL and TPA induced the activation of JNK. Although TPA had inhibitory effect on NF-κB activation, it had no or little effect on the RANKL-induced activation of JNK (Figure 6.7A).

6.2.4 TPA suppresses RANKL-induced activation of the ERK but not the p38 pathway

The MEK/ERK and p38 MAP kinase pathways have been shown to play an important role in RANKL-induced osteoclastogenesis (Hotokezaka et al., 2002a; Matsumoto et al., 2000c). In examining the effect of TPA on the RANKL-induced activation of ERK and p38, Western blotting analysis was performed using antibodies to the phosphorylated forms of ERK and P38. The results showed that both RANKL and TPA induced the phosphorylation of ERK and p38. However, while TPA prevented the RANKL-induced activation of ERK, it had little or no effect on the RANKL-induced activation of p38 (Figure 6.7B).

Figure 6.6

Figure 6.7

6.3 DISCUSSION

Many cytokines such as IL-1, IL-6, and TNF-α have stimulative effects on the formation of osteoclasts *in vivo* or in co-culture systems, but they are not capable of directly inducing such formation from their precursors. Knockout mice lacking IL-1, IL-6, TNF-α or their receptors do not exhibit osteopetrosis (Lorenzo et al., 1998; Poli et al., 1994; Vargas et al., 1996), further suggesting that these cytokines enhance osteoclast formation indirectly either by increasing the production of M-CSF (Cenci et al., 2000) or by potentiating the osteoclastogenic effects of RANKL (Lam et al., 2000). In contrast, RANKL is a key inducer of osteoclastogenesis (Kong et al., 1999d; Lacey et al., 1998a), and intracellular mechanisms that inhibit RANKL-induced osteoclastogenesis are therefore of great interest as they offer possible means of curing bone diseases associated with enhanced osteoclastic bone resorption.

PKC is a family of serine/threonine protein kinases involved in many cellular responses. Although the analysis of PKC activity has provided crucial insights to its biologic function in many systems (Carter, 2000), its role in the differentiation of osteoclast progenitor cells into osteoclasts remains unclear. Previous studies have shown that calcitonin or TPA which increases PKC activity, inhibits bone pit formation *in-vitro* (Murrills et al., 1992; Su et al., 1992; Teti et al., 1992). The effect of PKC activation on osteoclastogenesis however remains controversial. Here we have used RAW264.7 cells culture for the study of TPA inhibition on RANKL-induced osteoclastogenesis and signaling pathways. The ability of the soluble form of RANKL alone to induce differentiation of RAW264.7 cells into osteoclasts in the absence of supportive cells allowed us to test whether TPA acts directly on RANKL-induced osteoclastogenesis in the absence of stromal cells.

Our studies showed that TPA acted directly on osteoclast precursor cells and prevented the differentiation of osteoclast precursors into osteoclasts. It appeared that the suppressive effect of TPA took place predominantly during the early stage of RANKL-induced osteoclastogenesis. Apart from a direct effect of TPA on osteoclast precursors demonstrated in this study, there were also reports of the indirect effects of PKC activators via stromal cells to modulate osteoclastogenesis by stimulating the expression of RANKL and OPG mRNAs in primary osteoblasts (Brandstrom et al., 2001; Takami et al., 2000b).

The interaction between RANKL and RANK results in a cascade of intracellular events including the activation of NF-κB and the protein kinase JNK (Hsu et al., 1999a; Yamamoto et al., 2002; Zhang et al., 2001). The NF-κB signaling has been shown to play an important role in osteoclastogenesis (Boyce et al., 1999b). NF-κB p50-/- and p52-/- double knockout mice exhibit severe osteopetrosis due to failure of osteoclast formation (Franzoso et al., 1997a; Iotsova et al., 1997a). NF-κB is activated by RANKL both in RAW264.7 cells and in monocytes (Hsu et al., 1999a; Jimi et al., 1999a; Lacey et al., 1998a; Wong et al., 1997a), and is required *in vivo* for osteoclast formation (Franzoso et al., 1997a).

More recent studies indicate that NF-kappaB p50 and p52 expressions are essential for RANK-expressing osteoclast precursors to differentiate into TRACP+ osteoclasts in response to RANKL and other osteoclastogenic cytokines (Xing et al., 2002). Therefore, the suppression of NF-κB activation would play an important role in osteoclast formation. Interestingly, in the present studies, the reduction of the RANKL-induced NF-κB-activity by TPA and the inhibition of RANKL-induced differentiation of RAW264.7 cells into osteoclasts occurred simultaneously. TPA alone has little effect on the activation of NF-κB in RAW264.7 cells. This is consistent with the previous findings (Vincenti et al., 1992) but in contrast with enhanced NF-κB activity in cell types such as JB6 mouse epidermal cell line (Nomura et al., 2000) and the human T cell leukemia Jurkat cells (Ariga et al., 2002). In addition, TPA has inhibitory effects on LPS, TNF-α and the IL-1-induced activation of NF-κB mediated transcription but at different degrees when compared with the control group.

RAW264.7 cells express eight PKC isoforms in three groups: conventional PKCs (alpha, betaI, betaII); novel PKCs (delta, epsilon, mu); and atypical PKCs (lambda and zeta) (Larsen et al., 2000; Lin and Chen, 1998). TPA induces the activation of alpha, betaI, betaII, delta, epsilon and mu isoforms in RAW264.7 cells (Lin and Chen, 1998). Interestingly, we have shown that a conventional PKC inhibitor named Go9676 prevented the inhibitory effect of TPA on the RANKL-induced activation of NF-κB in RAW264.7 cells. This indicated that the activation of one or more conventional PKC isoforms is likely to be involved in NF-κB suppression.

The c-Jun phosphorylation also plays an essential role in osteoclastogenesis (David et al., 2002b). The signaling pathways mediated by RANK/TRAF6/JNK/AP-1/C-Fos appear

to be critical for osteoclastogenesis as TRAF6 (Kim et al., 1999a; Lomaga et al., 1999a) and *c-fos*-deficient mice (Johnson et al., 1992b; Wang et al., 1992c) develop osteopetrosis. Using mice lacking JNK1 or JNK2, it has been demonstrated that JNK1, but not JNK2, is specifically activated by the osteoclast-differentiating factor RANKL, and the activation of JNK1 is required for efficient osteoclastogenesis from bone marrow derived monocytes (David et al., 2002b).

Furthermore, the estrogen-mediated suppression of JNK1 and transcription factors c-Jun and c-Fos were also found to decrease the ability of RANKL to induce osteoclastogenesis (Shevde et al., 2000; Srivastava et al., 2001). The activation of JNK is likely to play an important role in the early stage of osteoclast differentiation. We have found that TPA induced the activation of JNK in RAW264.7 cells which is consistent with the findings in other cell types (Engedal et al., 2002; Lin et al., 2002; Mauro et al., 2002; Zhou et al., 2000). However, TPA did not lead to the inhibition of RANKL-induced JNK activity in RAW264.7 cells, suggesting that the inhibition of osteoclastogenesis might be independent of TPA's action on c-Jun signaling.

On the other hand, in addition to activating the JNK pathway, TPA might lead to the activation of factors that inhibit the RANKL-induced c-Jun transcriptional activity. While TPA is able to activate both classical (α, β, γ) and novel (δ, ε, θ) PKC isozymes in several cell types (Carter, 2000), its activation is predominantly on the classical PKC isozymes in RAW264.7 cells (Lin and Chen, 1998). Further investigation of the PKC isozymes that regulate the RANKL-induced osteoclast formation might provide more insight into the cross interaction of these signaling pathways.

The MEK/ERK specific inhibitors namely U0126 and PD98059, have been shown to accelerate the differentiation of RAW264.7 cells into osteoclast-like cells. This indicated that the MEK/ERK pathway negatively regulates osteoclastogenesis, while the p38 pathway positively regulates osteoclastogenesis (Hotokezaka et al., 2002a; Matsumoto et al., 2000c). In addition, we have demonstrated that TPA prevented the RANKL-induced activation of ERK and had no effect on the p38 activation, both of which are outcomes which might be expected to confer a positive effect on osteoclastogenesis. In this study, it was found that TPA had an inhibitory effect on RANKL-induced osteoclastogenesis. It was likely that the NF-kB signaling pathway played a part in causing this effect but the same cannot be said for the MEK/ERK and

p38 pathways.

In summary, our findings demonstrated that TPA suppressed the RANKL-induced RAW264.7 cells differentiation into osteoclasts and the expression of osteoclast specific genes. It appeared that the inhibitory effect took place predominantly during the early stage of osteoclast differentiation induced by RANKL. The suppression of NF-κB activation accounted, at least in part, for the mechanism of action.

CHAPTER 7

Protein Kinase Inhibitors, Gö 6976 and GF 109203X, Inhibit RANKL-induced Osteoclastogenesis Via NF-κB Signaling Pathways

Key message:

Selective inhibition of Protein Kinase C signaling pathways involved in osteoclastogenesis might be a potential treatment method for osteoclast-related bone diseases

CHAPTER 7– PROTEIN KINASE INHIBITORS, GÖ 6976 AND GF 109203X, INHIBIT RANKL-INDUCED OSTEOCLASTOGENESIS VIA NF-KB SIGNALING PATHWAYS

7.1 INTRODUCTION

RANKL is a key cytokine for osteoclastogenesis (Kong et al., 1999a; Lacey et al., 1998a) and the intracellular mechanisms by which RANKL-induced osteoclastogenesis are of major interest in the research of bone diseases associated with enhanced osteoclastic bone resorption. The protein kinase C (PKC) pathway has been suggested to be an important regulator of osteoclastic bone resorption (Su et al., 1992). Activation of PKC via 12-O-tetradecanoyl phorbol-13-acetate (TPA) is known to decrease osteoclastic bone-resorbing activity (Mano et al., 2000). In addition, TPA has been shown to suppress RANKL-induced osteoclast differentiation and the expression of osteoclast-specific genes (Wang et al., 2003b). In addition, studies using synthetic peptide fragments of PKC provide further evidence to suggest that PKC plays an important physiological role in osteoclast function (Moonga and Dempster, 1998). Collectively, these studies provide evidence for an important role of PKC in the modulation of osteoclast differentiation and function.

The activation of protein kinase C (Serine/Threonine) is one of the earliest events in the cascade of signal transduction pathways leading to a variety of cellular responses in many biological functions including cell proliferation, secretion, gene expression as well as muscle contraction (Nishizuka, 1989). More recently, PKCs have been found to be involved in intracellular signal transduction pathways that regulate cell growth, differentiation and apoptosis, and implicated in the rearrangement of the cytoskeleton and migration (Keenan and Kelleher, 1998).

There are 12 common isozymes of PKC which are categorized into 3 classes based on their structure and co-factor requirement for activation: 1) the conventional PKCs (α, βI, βII and γ) which require both Ca^{2+} and phosphatidylserine, diacylglycerol (DAG) or phorbolesters as cofactors; 2) the novel PKCs (δ, ε, η, μ and θ) which can be stimulated by DAG, phosphatidylserine or phorbolesters alone, independent of Ca^{2+}; and 3) the atypical PKCs (λ, ι and ζ) which are independent of both Ca^{2+} and DAG stimuli (Dekker

and Parker, 1994; Keenan and Kelleher, 1998; Knopf et al., 1986; Newton, 1995; Nishizuka, 1986). One of the major approaches used to study the role of PKC in cellular responses is to inhibit the kinase activity involved in cells. For this purpose, permeable, potent and selective compounds are required. In this study, the effects of two PKC inhibitors named Gö 6976 and GF 109203X were examined on RANKL-induced osteoclastogenesis.

Gö 6976, Indolocarbazole is a cell-permeable inhibitor of PKC and selectively inhibits Ca^{2+}-dependent PKC α, and β_1 -isozyme but not the kinase activity of Ca^{2+}-independent PKC δ-, ε- and ζ-isozymes even at micromolar levels (Martiny-Baron et al., 1993). It is a conventional PKC catalytic activity inhibitor and has been reported to inhibit PKC_{μ} at higher concentrations (Gschwendt et al., 1996). Moreover, Gö 6976 selectively differentiates between PKC isoenzymes (Gschwendt et al., 1995; Martiny-Baron et al., 1993; Zang et al., 1994), inhibiting cPKC (α, β, γ) with much greater efficacy than nPKC (δ, ε, η) and aPKC (ζ) (Gschwendt et al., 1996).

GF 109203X, Bisindolylmaleimide is a compound structurally related to the potent PKC inhibitor of PKC Staurosporine (Toullec et al., 1991). While Staurosporine is suggested to be the most potent inhibitor of PKC, this natural product has a wide spectrum of effect when assayed against other protein kinases. On the other hand, GF109203X has been shown to display higher selectivity for PKC and it is a competitive inhibitor with respect to ATP (Toullec et al., 1991). GF109203X selectively inhibits PKC in human platelet and Swiss 3T3 fibroblasts (Toullec et al., 1991).

The precise role of PKC in osteoclast differentiation and function is largely unclear. In this study, PKC inhibitors, Gö 6976 and GF109203X were used_to investigate the mechanisms of PKCs involved in RANKL-induced osteoclast formation and osteoclastic bone resorption. Both Gö 6976 and GF109203X potently inhibited RAW264.7 cell-derived osteoclast formation and RANKL-mediated NF-κB transcriptional activities. In addition, these inhibitors disrupted the bone resorptive activity of multinucleated cells derived from patients presenting Giant Cell Tumour (GCT) of bone. Based on these findings, Gö 6976 and GF109203X might be useful tools for studying the association of PKC and osteoclast formation and activity. Thus, they may also prove to be useful for the treatment of bone lytic disorders.

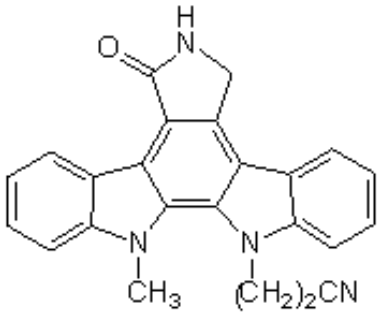

Gö 6976

Molecular formula: $C_{24}H_{18}N_4O$

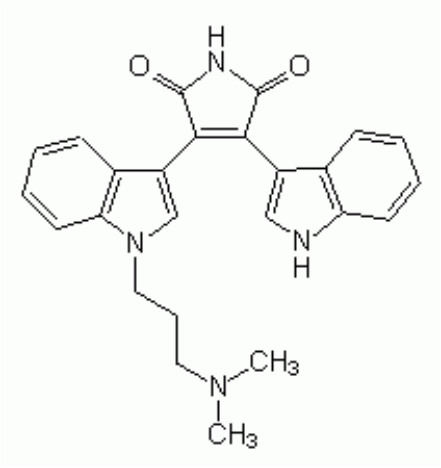

GF 109203X

Molecular formula: $C_{25}H_{24}N_4O_2$

7.2 RESULTS

7.2.1 Gö 6976 and GF 109203X inhibit RANKL-induced osteoclastogenesis

RAW264.7 cells require only RANKL to form *bona fide* bone resorbing osteoclasts (Hsu et al., 1999b; Xu et al., 2000c). Thus, RAW264.7 cells were used to study the effect of Gö 6976 and GF 109203X on RANKL-induced osteoclast formation and the relevant signal transduction pathways. RAW264.7 cells were treated for 5 days with differing concentrations of Gö 6976 (at a final concentration of 0.5, 1, 2, 4uM) and GF 109203X (0.5, 1, 2, 5, 10uM) in the presence or absence of 100ng/ml RANKL to induce osteoclast formation. As shown in Figure 7.1, Gö 6976 dose-dependently inhibited the RANKL-induced osteoclast formation at concentrations ranging from 0.1 to 2uM ($p<0.05$). Similarly, GF 109203X potently suppressed RANKL-induced osteoclast formation at concentrations greater than 2.5uM ($p<0.05$) (Figure 7.2).

Since Gö 6976 and GF 109203X had inhibited RANKL-induced osteoclastogensis, it was a next aim to examine if this effect is involved in the early or late stage of osteoclast differentiation. To this end, RAW264.7 cells were treated with Gö 6976 and GF 109203X at 3 different time points: 1) 24 hours before adding RANKL; 2) at the early time point (on day 1-2); and 3) at later time point (on day 3-4) in the presence of RANKL. The degree of osteoclast formation was examined by TRACP staining at the end of day 5 culture. The TRACP activities were also measured as absorbance at 410nm.

The results indicate that Gö 6976 inhibited osteoclast formation during pre-treatment and early phases of osteoclast differentiation. The greatest reduction in osteoclast formation was evidenced in the pre-treatment groups (Figure7.3A). It was observed that the exposure of GF 109203X at 2 and 5uM in the 24-hour pre-treatment and early treatment groups decreased the number of RAW264.7 cells differentiating to osteoclast-like cells in 5 days (Figure 7.3B). In addition, the greatest reduction in OCLs formation was evidenced in the early treatment group. GF 109203X had no effect on RAW264.7 cells during the late phase of osteoclastogenesis. Collectively, these results demonstrate that the inhibitory effects of Gö 6976 and GF 109203X occur predominantly during the pre-treatment and early phase of the RANKL-induced osteoclast formation respectively. Surprisingly, the late time treatment of GF109203 seems to enhance osteoclastogenesis.

Figure 7.1

Figure 7.2

Figure 7.3A

Figure 7.3B

In order to complement the osteoclastic assay, semi-quantitative RT-PCR was performed using primers that are recognized as the osteoclast differentiation markers such as Calcitonin receptor and Cathepsin K (Figure 7.4). Consistently, the results show that Gö 6976 reduces the gene expression of both calcitonin receptor and cathepsin K whereas GF 109203X had very weak effect from the 5 days of culture.

7.2.2 Gö 6976 and GF 109203X impair bone resorption by human osteoclast-like cells

Since both Gö 6976 and GF 109203X exhibited inhibitory effect on RANKL-induced osteoclastogenesis, it was of interest to examine the effect of these two PKC inhibitors on pathological bone resorption. Osteoclast-like cells derived from Giant cell tumour of bone (GCT) were used to examine the role of PKC in pathlogical bone resorption. The cells were seeded onto bone slices and cultured with either vehicle or differing concentrations of Gö 6976 and GF 109203X for 72 hours. Figure 7.5A depicts representative images of TRACP positive osteoclast-like cells on bone slices and their respective bone resorption pits taken by light and scanning electron microscopy (SEM). As shown in Figure 7.5A, 0.5 and 1uM of Gö 6976 reduced the size of OCL derived from GCT. 1 and 2uM of GF 109203X also displayed the similar effect on GCT as the size of the OCL was smaller without changing the cell number. The SEM images presented in Figure 7.5A showed that Gö 6976 at concentration levels of 0.5uM and 1uM inhibited GCT-induced bone resorption. There were less resorbing pits on the bone slice. Remarkably, GF 109203X at 1 and 2uM profoundly inhibited the bone resorption by GCT as there was almost no resorption pits evident that on all bone slices examined. Together, these data convincingly demonstrated that Gö 6976 and GF 109203X impair bone resorption by GCT. (for quantitative analysis, see Figure 7.5B)

7.2.3 Gö 6976 and GF 109203X suppress RANKL-induced NF-κB activation

Next, to gain insights into the molecular mechanism underlying the inhibition in osteoclast formation and activities, the effect of Gö 6976 and GF 109203X on RANKL-induced signaling pathways was examined. To this end, the effects of Gö 6976 and GF 109203X on RANKL-induced NF-κB activity in osteoclast precursors was determined. RAW264.7 cells were transiently transfected with a NF-κB luciferase

Figure 7.4

Figure 7.5A

Figure 7.5B

reporter construct and pre-treated with various doses of Gö 6976 and GF 109203X ranging from 0.1 to 5uM for 30 minutes before stimulating them with 100ng/ml RANKL for another 8 hours. The firefly luciferase activity was then measured.

As shown in Figure 7.6A, RANKL induced a 5-fold increase in the activation of NF-κB activity compared to the unstimulated cells. Gö 6976 dose-dependently inhibited the RANKL-induced NF-κB activation at a dose range of 0.5-5uM. It significantly suppressed the RANKL-induced NF-κB activation at 1, 2 and 5uM. However, the inhibitor had no significant effect on the basal NF-κB activity at any concentration level. By comparison, GF 109203X significantly decreased the RANKL NF-κB activity only at 5uM ($p<0.05$). Interestingly, GF 109203X elevated the basal NF-κB activity at 1, 2, and 5uM. Both Gö 6976 and GF 109203X did not alter the RANKL-induced IKK-α degradation (Figure 7.6B).

Next, to further examine the effects of the PKC inhibition on NF-κB signaling pathway, their ability to block p65 translocation was examined. To this end, BMM cells were pre-treated with 1 and 5uM Gö 6976 as well as GF 109203X for 1 hour and then stimulated with LPS for 30 minutes. Cells were then fixed and stained for p65. The results in Figure 7.7 illustrate that LPS induced the p65 translocation from cytoplasm to the nuclei. GF 109203X at 1 and 5uM partially inhibited the translocation of p65 to the nuclei. On the other hand, Gö 6976 had a partial effect but at lesser degree on the LPS-induced p65 translocation when compared with GF 109203X. In short, these results indicated that Gö 6976 and GF 109203X inhibited NF-κB activity by blocking the p65 translocation, and not the IκBα degradation.

7.2.4 Gö 6976 and GF 109203X modulate RANKL-induced NFAT activity

The synthesis of the transcriptional factor NFAT2/NFATc1 has been shown to play a crucial role in RANKL-stimulated signaling pathways, and the activation of this transcription factor is both necessary and sufficient for osteoclastogenesis. Therefore, it was a next aim to examine whether PKC inhibitor Gö 6976 and GF 109203X effect NFATc1 signaling. RAW264.7 cells were pre-treated with two different doses of Gö 6976 (0.5 and 1uM) and GF 109203X (1 and 2uM) and subsequently cultured for 3 days in the presence and absence of 100ng/ml RANKL. Cells were lysed and subjected to Western blotting using a specific antibody to NFATC1. The results show that GF

Figure 7.6

Figure 7.7

109203X increase the level of NFATc1 protein expression at both concentration levels of 1 and 2uM. Interestingly, Gö 6976 greatly enhanced the level of NFATc1 protein at the concentration level of 0.5uM but the enhancement was lesser when at 1uM (Figure 7.8A).

In addition, the effects of Gö 6976 and GF 109203X on RANKL-induced NFAT transcription were also examined. A luciferase reporter plasmid named pNFAT-Luc was transiently transfected into RAW264.7 cells. After 48 hours of post-transfection, the transfected cells were treated with various doses of Gö 6976 and GF 109203X in the presence and absence of RANKL for another 8 hours before the luciferase activities were measured. Both Gö 6976 and GF 109203X significantly decreased the RANKL-induced NFAT activity when compared with the controls (Figure 7.8B). In contrast to the potentiated effects of Gö 6976 and GF 109203X on the RANKL-induced phosphorylation of NFATc1 after 72 hours; these two PKC inhibitors suppressed the NFAT transcription 8 hours after RANKL stimulation. Interestingly, it was found that the two PKC inhibitors, Gö 6976 and GF 109203X, potentiated the RANKL-induced phosphorylation of NFATc1 protein expression after 72 hours, but inhibited the NFAT transcription only 8 hours after RANKL stimulation.

7.2.5 Gö 6976 and GF 109203X increase the total c-SRC induced by RANKL

In order to further examine the effects of Gö 6976 and GF 109203X on key osteoclast signaling pathways, their effect on total c-SRC levels was examined by immunoblotting. RAW264.7 cells were cultured with 0.5 and 1uM of Gö 6976 as well as 1 and 2uM of GF 109203X in the presence and absence of RANKL for 72 hours before the cell lysates were collected for proceeding standard immunoblotting. After 72 hours, the RANKL-stimulated group of cells started to form multinucleated OCLs. However, the two PKC inhibitors, Gö 6976 and GF 109203X, reduced osteoclast formation. As shown in Figure 7.9, both potentiated the total c-SRC of RANKL-stimulated RAW264.7 cells. Interestingly, 0.5 and 1uM Gö 6976-treated cells had greater amount of total c-SRC than the GF 109203X-treated cells.

Figure 7.8

Figure 7.9

7.3 DISCUSSION

Bone remodeling is regulated by the coupled activities of osteoclast-mediated bone resorption and osteoblast-mediated bone formation. Excessive osteoclastic bone resorption is a major hallmark of several common pathological bone disorders including osteoporosis, osteoarthritis, Paget's disease and tumour metastasis of bone. RANKL is the key cytokine for osteoclast differentiation and activity (Kong et al., 1999a; Lacey et al., 1998a), and its biological signaling pathways are one of the major interests for the understanding of mechanisms on the excessive osteoclast-associated bone disorders. Despite the fact that protein kinase C (PKC) signaling pathways have been suggested to play a role in osteoclastic bone resorption, the underlying mechanisms of PKC involved in osteoclastogenesis and osteoclast activity remain unclear. One of the most direct approaches to study the role of PKC in osteoclastogenesis as well as osteoclast activity, is to inhibit the enzymatic activity of the kinase.

Therefore, the inhibitors of PKC can be the important experimental tools to determine the PKC dependence of a particular signal transduction mechanism on osteoclasts. In this study, two potent PKC inhibitors Gö 6976 and GF 109203X were employed to examine the role by PKC in osteoclast differentiation and activation. Gö 6976 is a conventional PCK inhibitor with selectivity to PKCβ (Martiny-Baron et al., 1993), while GF 109203X is a broad spectrum PKC inhibitor. The effects of both inhibitors on osteoclast formation were documented. Moreover, it was demonstrated that they inhibited the bone resorption activity of the giant multinucleated cells-derived from patients with Giant cell tumour of bone.

PKCβ gene expression is upregulated during osteoclastogenesis and has a functional role in osteoclast differentiation, fusion and resorption activity (Lee et al., 2003). The results presented here also suggested that the inhibitory effects of Gö 6976 and GF 109203X on osteoclast differentiation and activity might be due to their inhibition of PKCβ. Since Gö 6976 is a conventional PKC inhibitor and GF 109203X, a broad spectrum PKC inhibitor, it is possible that other PKC isoenzymes might play a role in modulating osteoclast differentiation and activity.

It is known that PKC triggers cellular signals that regulate the proliferation or death in a cell- and stimulus-specific manner (Byun et al., 2006). The PKC inhibitor, Gö 6976, had

been reported to abrogate S and G_2 phases of a cell cycle arrest (Kohn et al., 2003). Since the S and G_2 arrest do not require p53, cells mutated for p53 (about 50% of tumours) arrest primarily in S or G_2 in response to damages (Kohn et al., 2003). Therefore, Gö 6976 was suggested to be a potential therapy for the sensitization of tumour cells to DNA-damaging agents.

RAW264.7 cells express eight PKC isoforms; conventional PKCα, βI, βII, novel PKCδ, ε, μ and atypical PKCλ and ζ (Larsen et al., 2000; Lin and Chen, 1998). NF-κB is activated by RANKL both in RAW264.7 cells and in monocytes (Hsu et al., 1999b; Jimi et al., 1999b; Lacey et al., 1998a; Wong et al., 1997a), and is required *in vivo* for osteoclast formation (Franzoso et al., 1997b). Our previous studies demonstrated that RANKL activation induced the DNA binding of NF-κB complexes consisting of C-Rel, NF-κB1 (p50), and Rel-A (p65) (Wang et al., 2003b). While earlier studies have demonstrated that the inhibitors of PKC, Gö 6976 and GF 109203X, prevent NF-κB-dependent transcription, the NF-κB DNA binding is unaffected in pulmonary A549 cells (Catley et al., 2004).

Given the inhibitory effects of Gö 6976 and GF 109203X on NF-κB, it was also demonstrated that these two PKC inhibitors inhibited the NF-κB transcription induced by RANKL although there was no effect on the loss of IκBα. In addition, both inhibitors had a partial effect on the nuclear translocation of p65 following the LPS stimulation of BMM. From the results presented here and coupled with previously published data, it is tempting to speculate that these two PKC inhibitors exert their inhibitory effects on the p65/RelA involved in the classical NF-κB signaling pathway in osteoclastogenesis. The upstream of NF-κB signaling pathways, IκBα degradation, is unlikely to be involved in the inhibitory mechanism of these two PKC inhibitors. These findings hint that PKCs play an important role in NF-κB signaling pathways induced by RANKL in osteoclastogenesis.

In this study, it was also found that the two PKC inhibitors, Gö 6976 and GF 109203X, potentiated the RANKL-induced protein expression of NFATc1 after 72 hours, but inhibited the NFAT transcription only 8 hours after RANKL stimulation. From this surprising observation, it is possible that the effects of these two PKC inhibitors on the expression of NFATc1 and the NFAT transcription induced by RANKL were preceded at different time points, thus displaying opposing results. These results also correlate

well with osteoclastogenesis assays which showed that late treatment of Gö 6976 and GF 109203X potentiated osteoclastogenesis whereas early treatment inhibited this process. To date, the association of NFAT and PKC in osteoclastogenesis has not been investigated. Hence, further studies are required to explore the precise relationship between NFAT and PKC signaling.

In the case of TPA in RAW264.7 cells, it is possible that many PKC isoforms activated by TPA might become degradaded at late time points. TPA exhibits an inhibitory effect on RANKL-induced NF-κB activation in RAW264.7 cells (Wang et al., 2003b), and induces the activation of PKC α, βI, βII, δ, ε, and μ isoforms in RAW264.7 cells, where as pre-treatment for 2-24 hours could result in the down-regulation of PKC α, βI, βII, and δ expressions (Lin et al., 1998). Thus, different isoforms of PKC might play distinctive roles and are involved in distinctive cellular processes in different cell types.

To summarize, these results suggest that PKCs play an important role in osteoclast differentiation and activity by interacting with the RANKL-induced NF-κB signaling pathway. The two PKC inhibitors namely Gö 6976 and GF 109203X, might be potential therapeutics for bone lytic disorders. It is interesting to note that Gö 6976 might be a potential candidate for clinical therapy for treating metastasis of bones due to its inhibitory effect on osteoclastogenesis as well as inhibitory property in DNA-damage-induced S and G_2 cell cycle checkpoints. Nonetheless, more in-depth studies using potent and selective inhibitors for each subtype of PKCs are required to provide a more comprehensive approach to ascertain the distinctive role of each PKC isoenzyme in osteoclastogenesis and activity.

CHAPTER 8

Protein Kinase C Delta Modulates RANKL-induced Osteoclastogenesis and osteoclastic bone resorption

Key message:

Protein Kinase C delta signaling pathways regulate osteoclast formation and function

CHAPTER 8– PROTEIN KINASE C DELTA MODULATES RANKL-INDUCED OSTEOCLASTOGENESIS AND OSTEOCLASTIC BONE RESORPTION

8.1 INTRODUCTION

The activation of intracellular signaling pathways by extracellular stimuli usually requires the involvement of one or more integral membrane proteins. **Protein Kinase C (PKC)** is widely involved in the intracellular signal transduction pathways that regulate cell growth, differentiation, apoptosis, tumour developments as well as in the rearrangement of the cytoskeleton and cellular migration. PKCs belong to a family of phospholipids-dependent serine/threonine kinases. Based on their structure and cofactor requirements for activation, PKC isozymes are subdivided into three classes: 1) **conventional PKCs** (α, βI, βII and γ); 2) **novel PKCs** (δ, ε, η and θ); and 3) **atypical PKCs** (λ, ι and ζ) (Dekker and Parker, 1994; Keenan and Kelleher, 1998; Knopf et al., 1986; Newton, 1995; Nishizuka, 1986). The individual isotypes of PKCs have distinctive functions in the signal transduction and cellular metabolism of different cell types (Brandt et al., 2002; Dekker and Parker, 1994; Hug and Sarre, 1993; Jaken, 1996; Nishizuka, 1986).

The PKC pathway has been suggested to be an important regulator of osteoclastic bone resorption (Su et al., 1992). A PKC activator called 12-O-tetradecanoyl phorbol-13-acetate (TPA) has been shown to inhibit RANKL-induced osteoclastogenesis by suppressing NF-κB activation (Wang et al., 2003b). In addition, TPA has been shown to decrease osteoclastic bone-resorption (Mano et al., 2000). Interestingly, it was also observed that a conventional and a broad spectrum PKC inhibitor named Gö 6976 and GF 109203X respectively, exerted inhibitory effects on RANKL-induced osteoclast formation and osteoclastic bone resorption (Chapter 6, unpublished results). These results suggest that PKCs play an important role in osteoclast formation and function. However, to date, the role of individual PKCs in osteoclast differentiation as well as their activity remains to be elucidated.

In the present study, it is sought to investigate the role(s) of specific PKC in osteoclast formation and activity as they have yet to be elucidated. For this purpose, the specific PKCδ inhibitor **Rottlerin** and activator **Bryostatin 1 were utilized**, and their effects on

osteoclastogenesis were examined. Macrolactone, Bryostatin 1 is isolated from the marine bryozoan *Bugula neritina* that initially activates and subsequently down-regulates PKC (Mutter and Wills, 2000). It is more potent than phorbol myristate acetate for translocating PKCδ and ε (Mutter and Wills, 2000). It has been widely used as a PKCδ activator to study the role of PKCδ in different cell types. On the other hand, Rottlerin is a widely selective PKCδ inhibitor isolated from *Mallotus phillippinensis*. It has been shown to be effective against several human tumour cell lines and in potentiating chemotherapy-induced cell death (Liao et al., 2005). It is also recognized as a PKCδ-selective inhibitor and is used extensively in the studies for examining the cellular response of PKCδ in different cell types (Bartimole et al., 1997; Bosco et al., 1997; Chelliah et al., 1997; Song et al., 1999; Stone, 1997).

In this chapter, it is demonstrated that Rottlerin potently inhibits RANKL-induced osteoclastogenesis. By comparison, Bryostatin 1 was found to enhance osteoclastogenesis. Together, these data suggest that PKCδ is an important signaling pathway required for both osteoclast formation and activation. Our studies hint that the modulation of PKCδ might offer therapeutic value for osteoclast-mediated bone disorders.

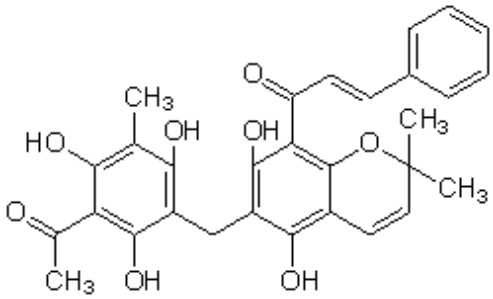

Rottlerin

Molecular formula: $C_{30}H_{28}O_8$

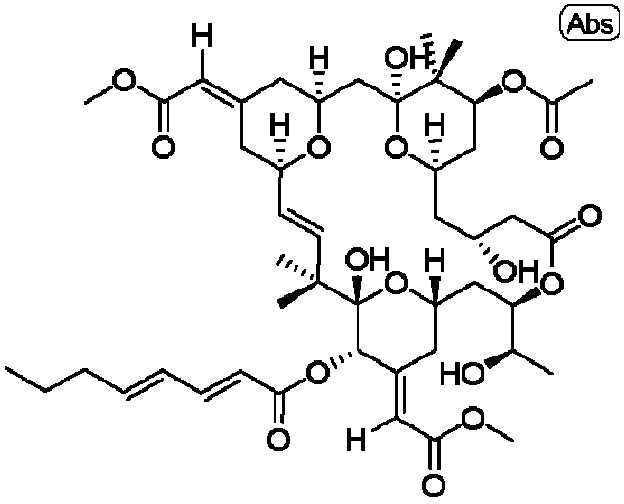

Bryostatin 1

Molecular formula: $C_{47}H_{68}O_{17}$

8.2 RESULTS

8.2.1 Rottlerin inhibits RANKL-induced osteoclast formation

As an initial step, to explore the role of individual PKC isotypes in osteoclast formation, the direct effect of Rottlerin on RANKL-induced osteoclast formation was examined using the RAW264.7 cell culture system. The RAW264.7 cells were treated with Rottlerin at various concentrations (10, 5, 2, 1, 0.5, and 0.1uM), in the presence or absence of 100ng/ml RANKL to form osteoclasts. When the RAW264.7 cells were treated with RANKL, osteoclasts-like cells were formed and the latter displayed multinucleation and TRACP positive staining. Treatment of Rottlerin dose-dependently reduced the osteoclasts formation as evidenced by TRACP activity in culture.

Morphologically, it appeared that the TRACP positive multinucleated osteoclast-like cells induced by RANKL are smaller in the presence of Rottlerin when compared with those in the absence of Rottlerin. At 2uM doses of Rottlerin, the formation of osteoclast-like cells was almost completely abolished. The culture showed only mononucleated osteoclast-like cells with a very low number of TRACP positive cells. It was observed that Rottlerin caused some cell death at concentration levels higher than 5uM (Figure 8.1). In order to further validate the inhibitory effect of Rottlerin on osteoclastogenesis, its effect was also examined using the primary mouse bone marrow macrophage (BMM) osteoclastogenic culture system**.** The result was consistent with those shown in RAW cell culture. Two micromolars of Rottlerin almost completely inhibited RANKL-induced osteoclastogenesis (Data not shown).

Next, a study was conducted to examine whether the inhibitory effect of Rottlerin on RANKL-induced osteoclastogenesis occurs at the early stage of osteoclast differentiation. The RAW264.7 cells were pre-treated with Rottlerin for 24 hours before the addition of RANKL. In addition, RAW264.7 cells were also treated with Rottlerin at early time point (on day 1-2) and late time point (on day 3-4) in the presence of RANKL. The degree of osteoclast formation was assessed by TRACP staining at the end of day 5 of culture. It was observed that the exposure of 2uM of Rottlerin at the early and late time points decreased the number of RAW264.7 cells differentiating to osteoclast-like cells in 5 days. Also, the greatest reduction in OCL formation was evidenced in the late treatment group. Rottlerin had no effect on the RAW264.7 cells when pre-treated for 24 hours (Figure 8.2). Collectively, these results demonstrate that

Figure 8.1

the inhibitory effect of Rottlerin occurs predominantly during the end stages of the RANKL-induced osteoclast formation.

In order to further investigate the inhibitory effect of Rottlerin on RANKL-induced osteoclastogenesis, RAW264.7 cells were treated with RANKL in the presence or absence of Rottlerin at 2uM, and total RNA isolated. Semiquantitative RT-PCR was performed using primers against markers for osteoclast differentiation including calcitonin receptor and cathepsin K. The results showed that Rottlerin reduced the gene expression of both calcitonin receptor and cathepsin K (Figure 8.2C and D).

In examining the effect of Bryostatin 1 on osteoclastogenesis, RAW264.7 cells and bone marrow macrophages (BMMs) were treated with Bryostatin 1 at concentrations of 25, 50, 100, 200 and 400nM in the presence of RANKL. Remarkably, the treatment with Bryostatin 1 led to the formation of uncharacteristically large OCLs exhibiting greater multinucleation in the RAW264.7 culture (Figure 8.3A). Similarly, in Bryostatin 1-treated BMMs, enhanced clusters of nuclei were observed in OCLs (Figure 8.3B).

In order to further validate the dramatic increase in the number of nuclei in osteoclast after the Bryostatin 1 treatment, a semiquantitative RT-PCR was performed using DC STAMP primer which is recognized as the marker for osteoclast fusion. RAW264.7 cells were treated with Bryostatin 1 and Rottlerin at a final concentration of 200nM and 2uM respectively, in the presence of RANKL for 3 days. It was observed that the gene expression of DC-STAMP increased in Bryostatin 1-treated cells compared to cells that were stimulated with RANKL only. On the other hand, Rottlerin had no effect on DC-STAMP gene expression (Figure 8.4). In short, these findings indicated that Rottlerin inhibited RANKL-induced osteoclast differentiation whereas Bryostatin 1 potentiated osteoclastogenesis and fusion of osteoclasts.

8.2.2 Rottlerin inhibits osteoclastic bone resorption

Giant cell tumour (GCT) of bone is a primary osteolytic tumour of bone which is characterized by the pathological bone destruction at the epiphysis of lone bones with locally massive increase of multinucleated osteoclast-like giant cells. The unique function of osteoclast is bone resorption. Given the dramatic inhibitory properties of Rottlerin on RANKL-induced osteoclast formation, it was therefore of interest to

Figure 8.2A and B

Figure 8.2C and D

Figure 8.3

Figure 8.4

determine the effect(s) of Rottlerin on pathological bone resorption caused by GCT. GCT-derived multinucleated cells were seeded onto the bone slices with approximately 50% surface area. They were cultured in the presence of either vehicle or different concentrations of Rottlerin (2 and 4uM) for 72 hours. The representative images of TRACP positive osteoclast-like cells on bone slices and bone resorption pits examined by SEM are shown in Figure 8.5A. In the presence of Rottlerin, the osteoclast-like cells exhibited morphological changes, being markedly smaller and less multinucleated compared to the control group. In addition, both 2 and 4uM of Rottlerin attenuated the osteoclast-like cell formation. No apparent cell death was observed at the doses applied. As shown in the results of semiquantitative analysis of resorbing area, the bone resorption from GCT was significantly reduced by Rottlerin. Surprisingly, although Bryostatin 1 enlarged the OCLs and its number, the bone resorbing area induced by GCT is significantly reduced by 50% by Bryostatin 1 (Figure 8.5B). However, cell death was not observed from cells treated with Bryostatin 1.

8.2.3 Rottlerin induces apoptosis in RAW264.7 cell-derived osteoclast and GCT

In search for an explanation for the loss of osteoclasts in cultures exposed to higher concentrations of Rottlerin (5 and 10uM), the apoptotic effect of Rottlerin on mature osteoclast-like cells was explored. Osteoclast-like cells were seeded onto coverslips in either the presence of vehicle or Rottlerin (1 and 10uM) separately for 24 hours. The cells were then fixed and immunostained with Rhodamine-conjugated Palloidin and Hoechst 33342 to visualized cytoskeletal (F-actin) and nuclear morphology, respectively. Using confocal microscopy, it was observed that OCLs treated with 10uM of Rottlerin displayed striking morphological aberrations, as the cytoskeletal organization was disorganized and the nuclei were displaying fragmentation each a characteristics of cellular apoptosis. In contrast, no nuclear fragmentation was observed with 1uM of Rottlerin. Although no apoptotic effect was displayed at low concentration levels of Rottlerin, the change of cytoskeletal structures was evident as the F-actin rings displayed a somewhat diffuse distribution pattern (Figure 8.6).

Next, the apoptotic effect of Rottlerin on osteoclasts under pathological condition was examined by using OCLs derived from Giant cell tumour (GCT). First, the OCLs were treated with Rottlerin at a final concentration level of 2uM, 5uM and 10uM for 24 hours.

Figure 8.5A

Figure 8.5B

Figure 8.6

Subsequently, the OCLs were fixed and triple-stained with Rhodamine-conjugated Phalloidin, α-tubulin and Hoechst 33342 to visualized microfilaments, microtubules and chromatin, respectively. The untreated OCLs displayed the characteristic F-actin rings (red), a spatially organized microtubule array (Green and Flavell) and intact nuclei (blue). In contrast, the Rottlerin-treated OCLs exhibited changes in the integrity of F-actin ring, microtubule organization, and marked nuclear fragmentation. At lower concentration levels, it was observed that the cells had fewer nuclei. While there were subtle changes in the actin filament, the nuclei remained normal. On the contrary, 10uM of Rottlerin induced obvious morphological changes of OCLs. Interestingly, the clustering of F-actin was observed, and the F-actin ring and podosome arrangement were disrupted. The OCLs displayed the micronucleation and fragmentation of the nuclei as well as chromatin condensation (Figure 8.7A).

The effect of Bryostatin 1 on osteoclast morphology was also examined using the OCLs derived from GCT. The latter was treated with Bryostatin 1 at final concentrations of 100, 200 and 400 nM. It was observed a notable increase in the number of OCLs. Even though the OCLs were slightly enlarged with a high concentration of Bryostatin 1, the architecture of microtubules, F-actin arrangements as well as the nucleations of those cells were normal. In short, these results suggest that Bryostatin 1 has no apoptotic effect on the OCLs derived from GCT (Figure 8.7B).

8.2.4 Rottlerin suppresses RANKL-induced NF-κB activation, and Bryostatin 1 potentiates RANKL-induced NF-κB activity

In order to study the underlying mechanisms of the inhibitory effect of Rottlerin on osteoclastogenesis, the major signaling pathways activated by RANKL was investigated. To this end, RAW264.7 cells were transiently transfected with a NF-κB-driven luciferase reporter gene construct named *3κB-Luc-SV40,* and then treated with RANKL, Rottlerin and the combination of both after 48 hours post-transfection. The transfected cells were pre-treated separately with various doses of concentration ranging from 0-5uM, and subsequently stimulated with RANKL for 8 hours to achieve the maximum activation of NF-κB. As shown in Figure 8.8A, RANKL induced a four-fold increase in the activation of NF-κB activity as compared to the unstimulated cells. Rottlerin dose-dependently significantly suppressed the RANKL-induced NF-κB activation at 2uM and 5uM. However, it did not significantly decrease the basal NF-κB activity at

Figure 8.7A

Figure 8.7B

any concentration level. In contrast to the effect of Rottlerin on RANKL-induced NF-κB activation, Bryostatin 1 significantly potentiated the RANKL-induced NF-κB activity at both concentration levels (50 and 100nM) ($p<0.05$). In addition, Bryostatin 1 also significantly increased the basal level of NF-κB ($p<0.05$).

Next, to examine the effects of Rottlerin and Bryostatin 1 on the p65 translocation in BMM, immnohistochemistry was performed using an anti-p65 antibody. The BMMs were treated individually with 1 and 10uM of Rottlerin as well as 100 and 200nM of Bryostatin 1 for 2 hours, and then stimulated with 1ug/ml of LPS for another 30 minutes before proceeding with immunohistochemistry. As shown in Figure 8.8B, p65 was translocated from the cell cytoplasm to the nucleus upon LPS stimulation. It was observed that 1uM of Rottlerin partially inhibited the p65 translocation as p65 was found in both cytoplasm and nuclei in some BMM cells. At 10uM of Rottlerin, the translocation of p65 to the nuclei by LPS stimulation was completely abolished. In contrast, p65 was localized in the cell cytoplasm and nuclei with 100nM and 200nM of Bryostatin 1. These results suggest that Bryostatin 1 had potentiated the effect on the LPS-induced p65 translocation.

The NF-κB factors undergo nuclear translocation after their release from cytoplasmic inhibitory proteins of the I-κB family. The proteosomal degradation of I-κB proteins follows the signal-dependent phosphorylation and ubiquitination. To further examine whether Rottlerin inhibited NF-κB nuclear translocation by preventing IκB-α degradation, the RAW264.7 cells were seeded at the density of 5×10^5 cells per well in 6-well plates and cultured in complete α-MEM. The cells were pre-treated separately with 2 uM of Rottlerin, as well as 200 nM of Bryostatin 1 for 30 minutes and subsequently stimulated with RANKL for 5-60 minutes. Western blot analysis was performed using a polyclonal antibody against IκB-α. The results showed that the RANKL-induced IκB-α degradation peaked between 15 to 30 minutes and followed by IκB-α re-synthesis at 45 and 60 minutes. Bryostatin 1 increased and prolonged the RANKL-induced IκB-α degradation (Figure 8.8C), whereas Rottlerin prolonged the RANKL-induced IκB-α degradation from 15 to 60 minutes (Figure 8.8C). These results suggest that Rottlerin might inhibit NF-kB via an alternative pathway.

Figure 8.8A

Figure 8.8B

Figure 8.8C

8.2.5 Rottlerin reduces RANKL-induced NFAT activity

The synthesis of the transcription factors NFAT2/NFATc1 has been demonstrated to play a crucial role in RANKL-stimulated signaling pathways, and the activation of both transcription factors is necessary and sufficient for osteoclastogenesis (Ikeda et al., 2004). The effect of Rottlerin on RANKL-induced NFAT activity was therefore examined. A luciferase reporter plasmid named pNFAT-luc was transiently transfected into the RAW264.7 cells, and subsequently pre-treated with Rottlerin (1, 2 and 5uM) and stimulated with 100ng/ml of RANKL for 8 hours. The NFAT activities were measured as the luciferase activity, and it increased by two-folds after the RANKL stimulation. Rottlerin at 2uM and 5uM significantly reduced the RANKL-induced NFAT activation. However, the basal level of NFAT luciferase activity was reduced only at 5uM of Rottlerin (Figure 8.9). This result might be due to cell apoptosis caused at 5uM of Rottlerin (shown previously in Figure 8.6).

8.2.6 The effect of Bryostatin 1 and Rottlerin on cSrc protein expression

To examine the effect of Bryostatin 1 and Rottlerin on cSrc protein expression, RAW cells were treated for 1 hour with Bryostatin 1 (200 nM) and Rottlerin (2 uM) prior to stimulation with RANKL for 3 days. Whole cell extract were analyzed for total cSrc protein expression by Western blotting. The results showed that Bryostatin 1 decreased cSrc protein expression, whereas Rottlerin increased cSrc protein levels (Figure 8.10).

Figure 8.9

Figure 8.10

8.3 DISCUSSION

The PKC family comprises at least 12 closely related isoenzymes. Their differences in structure, cofactor requirement for activation, substrate specificity, tissue distribution and subcellular localization suggest that PKCs function in an isoenzyme-specific manner in any given cell type. The whole range of PKCs' isozymes has been relatively well studied in different cell types. However, very little understanding of the role of PKCs in bone biology is known. The role of individual isoenzymes of PKCs involved in osteoclast differentiation and activation remains unidentified. We have previously shown that PKCs play an important role in osteoclastogenesis as well as in osteoclast activity employing the PKC modulator, TPA (Wang et al., 2003b) and inhibitors (refer to chapter 7). In order to unravel the role of individual PKC isotypes in osteoclast differentiation and activity, a potent PKCδ-selective inhibitor and activator, Rottlerin and Bryostatin 1 respectively, were employed to explore the involvement of PKCδ in osteoclasts. Both Rottlerin and Bryostatin 1 have been used to study the function and cellular responses of PKCδ in other cell types (Mutter and Wills, 2000; Ringshausen et al., 2006; Tillman et al., 2003).

The cells of monocyte and macrophage lineage express not only the classical isoenzymes (α, βI, and βII), but also the novel (δ and ε) and atypical (ζ) isoenzymes (Chang and Beezhold, 1993; Fujihara et al., 1994; Kontny et al., 1999). Besides the PKC isozymes mentioned above, the RAW264.7 cells also express PKCμ and λ (Larsen et al., 2000; Lin and Chen, 1998).

Studies regarding the contribution of the PKC isoenzymes to the regulation of cell functions are scarce. In this study, it was found that Rottlerin inhibits osteoclastogenesis and osteoclast activity. Rottlerin has been reported to be a selective inhibitor of PKC that exerts different IC_{50} values for PKC δ (3-6uM) and PKCα (30-42uM) (Gschwendt et al., 1994). It has been shown to inhibit LPS-induced translocation of PKCδ and α at a concentration of 15uM and 50uM respectively (Kontny et al., 2000) and can discriminate between these two isoenzymes. In this study, it was found that 2uM of Rottlerin remarkably impaired RANKL-induced osteoclastogenesis in both RAW264.7 cells and BMM culture with suppressed TRACP activity and gene expression of the calcitonin receptor.

On the contrary, the PKCδ activator, Bryostatin 1, markedly enhanced RANKL-induced osteoclastogenesis with a dramatic increase in osteoclast size and nuclei number. The formation of multinuclear osteoclasts involves the movement of mononuclear osteoclasts to adjacent cells and the subsequent occurrence of fusion. The enlargement of osteoclasts by Bryotatin 1 might be due to the enhancement of fusion of precursors as the gene expression of DC-STAMP is increased. Briefly, these findings indicated that PKCδ plays a role in modulating osteoclastogenesis and its mechanism might involve the fusion of mononuclear osteoclast into multinucleated mature osteoclast. In addition, the mechanincal stress-activated PKCδ was found to regulate a smooth muscle cell migration as demonstrated by the PKCδ$^{-/-}$ mice (Li et al., 2003). However, the role of PKCδ in cell migration in other cell types including osteoclast remains to be elucidated.

The precise role of PKCδ in the regulation of apoptosis remains controversial. The important roles of PKCδ might be pro-apoptotic or anti-apoptotic, depending on the stimulus and cell type (Gschwendt, 1999). Several studies have documented the activation, translocation and cleavage of PKCδ in response to the apoptotic stimuli, while others have demonstrated the role of PKCδ in cell apoptosis using specific PKC inhibitors. Our results showed that the apoptotic effect of Rottlerin is dose-dependent. Treatment of Rottlerin at 10uM concentration for 24 hours induced apoptosis in mature osteoclasts generated from the RAW264.7 cells as the OCLs displayed nuclei fragmentation and disrupted F-actin rings.

Previous studies have also shown that the RAW264.7 cells undergo apoptosis when treated with 10uM of Rottlerin for 24 hours and the apoptosis occurs via mitochondrial membrane depolarization and caspases' cascade (Gschwendt, 1999). In addition, it was found that a high concentration of Rottlerin induced obvious morphological changes in OCLs derived form GCT, and resulted in the apoptosis of OCLs. The bone resorption from GCT was significantly decreased by Rottlerin. On the other hand, although Bryostatin 1 enlarged the OCLs derived from RAW264.7 cells as well as GCTs, it has no apoptotic effect on OCLs. Interestingly, the bone resorption by the OCLs derived from RAW264.7 cells and GCT is reduced by Bryostatin 1. It is possible that the morphological changes of enlarged OCLs might affect the resorbing.

The NF-κB activation is central to the RANKL-induced osteoclastogenesis (Boyce et al., 1999b; Franzoso et al., 1997b; Iotsova et al., 1997c). There are two NF-κB signaling

pathways: 1) **classical pathway**, which depends on three subunit IKK holocomplexes that phosphrylate IκBs to induce degradation; and 2) **alternative pathways**, which depends on IKK-α homodimers to induce p100 and nuclear translocation of RelB-p52 dimers (Karin et al., 2004). The effects of PKC inhibitor and activator on IκBα degradation were examined since it is involved in the upstream of classical NF-κB signaling pathways and subsequently examined the NF-κB transcription. The RANKL-induced NF-κB transcription was inhibited by Rottlerin and potentiated by Bryostatin 1. Surprisingly, the degradation of IκBα were prolonged by Rottlerin and Bryostatin 1, are contradictory to the results of NF-κB transcription activation. These results might suggest the alternative pathways of NF-κB are important in the regulation by Rottlerin.

In line with the results of NF-κB transcription, the p65 translocation was inhibited by Rottlerin but enhanced by Bryostatin 1, consistent with the effect of NF-κB activation. It is also possible that these two PKC modulators might have effect on the alternative NF-κB pathway. Although further investigation is required to determine the mechanisms of these two PKC modulators, these data demonstrated that the induction of NF-κB-dependent transcription by RANKL was inhibited by the PKCδ inhibitor (Rottlerin) and potentiated by the PKCδ activator (Bryostatin 1), further supporting the involvement of PKCδ in osteoclastogenesis.

Both NFAT and c-Src have been shown to play an important role in osteoclastgenesis. Induction of NFAT potentiates osteoclastogenesis (Ikeda et al., 2004), whereas induction of c-Src protein expression reduces osteoclastogenesis (Soriano et al., 1991). The effects of Byrostatin and Rottlerin on the expression of NFAT and cSrc are consistent with their effects osteoclastogenesis.

Our findings indicated that PKCδ has a role in the regulation of osteoclast formation and function potentially by participating in the NF-kB signaling pathway of RANKL. More stringent approaches like a dominant negative PKCδ or even a PKCδ knockout mice model are required for future studies to ascertain the precise role of PKCδ in osteoclast differentiation and activation.

CHAPTER 9

General Summary, Conclusions and Future Directions

CHAPTER 9– GENERAL SUMMARY, CONCLUSIONS AND FUTURE DIRECTIONS

9.1 OVERVIEW OF THESIS

RANKL is a key cytokine for osteoclast differentiation and activation (Kong et al., 1999a; Lacey et al., 1998a). The association of RANKL to its cognate receptor, RANK, which is expressed on osteoclast precursors and mature osteoclasts, is essential for osteoclast formation and activation (Fuller et al., 1998; Hsu et al., 1999a).

In order to shed new light on the mechanism(s) of osteoclast physiology, four truncation mutants of RANKL within the TNF-like core domain were generated. The predicted crystal structures of truncation mutants of RANKL based on the proposed crystal structure of RANKL, display distinctive structural variations when compared to the wild-type RANKL. These structural deficiencies in RANKL were predicted to alter the folding of proteins and sequentially effect their binding to receptor RANK and the biological activity of osteoclast precursors and osteoclast. In this study, our results demonstrated that the truncation mutants of RANKL within the TNF-like domain showed impaired osteoclastogenesis and bone resorption as compared to the wild-type RANKL. The impaired function of the truncation mutants of RANKL showed a highly positive correlation with their reduced effect on RANK signaling including NF-κB, IκBα, ERK and JNK.

Interestingly, also it was also found that these truncation mutants of RANKL were able to bind to RANK differentially. The differential binding affinity of these truncation mutants of RANKL and their lack of signaling induction might account for their inhibition of osteoclast differentiation and activity. Furthermore, it was found that RANKL mutants were capable of inhibiting the interaction of wild-type RANKL and wild-type RANKL-induced osteoclastogenesis in a dose-dependent manner. Among the four truncation mutants of RANKL examined, mutant RANKL5 (aa246-318) displayed only minor effect on osteoclastogenesis, but exhibited the most potent inhibitory effect on wild-type RANKL-induced osteoclast formation and bone resorption.

These findings are consistent with previous studies which show that naturally occurring shorter isoforms of RANKL have no effect on osteoclast formation, but inhibit the fusion of pre-osteoclasts when co-expressed with full-length RANKL (Ikeda et al.,

2003). Collectively, the results of this study highlight the potential of RANKL mutant molecules in blocking the deleterious biological effects in RANKL-induced osteoclastogenesis and bone resorption. The RANKL mutants may act as inhibitory peptides for RANKL-induced osteoclast formation and function. Studies on the structural determinants of RANKL interaction could facilitate the pharmacological design of small molecule mimetics that block osteoclast activity and hence, ameliorate bone lytic disorders.

During bone resorption, osteoclasts are exposed to a high extracelluar level of Ca^{2+} (Silver et al., 1988b). The latter has been shown to trigger an increase in cytosolic Ca^{2+}, through Ca^{2+} release from internal stores and/or Ca^{2+} influx, and this results in the inhibition of bone resorption (Zaidi et al., 1999b; Zaidi et al., 1999c) and induction of osteoclast apoptosis (Lorget et al., 2000). In this study, it was determined to examine the regulatory mechanisms which allow osteoclasts to tolerate the high level of Ca^{2+} in their immediate microenvironments. The findings documented in this thesis demonstrate that RANKL protects against high extracellular Ca^{2+}-induced loss of OCLs, indicating a paracrine action of RANKL on combating the deleterious effects of elevated extracellular Ca^{2+} on osteoclasts. The inhibition of RANKL-induced activation of NF-κB and AP-1 by the high extracellular Ca^{2+} level was also observed in this study, suggesting that it might act as a negative feedback mechanism. Recent studies reported that the release of RANKL-elevated cytosolic Ca^{2+} from the intracellular stores via a PLC pathway resulted in an increased NF-κB nuclear translocation and transcription, which in turn promoted osteoclast survival under normal Ca^{2+} concentration (Komarova et al., 2003). Likewise, it was found that RANKL activates NF-κB, JNK and ERK signaling pathways and increases the survival chances of osteoclasts. In conclusion, this study highlights a reciprocal regulation of the high extracellular Ca^{2+} and RANKL signaling pathways, hence indicating that the cross-talk between them plays an important role in the regulation of osteoclast function.

Since the unraveling of RANKL/RANK system, great efforts have made towards dissecting RANK-initiated intracellular signaling. Although RANKL-induced signaling pathways such as NF-κB, NFAT, JNK, ERK and PI3 kinase have been studied extensively, additional signaling pathways involved in the osteoclast growth and activity have yet to be determined. The protein kinase C (PKC) pathway has been suggested to be an important regulator of osteoclastic bone resorption (Rucci et al., 2005). The role

of PKC in RANKL-induced osteoclastogenesis, however, is not clear.

In this thesis, a PKC activator named 12-*O*-tetradecanoylphorbol-13-acetate (TPA) was first used to study the role of PKC in osteoclastogenesis. The findings indicate that TPA inhibits osteoclastogenesis by suppressing the RANKL-induced NF-κB activation. Given that NF-κB activation is obligatory for osteoclast differentiation; our studies imply that the inhibition of osteoclastogenesis by TPA is, at least in part, caused by the suppression of RANKL-induced activation of NF-κB during the early stage of osteoclastogenesis. The selective modulation of RANKL signaling pathways by TPA (as shown in this study) led us to discover the possible mechanisms involved in these signaling events. Therefore, a conventional and a broad spectrum PKC inhibitor namely GÖ 6976 and GF 109203X were used, respectively. Both PKC inhibitors demonstrated inhibitory effect on RANKL-induced osteoclastogenesis and bone resorption. They also inhibited p65 translocation and its downstream signaling pathway NF-κB but not upstream signaling pathways like IκBα degradation.

Our results suggest that GÖ 6976 and GF 109203X prevent osteoclastogenesis and bone resorption by selectively inhibiting the downstream of RANKL-induced NF-κB signaling pathways. There are two possible reasons for the inhibition of NF-κB signaling: 1) to prevent RANKL-induced phosphorylation of p65; 2) to prevent phosphorylated p65 into nucleus.

PKC inhibitors GÖ 6976 and GF 109203X inhibited RANKL-induced osteoclastogenesis as well as bone resorption. Intriguingly, it was observed that the suppressive effect of TPA on RANKL-induced NF-κB activation was prevented by GÖ 6976, a conventional PKC inhibitor. TPA exhibits an inhibitory effect on RANKL-induced NF-κB activation in $RAW_{246.7}$ cells (Wang et al., 2003b), and induces the activation of PKC α, βI, βII, δ, ε, and μ isoforms in $RAW_{246.7}$ cells, where the pre-treatment for 2-24 hours could result in the down-regulation of PKC α, βI, βII, and δ expressions (Lin and Chen, 1998). From the results presented here, together with previously published data, it is possible to deduce that the modulation of PKC by TPA is not only dose-dependent but also time-dependent. Moreover, even though both GÖ 6976 and GF 109203X are selective inhibitors, they are specific for PKC isoenzymes and thus, it is difficult to ascertain the mechanisms for their inhibitory effect on osteoclastogenesis and bone resorption. Nonetheless, these results indicate that PKC

plays an important role in osteoclast differentiation and activity.

In order to provide further mechanistic insight into the role of PKC in RANKL-mediated osteoclast differentiation and activity, the individual isoenzyme, PKCδ was investigated using the potent selective PKCδ inhibitor and activator, Rottlerin and Bryostatin 1, respectively. Rottlerin was shown to exert inhibitory effect on RANKL-induced osteoclastogenesis and bone resorption. In support of the inhibitory effect of Rottlerin, Bryostatin 1 enhances osteoclastogenesis possibly through the fusion mechanism as the RANKL-induced OCLs are enlarged with more nuclei. Interestingly, the bone resorption from OCLs derived from GCT was reduced by Bryostatin 1.

The morphological changes observed in OCLs that were treated with Bryostatin 1 reflect their reduced ability to resorb bone. This disturbed osteoclast morphology and function might be caused by the excessive fusion of the osteoclast precursors. Furthermore, Rottlerin has also shown to inhibite NF-κB activity but not IκB-α degradation, whereas Bryostatin 1 enhanced NF-κB activity and IκB-α degradation. They have also shown modulation of other signaling pathways like NFAT and total c-Src. At present, the precise reasons for these intracellular mechanisms of PKCδ in osteoclastogenesis and bone resorption remain unknown. To our knowledge, this is the report that demonstrates the involvement of PKCδ in osteoclastogenesis and resorption as well as the modulation of RANKL-induced signaling pathways. Although further research is required to determine the intracellular mechanisms of PKCδ in osteoclastogenesis and bone resorption, our findings indicate that PKCδ plays an important role in RANKL-induced osteoclast differentiation and activity.

9.2 FUTURE DIRECTIONS

The results of this thesis have revealed several new avenues of future research which should be pursued in order to better define the extracellular and intracellular mechanisms involved in osteoclast differentiation and activity:

Truncation Mutants of RANKL and Clinical Application

a) It was demonstrated that truncation mutants of RANKL can inhibit RANKL-induced osteoclastogenesis and bone resorption. The truncation mutants were capable of binding to RANK differentially and compete in binding with wild-type RANKL. While there is no doubt that these RANKL mutants impaired osteoclastogenesis and bone resorption *in vivo*, whether their inhibitory effects translate *in vitro* remains to be determined. Thus, it would be of interest to examine the effect of these RANKL mutants *in vivo* by using the animal model. This may be achieved by injecting the RANKL mutants and wild-type RANKL intravenously into mice and measure the calcium level in the blood. The inhibition of RANKL-induced hypercalceamia would be an important indicator to demonstrate the therapeutic potential of these RANKL mutants.

b) In this thesis, all truncation mutants of RANKL had deletions at either the N- or C-terminal of TNF-like core domain. The size of these RANKL mutants ranges from 72-142aa, and they have different deletions of bF, bG, bH strands and/or bA, AA' loop, bB, bC, CD loop and bD. Despite the fact that they all have inhibitory effect on RANKL-induced osteoclastogenesis, RANKL5 (aa246-318) is the best candidate to be studied comprehensively due to its inhibitory potency on osteoclast differentiation and activity. These results led to the concept of generating smaller peptides where their amino acids coincide with RANKL5. Four small peptides evenly cut RANKL5 consisting of approximately 20 amino acids might be the ideal choices to facilitate further investigation. (REF of small RANKL peptides). In addition, it would be of interest to examine whether these TNF-like core domains have any effect on the RANKL-RANK interaction as well as the signaling pathway.

c) The results of this dissertation have also led to the hypothesis that particular amino acid(s) might be critical in its binding to RANK and/or activate the important signaling events. The generation of RANKL mutants by using the

site-direct mutagenesis approach to mutate the key residues, would also present a useful tool for pin pointing the exact mechanisms involved in osteoclast differentiation and activation. Such studies might yield important new information and aid the development of basic scientific research into future clinical application.

Protein Kinase C (PKC) Pathways Characterization

In the present investigation, the PKC pathways involved in osteoclast differentiation and activation were extensively studied using the PKC modulator (TPA) and general PKC inhibitors (GÖ 6976 and GF 109203X) as well as PKCδ inhibitor and activator (Rottlerin and Bryostatin 1, respectively). While all PKC inhibitors have shown inhibitory effects on RANKL-induced osteoclast formation and activity, the PKC activator was found to potentiate osteoclast fusion. Interestingly, compounds such GÖ 6976 and Rottlerin have known anti-cancer properties, suggesting their potential use in tumour-mediated osteolysis. Although these selective PKC inhibitors effectively and potently inhibit osteoclastogenesis and prevent bone resorption, their inhibitory specificity in PKC is not clear. Therefore, their modulation of PKC involved in osteoclast differentiation and activation might be interfered and/or effected by other mechanisms. Two alternative approaches to better define the underlying mechanisms involved are as follow:

a) Introduce over-expression of constitutively active and dominant-negative PKC isotypes into the osteoclast culture system using a retrovirus-mediated approach. Recently four constructs were obtained including a wild-type PKCδ, two constitutive active PKCδ, and one dominant-negative PKCδ (kinase inactive) and have been subcloned into pMX-IRIS retroviral vectors. This approach would give us a greater insight into understanding the role of PKCδ in osteoclast differentiation and activity. In addition, it has been shown that while the PKC activator induced fusion and the morphological changes of osteoclasts, it surprisingly inhibited bone resorption. It would be of interest to examine whether PKCδ plays an important role in the cytoskeletal organization of osteoclast. The signalling events of RANKL/RANK should also be determined.

b) The results from this thesis suggest that PKCδ plays an important role in osteoclastogenesis and function. Perhaps the most comprehensive approach is to

further study the role of PKCδ in osteoclast is to examine its role through knockout mice. We have recently aquired PKCδ$^{-/-}$ mice which are in the process of breeding. Notably, no studies relating to bone have been performed previously. It would be of interest to characterize the micro-architecture and biochemical properties of bone derived from PKCδ$^{-/-}$ mice by microCT, histomorphometry and loading studies. More importantly, it is also essential to examine whether there are any resorptive or osteoclastogenesis deficiencies in PKCδ-deficient mice.

CHAPTER 10

Bibliography

CHAPTER 10 – BIBLIOGRAPHY

Abbas, S., J.C. Clohisy, and Y. Abu-Amer. 2003. Mitogen-activated protein (MAP) kinases mediate PMMA-induction of osteoclasts. *J Orthop Res*. 21:1041-8.

Abramson, J., and I. Pecht. 2002. Clustering the mast cell function-associated antigen (MAFA) leads to tyrosine phosphorylation of p62Dok and SHIP and affects RBL-2H3 cell cycle. *Immunol Lett*. 82:23-8.

Adebanjo, O.A., B.S. Moonga, T. Yamate, L. Sun, C. Minkin, E. Abe, and M. Zaidi. 1998. Mode of action of interleukin-6 on mature osteoclasts. Novel interactions with extracellular Ca2+ sensing in the regulation of osteoclastic bone resorption. *In* J Cell Biol. Vol. 142. 1347-56.

Akisaka, T., T. Yamamoto, and C.V. Gay. 1988. Ultracytochemical investigation of calcium-activated adenosine triphosphatase (Ca++-ATPase) in chick tibia. *J Bone Miner Res*. 3:19-25.

Alimzhanov, M.B., D.V. Kuprash, M.H. Kosco-Vilbois, A. Luz, R.L. Turetskaya, A. Tarakhovsky, K. Rajewsky, S.A. Nedospasov, and K. Pfeffer. 1997. Abnormal development of secondary lymphoid tissues in lymphotoxin beta-deficient mice. *Proc Natl Acad Sci U S A*. 94:9302-7.

Andela, V.B., A.H. Gordon, G. Zotalis, R.N. Rosier, J.J. Goater, G.D. Lewis, E.M. Schwarz, J.E. Puzas, and R.J. O'Keefe. 2003. NFkappaB: a pivotal transcription factor in prostate cancer metastasis to bone. *Clin Orthop*:S75-85.

Anderson, D.M., E. Maraskovsky, W.L. Billingsley, W.C. Dougall, M.E. Tometsko, E.R. Roux, M.C. Teepe, R.F. DuBose, D. Cosman, and L. Galibert. 1997a. A homologue of the TNF receptor and its ligand enhance T-cell growth and dendritic-cell function. *Nature*. 390:175-9.

Anderson, D.M., E. Maraskovsky, W.L. Billingsley, W.C. Dougall, M.E. Tometsko, E.R. Roux, M.C. Teepe, R.F. DuBose, D. Cosman, and L. Galibert. 1997b. A homologue of the TNF receptor and its ligand enhance T-cell growth and dendritic-cell function. *Nature*. 390:175-9.

Aoki, K., H. Saito, C. Itzstein, M. Ishiguro, T. Shibata, R. Blanque, A.H. Mian, M. Takahashi, Y. Suzuki, M. Yoshimatsu, A. Yamaguchi, P. Deprez, P. Mollat, R. Murali, K. Ohya, W.C. Horne, and R. Baron. 2006. A TNF receptor loop peptide mimic blocks RANK ligand-induced signaling, bone resorption, and bone loss. *J Clin Invest*. 116:1525-34.

Arai, F., T. Miyamoto, O. Ohneda, T. Inada, T. Sudo, K. Brasel, T. Miyata, D.M. Anderson, and T. Suda. 1999. Commitment and differentiation of osteoclast precursor cells by the sequential expression of c-Fms and receptor activator of nuclear factor kappaB (RANK) receptors. *J Exp Med*. 190:1741-54.

Ariga, A., J. Namekawa, N. Matsumoto, J. Inoue, and K. Umezawa. 2002. Inhibition of tumor necrosis factor-alpha -induced nuclear translocation and activation of NF-kappa B by dehydroxymethylepoxyquinomicin. *J Biol Chem*. 277:24625-30.

Arthur, J.M., M.S. Lawrence, C.R. Payne, M.J. Rane, and K.R. McLeish. 2000. The calcium-sensing receptor stimulates JNK in MDCK cells. *In* Biochem Biophys Res Commun. Vol. 275. 538-41.

Aubin, J.E. 2001. Regulation of osteoblast formation and function. *Rev Endocr Metab Disord*. 2:81-94.

Banner, D.W., A. D'Arcy, W. Janes, R. Gentz, H.J. Schoenfeld, C. Broger, H. Loetscher, and W. Lesslauer. 1993. Crystal structure of the soluble human 55 kd TNF receptor-human TNF beta complex: implications for TNF receptor activation. *Cell*. 73:431-45.

Baron, R., L. Neff, W. Brown, P.J. Courtoy, D. Louvard, and M.G. Farquhar. 1988. Polarized secretion of lysosomal enzymes: co-distribution of cation-independent

mannose-6-phosphate receptors and lysosomal enzymes along the osteoclast exocytic pathway. *J Cell Biol*. 106:1863-72.

Baron, R., L. Neff, W. Brown, D. Louvard, and P.J. Courtoy. 1990. Selective internalization of the apical plasma membrane and rapid redistribution of lysosomal enzymes and mannose 6-phosphate receptors during osteoclast inactivation by calcitonin. *J Cell Sci*. 97 (Pt 3):439-47.

Baron, R., L. Neff, D. Louvard, and P.J. Courtoy. 1985. Cell-mediated extracellular acidification and bone resorption: evidence for a low pH in resorbing lacunae and localization of a 100-kD lysosomal membrane protein at the osteoclast ruffled border. *J Cell Biol*. 101:2210-22.

Baron, R., L. Neff, C. Roy, A. Boisvert, and M. Caplan. 1986a. Evidence for a high and specific concentration of (Na+,K+)ATPase in the plasma membrane of the osteoclast. *Cell*. 46:311-20.

Baron, R., L. Neff, P. Tran Van, J.R. Nefussi, and A. Vignery. 1986b. Kinetic and cytochemical identification of osteoclast precursors and their differentiation into multinucleated osteoclasts. *Am J Pathol*. 122:363-78.

Barrett, J., E. Worth, F. Bauss, and S. Epstein. 2004. Ibandronate: a clinical pharmacological and pharmacokinetic update. *J Clin Pharmacol*. 44:951-65.

Bartimole, T.M., J.A. Vrana, A.J. Freemerman, W.D. Jarvis, J.C. Reed, L.H. Boise, and S. Grant. 1997. Modulation of the expression of Bcl-2 and related proteins in human leukemia cells by protein kinase C activators: relationship to effects on 1-[beta-D-arabinofuranosyl]cytosine-induced apoptosis. *Cell Death Differ*. 4:294-303.

Battaglino, R., D. Kim, J. Fu, B. Vaage, X.Y. Fu, and P. Stashenko. 2002. c-myc is required for osteoclast differentiation. *J Bone Miner Res*. 17:763-73.

Bennett, B.D., U. Alvarez, and K.A. Hruska. 2001. Receptor-operated osteoclast calcium sensing. *In* Endocrinology. Vol. 142. 1968-74.

Berridge, M.J., P. Lipp, and M.D. Bootman. 2000. The versatility and universality of calcium signalling. *Nat Rev Mol Cell Biol*. 1:11-21.

Bharti, A.C., Y. Takada, and B.B. Aggarwal. 2004. Curcumin (diferuloylmethane) inhibits receptor activator of NF-kappa B ligand-induced NF-kappa B activation in osteoclast precursors and suppresses osteoclastogenesis. *J Immunol*. 172:5940-7.

Biskobing, D.M., X. Fan, and J. Rubin. 1995. Characterization of MCSF-induced proliferation and subsequent osteoclast formation in murine marrow culture. *J Bone Miner Res*. 10:1025-32.

Blair, H.C., A.J. Kahn, E.C. Crouch, J.J. Jeffrey, and S.L. Teitelbaum. 1986. Isolated osteoclasts resorb the organic and inorganic components of bone. *J Cell Biol*. 102:1164-72.

Blair, H.C., and P.H. Schlesinger. 1990. Purification of a stilbene sensitive chloride channel and reconstitution of chloride conductivity into phospholipid vesicles. *Biochem Biophys Res Commun*. 171:920-5.

Blair, H.C., S.L. Teitelbaum, R. Ghiselli, and S. Gluck. 1989. Osteoclastic bone resorption by a polarized vacuolar proton pump. *Science*. 245:855-7.

Borner, C., S.N. Guadagno, D. Fabbro, and I.B. Weinstein. 1992. Expression of four protein kinase C isoforms in rat fibroblasts. Distinct subcellular distribution and regulation by calcium and phorbol esters. *J Biol Chem*. 267:12892-9.

Bosco, M.C., S. Rottschafer, L.S. Taylor, J.R. Ortaldo, D.L. Longo, and I. Espinoza-Delgado. 1997. The antineoplastic agent bryostatin-1 induces proinflammatory cytokine production in human monocytes: synergy with interleukin-2 and modulation of interleukin-2Rgamma chain expression. *Blood*. 89:3402-11.

Bossard, M.J., T.A. Tomaszek, S.K. Thompson, B.Y. Amegadzie, C.R. Hanning, C. Jones, J.T. Kurdyla, D.E. McNulty, F.H. Drake, M. Gowen, and M.A. Levy. 1996. Proteolytic activity of human osteoclast cathepsin K. Expression, purification, activation, and substrate identification. *J Biol Chem*. 271:12517-24.

Boyce, B.F., L. Xing, G. Franzoso, and U. Siebenlist. 1999a. Required and nonessential functions of nuclear factor-kappa B in bone cells. *In* Bone. Vol. 25. 137-9.

Boyce, B.F., L. Xing, G. Franzoso, and U. Siebenlist. 1999b. Required and nonessential functions of nuclear factor-kappa B in bone cells. *Bone*. 25:137-9.

Boyce, B.F., T. Yoneda, C. Lowe, P. Soriano, and G.R. Mundy. 1992. Requirement of pp60c-src expression for osteoclasts to form ruffled borders and resorb bone in mice. *J Clin Invest*. 90:1622-7.

Boyle, W.J., W.S. Simonet, and D.L. Lacey. 2003. Osteoclast differentiation and activation. *Nature*. 423:337-42.

Brandstrom, H., T. Bjorkman, and O. Ljunggren. 2001. Regulation of osteoprotegerin secretion from primary cultures of human bone marrow stromal cells. *Biochem Biophys Res Commun*. 280:831-5.

Brandt, D., M. Gimona, M. Hillmann, H. Haller, and H. Mischak. 2002. Protein kinase C induces actin reorganization via a Src- and Rho-dependent pathway. *J Biol Chem*. 277:20903-10.

Bucay, N., I. Sarosi, C.R. Dunstan, S. Morony, J. Tarpley, C. Capparelli, S. Scully, H.L. Tan, W. Xu, D.L. Lacey, W.J. Boyle, and W.S. Simonet. 1998. osteoprotegerin-deficient mice develop early onset osteoporosis and arterial calcification. *Genes Dev*. 12:1260-8.

Burger, E.H., J.W. van der Meer, and P.J. Nijweide. 1984. Osteoclast formation from mononuclear phagocytes: role of bone-forming cells. *J Cell Biol*. 99:1901-6.

Burger, E.H., J.W. Van der Meer, J.S. van de Gevel, J.C. Gribnau, G.W. Thesingh, and R. van Furth. 1982. In vitro formation of osteoclasts from long-term cultures of bone marrow mononuclear phagocytes. *J Exp Med*. 156:1604-14.

Burgess, T.L., Y. Qian, S. Kaufman, B.D. Ring, G. Van, C. Capparelli, M. Kelley, H. Hsu, W.J. Boyle, C.R. Dunstan, S. Hu, and D.L. Lacey. 1999a. The ligand for osteoprotegerin (OPGL) directly activates mature osteoclasts. *J Cell Biol*. 145:527-38.

Burgess, T.L., Y. Qian, S. Kaufman, B.D. Ring, G. Van, C. Capparelli, M. Kelley, H. Hsu, W.J. Boyle, C.R. Dunstan, S. Hu, and D.L. Lacey. 1999b. The ligand for osteoprotegerin (OPGL) directly activates mature osteoclasts. *In* J Cell Biol. Vol. 145. 527-38.

Byun, H.S., K.A. Park, M. Won, K.J. Yang, S. Shin, L. Piao, J.Y. Kwak, Z.W. Lee, J. Park, J.H. Seok, Z.G. Liu, and G.M. Hur. 2006. Phorbol 12-myristate 13-acetate protects against tumor necrosis factor (TNF)-induced necrotic cell death by modulating the recruitment of TNF receptor 1-associated death domain and receptor-interacting protein into the TNF receptor 1 signaling complex: Implication for the regulatory role of protein kinase C. *Mol Pharmacol*. 70:1099-108.

Cano, E., and L.C. Mahadevan. 1995. Parallel signal processing among mammalian MAPKs. *Trends Biochem Sci*. 20:117-22.

Capparelli, C., S. Morony, K. Warmington, S. Adamu, D. Lacey, C.R. Dunstan, B. Stouch, S. Martin, and P.J. Kostenuik. 2003. Sustained antiresorptive effects after a single treatment with human recombinant osteoprotegerin (OPG): a pharmacodynamic and pharmacokinetic analysis in rats. *J Bone Miner Res*. 18:852-8.

Carron, C.P., D.M. Meyer, V.W. Engleman, J.G. Rico, P.G. Ruminski, R.L. Ornberg, W.F. Westlin, and G.A. Nickols. 2000. Peptidomimetic antagonists of alphavbeta3

inhibit bone resorption by inhibiting osteoclast bone resorptive activity, not osteoclast adhesion to bone. *J Endocrinol*. 165:587-98.

Carter, C.A. 2000. Protein kinase C as a drug target: implications for drug or diet prevention and treatment of cancer. *Curr Drug Targets*. 1:163-83.

Cassady, A.I., A. Luchin, M.C. Ostrowski, and D.A. Hume. 2003. Regulation of the murine TRACP gene promoter. *J Bone Miner Res*. 18:1901-4.

Catley, M.C., L.M. Cambridge, Y. Nasuhara, K. Ito, J.E. Chivers, A. Beaton, N.S. Holden, M.W. Bergmann, P.J. Barnes, and R. Newton. 2004. Inhibitors of protein kinase C (PKC) prevent activated transcription: role of events downstream of NF-kappaB DNA binding. *J Biol Chem*. 279:18457-66.

Cenci, S., M.N. Weitzmann, M.A. Gentile, M.C. Aisa, and R. Pacifici. 2000. M-CSF neutralization and egr-1 deficiency prevent ovariectomy-induced bone loss. *J Clin Invest*. 105:1279-87.

Chalfant, C.E., S. Ohno, Y. Konno, A.A. Fisher, L.D. Bisnauth, J.E. Watson, and D.R. Cooper. 1996. A carboxy-terminal deletion mutant of protein kinase C beta II inhibits insulin-stimulated 2-deoxyglucose uptake in L6 rat skeletal muscle cells. *Mol Endocrinol*. 10:1273-81.

Chambers, T.J. 2000. Regulation of the differentiation and function of osteoclasts. *J Pathol*. 192:4-13.

Chang, Z.L., and D.H. Beezhold. 1993. Protein kinase C activation in human monocytes: regulation of PKC isoforms. *Immunology*. 80:360-6.

Chellaiah, M., C. Fitzgerald, U. Alvarez, and K. Hruska. 1998. c-Src is required for stimulation of gelsolin-associated phosphatidylinositol 3-kinase. *J Biol Chem*. 273:11908-16.

Chelliah, J., A.J. Freemerman, S. Wu-Pong, W.D. Jarvis, and S. Grant. 1997. Potentiation of ara-C-induced apoptosis by the protein kinase C activator bryostatin 1 in human leukemia cells (HL-60) involves a process dependent upon c-Myc. *Biochem Pharmacol*. 54:563-73.

Chiba, M., S.L. Teitelbaum, X. Cao, and F.P. Ross. 1996. Retinoic acid stimulates expression of the functional osteoclast integrin alpha v beta 3: transcriptional activation of the beta 3 but not the alpha v gene. *J Cell Biochem*. 62:467-75.

Clohisy, J.C., T. Hirayama, E. Frazier, S.K. Han, and Y. Abu-Amer. 2004. NF-kB signaling blockade abolishes implant particle-induced osteoclastogenesis. *J Orthop Res*. 22:13-20.

Coussens, L., C. Van Beveren, D. Smith, E. Chen, R.L. Mitchell, C.M. Isacke, I.M. Verma, and A. Ullrich. 1986. Structural alteration of viral homologue of receptor proto-oncogene fms at carboxyl terminus. *Nature*. 320:277-80.

Coxon, F.P., M.H. Helfrich, R. Van't Hof, S. Sebti, S.H. Ralston, A. Hamilton, and M.J. Rogers. 2000. Protein geranylgeranylation is required for osteoclast formation, function, and survival: inhibition by bisphosphonates and GGTI-298. *J Bone Miner Res*. 15:1467-76.

Crippes, B.A., V.W. Engleman, S.L. Settle, J. Delarco, R.L. Ornberg, M.H. Helfrich, M.A. Horton, and G.A. Nickols. 1996. Antibody to beta3 integrin inhibits osteoclast-mediated bone resorption in the thyroparathyroidectomized rat. *Endocrinology*. 137:918-24.

Crotti, T., M.D. Smith, R. Hirsch, S. Soukoulis, H. Weedon, M. Capone, M.J. Ahern, and D. Haynes. 2003. Receptor activator NF kappaB ligand (RANKL) and osteoprotegerin (OPG) protein expression in periodontitis. *J Periodontal Res*. 38:380-7.

Croucher, P.I., C.M. Shipman, B. Van Camp, and K. Vanderkerken. 2003. Bisphosphonates and osteoprotegerin as inhibitors of myeloma bone disease. *Cancer*. 97:818-24.

Dando, T.M., and L.R. Wiseman. 2004. Clodronate : a review of its use in the prevention of bone metastases and the management of skeletal complications associated with bone metastases in patients with breast cancer. *Drugs Aging*. 21:949-62.

Darnay, B.G., V. Haridas, J. Ni, P.A. Moore, and B.B. Aggarwal. 1998. Characterization of the intracellular domain of receptor activator of NF-kappaB (RANK). Interaction with tumor necrosis factor receptor- associated factors and activation of NF-kappab and c-Jun N-terminal kinase. *J Biol Chem*. 273:20551-5.

David, J.P., K. Sabapathy, O. Hoffmann, M.H. Idarraga, and E.F. Wagner. 2002a. JNK1 modulates osteoclastogenesis through both c-Jun phosphorylation- dependent and -independent mechanisms. *In* J Cell Sci. Vol. 115. 4317-4325.

David, J.P., K. Sabapathy, O. Hoffmann, M.H. Idarraga, and E.F. Wagner. 2002b. JNK1 modulates osteoclastogenesis through both c-Jun phosphorylation-dependent and -independent mechanisms. *J Cell Sci*. 115:4317-25.

De Jesus Ferreira, M.C., and C. Bailly. 1998. Extracellular Ca2+ decreases chloride reabsorption in rat CTAL by inhibiting cAMP pathway. *In* Am J Physiol. Vol. 275. F198-203.

de Jesus Ferreira, M.C., C. Helies-Toussaint, M. Imbert-Teboul, C. Bailly, J.M. Verbavatz, A.C. Bellanger, and D. Chabardes. 1998. Co-expression of a Ca2+-inhibitable adenylyl cyclase and of a Ca2+-sensing receptor in the cortical thick ascending limb cell of the rat kidney. Inhibition of hormone-dependent cAMP accumulation by extracellular Ca2+. *In* J Biol Chem. Vol. 273. 15192-202.

De Togni, P., J. Goellner, N.H. Ruddle, P.R. Streeter, A. Fick, S. Mariathasan, S.C. Smith, R. Carlson, L.P. Shornick, J. Strauss-Schoenberger, and et al. 1994. Abnormal development of peripheral lymphoid organs in mice deficient in lymphotoxin. *Science*. 264:703-7.

Dekker, L.V., and P.J. Parker. 1994. Protein kinase C--a question of specificity. *Trends Biochem Sci*. 19:73-7.

Dekker, L.V., and P.J. Parker. *Protein Kinase C*. 1997. Springer. New York, N. Y., U.S.A.

Dekker, L.V. Protein Kinase C. (2nd Edition) 2004. Plenum Publishers. New York, N.Y., U.S.A.

Delaisse, J.M., T.L. Andersen, M.T. Engsig, K. Henriksen, T. Troen, and L. Blavier. 2003. Matrix metalloproteinases (MMP) and cathepsin K contribute differently to osteoclastic activities. *Microsc Res Tech*. 61:504-13.

Delaisse, J.M., Y. Eeckhout, L. Neff, C. Francois-Gillet, P. Henriet, Y. Su, G. Vaes, and R. Baron. 1993. (Pro)collagenase (matrix metalloproteinase-1) is present in rodent osteoclasts and in the underlying bone-resorbing compartment. *J Cell Sci*. 106:1071-82.

Delaisse, J.M., P. Ledent, and G. Vaes. 1991. Collagenolytic cysteine proteinases of bone tissue. Cathepsin B, (pro)cathepsin L and a cathepsin L-like 70 kDa proteinase. *Biochem J*. 279 (Pt 1):167-74.

Dixit, V., and T.W. Mak. 2002. NF-kappaB signaling. Many roads lead to madrid. *Cell*. 111:615-9.

Dougall, W.C., M. Glaccum, K. Charrier, K. Rohrbach, K. Brasel, T. De Smedt, E. Daro, J. Smith, M.E. Tometsko, C.R. Maliszewski, A. Armstrong, V. Shen, S. Bain, D. Cosman, D. Anderson, P.J. Morrissey, J.J. Peschon, and J. Schuh. 1999. RANK is essential for osteoclast and lymph node development. *Genes Dev*. 13:2412-24.

Drake, F.H., R.A. Dodds, I.E. James, J.R. Connor, C. Debouck, S. Richardson, E. Lee-Rykaczewski, L. Coleman, D. Rieman, R. Barthlow, G. Hastings, and M. Gowen. 1996. Cathepsin K, but not cathepsins B, L, or S, is abundantly

expressed in human osteoclasts. *J Biol Chem*. 271:12511-6.

Ducy, P., T. Schinke, and G. Karsenty. 2000. The osteoblast: a sophisticated fibroblast under central surveillance. *Science*. 289:1501-4.

Dulce, H.J., P. Siegmund, F. Koerber, and E. Schuette. 1960. [On the biochemistry of the dissolution of bone. 3. On the presence of carbonic anhydrase in bones]. *Hoppe Seylers Z Physiol Chem*. 320:163-7.

Duong, L.T., P. Lakkakorpi, I. Nakamura, and G.A. Rodan. 2000. Integrins and signaling in osteoclast function. *Matrix Biol*. 19:97-105.

Duong, L.T., P.T. Lakkakorpi, I. Nakamura, M. Machwate, R.M. Nagy, and G.A. Rodan. 1998. PYK2 in osteoclasts is an adhesion kinase, localized in the sealing zone, activated by ligation of alpha(v)beta3 integrin, and phosphorylated by src kinase. *J Clin Invest*. 102:881-92.

Efimova, T., A. Deucher, T. Kuroki, M. Ohba, and R.L. Eckert. 2002. Novel protein kinase C isoforms regulate human keratinocyte differentiation by activating a p38 delta mitogen-activated protein kinase cascade that targets CCAAT/enhancer-binding protein alpha. *J Biol Chem*. 277:31753-60.

Efimova, T., and R.L. Eckert. 2000. Regulation of human involucrin promoter activity by novel protein kinase C isoforms. *J Biol Chem*. 275:1601-7.

Engedal, N., C.G. Korkmaz, and F. Saatcioglu. 2002. C-Jun N-terminal kinase is required for phorbol ester- and thapsigargin- induced apoptosis in the androgen responsive prostate cancer cell line LNCaP. *Oncogene*. 21:1017-27.

Engleman, V.W., G.A. Nickols, F.P. Ross, M.A. Horton, D.W. Griggs, S.L. Settle, P.G. Ruminski, and S.L. Teitelbaum. 1997. A peptidomimetic antagonist of the alpha(v)beta3 integrin inhibits bone resorption in vitro and prevents osteoporosis in vivo. *J Clin Invest*. 99:2284-92.

Everts, V., J.M. Delaisse, W. Korper, A. Niehof, G. Vaes, and W. Beertsen. 1992. Degradation of collagen in the bone-resorbing compartment underlying the osteoclast involves both cysteine-proteinases and matrix metalloproteinases. *J Cell Physiol*. 150:221-31.

Faccio, R., M. Grano, S. Colucci, A. Villa, G. Giannelli, V. Quaranta, and A. Zallone. 2002. Localization and possible role of two different alpha v beta 3 integrin conformations in resting and resorbing osteoclasts. *J Cell Sci*. 115:2919-29.

Falgueyret, J.P., R.M. Oballa, O. Okamoto, G. Wesolowski, Y. Aubin, R.M. Rydzewski, P. Prasit, D. Riendeau, S.B. Rodan, and M.D. Percival. 2001. Novel, nonpeptidic cyanamides as potent and reversible inhibitors of human cathepsins K and L. *J Med Chem*. 44:94-104.

Fallon, M.D. 1984. Bone resorbing fluid from osteoclasts is acidic – an in vitro micropuncture study. *In* Endocrine control of bone and calcium
metabolism. Vol. 619. Elsevier Science, Amsterdam. pp 144–146.

Fallon, M.D., and H.A. Schwamm. 1989. Paget's disease of bone. An update on the pathogenesis, pathophysiology, and treatment of osteitis deformans. *Pathol Annu*. 24 Pt 1:115-59.

Fallon, M.D., S.L. Teitelbaum, and A.J. Kahn. 1983. Multinucleation enhances macrophage-mediated bone resorption. *Lab Invest*. 49:159-64.

Farina, C., and S. Gagliardi. 2002. Selective inhibition of osteoclast vacuolar H(+)-ATPase. *Curr Pharm Des*. 8:2033-48.

Fata, J.E., Y.Y. Kong, J. Li, T. Sasaki, J. Irie-Sasaki, R.A. Moorehead, R. Elliott, S. Scully, E.B. Voura, D.L. Lacey, W.J. Boyle, R. Khokha, and J.M. Penninger. 2000. The osteoclast differentiation factor osteoprotegerin-ligand is essential for mammary gland development. *Cell*. 103:41-50.

Felix, R., M.G. Cecchini, W. Hofstetter, P.R. Elford, A. Stutzer, and H. Fleisch. 1990. Impairment of macrophage colony-stimulating factor production and lack of

resident bone marrow macrophages in the osteopetrotic op/op mouse. *J Bone Miner Res*. 5:781-9.

Feng, X., D.V. Novack, R. Faccio, D.S. Ory, K. Aya, M.I. Boyer, K.P. McHugh, F.P. Ross, and S.L. Teitelbaum. 2001. A Glanzmann's mutation in beta 3 integrin specifically impairs osteoclast function. *J Clin Invest*. 107:1137-44.

Fisher, J.E., M.P. Caulfield, M. Sato, H.A. Quartuccio, R.J. Gould, V.M. Garsky, G.A. Rodan, and M. Rosenblatt. 1993. Inhibition of osteoclastic bone resorption in vivo by echistatin, an "arginyl-glycyl-aspartyl" (RGD)-containing protein. *Endocrinology*. 132:1411-3.

Franzoso, G., L. Carlson, L. Xing, L. Poljak, E.W. Shores, K.D. Brown, A. Leonardi, T. Tran, B.F. Boyce, and U. Siebenlist. 1997a. Requirement for NF-kappaB in osteoclast and B-cell development. *Genes Dev*. 11:3482-96.

Franzoso, G., L. Carlson, L. Xing, L. Poljak, E.W. Shores, K.D. Brown, A. Leonardi, T. Tran, B.F. Boyce, and U. Siebenlist. 1997b. Requirement for NF-kappaB in osteoclast and B-cell development. *Genes Dev*. 11:3482-96.

Franzoso, G., L. Carlson, L. Xing, L. Poljak, E.W. Shores, K.D. Brown, A. Leonardi, T. Tran, B.F. Boyce, and U. Siebenlist. 1997c. Requirement for NF-kappaB in osteoclast and B-cell development. *In* Genes Dev. Vol. 11. 3482-96.

Fujihara, M., N. Connolly, N. Ito, and T. Suzuki. 1994. Properties of protein kinase C isoforms (beta II, epsilon, and zeta) in a macrophage cell line (J774) and their roles in LPS-induced nitric oxide production. *J Immunol*. 152:1898-906.

Fuller, K., J.M. Owens, C.J. Jagger, A. Wilson, R. Moss, and T.J. Chambers. 1993. Macrophage colony-stimulating factor stimulates survival and chemotactic behavior in isolated osteoclasts. *J Exp Med*. 178:1733-44.

Fuller, K., B. Wong, S. Fox, Y. Choi, and T.J. Chambers. 1998. TRANCE is necessary and sufficient for osteoblast-mediated activation of bone resorption in osteoclasts. *J Exp Med*. 188:997-1001.

Galibert, L., M.E. Tometsko, D.M. Anderson, D. Cosman, and W.C. Dougall. 1998. The involvement of multiple tumor necrosis factor receptor (TNFR)-associated factors in the signaling mechanisms of receptor activator of NF-kappaB, a member of the TNFR superfamily. *J Biol Chem*. 273:34120-7.

Ghosh, S., and M. Karin. 2002. Missing pieces in the NF-kappaB puzzle. *Cell*. 109 Suppl:S81-96.

Gibbs, J.B., and A. Oliff. 1997. The potential of farnesyltransferase inhibitors as cancer chemotherapeutics. *Annu Rev Pharmacol Toxicol*. 37:143-66.

Giuliani, C., G. Napolitano, I. Bucci, V. Montani, and F. Monaco. 2001. [Nf-kB transcription factor: role in the pathogenesis of inflammatory, autoimmune, and neoplastic diseases and therapy implications]. *Clin Ter*. 152:249-53.

Givant-Horwitz, V., B. Davidson, P. Lazarovici, E. Schaefer, J.M. Nesland, C.G. Trope, and R. Reich. 2003. Mitogen-activated protein kinases (MAPK) as predictors of clinical outcome in serous ovarian carcinoma in effusions. *Gynecol Oncol*. 91:160-72.

Gothlin, G., and J.L. Ericsson. 1973. On the histogenesis of the cells in fracture callus. Electron microscopic autoradiographic observations in parabiotic rats and studies on labeled monocytes. *Virchows Arch B Cell Pathol*. 12:318-29.

Goto, T., T. Kiyoshima, R. Moroi, T. Tsukuba, Y. Nishimura, M. Himeno, K. Yamamoto, and T. Tanaka. 1994. Localization of cathepsins B, D, and L in the rat osteoclast by immuno- light and -electron microscopy. *Histochemistry*. 101:33-40.

Green, E.A., and R.A. Flavell. 1999. TRANCE-RANK, a new signal pathway involved in lymphocyte development and T cell activation. *J Exp Med*. 189:1017-20.

Grigoriadis, A.E., Z.Q. Wang, M.G. Cecchini, W. Hofstetter, R. Felix, H.A. Fleisch, and E.F. Wagner. 1994. c-Fos: a key regulator of osteoclast-macrophage lineage

determination and bone remodeling. *Science*. 266:443-8.

Gschwendt, M. 1999. Protein kinase C delta. *Eur J Biochem*. 259:555-64.

Gschwendt, M., S. Dieterich, J. Rennecke, W. Kittstein, H.J. Mueller, and F.J. Johannes. 1996. Inhibition of protein kinase C mu by various inhibitors. Differentiation from protein kinase c isoenzymes. *FEBS Lett*. 392:77-80.

Gschwendt, M., G. Furstenberger, H. Leibersperger, W. Kittstein, D. Lindner, C. Rudolph, H. Barth, J. Kleinschroth, D. Marme, C. Schachtele, and et al. 1995. Lack of an effect of novel inhibitors with high specificity for protein kinase C on the action of the phorbol ester 12-O-tetradecanoylphorbol-13-acetate on mouse skin in vivo. *Carcinogenesis*. 16:107-11.

Gschwendt, M., H.J. Muller, K. Kielbassa, R. Zang, W. Kittstein, G. Rincke, and F. Marks. 1994. Rottlerin, a novel protein kinase inhibitor. *Biochem Biophys Res Commun*. 199:93-8.

Hall, T.J., M. Schaeublin, and T.J. Chambers. 1992. Na+/H(+)-antiporter activity is essential for the induction, but not the maintenance of osteoclastic bone resorption and cytoplasmic spreading. *Biochem Biophys Res Commun*. 188:1097-103.

Hayashi, S., T. Yamane, A. Miyamoto, H. Hemmi, H. Tagaya, Y. Tanio, H. Kanda, H. Yamazaki, and T. Kunisada. 1998. Commitment and differentiation of stem cells to the osteoclast lineage. *Biochem Cell Biol*. 76:911-22.

Haynes, D.R., and T.N. Crotti. 2003. Regulation of bone lysis in inflammatory diseases. *Inflammopharmacology*. 11:323-31.

Haynes, D.R., T.N. Crotti, M. Loric, G.I. Bain, G.J. Atkins, and D.M. Findlay. 2001. Osteoprotegerin and receptor activator of nuclear factor kappaB ligand (RANKL) regulate osteoclast formation by cells in the human rheumatoid arthritic joint. *Rheumatology (Oxford)*. 40:623-30.

Helfrich, M.H., S.A. Nesbitt, P.T. Lakkakorpi, M.J. Barnes, S.C. Bodary, G. Shankar, W.T. Mason, D.L. Mendrick, H.K. Vaananen, and M.A. Horton. 1996. Beta 1 integrins and osteoclast function: involvement in collagen recognition and bone resorption. *Bone*. 19:317-28.

Heymann, D., J. Guicheux, F. Gouin, N. Passuti, and G. Daculsi. 1998. Cytokines, growth factors and osteoclasts. *Cytokine*. 10:155-68.

Hill, M.A., L. Schedlich, and P. Gunning. 1994a. Serum-induced signal transduction determines the peripheral location of beta-actin mRNA within the cell. *J Cell Biol*. 126:1221-9.

Hill, P.A., G. Murphy, A.J. Docherty, R.M. Hembry, T.A. Millican, J.J. Reynolds, and M.C. Meikle. 1994b. The effects of selective inhibitors of matrix metalloproteinases (MMPs) on bone resorption and the identification of MMPs and TIMP-1 in isolated osteoclasts. *J Cell Sci*. 107 (Pt 11):3055-64.

Hirotani, H., N.A. Tuohy, J.T. Woo, P.H. Stern, and N.A. Clipstone. 2004. The calcineurin/NFAT signaling pathway regulates osteoclastogenesis in RAW264.7 cells. *J Biol Chem*.

Hobson, S.A., J. Wright, F. Lee, S.E. McNeil, T. Bilderback, and K.D. Rodland. 2003. Activation of the MAP kinase cascade by exogenous calcium-sensing receptor. *In* Mol Cell Endocrinol. Vol. 200. 189-98.

Hofbauer, L.C. 1999. Osteoprotegerin ligand and osteoprotegerin: novel implications for osteoclast biology and bone metabolism. *Eur J Endocrinol*. 141:195-210.

Hofbauer, L.C., and M. Schoppet. 2004. Clinical implications of the osteoprotegerin/RANKL/RANK system for bone and vascular diseases. *Jama*. 292:490-5.

Hofer, A.M., and E.M. Brown. 2003. Extracellular calcium sensing and signalling. *In* Nat Rev Mol Cell Biol. Vol. 4. 530-8.

Hogan, P.G., L. Chen, J. Nardone, and A. Rao. 2003. Transcriptional regulation by calcium, calcineurin, and NFAT. *Genes Dev*. 17:2205-32.

Holt, I., and M.J. Marshall. 1998. Integrin subunit beta3 plays a crucial role in the movement of osteoclasts from the periosteum to the bone surface. *J Cell Physiol*. 175:1-9.

Holtrop, M.E., and G.J. King. 1977. The ultrastructure of the osteoclast and its functional implications. *Clin Orthop Relat Res*:177-96.

Horne, W.C., L. Neff, D. Chatterjee, A. Lomri, J.B. Levy, and R. Baron. 1992. Osteoclasts express high levels of pp60c-src in association with intracellular membranes. *J Cell Biol*. 119:1003-13.

Horton, M.A., E.L. Dorey, S.A. Nesbitt, J. Samanen, F.E. Ali, J.M. Stadel, A. Nichols, R. Greig, and M.H. Helfrich. 1993. Modulation of vitronectin receptor-mediated osteoclast adhesion by Arg-Gly-Asp peptide analogs: a structure-function analysis. *J Bone Miner Res*. 8:239-47.

Horton, M.A., M.L. Taylor, T.R. Arnett, and M.H. Helfrich. 1991. Arg-Gly-Asp (RGD) peptides and the anti-vitronectin receptor antibody 23C6 inhibit dentine resorption and cell spreading by osteoclasts. *Exp Cell Res*. 195:368-75.

Hotokezaka, H., E. Sakai, K. Kanaoka, K. Saito, K. Matsuo, H. Kitaura, N. Yoshida, and K. Nakayama. 2002a. U0126 and PD98059, specific inhibitors of MEK, accelerate differentiation of RAW264.7 cells into osteoclast-like cells. *J Biol Chem*. 277:47366-72.

Hotokezaka, H., E. Sakai, K. Kanaoka, K. Saito, K. Matsuo, H. Kitaura, N. Yoshida, and K. Nakayama. 2002b. U0126 and PD98059, specific inhibitors of MEK, accelerate differentiation of RAW264.7 cells into osteoclast-like cells. *In* J Biol Chem. Vol. 277. 47366-72.

Hsu, H., D.L. Lacey, C.R. Dunstan, I. Solovyev, A. Colombero, E. Timms, H.L. Tan, G. Elliott, M.J. Kelley, I. Sarosi, L. Wang, X.Z. Xia, R. Elliott, L. Chiu, T. Black, S. Scully, C. Capparelli, S. Morony, G. Shimamoto, M.B. Bass, and W.J. Boyle. 1999a. Tumor necrosis factor receptor family member RANK mediates osteoclast differentiation and activation induced by osteoprotegerin ligand. *Proc Natl Acad Sci U S A*. 96:3540-5.

Hsu, H., D.L. Lacey, C.R. Dunstan, I. Solovyev, A. Colombero, E. Timms, H.L. Tan, G. Elliott, M.J. Kelley, I. Sarosi, L. Wang, X.Z. Xia, R. Elliott, L. Chiu, T. Black, S. Scully, C. Capparelli, S. Morony, G. Shimamoto, M.B. Bass, and W.J. Boyle. 1999b. Tumor necrosis factor receptor family member RANK mediates osteoclast differentiation and activation induced by osteoprotegerin ligand. *Proc Natl Acad Sci U S A*. 96:3540-5.

Hsu, H., D.L. Lacey, C.R. Dunstan, I. Solovyev, A. Colombero, E. Timms, H.L. Tan, G. Elliott, M.J. Kelley, I. Sarosi, L. Wang, X.Z. Xia, R. Elliott, L. Chiu, T. Black, S. Scully, C. Capparelli, S. Morony, G. Shimamoto, M.B. Bass, and W.J. Boyle. 1999c. Tumor necrosis factor receptor family member RANK mediates osteoclast differentiation and activation induced by osteoprotegerin ligand. *In* Proc Natl Acad Sci U S A. Vol. 96. 3540-5.

Huang, L., J. Xu, D.J. Wood, and M.H. Zheng. 2000. Gene expression of osteoprotegerin ligand, osteoprotegerin, and receptor activator of NF-kappaB in giant cell tumor of bone: possible involvement in tumor cell-induced osteoclast-like cell formation. *Am J Pathol*. 156:761-7.

Hug, H., and T.F. Sarre. 1993. Protein kinase C isoenzymes: divergence in signal transduction? *Biochem J*. 291 (Pt 2):329-43.

Hunter, S.J., H. Schraer, and C.V. Gay. 1989. Characterization of the cytoskeleton of isolated chick osteoclasts: effect of calcitonin. *J Histochem Cytochem*. 37:1529-37.

Igarashi, K., H. Hirotani, J.T. Woo, and P.H. Stern. 2004. Cyclosporine A and FK506 induce osteoclast apoptosis in mouse bone marrow cell cultures. *Bone*. 35:47-56.

Ikeda, F., R. Nishimura, T. Matsubara, S. Tanaka, J. Inoue, S.V. Reddy, K. Hata, K. Yamashita, T. Hiraga, T. Watanabe, T. Kukita, K. Yoshioka, A. Rao, and T. Yoneda. 2004. Critical roles of c-Jun signaling in regulation of NFAT family and RANKL-regulated osteoclast differentiation. *J Clin Invest*. 114:475-84.

Ikeda, T., M. Kasai, J. Suzuki, H. Kuroyama, S. Seki, M. Utsuyama, and K. Hirokawa. 2003. Multimerization of the RANKL isoforms and regulation of osteoclastogenesis. *J Biol Chem*.

Inoue, K., Y. Ozaki, K. Satoh, Y. Wu, Y. Yatomi, Y. Shin, and T. Morita. 1999. Signal transduction pathways mediated by glycoprotein Ia/IIa in human platelets: comparison with those of glycoprotein VI. *Biochem Biophys Res Commun*. 256:114-20.

Iotsova, V., J. Caamano, J. Loy, Y. Yang, A. Lewin, and R. Bravo. 1997a. Osteopetrosis in mice lacking NF-kappaB1 and NF-kappaB2. *Nat Med*. 3:1285-9.

Iotsova, V., J. Caamano, J. Loy, Y. Yang, A. Lewin, and R. Bravo. 1997b. Osteopetrosis in mice lacking NF-kappaB1 and NF-kappaB2. *In* Nat Med. Vol. 3. 1285-9.

Iotsova, V., J. Caamano, J. Loy, Y. Yang, A. Lewin, and R. Bravo. 1997c. Osteopetrosis in mice lacking NF-kappaB1 and NF-kappaB2. *Nat Med*. 3:1285-9.

Ito, S., and T. Hata. 2004. Crystal structure of RANK ligand involved in bone metabolism. *Vitam Horm*. 67:19-33.

Ito, S., K. Wakabayashi, O. Ubukata, S. Hayashi, F. Okada, and T. Hata. 2002. Crystal structure of the extracellular domain of mouse RANK ligand at 2.2-A resolution. *J Biol Chem*. 277:6631-6.

Jaken, S. 1996. Protein kinase C isozymes and substrates. *Curr Opin Cell Biol*. 8:168-73.

Janssens, K., M.C. de Vernejoul, F. de Freitas, F. Vanhoenacker, and W. Van Hul. 2005. An intermediate form of juvenile Paget's disease caused by a truncating TNFRSF11B mutation. *Bone*. 36:542-8.

Jimi, E., S. Akiyama, T. Tsurukai, N. Okahashi, K. Kobayashi, N. Udagawa, T. Nishihara, N. Takahashi, and T. Suda. 1999a. Osteoclast differentiation factor acts as a multifunctional regulator in murine osteoclast differentiation and function. *J Immunol*. 163:434-42.

Jimi, E., S. Akiyama, T. Tsurukai, N. Okahashi, K. Kobayashi, N. Udagawa, T. Nishihara, N. Takahashi, and T. Suda. 1999b. Osteoclast differentiation factor acts as a multifunctional regulator in murine osteoclast differentiation and function. *J Immunol*. 163:434-42.

Jimi, E., S. Akiyama, T. Tsurukai, N. Okahashi, K. Kobayashi, N. Udagawa, T. Nishihara, N. Takahashi, and T. Suda. 1999c. Osteoclast differentiation factor acts as a multifunctional regulator in murine osteoclast differentiation and function. *In* J Immunol. Vol. 163. 434-42.

Jimi, E., K. Aoki, H. Saito, F. D'Acquisto, M.J. May, I. Nakamura, T. Sudo, T. Kojima, F. Okamoto, H. Fukushima, K. Okabe, K. Ohya, and S. Ghosh. 2004. Selective inhibition of NF-kappa B blocks osteoclastogenesis and prevents inflammatory bone destruction in vivo. *Nat Med*. 10:617-24.

Johnson, R.S., B.M. Spiegelman, and V. Papaioannou. 1992a. Pleiotropic effects of a null mutation in the c-fos proto-oncogene. *In* Cell. Vol. 71. 577-86.

Johnson, R.S., B.M. Spiegelman, and V. Papaioannou. 1992b. Pleiotropic effects of a null mutation in the c-fos proto-oncogene. *Cell*. 71:577-86.

Jones, D.H., T. Nakashima, O.H. Sanchez, I. Kozieradzki, S.V. Komarova, I. Sarosi, S. Morony, E. Rubin, R. Sarao, C.V. Hojilla, V. Komnenovic, Y.Y. Kong, M. Schreiber, S.J. Dixon, S.M. Sims, R. Khokha, T. Wada, and J.M. Penninger.

2006. Regulation of cancer cell migration and bone metastasis by RANKL. *Nature*. 440:692-6.

Joyce, D., C. Albanese, J. Steer, M. Fu, B. Bouzahzah, and R.G. Pestell. 2001. NF-kappaB and cell-cycle regulation: the cyclin connection. *Cytokine Growth Factor Rev*. 12:73-90.

Joyce, D.A., and J.H. Steer. 1992. Differentiation of the U-937 promonocytic cell line induced by phorbol myristate acetate or retinoic acid: effect of aurothiomalate. *Agents Actions*. 37:305-10.

Kakegawa, H., T. Nikawa, K. Tagami, H. Kamioka, K. Sumitani, T. Kawata, M. Drobnic-Kosorok, B. Lenarcic, V. Turk, and N. Katunuma. 1993. Participation of cathepsin L on bone resorption. *FEBS Lett*. 321:247-50.

Kameda, T., H. Mano, Y. Yamada, H. Takai, N. Amizuka, M. Kobori, N. Izumi, H. Kawashima, H. Ozawa, K. Ikeda, A. Kameda, Y. Hakeda, and M. Kumegawa. 1998. Calcium-sensing receptor in mature osteoclasts, which are bone resorbing cells. *In* Biochem Biophys Res Commun. Vol. 245. 419-22.

Kanatani, M., T. Sugimoto, M. Kanzawa, S. Yano, and K. Chihara. 1999. High extracellular calcium inhibits osteoclast-like cell formation by directly acting on the calcium-sensing receptor existing in osteoclast precursor cells. *In* Biochem Biophys Res Commun. Vol. 261. 144-8.

Kanehisa, J., T. Yamanaka, S. Doi, K. Turksen, J.N. Heersche, J.E. Aubin, and H. Takeuchi. 1990. A band of F-actin containing podosomes is involved in bone resorption by osteoclasts. *Bone*. 11:287-93.

Karin, M., Y. Yamamoto, and Q.M. Wang. 2004. The IKK NF-kappa B system: a treasure trove for drug development. *Nat Rev Drug Discov*. 3:17-26.

Kashiwada, M., Y. Shirakata, J.I. Inoue, H. Nakano, K. Okazaki, K. Okumura, T. Yamamoto, H. Nagaoka, and T. Takemori. 1998. Tumor necrosis factor receptor-associated factor 6 (TRAF6) stimulates extracellular signal-regulated kinase (ERK) activity in CD40 signaling along a ras-independent pathway. *J Exp Med*. 187:237-44.

Katoh, M., K. Kitamura, and H. Kitagawa. 1995. Induction of bone resorbing-activity by mouse stromal cell line, MC3T3- G2/PA6. *Bone*. 16:97-102.

Keenan, C., and D. Kelleher. 1998. Protein kinase C and the cytoskeleton. *Cell Signal*. 10:225-32.

Key, L.L., Jr., W.C. Wolf, C.M. Gundberg, and W.L. Ries. 1994. Superoxide and bone resorption. *Bone*. 15:431-6.

Kifor, O., R. Diaz, R. Butters, and E.M. Brown. 1997. The Ca2+-sensing receptor (CaR) activates phospholipases C, A2, and D in bovine parathyroid and CaR-transfected, human embryonic kidney (HEK293) cells. *In* J Bone Miner Res. Vol. 12. 715-25.

Kim, B.Y., R.B. Gaynor, K. Song, A. Dritschilo, and M. Jung. 2002. Constitutive activation of NF-kappaB in Ki-ras-transformed prostate epithelial cells. *Oncogene*. 21:4490-7.

Kim, H.H., D.E. Lee, J.N. Shin, Y.S. Lee, Y.M. Jeon, C.H. Chung, J. Ni, B.S. Kwon, and Z.H. Lee. 1999a. Receptor activator of NF-kappaB recruits multiple TRAF family adaptors and activates c-Jun N-terminal kinase. *FEBS Lett*. 443:297-302.

Kim, H.H., D.E. Lee, J.N. Shin, Y.S. Lee, Y.M. Jeon, C.H. Chung, J. Ni, B.S. Kwon, and Z.H. Lee. 1999b. Receptor activator of NF-kappaB recruits multiple TRAF family adaptors and activates c-Jun N-terminal kinase. *In* FEBS Lett. Vol. 443. 297-302.

King, G.J., and M.E. Holtrop. 1975. Actin-like filaments in bone cells of cultured mouse calvaria as demonstrated by binding to heavy meromyosin. *J Cell Biol*. 66:445-51.

Knopf, J.L., M.H. Lee, L.A. Sultzman, R.W. Kriz, C.R. Loomis, R.M. Hewick, and R.M. Bell. 1986. Cloning and expression of multiple protein kinase C cDNAs. *Cell*. 46:491-502.

Kobayashi, N., Y. Kadono, A. Naito, K. Matsumoto, T. Yamamoto, S. Tanaka, and J. Inoue. 2001. Segregation of TRAF6-mediated signaling pathways clarifies its role in osteoclastogenesis. *Embo J*. 20:1271-80.

Kodama, H., M. Nose, S. Niida, and A. Yamasaki. 1991. Essential role of macrophage colony-stimulating factor in the osteoclast differentiation supported by stromal cells. *J Exp Med*. 173:1291-4.

Kohn, E.A., C.J. Yoo, and A. Eastman. 2003. The protein kinase C inhibitor Go6976 is a potent inhibitor of DNA damage-induced S and G2 cell cycle checkpoints. *Cancer Res*. 63:31-5.

Komarova, S.V., M.F. Pilkington, A.F. Weidema, S.J. Dixon, and S.M. Sims. 2003. RANK Ligand-induced Elevation of Cytosolic Ca2+ Accelerates Nuclear Translocation of Nuclear Factor kappa B in Osteoclasts. *In* J Biol Chem. Vol. 278. 8286-93.

Kong, Y.Y., W.J. Boyle, and J.M. Penninger. 1999a. Osteoprotegerin ligand: a common link between osteoclastogenesis, lymph node formation and lymphocyte development. *Immunol Cell Biol*. 77:188-93.

Kong, Y.Y., U. Feige, I. Sarosi, B. Bolon, A. Tafuri, S. Morony, C. Capparelli, J. Li, R. Elliott, S. McCabe, T. Wong, G. Campagnuolo, E. Moran, E.R. Bogoch, G. Van, L.T. Nguyen, P.S. Ohashi, D.L. Lacey, E. Fish, W.J. Boyle, and J.M. Penninger. 1999b. Activated T cells regulate bone loss and joint destruction in adjuvant arthritis through osteoprotegerin ligand. *Nature*. 402:304-9.

Kong, Y.Y., H. Yoshida, I. Sarosi, H.L. Tan, E. Timms, C. Capparelli, S. Morony, A.J. Oliveira-dos-Santos, G. Van, A. Itie, W. Khoo, A. Wakeham, C.R. Dunstan, D.L. Lacey, T.W. Mak, W.J. Boyle, and J.M. Penninger. 1999c. OPGL is a key regulator of osteoclastogenesis, lymphocyte development and lymph-node organogenesis. *In* Nature. Vol. 397. 315-23.

Kong, Y.Y., H. Yoshida, I. Sarosi, H.L. Tan, E. Timms, C. Capparelli, S. Morony, A.J. Oliveira-dos-Santos, G. Van, A. Itie, W. Khoo, A. Wakeham, C.R. Dunstan, D.L. Lacey, T.W. Mak, W.J. Boyle, and J.M. Penninger. 1999d. OPGL is a key regulator of osteoclastogenesis, lymphocyte development and lymph-node organogenesis. *Nature*. 397:315-23.

Koni, P.A., R. Sacca, P. Lawton, J.L. Browning, N.H. Ruddle, and R.A. Flavell. 1997. Distinct roles in lymphoid organogenesis for lymphotoxins alpha and beta revealed in lymphotoxin beta-deficient mice. *Immunity*. 6:491-500.

Kontny, E., M. Kurowska, K. Szczepanska, and W. Maslinski. 2000. Rottlerin, a PKC isozyme-selective inhibitor, affects signaling events and cytokine production in human monocytes. *J Leukoc Biol*. 67:249-58.

Kontny, E., M. Ziolkowska, A. Ryzewska, and W. Maslinski. 1999. Protein kinase c-dependent pathway is critical for the production of pro-inflammatory cytokines (TNF-alpha, IL-1beta, IL-6). *Cytokine*. 11:839-48.

Kornak, U., D. Kasper, M.R. Bosl, E. Kaiser, M. Schweizer, A. Schulz, W. Friedrich, G. Delling, and T.J. Jentsch. 2001. Loss of the ClC-7 chloride channel leads to osteopetrosis in mice and man. *Cell*. 104:205-15.

Kornak, U., A. Schulz, W. Friedrich, S. Uhlhaas, B. Kremens, T. Voit, C. Hasan, U. Bode, T.J. Jentsch, and C. Kubisch. 2000. Mutations in the a3 subunit of the vacuolar H(+)-ATPase cause infantile malignant osteopetrosis. *Hum Mol Genet*. 9:2059-63.

Koths, K. 1997. Structure-function studies on human macrophage colony-stimulating factor (M-CSF). *Mol Reprod Dev*. 46:31-7; discussion 37-8.

Kurihara, N., C. Civin, and G.D. Roodman. 1991. Osteotropic factor responsiveness of highly purified populations of early and late precursors for human multinucleated cells expressing the osteoclast phenotype. *J Bone Miner Res*. 6:257-61.

Lacey, D.L., E. Timms, H.L. Tan, M.J. Kelley, C.R. Dunstan, T. Burgess, R. Elliott, A. Colombero, G. Elliott, S. Scully, H. Hsu, J. Sullivan, N. Hawkins, E. Davy, C. Capparelli, A. Eli, Y.X. Qian, S. Kaufman, I. Sarosi, V. Shalhoub, G. Senaldi, J. Guo, J. Delaney, and W.J. Boyle. 1998a. Osteoprotegerin ligand is a cytokine that regulates osteoclast differentiation and activation. *Cell*. 93:165-76.

Lacey, D.L., E. Timms, H.L. Tan, M.J. Kelley, C.R. Dunstan, T. Burgess, R. Elliott, A. Colombero, G. Elliott, S. Scully, H. Hsu, J. Sullivan, N. Hawkins, E. Davy, C. Capparelli, A. Eli, Y.X. Qian, S. Kaufman, I. Sarosi, V. Shalhoub, G. Senaldi, J. Guo, J. Delaney, and W.J. Boyle. 1998b. Osteoprotegerin ligand is a cytokine that regulates osteoclast differentiation and activation. *In* Cell. Vol. 93. 165-76.

Lagasse, E., and I.L. Weissman. 1997. Enforced expression of Bcl-2 in monocytes rescues macrophages and partially reverses osteopetrosis in op/op mice. *Cell*. 89:1021-31.

Laitala, T., and H.K. Vaananen. 1994. Inhibition of bone resorption in vitro by antisense RNA and DNA molecules targeted against carbonic anhydrase II or two subunits of vacuolar H(+)-ATPase. *J Clin Invest*. 93:2311-8.

Laitala, T., and K. Vaananen. 1993. Proton channel part of vacuolar H(+)-ATPase and carbonic anhydrase II expression is stimulated in resorbing osteoclasts. *J Bone Miner Res*. 8:119-26.

Laitala-Leinonen, T., M.L. Howell, G.E. Dean, and H.K. Vaananen. 1996. Resorption-cycle-dependent polarization of mRNAs for different subunits of V-ATPase in bone-resorbing osteoclasts. *Mol Biol Cell*. 7:129-42.

Lakkakorpi, P.T., and H.K. Vaananen. 1990. Calcitonin, prostaglandin E2, and dibutyryl cyclic adenosine 3',5'-monophosphate disperse the specific microfilament structure in resorbing osteoclasts. *J Histochem Cytochem*. 38:1487-93.

Lakkakorpi, P.T., and H.K. Vaananen. 1991. Kinetics of the osteoclast cytoskeleton during the resorption cycle in vitro. *J Bone Miner Res*. 6:817-26.

Lallena, M.J., M.T. Diaz-Meco, G. Bren, C.V. Paya, and J. Moscat. 1999. Activation of IkappaB kinase beta by protein kinase C isoforms. *Mol Cell Biol*. 19:2180-8.

Lam, J., C.A. Nelson, F.P. Ross, S.L. Teitelbaum, and D.H. Fremont. 2001a. Crystal structure of the TRANCE/RANKL cytokine reveals determinants of receptor-ligand specificity. *J Clin Invest*. 108:971-9.

Lam, J., C.A. Nelson, F.P. Ross, S.L. Teitelbaum, and D.H. Fremont. 2001b. Crystal structure of the TRANCE/RANKL cytokine reveals determinants of receptor-ligand specificity. *J Clin Invest*. 108:971-9.

Lam, J., S. Takeshita, J.E. Barker, O. Kanagawa, F.P. Ross, and S.L. Teitelbaum. 2000. TNF-alpha induces osteoclastogenesis by direct stimulation of macrophages exposed to permissive levels of RANK ligand. *J Clin Invest*. 106:1481-8.

Lark, M.W., G.B. Stroup, S.M. Hwang, I.E. James, D.J. Rieman, F.H. Drake, J.N. Bradbeer, A. Mathur, K.F. Erhard, K.A. Newlander, S.T. Ross, K.L. Salyers, B.R. Smith, W.H. Miller, W.F. Huffman, and M. Gowen. 1999. Design and characterization of orally active Arg-Gly-Asp peptidomimetic vitronectin receptor antagonist SB 265123 for prevention of bone loss in osteoporosis. *J Pharmacol Exp Ther*. 291:612-7.

Lark, M.W., G.B. Stroup, I.E. James, R.A. Dodds, S.M. Hwang, S.M. Blake, B.A. Lechowska, S.J. Hoffman, B.R. Smith, R. Kapadia, X. Liang, K. Erhard, Y. Ru, X. Dong, R.W. Marquis, D. Veber, and M. Gowen. 2002. A potent small molecule, nonpeptide inhibitor of cathepsin K (SB 331750) prevents bone

matrix resorption in the ovariectomized rat. *Bone*. 30:746-53.

Larsen, E.C., J.A. DiGennaro, N. Saito, S. Mehta, D.J. Loegering, J.E. Mazurkiewicz, and M.R. Lennartz. 2000. Differential requirement for classic and novel PKC isoforms in respiratory burst and phagocytosis in RAW 264.7 cells. *J Immunol*. 165:2809-17.

Lee, S.E., K.M. Woo, S.Y. Kim, H.M. Kim, K. Kwack, Z.H. Lee, and H.H. Kim. 2002. The phosphatidylinositol 3-kinase, p38, and extracellular signal-regulated kinase pathways are involved in osteoclast differentiation. *Bone*. 30:71-7.

Lee, S.W., H.B. Kwak, W.J. Chung, H. Cheong, H.H. Kim, and Z.H. Lee. 2003. Participation of protein kinase C beta in osteoclast differentiation and function. *Bone*. 32:217-27.

Lee, Z.H., and H.H. Kim. 2003. Signal transduction by receptor activator of nuclear factor kappa B in osteoclasts. *Biochem Biophys Res Commun*. 305:211-4.

Leitges, M., C. Schmedt, R. Guinamard, J. Davoust, S. Schaal, S. Stabel, and A. Tarakhovsky. 1996. Immunodeficiency in protein kinase cbeta-deficient mice. *Science*. 273:788-91.

Li, C., F. Wernig, M. Leitges, Y. Hu, and Q. Xu. 2003. Mechanical stress-activated PKCdelta regulates smooth muscle cell migration. *Faseb J*. 17:2106-8.

Li, J., I. Sarosi, X.Q. Yan, S. Morony, C. Capparelli, H.L. Tan, S. McCabe, R. Elliott, S. Scully, G. Van, S. Kaufman, S.C. Juan, Y. Sun, J. Tarpley, L. Martin, K. Christensen, J. McCabe, P. Kostenuik, H. Hsu, F. Fletcher, C.R. Dunstan, D.L. Lacey, and W.J. Boyle. 2000. RANK is the intrinsic hematopoietic cell surface receptor that controls osteoclastogenesis and regulation of bone mass and calcium metabolism. *Proc Natl Acad Sci U S A*. 97:1566-71.

Li, X., N. Udagawa, K. Itoh, K. Suda, Y. Murase, T. Nishihara, T. Suda, and N. Takahashi. 2002. p38 MAPK-mediated signals are required for inducing osteoclast differentiation but not for osteoclast function. *Endocrinology*. 143:3105-13.

Li, Y.P., W. Chen, Y. Liang, E. Li, and P. Stashenko. 1999. Atp6i-deficient mice exhibit severe osteopetrosis due to loss of osteoclast-mediated extracellular acidification. *Nat Genet*. 23:447-51.

Liao, Y.F., Y.C. Hung, W.H. Chang, G.J. Tsay, T.C. Hour, H.C. Hung, and G.Y. Liu. 2005. The PKC delta inhibitor, rottlerin, induces apoptosis of haematopoietic cell lines through mitochondrial membrane depolarization and caspases' cascade. *Life Sci*. 77:707-19.

Lin, K.I., J.A. DiDonato, A. Hoffmann, J.M. Hardwick, and R.R. Ratan. 1998. Suppression of steady-state, but not stimulus-induced NF-kappaB activity inhibits alphavirus-induced apoptosis. *J Cell Biol*. 141:1479-87.

Lin, S.Y., Y.C. Liang, Y.S. Ho, S.H. Tsai, S. Pan, and W.S. Lee. 2002. Involvement of both extracellular signal-regulated kinase and c-jun N- terminal kinase pathways in the 12-O-tetradecanoylphorbol-13-acetate- induced upregulation of p21(Cip1) in colon cancer cells. *Mol Carcinog*. 35:21-8.

Lin, W.W., and B.C. Chen. 1998. Distinct PKC isoforms mediate the activation of cPLA2 and adenylyl cyclase by phorbol ester in RAW264.7 macrophages. *Br J Pharmacol*. 125:1601-9.

Liu, B., M. Fang, Y. Lu, G.B. Mills, and Z. Fan. 2001. Involvement of JNK-mediated pathway in EGF-mediated protection against paclitaxel-induced apoptosis in SiHa human cervical cancer cells. *Br J Cancer*. 85:303-11.

Liu, D., J.K. Xu, L. Figliomeni, L. Huang, N.J. Pavlos, M. Rogers, A. Tan, P. Price, and M.H. Zheng. 2003. Expression of RANKL and OPG mRNA in periodontal disease: Possible involvement in bone destruction. *Int J Mol Med*. 11:17-21.

Lomaga, M.A., W.C. Yeh, I. Sarosi, G.S. Duncan, C. Furlonger, A. Ho, S. Morony, C.

Capparelli, G. Van, S. Kaufman, A. van der Heiden, A. Itie, A. Wakeham, W. Khoo, T. Sasaki, Z. Cao, J.M. Penninger, C.J. Paige, D.L. Lacey, C.R. Dunstan, W.J. Boyle, D.V. Goeddel, and T.W. Mak. 1999a. TRAF6 deficiency results in osteopetrosis and defective interleukin-1, CD40, and LPS signaling. *Genes Dev*. 13:1015-24.

Lomaga, M.A., W.C. Yeh, I. Sarosi, G.S. Duncan, C. Furlonger, A. Ho, S. Morony, C. Capparelli, G. Van, S. Kaufman, A. van der Heiden, A. Itie, A. Wakeham, W. Khoo, T. Sasaki, Z. Cao, J.M. Penninger, C.J. Paige, D.L. Lacey, C.R. Dunstan, W.J. Boyle, D.V. Goeddel, and T.W. Mak. 1999b. TRAF6 deficiency results in osteopetrosis and defective interleukin-1, CD40, and LPS signaling. *In* Genes Dev. Vol. 13. 1015-24.

Long, A., D. Kelleher, S. Lynch, and Y. Volkov. 2001. Cutting edge: protein kinase C beta expression is critical for export of Il-2 from T cells. *J Immunol*. 167:636-40.

Lorenzo, J.A., A. Naprta, Y. Rao, C. Alander, M. Glaccum, M. Widmer, G. Gronowicz, J. Kalinowski, and C.C. Pilbeam. 1998. Mice lacking the type I interleukin-1 receptor do not lose bone mass after ovariectomy. *Endocrinology*. 139:3022-5.

Lorget, F., S. Kamel, R. Mentaverri, A. Wattel, M. Naassila, M. Maamer, and M. Brazier. 2000. High extracellular calcium concentrations directly stimulate osteoclast apoptosis. *In* Biochem Biophys Res Commun. Vol. 268. 899-903.

Lowe, C., T. Yoneda, B.F. Boyce, H. Chen, G.R. Mundy, and P. Soriano. 1993. Osteopetrosis in Src-deficient mice is due to an autonomous defect of osteoclasts. *Proc Natl Acad Sci U S A*. 90:4485-9.

Lum, L., B.R. Wong, R. Josien, J.D. Becherer, H. Erdjument-Bromage, J. Schlondorff, P. Tempst, Y. Choi, and C.P. Blobel. 1999. Evidence for a role of a tumor necrosis factor-alpha (TNF-alpha)-converting enzyme-like protease in shedding of TRANCE, a TNF family member involved in osteoclastogenesis and dendritic cell survival. *J Biol Chem*. 274:13613-8.

Mackie, E.J. 2003. Osteoblasts: novel roles in orchestration of skeletal architecture. *Int J Biochem Cell Biol*. 35:1301-5.

Magnani, M., R. Crinelli, M. Bianchi, and A. Antonelli. 2000. The ubiquitin-dependent proteolytic system and other potential targets for the modulation of nuclear factor-kB (NF-kB). *Curr Drug Targets*. 1:387-99.

Mano, M., T. Arakawa, H. Mano, M. Nakagawa, T. Kaneda, H. Kaneko, T. Yamada, K. Miyata, H. Kiyomura, M. Kumegawa, and Y. Hakeda. 2000. Prostaglandin E2 directly inhibits bone-resorbing activity of isolated mature osteoclasts mainly through the EP4 receptor. *Calcif Tissue Int*. 67:85-92.

Mansky, K.C., U. Sankar, J. Han, and M.C. Ostrowski. 2002. Microphthalmia transcription factor is a target of the p38 MAPK pathway in response to receptor activator of NF-kappa B ligand signaling. *J Biol Chem*. 277:11077-83.

Marchisio, P.C., D. Cirillo, L. Naldini, M.V. Primavera, A. Teti, and A. Zambonin-Zallone. 1984. Cell-substratum interaction of cultured avian osteoclasts is mediated by specific adhesion structures. *J Cell Biol*. 99:1696-705.

Marks, C.R., M.F. Seifert, and S.C. Marks, 3rd. 1984. Osteoclast populations in congenital osteopetrosis: additional evidence of heterogeneity. *Metab Bone Dis Relat Res*. 5:259-64.

Marquis, R.W., Y. Ru, S.M. LoCastro, J. Zeng, D.S. Yamashita, H.J. Oh, K.F. Erhard, L.D. Davis, T.A. Tomaszek, D. Tew, K. Salyers, J. Proksch, K. Ward, B. Smith, M. Levy, M.D. Cummings, R.C. Haltiwanger, G. Trescher, B. Wang, M.E. Hemling, C.J. Quinn, H.Y. Cheng, F. Lin, W.W. Smith, C.A. Janson, B. Zhao, M.S. McQueney, K. D'Alessio, C.P. Lee, A. Marzulli, R.A. Dodds, S. Blake, S.M. Hwang, I.E. James, C.J. Gress, B.R. Bradley, M.W. Lark, M. Gowen, and D.F. Veber. 2001. Azepanone-based inhibitors of human and rat cathepsin K. *J*

Med Chem. 44:1380-95.

Martin, T.J., and M.T. Gillespie. 2001. Receptor activator of nuclear factor kappa B ligand (RANKL): another link between breast and bone. *Trends Endocrinol Metab*. 12:2-4.

Martiny-Baron, G., M.G. Kazanietz, H. Mischak, P.M. Blumberg, G. Kochs, H. Hug, D. Marme, and C. Schachtele. 1993. Selective inhibition of protein kinase C isozymes by the indolocarbazole Go 6976. *J Biol Chem*. 268:9194-7.

Masarachia, P., M. Yamamoto, C.T. Leu, G. Rodan, and L. Duong. 1998. Histomorphometric evidence for echistatin inhibition of bone resorption in mice with secondary hyperparathyroidism. *Endocrinology*. 139:1401-10.

Massey, H.M., and A.M. Flanagan. 1999. Human osteoclasts derive from CD14-positive monocytes. *Br J Haematol*. 106:167-70.

Matsumoto, M., T. Sudo, M. Maruyama, H. Osada, and M. Tsujimoto. 2000a. Activation of p38 mitogen-activated protein kinase is crucial in osteoclastogenesis induced by tumor necrosis factor. *FEBS Lett*. 486:23-8.

Matsumoto, M., T. Sudo, T. Saito, H. Osada, and M. Tsujimoto. 2000b. Involvement of p38 mitogen-activated protein kinase signaling pathway in osteoclastogenesis mediated by receptor activator of NF-kappa B ligand (RANKL). *In* J Biol Chem. Vol. 275. 31155-61.

Matsumoto, M., T. Sudo, T. Saito, H. Osada, and M. Tsujimoto. 2000c. Involvement of p38 mitogen-activated protein kinase signaling pathway in osteoclastogenesis mediated by receptor activator of NF-kappa B ligand (RANKL). *J Biol Chem*. 275:31155-61.

Matsuzaki, K., N. Udagawa, N. Takahashi, K. Yamaguchi, H. Yasuda, N. Shima, T. Morinaga, Y. Toyama, Y. Yabe, K. Higashio, and T. Suda. 1998. Osteoclast differentiation factor (ODF) induces osteoclast-like cell formation in human peripheral blood mononuclear cell cultures. *Biochem Biophys Res Commun*. 246:199-204.

Mattsson, J.P., K. Vaananen, B. Wallmark, and P. Lorentzon. 1991. Omeprazole and bafilomycin, two proton pump inhibitors: differentiation of their effects on gastric, kidney and bone H(+)-translocating ATPases. *Biochim Biophys Acta*. 1065:261-8.

Mauro, A., C. Ciccarelli, P. De Cesaris, A. Scoglio, M. Bouche, M. Molinaro, A. Aquino, and B.M. Zani. 2002. PKCalpha-mediated ERK, JNK and p38 activation regulates the myogenic program in human rhabdomyosarcoma cells. *J Cell Sci*. 115:3587-99.

May, M.J., and S. Ghosh. 1997. Rel/NF-kappa B and I kappa B proteins: an overview. *Semin Cancer Biol*. 8:63-73.

May, M.J., and S. Ghosh. 1999. IkappaB kinases: kinsmen with different crafts. *Science*. 284:271-3.

McClung, M.R., E.M. Lewiecki, M.A. Bolognese, G. Woodson, A. Moffett, M. Peacock, P.D. Miller, S. Lederman, C.H. Chesnut, R. Murphy, D. Holloway, and P.J. Bekker. 2004. AMG162 increases bone mineral density (BMD) within 1 moth in postmenopausal women with low BMD. *J Bone Miner Res*. 19:s20.

McHugh, K.P., K. Hodivala-Dilke, M.H. Zheng, N. Namba, J. Lam, D. Novack, X. Feng, F.P. Ross, R.O. Hynes, and S.L. Teitelbaum. 2000. Mice lacking beta3 integrins are osteosclerotic because of dysfunctional osteoclasts. *J Clin Invest*. 105:433-40.

McNeil, S.E., S.A. Hobson, V. Nipper, and K.D. Rodland. 1998. Functional calcium-sensing receptors in rat fibroblasts are required for activation of SRC kinase and mitogen-activated protein kinase in response to extracellular calcium. *In* J Biol Chem. Vol. 273. 1114-20.

Meldrum, D.R., X. Meng, B.C. Sheridan, R.C. McIntyre, Jr., A.H. Harken, and A. Banerjee. 1998. Tissue-specific protein kinase C isoforms differentially mediate macrophage TNFalpha and IL-1beta production. *Shock*. 9:256-60.

Mercurio, F., and A.M. Manning. 1999. Multiple signals converging on NF-kappaB. *Curr Opin Cell Biol*. 11:226-32.

Middleton-Hardie, C., Q. Zhu, H. Cundy, J.M. Lin, K. Callon, P.C. Tong, J. Xu, A. Grey, J. Cornish, and D. Naot. 2006. Deletion of aspartate 182 in OPG causes juvenile Paget's disease by impairing both protein secretion and binding to RANKL. *J Bone Miner Res*. 21:438-45.

Miyamoto, A., T. Kunisada, H. Hemmi, T. Yamane, H. Yasuda, K. Miyake, H. Yamazaki, and S.I. Hayashi. 1998. Establishment and characterization of an immortal macrophage-like cell line inducible to differentiate to osteoclasts. *Biochem Biophys Res Commun*. 242:703-9.

Miyazaki, T., H. Katagiri, Y. Kanegae, H. Takayanagi, Y. Sawada, A. Yamamoto, M.P. Pando, T. Asano, I.M. Verma, H. Oda, K. Nakamura, and S. Tanaka. 2000. Reciprocal role of ERK and NF-kappaB pathways in survival and activation of osteoclasts. *J Cell Biol*. 148:333-42.

Miyazaki, T., A. Sanjay, L. Neff, S. Tanaka, W.C. Horne, and R. Baron. 2004. Src kinase activity is essential for osteoclast function. *J Biol Chem*. 279:17660-6.

Mizukami, J., G. Takaesu, H. Akatsuka, H. Sakurai, J. Ninomiya-Tsuji, K. Matsumoto, and N. Sakurai. 2002. Receptor activator of NF-kappaB ligand (RANKL) activates TAK1 mitogen-activated protein kinase kinase kinase through a signaling complex containing RANK, TAB2, and TRAF6. *Mol Cell Biol*. 22:992-1000.

Mizuno, A., N. Amizuka, K. Irie, A. Murakami, N. Fujise, T. Kanno, Y. Sato, N. Nakagawa, H. Yasuda, S. Mochizuki, T. Gomibuchi, K. Yano, N. Shima, N. Washida, E. Tsuda, T. Morinaga, K. Higashio, and H. Ozawa. 1998. Severe osteoporosis in mice lacking osteoclastogenesis inhibitory factor/osteoprotegerin. *Biochem Biophys Res Commun*. 247:610-5.

Mizuno, A., T. Kanno, M. Hoshi, O. Shibata, K. Yano, N. Fujise, M. Kinosaki, K. Yamaguchi, E. Tsuda, A. Murakami, H. Yasuda, and K. Higashio. 2002. Transgenic mice overexpressing soluble osteoclast differentiation factor (sODF) exhibit severe osteoporosis. *J Bone Miner Metab*. 20:337-44.

Moonga, B.S., R. Davidson, L. Sun, O.A. Adebanjo, J. Moser, M. Abedin, N. Zaidi, C.L. Huang, and M. Zaidi. 2001. Identification and characterization of a sodium/calcium exchanger, NCX- 1, in osteoclasts and its role in bone resorption. *Biochem Biophys Res Commun*. 283:770-5.

Moonga, B.S., and D.W. Dempster. 1998. Effects of peptide fragments of protein kinase C on isolated rat osteoclasts. *Exp Physiol*. 83:717-25.

Moonga, B.S., L.S. Stein, J.M. Kilb, and D.W. Dempster. 1996. Effect of diacylglycerols on osteoclastic bone resorption. *Calcif Tissue Int*. 59:105-8.

Mostov, K., and Z. Werb. 1997. Journey across the osteoclast. *Science*. 276:219-20.

Motyckova, G., and D.E. Fisher. 2002. Pycnodysostosis: role and regulation of cathepsin K in osteoclast function and human disease. *Curr Mol Med*. 2:407-21.

Mulari, M.T., L. Patrikainen, T. Kaisto, K. Metsikko, J.J. Salo, and H.K. Vaananen. 2003a. The architecture of microtubular network and Golgi orientation in osteoclasts--major differences between avian and mammalian species. *Exp Cell Res*. 285:221-35.

Mulari, M.T., H. Zhao, P.T. Lakkakorpi, and H.K. Vaananen. 2003b. Osteoclast ruffled border has distinct subdomains for secretion and degraded matrix uptake. *Traffic*. 4:113-25.

Mundlos, S., and B.R. Olsen. 1997. Heritable diseases of the skeleton. Part I: Molecular

insights into skeletal development-transcription factors and signaling pathways. *Faseb J*. 11:125-32.

Murrills, R.J., L.S. Stein, W.R. Horbert, and D.W. Dempster. 1992. Effects of phorbol myristate acetate on rat and chick osteoclasts. *J Bone Miner Res*. 7:415-23.

Mutter, R., and M. Wills. 2000. Chemistry and clinical biology of the bryostatins. *Bioorg Med Chem*. 8:1841-60.

Nakamura, I., M.F. Pilkington, P.T. Lakkakorpi, L. Lipfert, S.M. Sims, S.J. Dixon, G.A. Rodan, and L.T. Duong. 1999. Role of alpha(v)beta(3) integrin in osteoclast migration and formation of the sealing zone. *J Cell Sci*. 112 (Pt 22):3985-93.

Nesbitt, S., A. Nesbit, M. Helfrich, and M. Horton. 1993. Biochemical characterization of human osteoclast integrins. Osteoclasts express alpha v beta 3, alpha 2 beta 1, and alpha v beta 1 integrins. *J Biol Chem*. 268:16737-45.

Newton, A.C. 1995. Protein kinase C: structure, function, and regulation. *J Biol Chem*. 270:28495-8.

Nicholson, G.C., J.M. Moseley, P.M. Sexton, and T.J. Martin. 1987. Chicken osteoclasts do not possess calcitonin receptors. *J Bone Miner Res*. 2:53-9.

Niikura, K., M. Takano, and M. Sawada. 2004. A novel inhibitor of vacuolar ATPase, FR167356, which can discriminate between osteoclast vacuolar ATPase and lysosomal vacuolar ATPase. *Br J Pharmacol*. 142:558-66.

Nijweide, P.J., E.H. Burger, and J.H. Feyen. 1986. Cells of bone: proliferation, differentiation, and hormonal regulation. *Physiol Rev*. 66:855-86.

Nishi, T., and M. Forgac. 2002. The vacuolar (H+)-ATPases--nature's most versatile proton pumps. *Nat Rev Mol Cell Biol*. 3:94-103.

Nishizuka, Y. 1984. The role of protein kinase C in cell surface signal transduction and tumour promotion. *Nature*. 308:693-8.

Nishizuka, Y. 1986. Studies and perspectives of protein kinase C. *Science*. 233:305-12.

Nishizuka, Y. 1989. Studies and prospectives of the protein kinase c family for cellular regulation. *Cancer*. 63:1892-903.

Nomura, M., W. Ma, N. Chen, A.M. Bode, and Z. Dong. 2000. Inhibition of 12-O-tetradecanoylphorbol-13-acetate-induced NF-kappaB activation by tea polyphenols, (-)-epigallocatechin gallate and theaflavins. *Carcinogenesis*. 21:1885-90.

Ohsawa, Y., T. Nitatori, S. Higuchi, E. Kominami, and Y. Uchiyama. 1993. Lysosomal cysteine and aspartic proteinases, acid phosphatase, and an endogenous cysteine proteinase inhibitor, cystatin-beta, in rat osteoclasts. *J Histochem Cytochem*. 41:1075-83.

Okada, Y., K. Naka, K. Kawamura, T. Matsumoto, I. Nakanishi, N. Fujimoto, H. Sato, and M. Seiki. 1995. Localization of matrix metalloproteinase 9 (92-kilodalton gelatinase/type IV collagenase = gelatinase B) in osteoclasts: implications for bone resorption. *Lab Invest*. 72:311-22.

Orrenius, S., B. Zhivotovsky, and P. Nicotera. 2003. Regulation of cell death: the calcium-apoptosis link. *Nat Rev Mol Cell Biol*. 4:552-65.

Partidos, C.D., C.L. Chirinos-Rojas, and M.W. Steward. 1997. The potential of combinatorial peptide libraries for the identification of inhibitors of TNF-alpha mediated cytotoxicity in vitro. *Immunol Lett*. 57:113-6.

Partidos, C.D., and M.W. Steward. 2002. Mimotopes of viral antigens and biologically important molecules as candidate vaccines and potential immunotherapeutics. *Comb Chem High Throughput Screen*. 5:15-27.

Pasparakis, M., L. Alexopoulou, V. Episkopou, and G. Kollias. 1996. Immune and inflammatory responses in TNF alpha-deficient mice: a critical requirement for TNF alpha in the formation of primary B cell follicles, follicular dendritic cell networks and germinal centers, and in the maturation of the humoral immune

response. *J Exp Med*. 184:1397-411.

Perry, C.M., and D.P. Figgitt. 2004. Zoledronic acid: a review of its use in patients with advanced cancer. *Drugs*. 64:1197-211.

Poli, V., R. Balena, E. Fattori, A. Markatos, M. Yamamoto, H. Tanaka, G. Ciliberto, G.A. Rodan, and F. Costantini. 1994. Interleukin-6 deficient mice are protected from bone loss caused by estrogen depletion. *Embo J*. 13:1189-96.

Quinn, J.M., J. Elliott, M.T. Gillespie, and T.J. Martin. 1998. A combination of osteoclast differentiation factor and macrophage- colony stimulating factor is sufficient for both human and mouse osteoclast formation in vitro. *Endocrinology*. 139:4424-7.

Rennert, P.D., D. James, F. Mackay, J.L. Browning, and P.S. Hochman. 1998. Lymph node genesis is induced by signaling through the lymphotoxin beta receptor. *Immunity*. 9:71-9.

Ringshausen, I., M. Oelsner, K. Weick, C. Bogner, C. Peschel, and T. Decker. 2006. Mechanisms of apoptosis-induction by rottlerin: therapeutic implications for B-CLL. *Leukemia*. 20:514-20.

Rodan, G.A., and T.J. Martin. 1981. Role of osteoblasts in hormonal control of bone resorption--a hypothesis. *Calcif Tissue Int*. 33:349-51.

Rogers, M.J., S. Gordon, H.L. Benford, F.P. Coxon, S.P. Luckman, J. Monkkonen, and J.C. Frith. 2000. Cellular and molecular mechanisms of action of bisphosphonates. *Cancer*. 88:2961-78.

Romas, E., N.A. Sims, D.K. Hards, M. Lindsay, J.W. Quinn, P.F. Ryan, C.R. Dunstan, T.J. Martin, and M.T. Gillespie. 2002. Osteoprotegerin reduces osteoclast numbers and prevents bone erosion in collagen-induced arthritis. *Am J Pathol*. 161:1419-27.

Roodman, G.D. 1999. Cell biology of the osteoclast. *Exp Hematol*. 27:1229-41.

Ross, F.P., J. Chappel, J.I. Alvarez, D. Sander, W.T. Butler, M.C. Farach-Carson, K.A. Mintz, P.G. Robey, S.L. Teitelbaum, and D.A. Cheresh. 1993. Interactions between the bone matrix proteins osteopontin and bone sialoprotein and the osteoclast integrin alpha v beta 3 potentiate bone resorption. *J Biol Chem*. 268:9901-7.

Roux, S., V. Meignin, J. Quillard, G. Meduri, A. Guiochon-Mantel, J.P. Fermand, E. Milgrom, and X. Mariette. 2002. RANK (receptor activator of nuclear factor-kappaB) and RANKL expression in multiple myeloma. *Br J Haematol*. 117:86-92.

Rucci, N., C. DiGiacinto, L. Orru, D. Millimaggi, R. Baron, and A. Teti. 2005. A novel protein kinase C alpha-dependent signal to ERK1/2 activated by alphaVbeta3 integrin in osteoclasts and in Chinese hamster ovary (CHO) cells. *J Cell Sci*. 118:3263-75.

Saftig, P., E. Hunziker, O. Wehmeyer, S. Jones, A. Boyde, W. Rommerskirch, J.D. Moritz, P. Schu, and K. von Figura. 1998. Impaired osteoclastic bone resorption leads to osteopetrosis in cathepsin-K-deficient mice. *Proc Natl Acad Sci U S A*. 95:13453-8.

Salo, J., P. Lehenkari, M. Mulari, K. Metsikko, and H.K. Vaananen. 1997. Removal of osteoclast bone resorption products by transcytosis. *Science*. 276:270-3.

Sambrook, J., E.F. Fritsch, and T. Maniatis. 1989. Molecular Cloning: A Laboratory Manual. Cold Spring Harbour Laboratory Press, New York.

Sanz, L., P. Sanchez, M.J. Lallena, M.T. Diaz-Meco, and J. Moscat. 1999. The interaction of p62 with RIP links the atypical PKCs to NF-kappaB activation. *Embo J*. 18:3044-53.

Sarma, U., and A.M. Flanagan. 1996. Macrophage colony-stimulating factor induces substantial osteoclast generation and bone resorption in human bone marrow

cultures. *Blood*. 88:2531-40.

Sasaki, A., K. Kitamura, R.E. Alcalde, T. Tanaka, A. Suzuki, Y. Etoh, and T. Matsumura. 1998. Effect of a newly developed bisphosphonate, YH529, on osteolytic bone metastases in nude mice. *Int J Cancer*. 77:279-85.

Sato, M., M.K. Sardana, W.A. Grasser, V.M. Garsky, J.M. Murray, and R.J. Gould. 1990. Echistatin is a potent inhibitor of bone resorption in culture. *J Cell Biol*. 111:1713-23.

Schwartzberg, P.L., L. Xing, O. Hoffmann, C.A. Lowell, L. Garrett, B.F. Boyce, and H.E. Varmus. 1997. Rescue of osteoclast function by transgenic expression of kinase-deficient Src in src-/- mutant mice. *Genes Dev*. 11:2835-44.

Schworer, C.M., R.J. Colbran, and T.R. Soderling. 1986. Reversible generation of a Ca2+-independent form of Ca2+(calmodulin)-dependent protein kinase II by an autophosphorylation mechanism. *J Biol Chem*. 261:8581-4.

Seales, E.C., K.J. Micoli, and J.M. McDonald. 2006. Calmodulin is a critical regulator of osteoclastic differentiation, function, and survival. *J Cell Biochem*. 97:45-55.

Shadle, P.J., L. Aldwin, D.E. Nitecki, and K. Koths. 1989. Human macrophage colony-stimulating factor heterogeneity results from alternative mRNA splicing, differential glycosylation, and proteolytic processing. *J Cell Biochem*. 40:91-107.

Shakespeare, W.C., C.A. Metcalf, 3rd, Y. Wang, R. Sundaramoorthi, T. Keenan, M. Weigele, R.S. Bohacek, D.C. Dalgarno, and T.K. Sawyer. 2003. Novel bone-targeted Src tyrosine kinase inhibitor drug discovery. *Curr Opin Drug Discov Devel*. 6:729-41.

Sharma, S.V., C. Oneyama, Y. Yamashita, H. Nakano, K. Sugawara, M. Hamada, N. Kosaka, and T. Tamaoki. 2001. UCS15A, a non-kinase inhibitor of Src signal transduction. *Oncogene*. 20:2068-79.

Shaw, J.P., P.J. Utz, D.B. Durand, J.J. Toole, E.A. Emmel, and G.R. Crabtree. 1988. Identification of a putative regulator of early T cell activation genes. *Science*. 241:202-5.

Shevde, N.K., A.C. Bendixen, K.M. Dienger, and J.W. Pike. 2000. Estrogens suppress RANK ligand-induced osteoclast differentiation via a stromal cell independent mechanism involving c-Jun repression. *Proc Natl Acad Sci U S A*. 97:7829-34.

Silver, I.A., R.J. Murrills, and D.J. Etherington. 1988a. Microelectrode studies on the acid microenvironment beneath adherent macrophages and osteoclasts. *In* Exp Cell Res. Vol. 175. 266-76.

Silver, I.A., R.J. Murrills, and D.J. Etherington. 1988b. Microelectrode studies on the acid microenvironment beneath adherent macrophages and osteoclasts. *Exp Cell Res*. 175:266-76.

Silverton, S. 1994. Osteoclast radicals. *J Cell Biochem*. 56:367-73.

Simmons, D.J., and A.J. Kahn. 1979. Cell lineage in fracture healing in chimeric bone grafts. *Calcif Tissue Int*. 27:247-53.

Sly, W.S., D. Hewett-Emmett, M.P. Whyte, Y.S. Yu, and R.E. Tashian. 1983. Carbonic anhydrase II deficiency identified as the primary defect in the autosomal recessive syndrome of osteopetrosis with renal tubular acidosis and cerebral calcification. *Proc Natl Acad Sci U S A*. 80:2752-6.

Sly, W.S., and P.Y. Hu. 1995. Human carbonic anhydrases and carbonic anhydrase deficiencies. *Annu Rev Biochem*. 64:375-401.

Solan, N.J., H. Miyoshi, E.M. Carmona, G.D. Bren, and C.V. Paya. 2002. RelB cellular regulation and transcriptional activity are regulated by p100. *J Biol Chem*. 277:1405-18.

Song, X., H.M. Sheppard, A.W. Norman, and X. Liu. 1999. Mitogen-activated protein kinase is involved in the degradation of p53 protein in the bryostatin-1-induced

differentiation of the acute promyelocytic leukemia NB4 cell line. *J Biol Chem*. 274:1677-82.

Soriano, P., C. Montgomery, R. Geske, and A. Bradley. 1991. Targeted disruption of the c-src proto-oncogene leads to osteopetrosis in mice. *Cell*. 64:693-702.

Srivastava, S., G. Toraldo, M.N. Weitzmann, S. Cenci, F.P. Ross, and R. Pacifici. 2001. Estrogen decreases osteoclast formation by down-regulating receptor activator of NF-kappa B ligand (RANKL)-induced JNK activation. *J Biol Chem*. 276:8836-40.

Steer, J.H., K.M. Kroeger, L.J. Abraham, and D.A. Joyce. 2000. Glucocorticoids suppress tumor necrosis factor-alpha expression by human monocytic THP-1 cells by suppressing transactivation through adjacent NF-kappa B and c-Jun-activating transcription factor-2 binding sites in the promoter. *J Biol Chem*. 275:18432-40.

Stenbeck, G. 2002. Formation and function of the ruffled border in osteoclasts. *Semin Cell Dev Biol*. 13:285-92.

Stenbeck, G., and M.A. Horton. 2000. A new specialized cell-matrix interaction in actively resorbing osteoclasts. *J Cell Sci*. 113:1577-87.

Stone, R.M. 1997. Bryostatin 1: differentiating agent from the depths. *Leuk Res*. 21:399-401.

Stroup, G.B., M.W. Lark, D.F. Veber, A. Bhattacharyya, S. Blake, L.C. Dare, K.F. Erhard, S.J. Hoffman, I.E. James, R.W. Marquis, Y. Ru, J.A. Vasko-Moser, B.R. Smith, T. Tomaszek, and M. Gowen. 2001. Potent and selective inhibition of human cathepsin K leads to inhibition of bone resorption in vivo in a nonhuman primate. *J Bone Miner Res*. 16:1739-46.

Su, Y., M. Chakraborty, M.H. Nathanson, and R. Baron. 1992. Differential effects of the 3',5'-cyclic adenosine monophosphate and protein kinase C pathways on the response of isolated rat osteoclasts to calcitonin. *Endocrinology*. 131:1497-502.

Suda, T., N. Takahashi, N. Udagawa, E. Jimi, M.T. Gillespie, and T.J. Martin. 1999. Modulation of osteoclast differentiation and function by the new members of the tumor necrosis factor receptor and ligand families. *Endocr Rev*. 20:345-57.

Sundquist, K., P. Lakkakorpi, B. Wallmark, and K. Vaananen. 1990. Inhibition of osteoclast proton transport by bafilomycin A1 abolishes bone resorption. *Biochem Biophys Res Commun*. 168:309-13.

Sundquist, K.T., M.G. Cecchini, and S.C. Marks, Jr. 1995. Colony-stimulating factor-1 injections improve but do not cure skeletal sclerosis in osteopetrotic (op) mice. *Bone*. 16:39.

Sundquist, K.T., and S.C. Marks, Jr. 1994. Bafilomycin A1 inhibits bone resorption and tooth eruption in vivo. *J Bone Miner Res*. 9:1575-82.

Takahashi, N., N. Udagawa, T. Akatsu, H. Tanaka, Y. Isogai, and T. Suda. 1991. Deficiency of osteoclasts in osteopetrotic mice is due to a defect in the local microenvironment provided by osteoblastic cells. *Endocrinology*. 128:1792-6.

Takami, A., N. Takahashi, N. Udagawa, C. Miyaura, K. Suda, J.T. Woo, T.J. Martin, K. Nagai, and T. Suda. 2000a. Intracellular calcium and protein kinase C mediate expression of receptor activator of nuclear factor-kappaB ligand and osteoprotegerin in osteoblasts. *In* Endocrinology. Vol. 141. 4711-9.

Takami, A., N. Takahashi, N. Udagawa, C. Miyaura, K. Suda, J.T. Woo, T.J. Martin, K. Nagai, and T. Suda. 2000b. Intracellular calcium and protein kinase C mediate expression of receptor activator of nuclear factor-kappaB ligand and osteoprotegerin in osteoblasts. *Endocrinology*. 141:4711-9.

Takayanagi, H., S. Kim, T. Koga, H. Nishina, M. Isshiki, H. Yoshida, A. Saiura, M. Isobe, T. Yokochi, J. Inoue, E.F. Wagner, T.W. Mak, T. Kodama, and T. Taniguchi. 2002. Induction and activation of the transcription factor NFATc1

(NFAT2) integrate RANKL signaling in terminal differentiation of osteoclasts. *Dev Cell*. 3:889-901.

Takeshita, S., K. Kaji, and A. Kudo. 2000. Identification and characterization of the new osteoclast progenitor with macrophage phenotypes being able to differentiate into mature osteoclasts. *J Bone Miner Res*. 15:1477-88.

Tanaka, S., M. Amling, L. Neff, A. Peyman, E. Uhlmann, J.B. Levy, and R. Baron. 1996. c-Cbl is downstream of c-Src in a signalling pathway necessary for bone resorption. *Nature*. 383:528-31.

Tegethoff, S., J. Behlke, and C. Scheidereit. 2003. Tetrameric oligomerization of IkappaB kinase gamma (IKKgamma) is obligatory for IKK complex activity and NF-kappaB activation. *Mol Cell Biol*. 23:2029-41.

Teitelbaum, S.L. 2000a. Bone resorption by osteoclasts. *Science*. 289:1504-8.

Teitelbaum, S.L. 2000b. Bone resorption by osteoclasts. *In* Science. Vol. 289. 1504-8.

Teitelbaum, S.L., H. Tanaka, H. Mimura, M. Inoue, M. Shima, A. Shioi, M. Chiba, S. Kitazawa, and F.P. Ross. 1997a. Integrins and osteoclast polarization. *Osteoporos Int*. 7 Suppl 3:S54-6.

Teitelbaum, S.L., M.M. Tondravi, and F.P. Ross. 1997b. Osteoclasts, macrophages, and the molecular mechanisms of bone resorption. *J Leukoc Biol*. 61:381-8.

Teti, A., H.C. Blair, S.L. Teitelbaum, J.A. Kahn, A. Carano, M. Grano, G. Santacroce, P. Schlesinger, and A. Zambonin Zallone. 1989. Cytoplasmic pH is regulated in isolated avian osteoclasts by a Cl-/HCO3- exchanger. *Boll Soc Ital Biol Sper*. 65:589-95.

Teti, A., S. Colucci, M. Grano, L. Argentino, and A. Zambonin Zallone. 1992. Protein kinase C affects microfilaments, bone resorption, and [Ca2+]o sensing in cultured osteoclasts. *Am J Physiol*. 263:C130-9.

Theill, L.E., W.J. Boyle, and J.M. Penninger. 2002. RANK-L and RANK: T cells, bone loss, and mammalian evolution. *Annu Rev Immunol*. 20:795-823.

Tillman, D.M., K. Izeradjene, K.S. Szucs, L. Douglas, and J.A. Houghton. 2003. Rottlerin sensitizes colon carcinoma cells to tumor necrosis factor-related apoptosis-inducing ligand-induced apoptosis via uncoupling of the mitochondria independent of protein kinase C. *Cancer Res*. 63:5118-25.

Toullec, D., P. Pianetti, H. Coste, P. Bellevergue, T. Grand-Perret, M. Ajakane, V. Baudet, P. Boissin, E. Boursier, F. Loriolle, and et al. 1991. The bisindolylmaleimide GF 109203X is a potent and selective inhibitor of protein kinase C. *J Biol Chem*. 266:15771-81.

Troen, B.R. 2003. Molecular mechanisms underlying osteoclast formation and activation. *Exp Gerontol*. 38:605-14.

Troen, B.R. 2004. The role of cathepsin K in normal bone resorption. *Drug News Perspect*. 17:19-28.

Udagawa, N., N. Takahashi, T. Akatsu, T. Sasaki, A. Yamaguchi, H. Kodama, T.J. Martin, and T. Suda. 1989. The bone marrow-derived stromal cell lines MC3T3-G2/PA6 and ST2 support osteoclast-like cell differentiation in cocultures with mouse spleen cells. *Endocrinology*. 125:1805-13.

Vaananen, H.K., and M. Horton. 1995. The osteoclast clear zone is a specialized cell-extracellular matrix adhesion structure. *J Cell Sci*. 108 (Pt 8):2729-32.

Vaananen, H.K., E.K. Karhukorpi, K. Sundquist, B. Wallmark, I. Roininen, T. Hentunen, J. Tuukkanen, and P. Lakkakorpi. 1990. Evidence for the presence of a proton pump of the vacuolar H(+)-ATPase type in the ruffled borders of osteoclasts. *J Cell Biol*. 111:1305-11.

Vaananen, H.K., H. Zhao, M. Mulari, and J.M. Halleen. 2000. The cell biology of osteoclast function. *J Cell Sci*. 113 (Pt 3):377-81.

van der Pluijm, G., H. Mouthaan, C. Baas, H. de Groot, S. Papapoulos, and C. Lowik.

1994. Integrins and osteoclastic resorption in three bone organ cultures: differential sensitivity to synthetic Arg-Gly-Asp peptides during osteoclast formation. *J Bone Miner Res*. 9:1021-8.

Vargas, S.J., A. Naprta, M. Glaccum, S.K. Lee, J. Kalinowski, and J.A. Lorenzo. 1996. Interleukin-6 expression and histomorphometry of bones from mice deficient in receptors for interleukin-1 or tumor necrosis factor. *J Bone Miner Res*. 11:1736-44.

Vincenti, M.P., T.A. Burrell, and S.M. Taffet. 1992. Regulation of NF-kappa B activity in murine macrophages: effect of bacterial lipopolysaccharide and phorbol ester. *J Cell Physiol*. 150:204-13.

Volkov, Y., A. Long, S. McGrath, D. Ni Eidhin, and D. Kelleher. 2001. Crucial importance of PKC-beta(I) in LFA-1-mediated locomotion of activated T cells. *Nat Immunol*. 2:508-14.

Vu, T.H., J.M. Shipley, G. Bergers, J.E. Berger, J.A. Helms, D. Hanahan, S.D. Shapiro, R.M. Senior, and Z. Werb. 1998. MMP-9/gelatinase B is a key regulator of growth plate angiogenesis and apoptosis of hypertrophic chondrocytes. *Cell*. 93:411-22.

Walker, D.G. 1973. Osteopetrosis cured by temporary parabiosis. *Science*. 180:875.

Walker, D.G. 1975. Bone resorption restored in osteopetrotic mice by transplants of normal bone marrow and spleen cells. *Science*. 190:784-5.

Wang, C., J. Steer, H., D.A. Joyce, K.H.M. Yip, M.H. Zheng, and J. Xu. 2003a. 12-O-tetradecanoylphorbol-13-acetate (TPA) inhibits osteoclastogenesis by suppressing RANKL-induced NF-kB activation. *In* J Bone Miner Res. Vol. 18. 2159-2168.

Wang, C., J.H. Steer, D.A. Joyce, K.H. Yip, M.H. Zheng, and J. Xu. 2003b. 12-O-tetradecanoylphorbol-13-acetate (TPA) inhibits osteoclastogenesis by suppressing RANKL-induced NF-kappaB activation. *J Bone Miner Res*. 18:2159-68.

Wang, Z.Q., P. Hemken, D. Menton, and S. Gluck. 1992a. Expression of vacuolar H(+)-ATPase in mouse osteoclasts during in vitro differentiation. *Am J Physiol*. 263:F277-83.

Wang, Z.Q., C. Ovitt, A.E. Grigoriadis, U. Mohle-Steinlein, U. Ruther, and E.F. Wagner. 1992b. Bone and haematopoietic defects in mice lacking c-fos. *In* Nature. Vol. 360. 741-5.

Wang, Z.Q., C. Ovitt, A.E. Grigoriadis, U. Mohle-Steinlein, U. Ruther, and E.F. Wagner. 1992c. Bone and haematopoietic defects in mice lacking c-fos. *Nature*. 360:741-5.

Wattel, A., S. Kamel, C. Prouillet, J.P. Petit, F. Lorget, E. Offord, and M. Brazier. 2004. Flavonoid quercetin decreases osteoclastic differentiation induced by RANKL via a mechanism involving NF kappa B and AP-1. *J Cell Biochem*. 92:285-95.

Whiteside, S.T., and A. Israel. 1997. I kappa B proteins: structure, function and regulation. *Semin Cancer Biol*. 8:75-82.

Wong, B.R., D. Besser, N. Kim, J.R. Arron, M. Vologodskaia, H. Hanafusa, and Y. Choi. 1999a. TRANCE, a TNF family member, activates Akt/PKB through a signaling complex involving TRAF6 and c-Src. *Mol Cell*. 4:1041-9.

Wong, B.R., R. Josien, and Y. Choi. 1999b. TRANCE is a TNF family member that regulates dendritic cell and osteoclast function. *J Leukoc Biol*. 65:715-24.

Wong, B.R., R. Josien, S.Y. Lee, B. Sauter, H.L. Li, R.M. Steinman, and Y. Choi. 1997a. TRANCE (tumor necrosis factor [TNF]-related activation-induced cytokine), a new TNF family member predominantly expressed in T cells, is a dendritic cell-specific survival factor. *J Exp Med*. 186:2075-80.

Wong, B.R., J. Rho, J. Arron, E. Robinson, J. Orlinick, M. Chao, S. Kalachikov, E.

Cayani, F.S. Bartlett, 3rd, W.N. Frankel, S.Y. Lee, and Y. Choi. 1997b. TRANCE is a novel ligand of the tumor necrosis factor receptor family that activates c-Jun N-terminal kinase in T cells. *J Biol Chem*. 272:25190-4.

Xing, L., T.P. Bushnell, L. Carlson, Z. Tai, M. Tondravi, U. Siebenlist, F. Young, and B.F. Boyce. 2002. NF-kappaB p50 and p52 expression is not required for RANK-expressing osteoclast progenitor formation but is essential for RANK- and cytokine-mediated osteoclastogenesis. *J Bone Miner Res*. 17:1200-10.

Xu, D., S. Wang, W. Liu, J. Liu, and X. Feng. 2006. A novel receptor activator of NF-kappaB (RANK) cytoplasmic motif plays an essential role in osteoclastogenesis by committing macrophages to the osteoclast lineage. *J Biol Chem*. 281:4678-90.

Xu, J., H.T. Feng, C. Wang, K.H. Yip, N. Pavlos, J.M. Papadimitriou, D. Wood, and M.H. Zheng. 2003. Effects of Bafilomycin A1: an inhibitor of vacuolar H (+)-ATPases on endocytosis and apoptosis in RAW cells and RAW cell-derived osteoclasts. *J Cell Biochem*. 88:1256-64.

Xu, J., J.W. Tan, L. Huang, X.H. Gao, R. Laird, D. Liu, S. Wysocki, and M.H. Zheng. 2000a. Cloning, sequencing, and functional characterization of the rat homologue of receptor activator of NF-kappaB ligand. *In* J Bone Miner Res. Vol. 15. 2178-86.

Xu, J., J.W. Tan, L. Huang, X.H. Gao, R. Laird, D. Liu, S. Wysocki, and M.H. Zheng. 2000b. Cloning, sequencing, and functional characterization of the rat homologue of receptor activator of NF-kappaB ligand. *J Bone Miner Res*. 15:2178-86.

Xu, J., J.W. Tan, L. Huang, X.H. Gao, R. Laird, D. Liu, S. Wysocki, and M.H. Zheng. 2000c. Cloning, sequencing, and functional characterization of the rat homologue of receptor activator of NF-kappaB ligand. *J Bone Miner Res*. 15:2178-86.

Yamamoto, A., T. Miyazaki, Y. Kadono, H. Takayanagi, T. Miura, H. Nishina, T. Katada, K. Wakabayashi, H. Oda, K. Nakamura, and S. Tanaka. 2002. Possible involvement of IkappaB kinase 2 and MKK7 in osteoclastogenesis induced by receptor activator of nuclear factor kappaB ligand. *J Bone Miner Res*. 17:612-21.

Yamamoto, M., M. Acevedo-Duncan, C.E. Chalfant, N.A. Patel, J.E. Watson, and D.R. Cooper. 2000. Acute glucose-induced downregulation of PKC-betaII accelerates cultured VSMC proliferation. *Am J Physiol Cell Physiol*. 279:C587-95.

Yamamoto, M., J.E. Fisher, M. Gentile, J.G. Seedor, C.T. Leu, S.B. Rodan, and G.A. Rodan. 1998. The integrin ligand echistatin prevents bone loss in ovariectomized mice and rats. *Endocrinology*. 139:1411-9.

Yang, S.Y., B. Wu, L. Mayton, P. Mukherjee, P.D. Robbins, C.H. Evans, and P.H. Wooley. 2004. Protective effects of IL-1Ra or vIL-10 gene transfer on a murine model of wear debris-induced osteolysis. *Gene Ther*. 11:483-91.

Yasuda, H., N. Shima, N. Nakagawa, K. Yamaguchi, M. Kinosaki, S. Mochizuki, A. Tomoyasu, K. Yano, M. Goto, A. Murakami, E. Tsuda, T. Morinaga, K. Higashio, N. Udagawa, N. Takahashi, and T. Suda. 1998a. Osteoclast differentiation factor is a ligand for osteoprotegerin/osteoclastogenesis-inhibitory factor and is identical to TRANCE/RANKL. *Proc Natl Acad Sci U S A*. 95:3597-602.

Yasuda, H., N. Shima, N. Nakagawa, K. Yamaguchi, M. Kinosaki, S. Mochizuki, A. Tomoyasu, K. Yano, M. Goto, A. Murakami, E. Tsuda, T. Morinaga, K. Higashio, N. Udagawa, N. Takahashi, and T. Suda. 1998b. Osteoclast differentiation factor is a ligand for osteoprotegerin/osteoclastogenesis-inhibitory factor and is identical to TRANCE/RANKL. *In* Proc Natl Acad Sci U S A. Vol. 95. 3597-602.

Yip, K.H., M.H. Zheng, H.T. Feng, J. Steer, H., D.A. Joyce, and J. Xu. 2004. Sesquiterpene Lactone Parthenolide Blocks Lipopolysaccharide Induced

Osteolysis through the Suppression of NF-kB Activity. *J Bone Miner Res*.

Yip, K.H., M.H. Zheng, J.H. Steer, T.M. Giardina, R. Han, S.Z. Lo, A.J. Bakker, A.I. Cassady, D.A. Joyce, and J. Xu. 2005. Thapsigargin modulates osteoclastogenesis through the regulation of RANKL-induced signaling pathways and reactive oxygen species production. *J Bone Miner Res*. 20:1462-71.

Yoneda, T., C. Lowe, C.H. Lee, G. Gutierrez, M. Niewolna, P.J. Williams, E. Izbicka, Y. Uehara, and G.R. Mundy. 1993. Herbimycin A, a pp60c-src tyrosine kinase inhibitor, inhibits osteoclastic bone resorption in vitro and hypercalcemia in vivo. *J Clin Invest*. 91:2791-5.

Yoshida, H., S. Hayashi, T. Kunisada, M. Ogawa, S. Nishikawa, H. Okamura, T. Sudo, and L.D. Shultz. 1990. The murine mutation osteopetrosis is in the coding region of the macrophage colony stimulating factor gene. *Nature*. 345:442-4.

Yoshizumi, M., Y. Fujita, Y. Izawa, Y. Suzaki, M. Kyaw, N. Ali, K. Tsuchiya, S. Kagami, S. Yano, S. Sone, and T. Tamaki. 2004. Ebselen inhibits tumor necrosis factor-alpha-induced c-Jun N-terminal kinase activation and adhesion molecule expression in endothelial cells. *Exp Cell Res*. 292:1-10.

Zaidi, M., O.A. Adebanjo, B.S. Moonga, L. Sun, and C.L. Huang. 1999a. Emerging insights into the role of calcium ions in osteoclast regulation. *J Bone Miner Res*. 14:669-74.

Zaidi, M., O.A. Adebanjo, B.S. Moonga, L. Sun, and C.L. Huang. 1999b. Emerging insights into the role of calcium ions in osteoclast regulation. *In* J Bone Miner Res. Vol. 14. 669-74.

Zaidi, M., H.C. Blair, B.S. Moonga, E. Abe, and C.L. Huang. 2003. Osteoclastogenesis, bone resorption, and osteoclast-based therapeutics. *J Bone Miner Res*. 18:599-609.

Zaidi, M., B.S. Moonga, and O.A. Adebanjo. 1999c. Novel mechanisms of calcium handling by the osteoclast: A review- hypothesis. *In* Proc Assoc Am Physicians. Vol. 111. 319-27.

Zaidi, M., V.S. Shankar, R. Tunwell, O.A. Adebanjo, J. Mackrill, M. Pazianas, D. O'Connell, B.J. Simon, B.R. Rifkin, A.R. Venkitaraman, and et al. 1995. A ryanodine receptor-like molecule expressed in the osteoclast plasma membrane functions in extracellular Ca2+ sensing. *In* J Clin Invest. Vol. 96. 1582-90.

Zambonin Zallone, A., A. Teti, M. Gaboli, and P.C. Marchisio. 1989. Beta 3 subunit of vitronectin receptor is present in osteoclast adhesion structures and not in other monocyte-macrophage derived cells. *Connect Tissue Res*. 20:143-9.

Zambonin-Zallone, A., A. Teti, A. Carano, and P.C. Marchisio. 1988. The distribution of podosomes in osteoclasts cultured on bone laminae: effect of retinol. *J Bone Miner Res*. 3:517-23.

Zang, R., H.J. Muller, K. Kielbassa, F. Marks, and M. Gschwendt. 1994. Partial purification of a type eta protein kinase C from murine brain: separation from other protein kinase C isoenzymes and characterization. *Biochem J*. 304 (Pt 2):641-7.

Zayzafoon, M., K. Fulzele, and J.M. McDonald. 2005. Calmodulin and calmodulin-dependent kinase IIalpha regulate osteoblast differentiation by controlling c-fos expression. *J Biol Chem*. 280:7049-59.

Zhang, Y.H., A. Heulsmann, M.M. Tondravi, A. Mukherjee, and Y. Abu-Amer. 2001. Tumor necrosis factor-alpha (TNF) stimulates RANKL-induced osteoclastogenesis via coupling of TNF type 1 receptor and RANK signaling pathways. *J Biol Chem*. 276:563-8.

Zhou, H., A. Lin, Z. Gu, S. Chen, N.H. Park, and R. Chiu. 2000. 12-O-tetradecanoylphorbol-13-acetate (TPA)-induced c-Jun N-terminal kinase

(JNK) phosphatase renders immortalized or transformed epithelial cells refractory to TPA-inducible JNK activity. *J Biol Chem*. 275:22868-75.

A

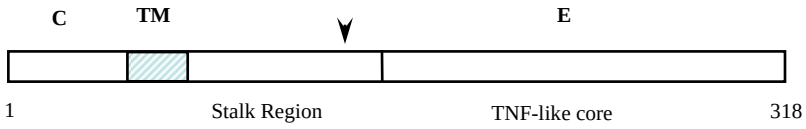

B

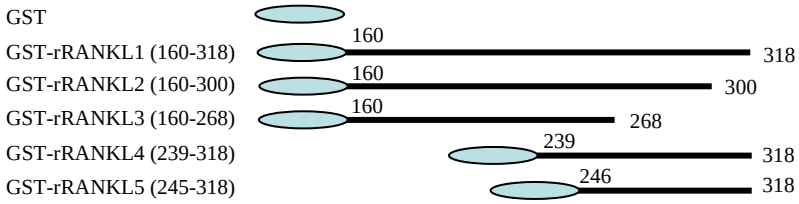

C

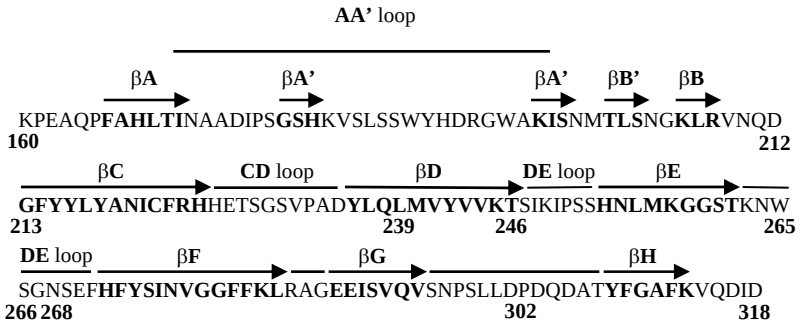

Figure 4.1 Structure of rat RANKL and expression of truncation mutants of rat RANKL within the TNF-like core domain. (A) Schematic diagram of the structure of rRANKL. C = cytoplasmic region; TM = transmembrane region; E = extracellular region; arrowhead indicate the potential TACE cleavage site. (B) Truncated regions of rRANKL cDNA cloned into the pGEX expression vectors. (C) Structure elements of TNF-like core domain of rat RANKL based on structural alignments of mouse RANKL and the crystal structure of mouse RANKL. The amino acid residues of truncation mutants are indicated.

A

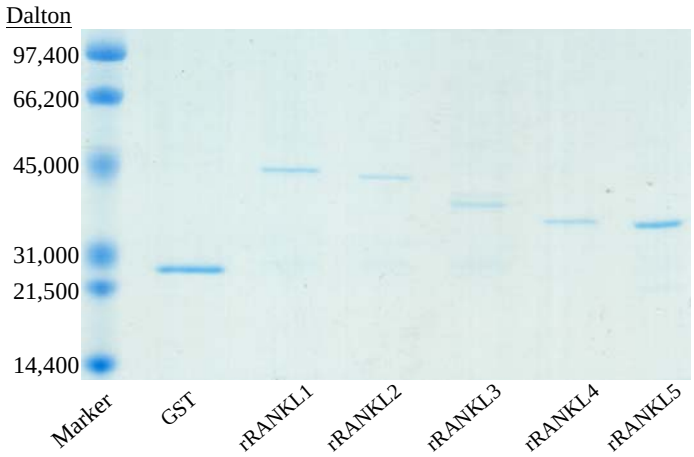

B

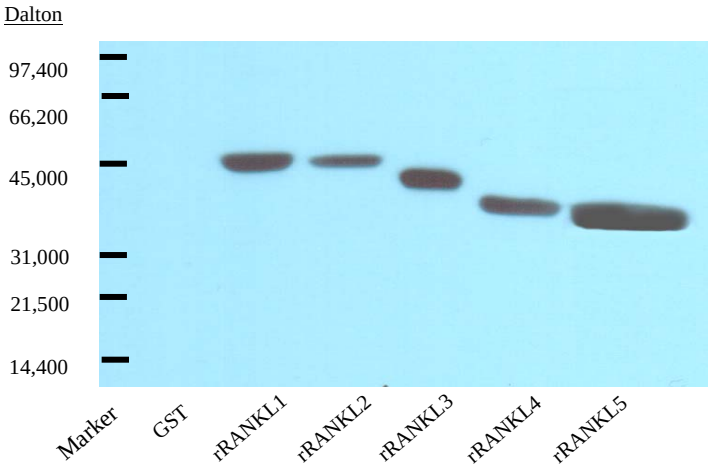

Figure 4.2 Protein purification of full-length and truncation mutants of rRANKL. (A) Coomassie blue-stained polyacrylamide gel showing the affinity-purified rat RANKL fusion proteins expressed in Escherichia coli. (B) An autoradiagraph showing that a monoclonal antibody to RANKL specifically interacts with the affinity-purified GST-rRANKL fusion proteins by Western blot analysis.

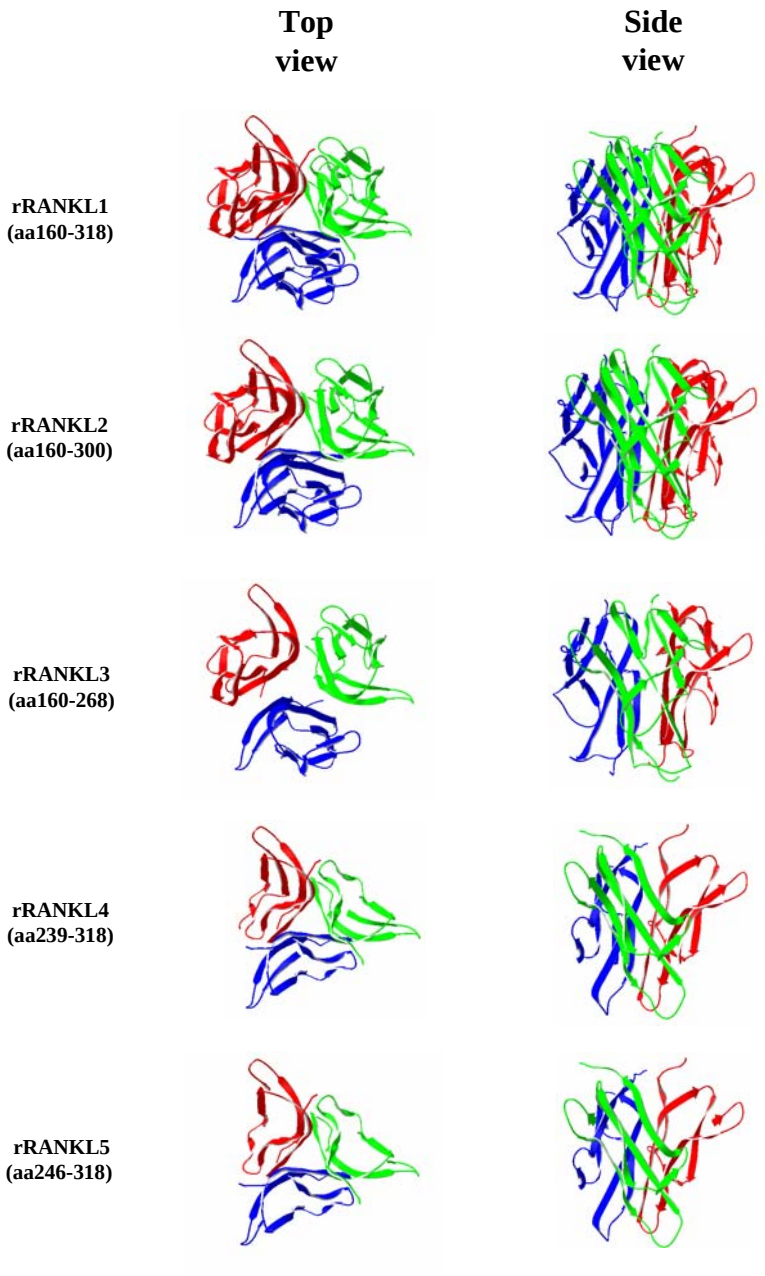

Figure 4.3 Predicted crystal structure of truncation mutants of rRANKL. Based on the proposed crystal structure of mouse RANKL, the crystal structure of rRANKL mutants (rRANKL1-5) were predicted by using Swiss PDB Viewer (version 3.7b1). Top and side views of the crystal structures were generated.

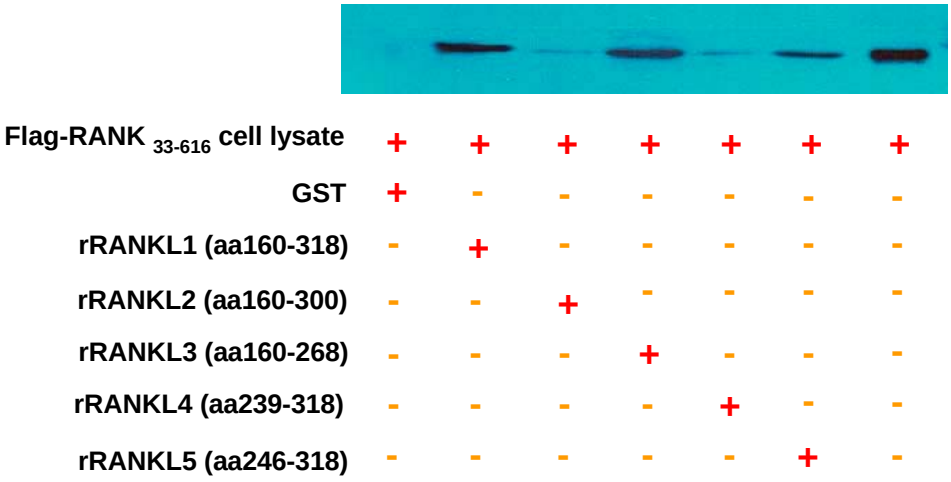

Figure 4.4 ***In vitro*** **Interaction of GST-rRANKL fusion proteins with RANK by GST pull-down assay.** An autoradiograph showing the binding of Flag-RANK to GST-RANKL mutants by GST pull-down assay. COS cells transfected with Flag-RANK were lysed and applied to immobilized GST-rRANKL in glutathione agarose beads. The binding complexes were separated on SDS-PAGE and Western blot was performed using the anti-Flag antibody.

A

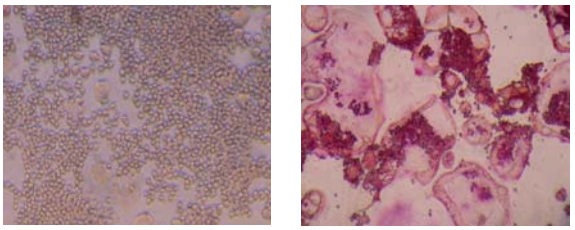

a. GST alone

b. rRANKL1 (aa160-318)

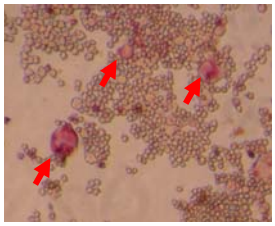

c. rRANKL2 (aa160-300)

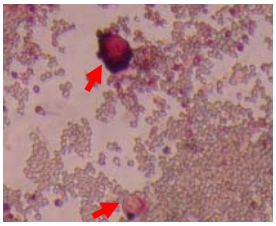

d. rRANKL3 (aa160-268)

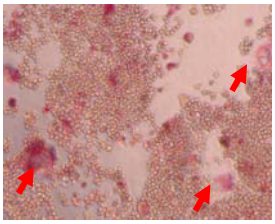

e. rRANKL4 (aa239-318)

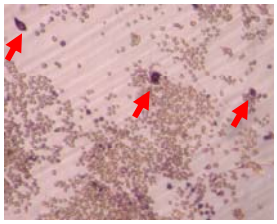

f. rRANKL5 (aa246-318)

B

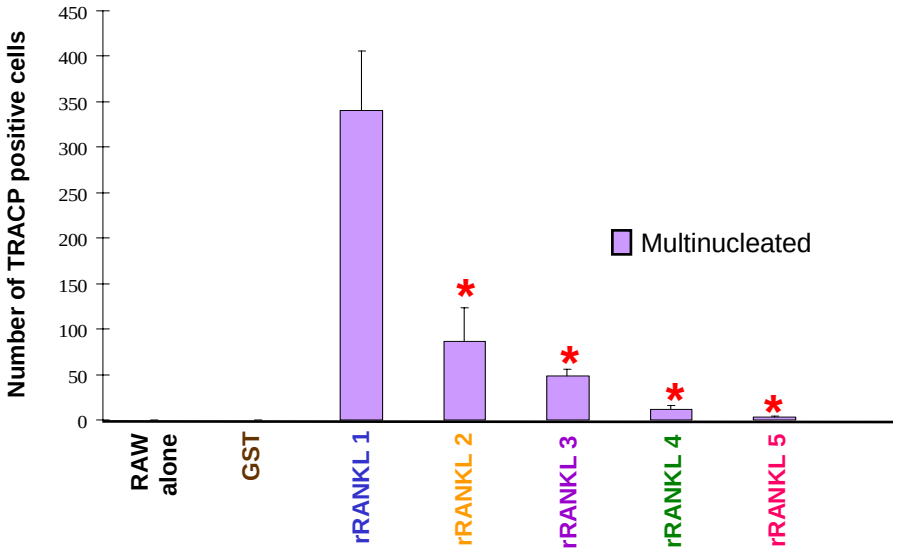

C

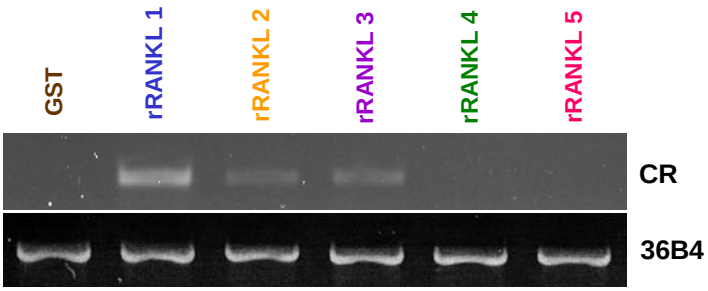

Figure 4.5 Inductive effects of RANKL mutants on osteoclastogenesis. RAW264.7 cells were stimulated with 100ng/ml of GST, full-length RANKL and 4 truncation mutants of rRANKL (aa160-302), (aa160-268), (aa239-318) and (aa246-318) for 5 days and fixed with 4% paraformaldehyde before being stained for TRACP activity. (A) Representative light microscopic images of TRACP-stained cells. Note that full-length rRANKL induces the formation of well-spread, TRACP-positive multinucleated (≥3 nuclei) osteoclasts. Truncation mutants of rRANKL generated TRACP-positive multinucleated (≥3 nuclei) cells (indicated by arrowheads), but the size of osteoclasts are smaller and they are lacking the characteristic morphology of osteoclasts. GST alone did not induce the formation of TRAP-positive cells. (B) A graph showing the total number of TRACP-positive multinucleated (≥3 nuclei) cells from RAW264.7 cells separately treated with 100 ng/ml of rRANKL mutants (aa160-302), (aa160-268), (aa239-318), (aa246-318), full-length RANKL (aa160-318), as well as GST control. (* $p<0.05$ compare with the full-length rRANKL-treated group) (C) RAW264.7 cells were separately stimulated with GST, full-length rRANKL as well as four truncation mutants of rRANKL (aa160-302), (aa160-268), (aa239-318) and (aa246-318) fusion proteins for 5 days. mRNA from cells was subjected to RT-PCR analysis using calcitonin receptor (CR) and 36B4.

A

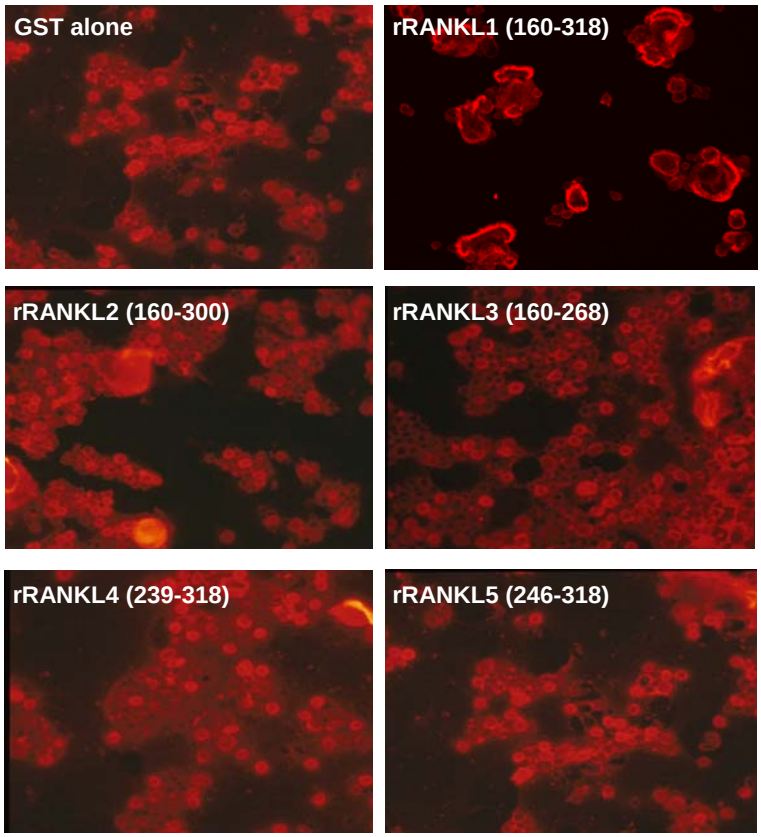
GST alone
rRANKL1 (160-318)
rRANKL2 (160-300)
rRANKL3 (160-268)
rRANKL4 (239-318)
rRANKL5 (246-318)

B

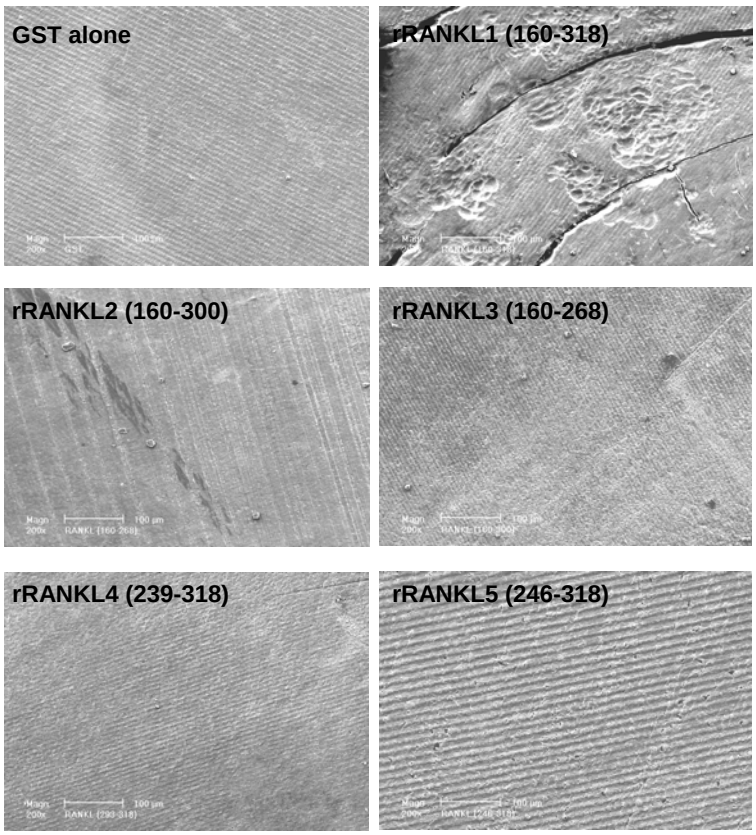

Figure 4.6 Truncation mutants of RANKL-induced osteoclast-like cells are incapable of bone resorption. (A) RAW264.7 cells were separately stimulated with GST, full-length rRANKL and truncation mutants of rRANKL for 5 days. The osteoclast-like cells were dissociated from the plate by using a cell dissociation buffer and then seeded on the glass overnight. The cells were fixed with 4% paraformaldehyde and stained with Rhodamine-conjugated Phalloidin (red) to visualize F-actin rings. (B) SEM images of bone slice. The truncation mutants of rRANKL-induced osteoclast-like cells are incapable of bone resorption. RAW264.7 cells were seeded on bone slices and separately stimulated with full-length rRANKL, truncation mutants of rRANKL and GST for 14 days. The bone slices were then processed and scanning electron microscopy (SEM) was performed.

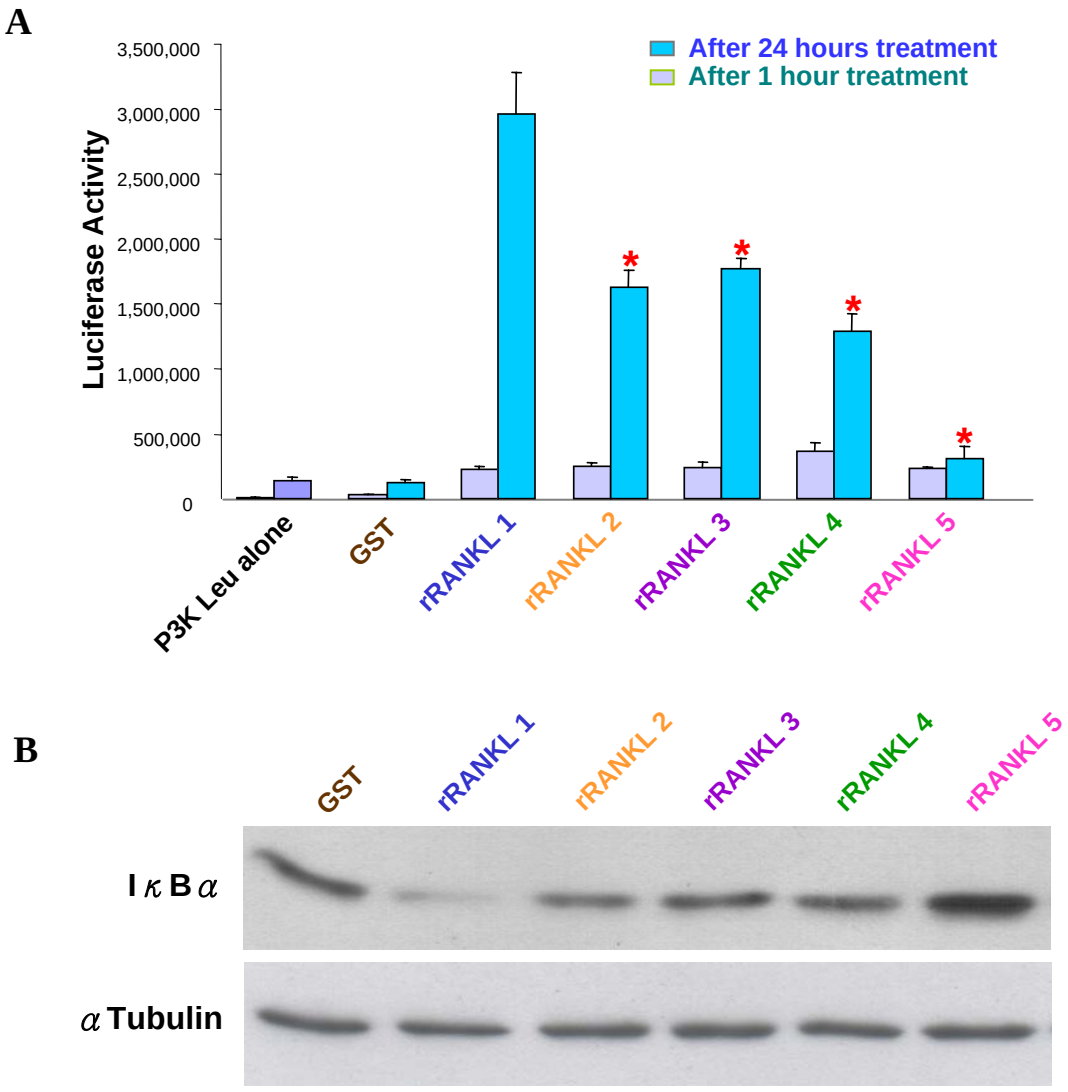

Figure 4.7 Activation of NF-κB by truncation mutants of rRANKL. (A) RAW264.7 cells which were stably transfected with the *3kB-Luc-SV40* reporter gene were separately treated with 200ng/ml of GST, rRANKL mutants (aa160-302), (aa160-268), (aa239-318), (aa246-318), and full-length rRANKL (aa160-318). The luciferase activity was measured at 1 hour and 24 hours after treatment. Note that the RANKL mutants have reduced effects on the activation of NF-κB compared with the full-length of RANKL, while GST control has no effects (* $p<0.05$ compare with full-length rRANKL-treated group). (B) RAW264.7 cells were separately stimulated with GST, full-length rRANKL and four truncation mutants of rRANKL for 20 minutes. The whole cell extracts were analyzed for IκBα degradation by using Western blotting. The proteins were separated by SDS-PAGE and transferred to the PVDF membrane. α Tubulin was used as internal control for protein loading. The bands were visualized by ECL.

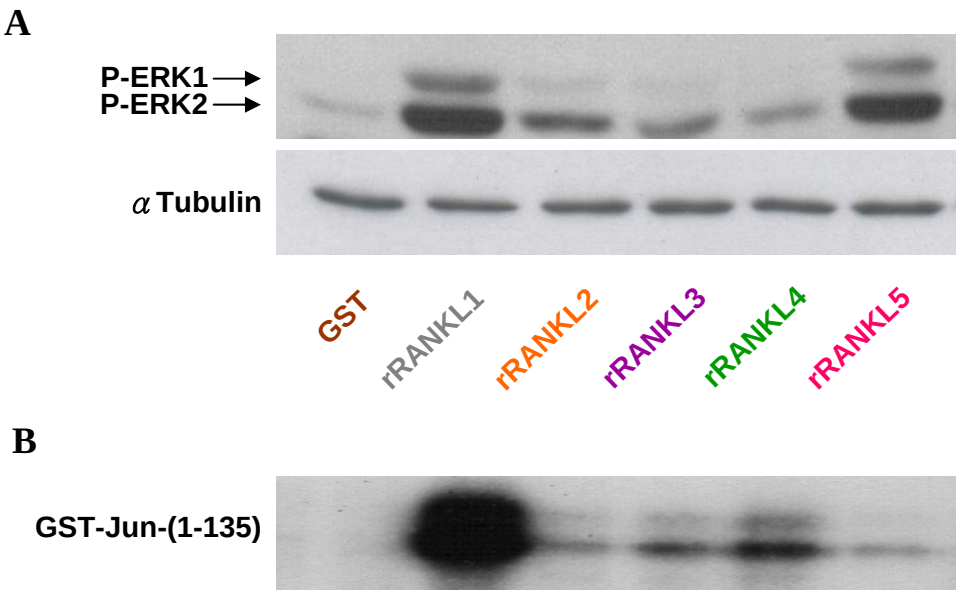

Figure 4.8 RANKL mutants impair the activation of pro-osteoclastogenic signalling pathways. (A) RAW264.7 cells were separately stimulated with GST, full-length rRANKL and four truncation mutants of rRANKL for 20 minutes. The whole cell extracts were analyzed for the phosphorylation of ERK by using Western blotting. The proteins were separated by SDS-PAGE and transferred to the PVDF membrane. α Tubulin was used as internal control for protein loading. The bands were visualized by ECL. (B) Activation of JNK by RANKL mutants. RAW264.7 cells were separately treated with 200 ng/ml of GST, truncation mutants of rRANKL (aa160-302), (aa160-268), (aa239-318), (aa246-318) and full-length RANKL (aa160-318). Cell lysates were precipitated with GST-c-jun sepharose. Precipitates were then assayed for their kinase activities using GST-c-Jun (1-135) as a substrate. Note that the RANKL mutants have reduced effects on the activation of JNK compared with the full-length of RANKL, while GST control has no effects.

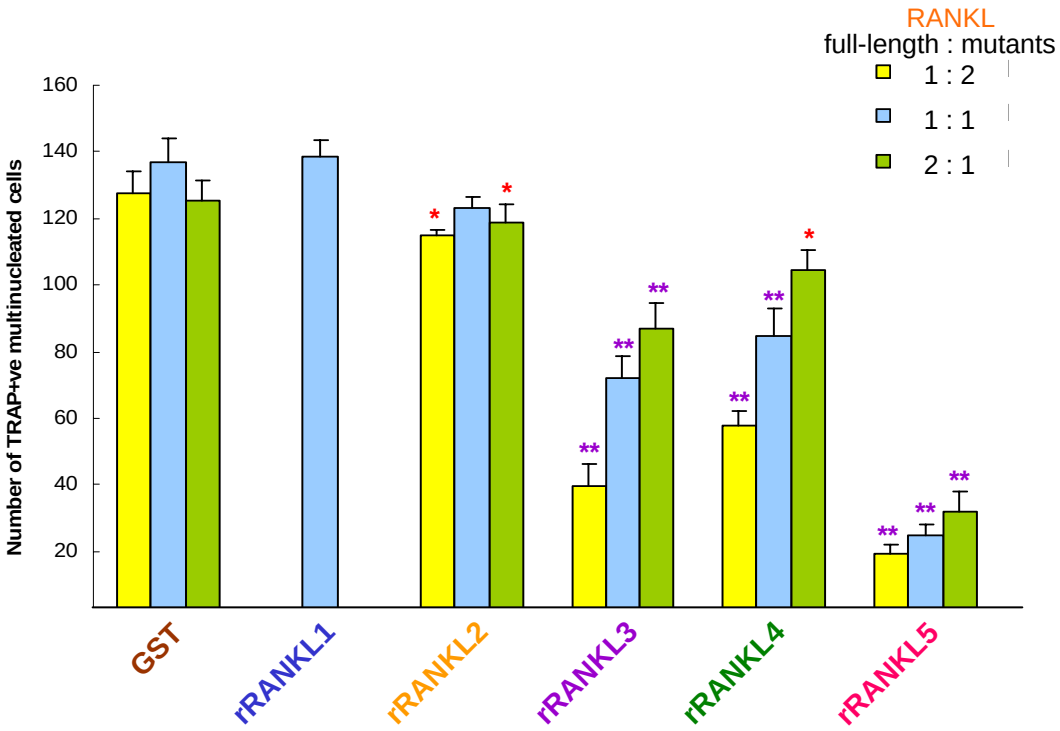

Figure 4.9 Truncation mutants of RANKL competitively inhibit full-length rRANKL-induced osteoclastogenesis. The graph represents of the total number of osteoclasts from each treated groups. RAW264.7 cells were treated with three different concentrations of truncation mutants of rRANKL (75, 150 and 300ng/ml) for 30 minutes before full-length RANKL (150ng/ml) was added. The ratio of truncation mutants of rRANKL to full-length rRANKL is 2:1 (yellow bars), 1:1 (blue bars) and 1:2 (green bars) (means±SD) (* $p<0.01$ and ** $p<0.001$ compare with the full-length rRANKL-treated groups). Note that the truncation mutants of rRANKL-treated cells appeared to be smaller compared with GST plus full-length rRANKL or rRANKL alone. The truncation mutants of rRANKL significantly inhibited the full-length rRANKL-induced osteoclastogenesis.

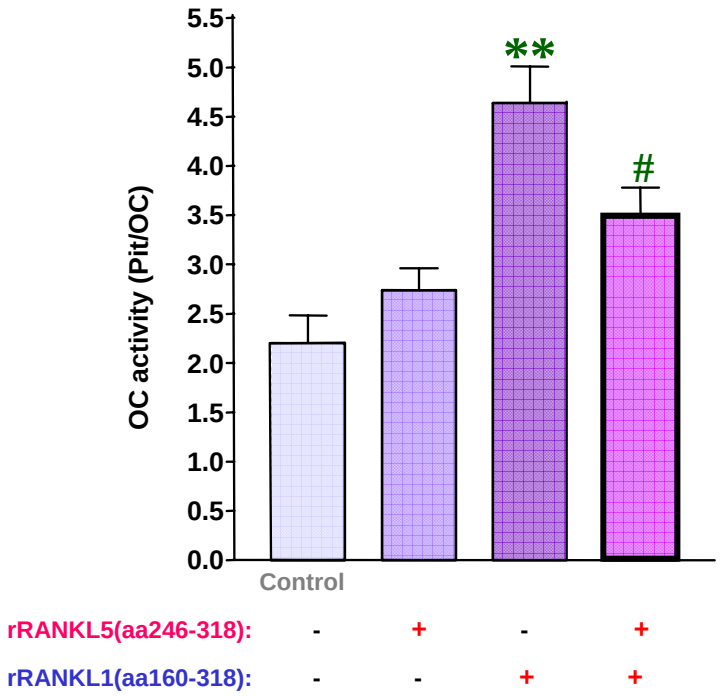

Figure 4.10 The inhibitory effect of RANKL5 (aa246-318) on full-length RANKL-induced osteoclastic bone resorption. Isolated rat osteoclasts (approximately 100 osteoclasts/slice) were cultured separately in the presence of RANKL5 (aa246-318), full-length RANKL (RANKL1, aa160-318) and both, and bone resorption pits were determined. Note that RANKL5 inhibited full-length rRANKL-induced bone resorption, although it marginally activates osteoclast bone resorption when applied alone (** significantly different from control, $p<0.01$ in t-test; # significantly different from full-length, $p<0.05$, in t-test).

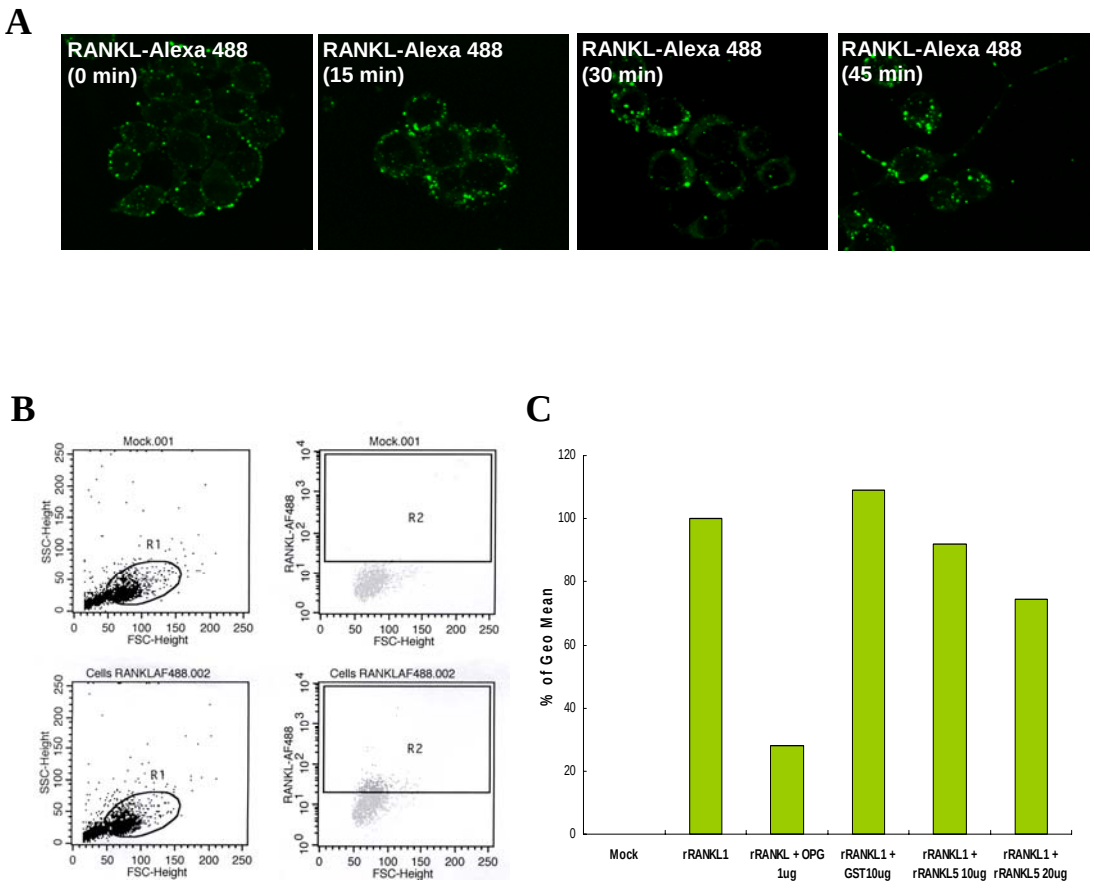

Figure 4.11 rRANKL5 competes with full-length RANKL to bind to the RANK receptor. (A) The full-length rRANKL was labelled Alexa Fluor (Molecular Probes). RAW264.7 cells were seeded on the glass overnight and then simulated with labelled RANKL-Alexa 488 for 5 to 45 minutes. The internalization of Alexa Fluor 488-labelled GST-rRANKL in RAW264.7 cells were analysed using confocal microscopy. (B) The competition binding of mutants and full-length rRANKL to the receptor RANK was examined by FACS analysis. RAW264.7 cells were separately pre-treated with GST (10ug) and rRANKL5 (10 and 20ug) for 1 hour at 4^{o}C. OPG (1ug) was mixed with rRANKL (500ng) for 1 hour prior adding to the cells suspension. The cells were separately treated with a labelled RANKL-Alexa 488 and, a mixture of OPG and labelled rRANKL-Alexa 488 for 1 hour at 4^{o}C and 30 minutes at 37^{o}C. The cells were then fixed with 4% paraformaldehyde and analysed by using FACS calibur to detect the fluorescence of the Alexa Fluor 488. The graphs represent the negative (no labelled RANKL-Alexa 488 were added) and positive (labelled rRANKL-Alexa 488 were added) controls. (C) A graph represent the percentage of Geo means from FACS analysis. The Geo means of the test groups were normalised with the positive control group (treated only with labelled rRANKL-Alexa 488).

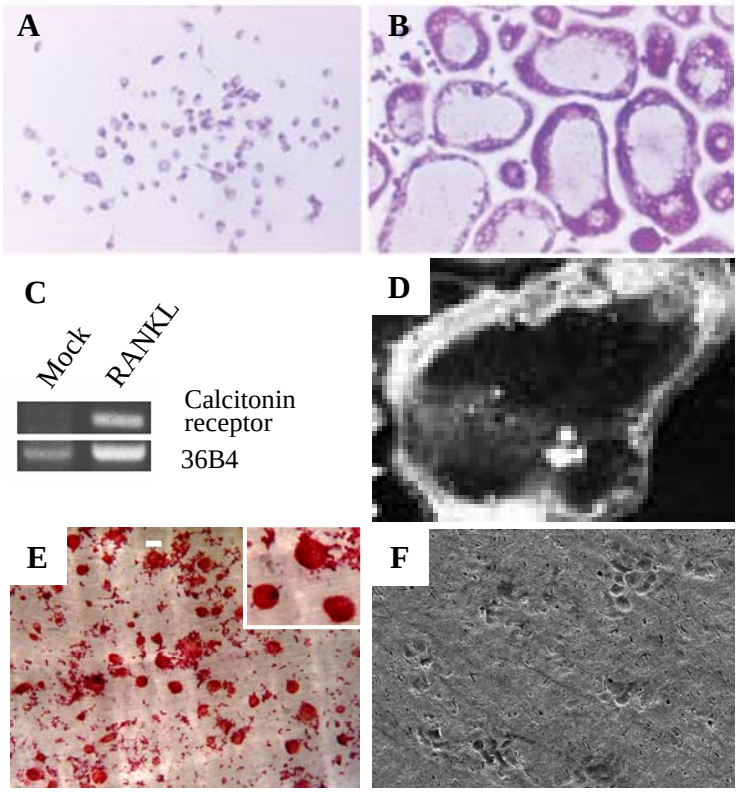

Figure 5.1 RAW264.7 cells derived osteoclasts were capable of resorbing bone. (A-B) Light microscopy images of TRACP activity of RAW cells treated with either 100 ng/ml of RANKL (B), or left untreated (A). (C) Expression of calcitonin receptor mRNA by RT-PCR in RAW264.7 cells treated with either 100 ng/ml of RANKL or left untreated. (D) Confocal microscopy image of the expression of calcitonin receptor proteins in RAW264.7 cell derived OCLs by immuno-fluorescence staining. (F) TRACP positive staining of RAW264.7 cells cultured on bovine bone slices in the presence of RANKL for 7 days. (E) Scanning electronic microscopy image of bone pit formation of RAW264.7 cell derived OLCs.

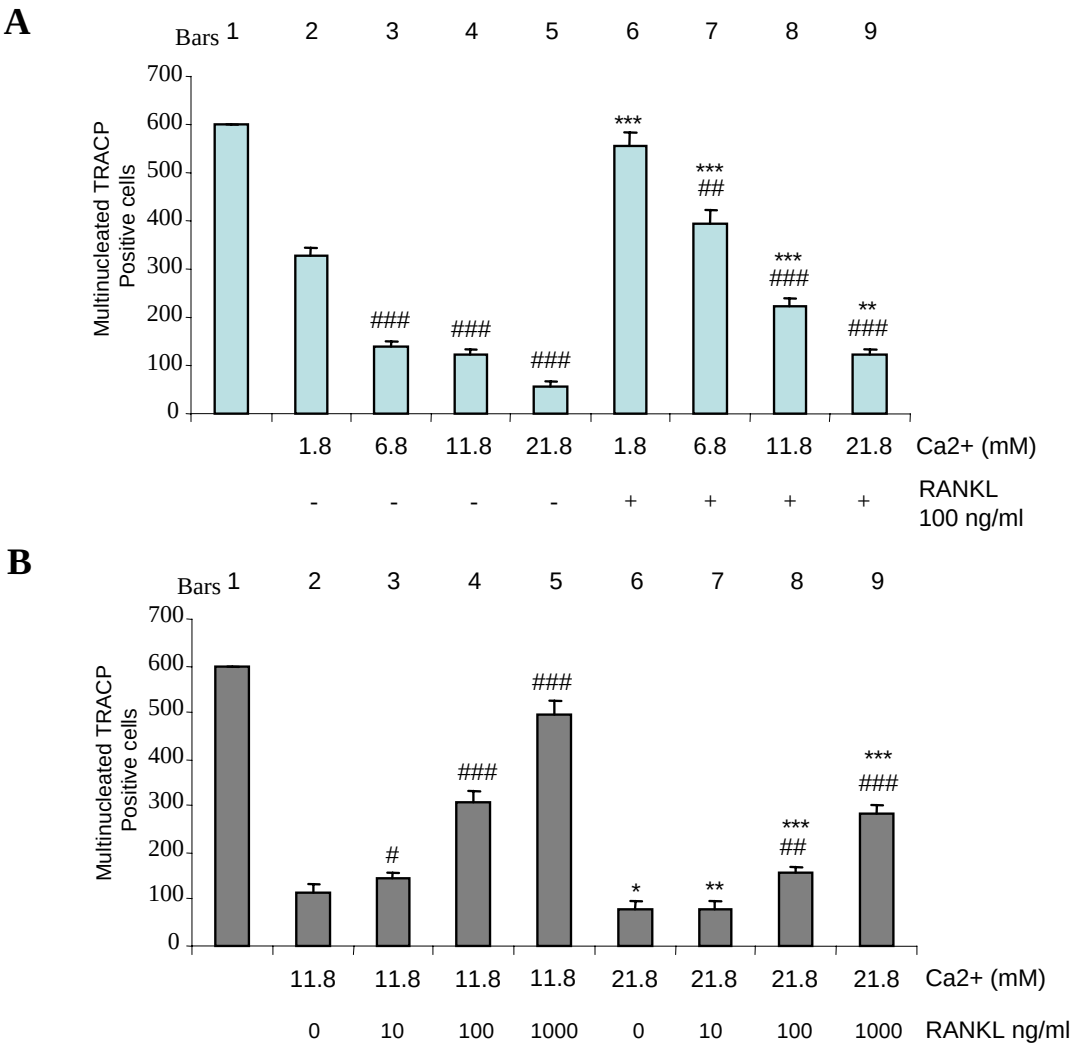

Figure 5.2 RANKL protects loss of osteoclast like cells induced by high extracellular Ca^{2+}. (A) The effect of extracellular Ca^{2+} and RANKL on osteoclast survival. RAW264.7 cell-derived OCLs were seeded at 600 cells (bar 1) per well in a 96 well plate and exposed to increasing concentration of $CaCl_2$ (1.8 of control, 6.8, 11.8 and 21.8 mM) in the presence or absence of 100 ng/ml of RANKL for 24 hours followed by fixation and TRACP staining. Bar 1 represents the number of OCLs seeded at the beginning of the 24 hour treatment. Total multinucleated TRACP positive OCLs were counted. Each bar represents mean ± SEM from triplicate wells. (B) RANKL dose dependently protected against elevated extracellular Ca^{2+}-induced cell death. RAW cell-derived OCLs were exposed to 11.8 or 21.8 mM $CaCl_2$ in the presence of 1, 10, 100 or 1000 ng/ml RANKL for 24 hours followed by fixation and TRACP staining. Representative results from three independent experiments are shown. # representing the P Values of the effect of calcium (bars 3-5, 7-9) compared to its respective controls (bars 2 and 6). * representing the P Values of the effect of RANKL (bars 6-9) compared to its respective controls (bars 2-5) (###/*** $p<0.001$, ##/** $p<0.01$, #/* $p<0.05$).

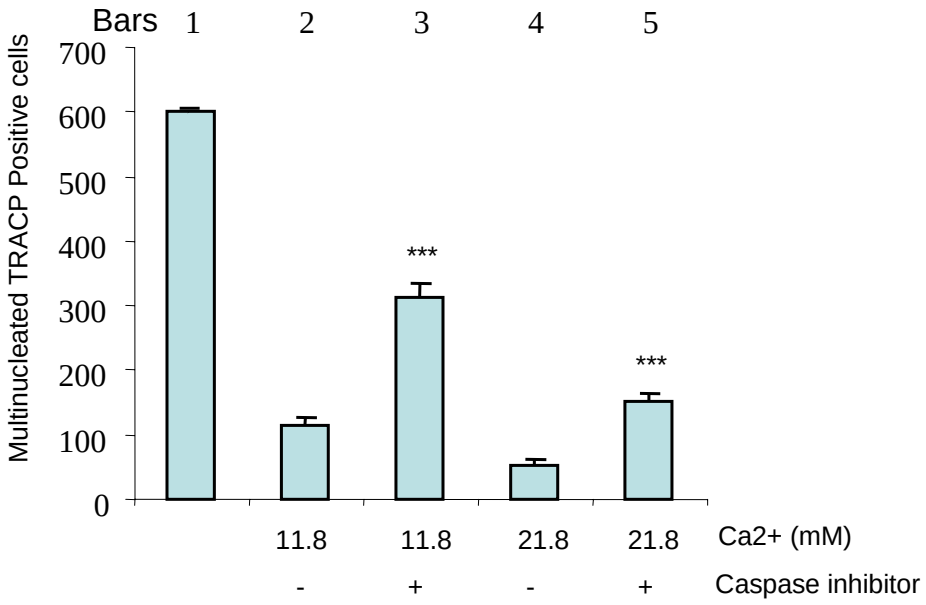

Figure 5.3 The caspase 3/7 inhibitor Ac-DEVD-CHO was protective against Ca^{2+}-induced cell death. RAW264.7 cell derived OCLs were exposed to 11.8 and 21.8 mM $CaCl_2$ in the presence or absence of 100 mM Ac-DEVD-CHO for 24 hours followed by fixation and TRACP staining. Bar 1 represents the number of OCLs seeded at the beginning of the 24 hour treatment. Total multinucleated TRACP positive OCLs were counted. Each bar represents mean ± SEM from triplicate wells. Representative results from three independent experiments are shown. * representing the P value of the effect caspase inhibitor (bars 3 and 5) compared to its respective controls (bars 2 and 4) (*** $p<0.001$).

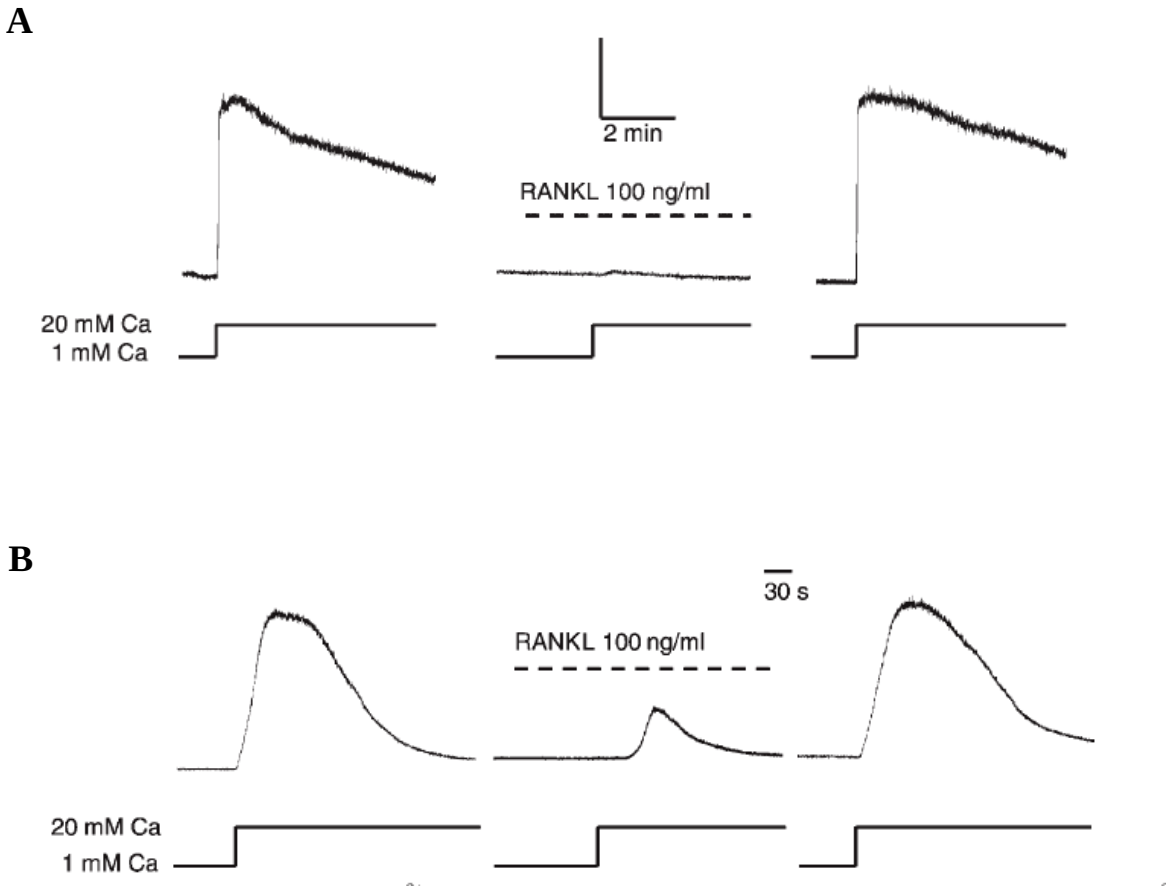

Figure 5.4 RANKL attenuates high extracellular Ca2+-induced elevations in cytosolic Ca^{2+} in RAW264.7 cell derived OCLs. In this experiment, OCLs (n=15) were initially exposed to 20 mM of Ca^{2+} to elicit a control cytosolic Ca^{2+} elevation (left panels). After washout, OCLs were exposed to RANKL and then re-exposed to 20 mM extracellular Ca^{2+}, and the resulting change in intracellular Ca^{2+} was recorded (middle panels). The cells were then re-exposed to 20 mM extracellular Ca^{2+} under control conditions to ensure that the cells retained viable Ca^{2+} signaling mechanisms (right panels). Traces are representative of those cells that showed that RANKL either completely, A (n=7), or partially, B (n=2), reduced high extracellular Ca^{2+}-induced elevations in cytosolic Ca^{2+} in the OCLs.

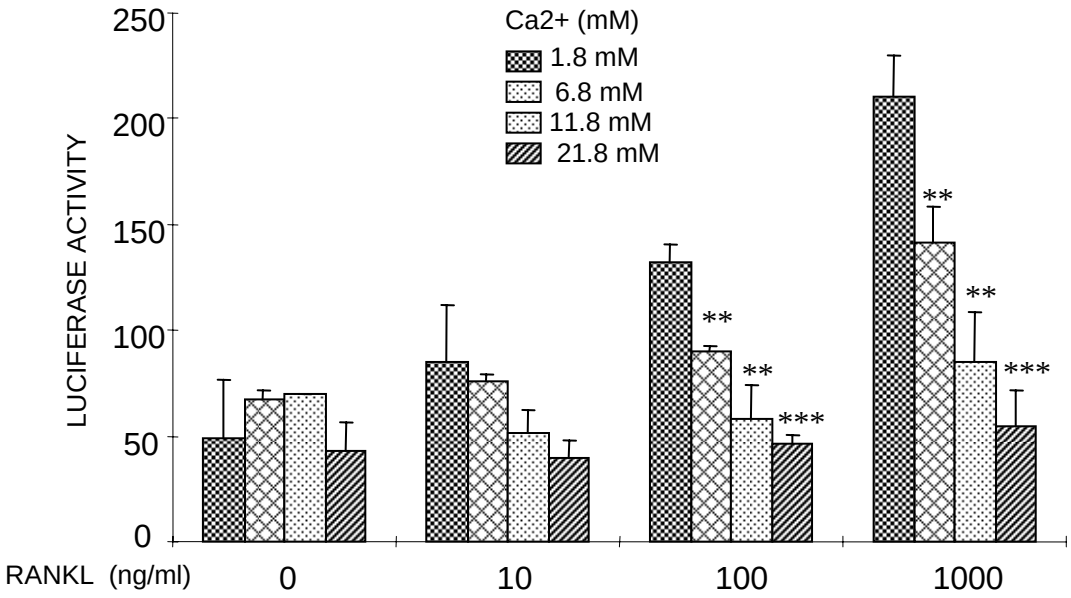

Figure 5.5 High Ca^{2+} inhibits RANKL-induced activation of NF-κB. RAW264.7 cells transiently transfected with the *3kB-Luc-SV40* reporter gene, were treated with a range of RANKL concentrations (0,10,100 or 100ng/ml) in the presence of a range of calcium concentrations (1.8, 6.8, 11.8 and 21.8 mM) for 8 hours and the luciferase activity in lysates determined. Each bar is the mean ± SEM from triplicate wells. Representative results from three independent experiments are shown. * representing the P value of the effect calcium (bars 2-4 of each group) compared to its respective controls (bars 1 of each group) (*** $p<0.001$, ** $p<0.01$, * $p<0.05$).

A

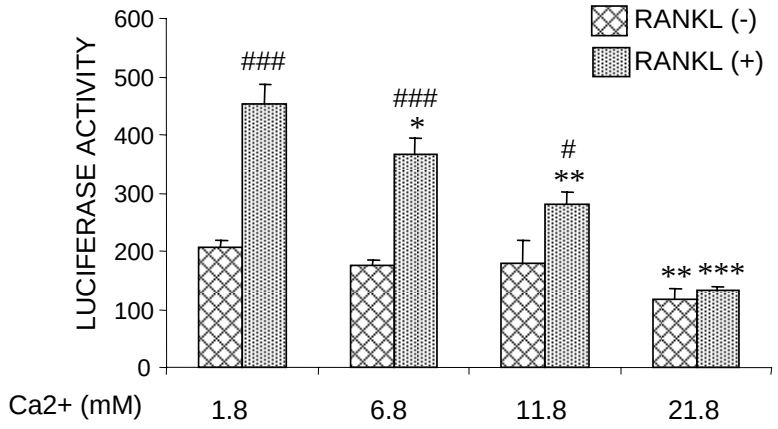

B

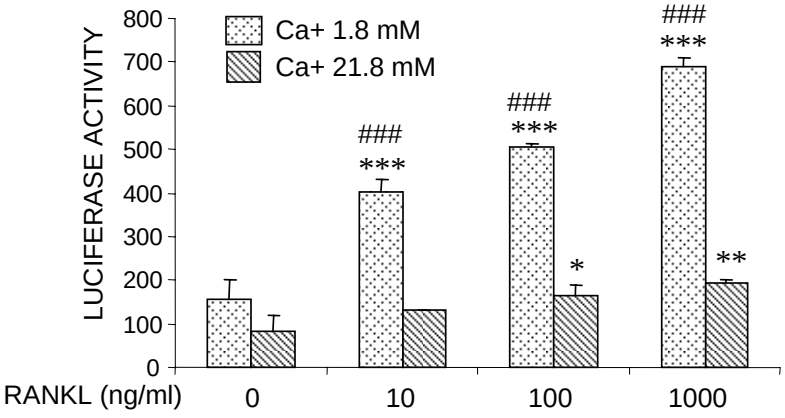

Figure 5.6 High Ca^{2+} inhibits RANKL-induced activation of JNK mediated AP-1. RAW264.7 cells transiently transfected with the *pAP1-TA-Luc* reporter gene, were treated with medium alone, RANKL, Ca^{2+} or RANKL plus Ca^{2+} for 8 hours and the luciferase activity in lysates determined. Each bar is the mean ± SEM from triplicate wells. (A) Dose dependent effect of Ca^{2+} (1.8, 6.8, 11.8 and 21.8) on RANKL (100 ng/ml) -induced activation of JNK. (B) Dose dependent effect of RANKL (1, 10, 100 and 1000 ng/ml) - induced activation of JNK in the presence of 1.8 mM or 21.8 mM of Ca^{2+}. Representative results from three independent experiments are shown. # representing the P Values of the effect of calcium compared to its respective controls. * representing the P Values of the effect of RANKL compared to its respective controls (###/*** $p<0.001$, ##/** $p<0.01$, #/* $p<0.05$).

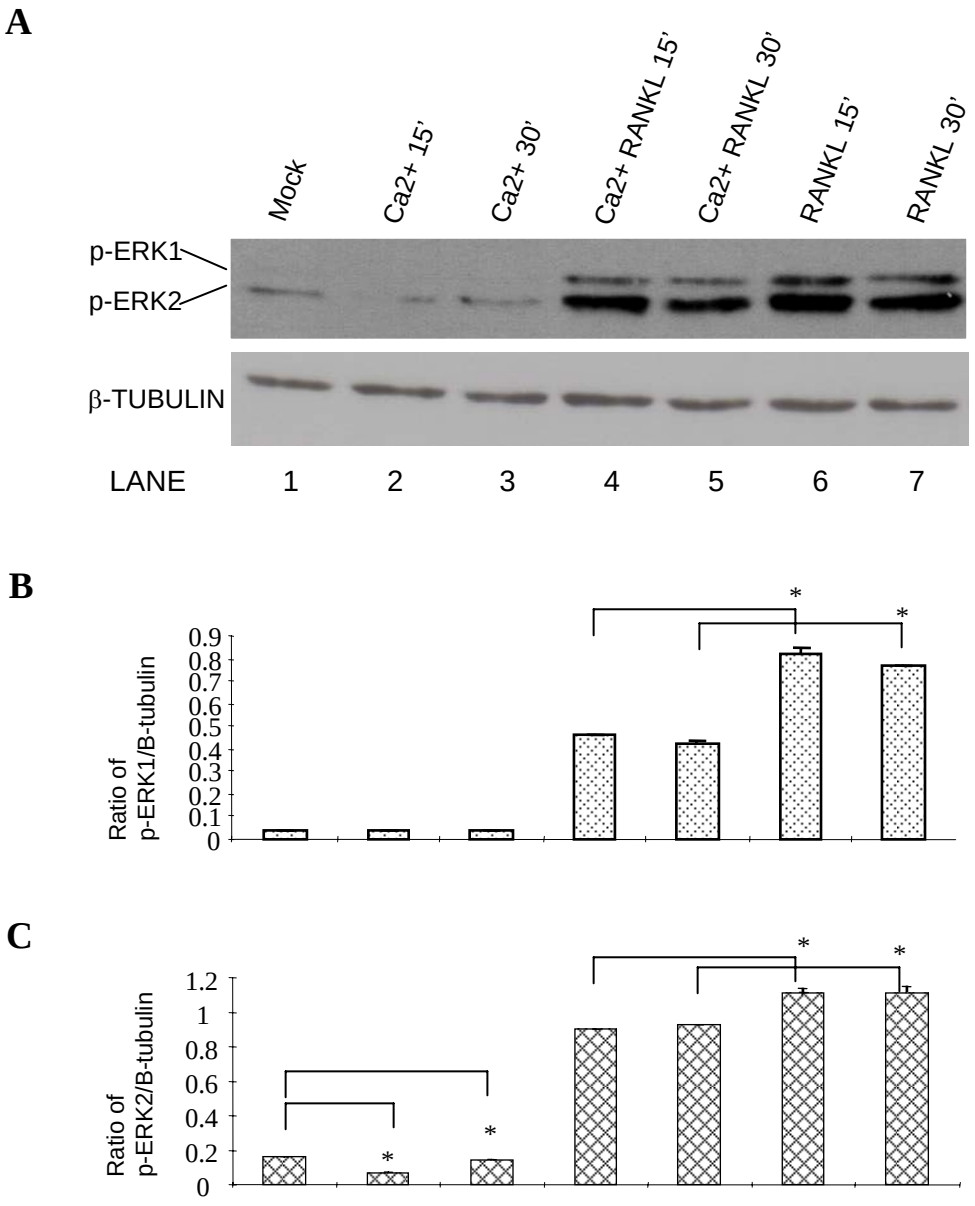

Figure 5.7 High $Ca2^+$ inhibits RANKL-induced phosphorylation of ERK. RAW264.7 cells were treated with vehicle alone (mock), 100 ng/ml RANKL, 11.8mM of Ca^{2+} or RANKL and Ca^{2+} for 0, 15 and 30 min and whole cell extracts analyzed for phosphorylated forms of ERK by Western blot analysis followed by ECL. The same membrane was stripped and re-probed with an antibody for β-tubulin which serves as an internal control for differences in loading and transfer (A). The levels of pERK1 (B) and pERK2 (C) proteins are shown as the ratio of pERK1 and pERK2 to β-tubulin. * representing the P value of the effect of calcium in comparison with its respective controls.(*$p<0.01$).

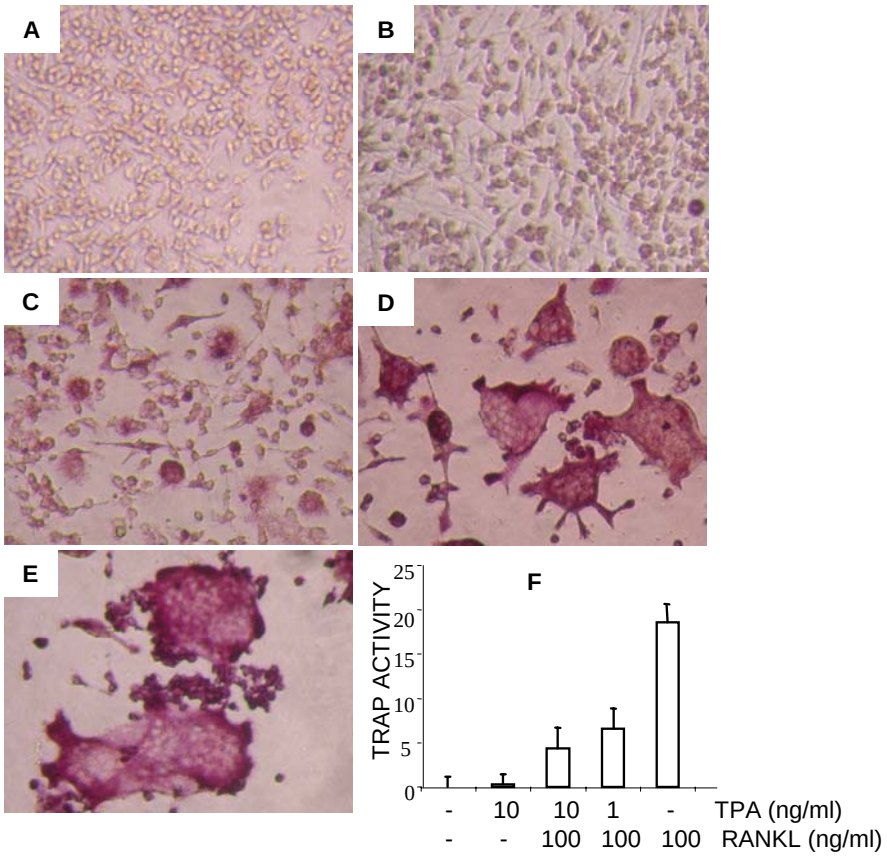

Figure 6.1 TPA inhibits RANKL-induced osteoclastogenesis. RAW264.7 cells were cultured in the presence of RANKL, TPA or RANKL plus TPA. After 5 days, the cells were fixed with 4% paraformaldehyde and stained for TRAP activity. (A) Light microscopy images showing the effect of TPA on RANKL-induced osteoclast formation with morphological changes. RAW264.7 cells were left untreated (A) or treated with 10 ng/ml of TPA (B), 1 ng/ml of TPA plus RANKL (C), 10 ng/ml of TPA plus RANKL (D), and RANKL alone (E). (F) A graph representing total TRAP activity calculated as arbitrary densitometry units.

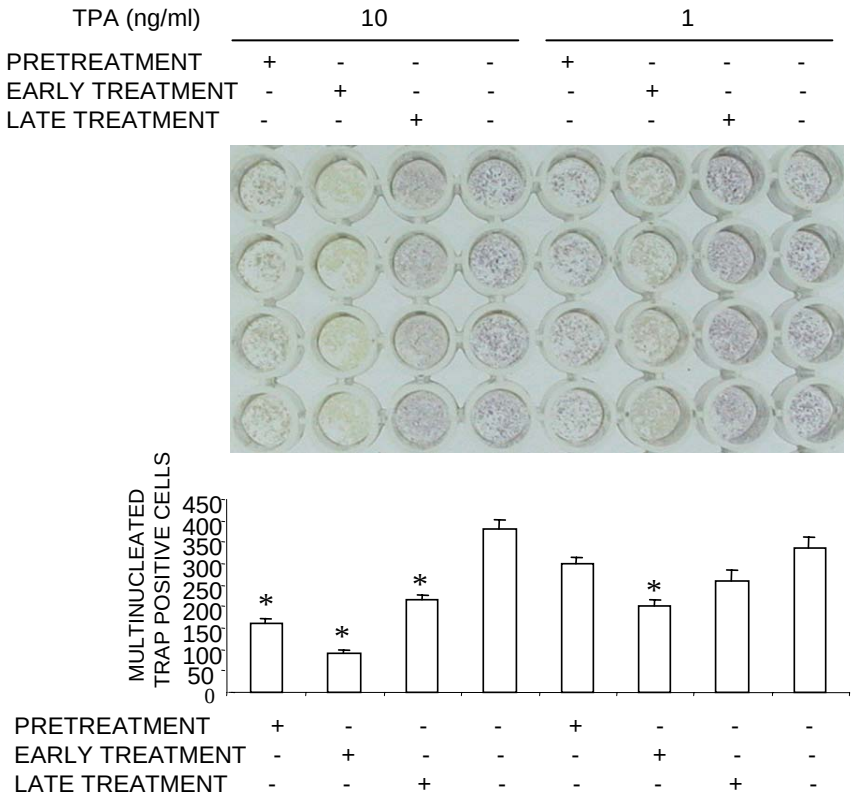

Figure 6.2 TPA inhibits RANKL-induced osteoclastogenesis predominantly during the early stage. RAW264.7 cells were pretreated with TPA for 24 hours before the addition of RANKL, or treated with TPA at the early time (at days 1-2), or late time course (at days 3-4), or left untreated, and cultured in the presence of RANKL for a total of 5 days. The treated cells were fixed with 4% paraformaldehyde and stained for TRAP activity. TRAP positive multinucleated (> 5 nuclei) cells were counted. Values are expressed as mean ± SEM from quadraplex wells (* $P<0.001$).

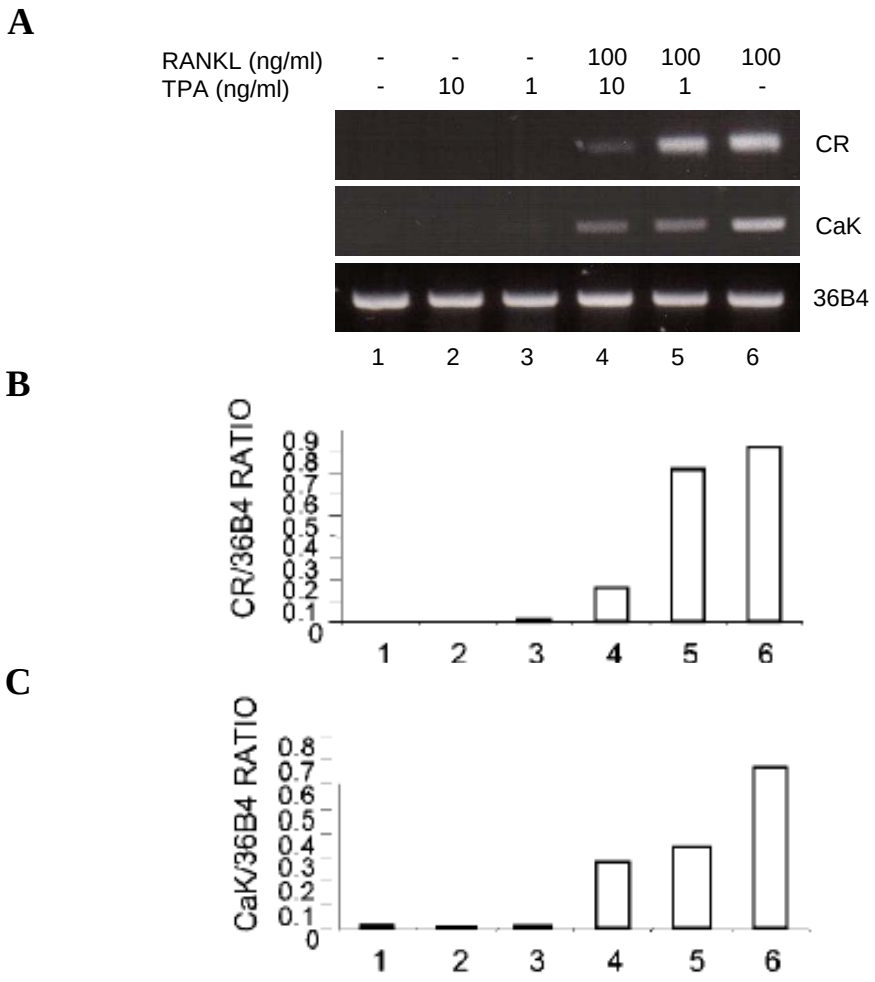

Figure 6.3 TPA dose-dependently reduced RANKL-induced expression of osteoclast genes. 1.5 x 10^5 RAW264.7 cells seeded into 6 well plates were incubated in the presence or absence of 100 ng/ml of RANKL for 5 days with various doses of TPA. Total cellular RNA was extracted and cDNA was synthesized using two mg of total RNA with oligo-dT. PCR amplification was performed using specific primers for, calcitonin receptor, cathepsin K and 36B4 genes. PCR products were separated on 1.2 % of agarose gels (A) and measured by densitometry. The levels of calcitonin receptor (CR) (B) or cathepsin K (CaK) (C) mRNA are shown as the ratio of calcitonin receptor or cathepsin K to 36B4.

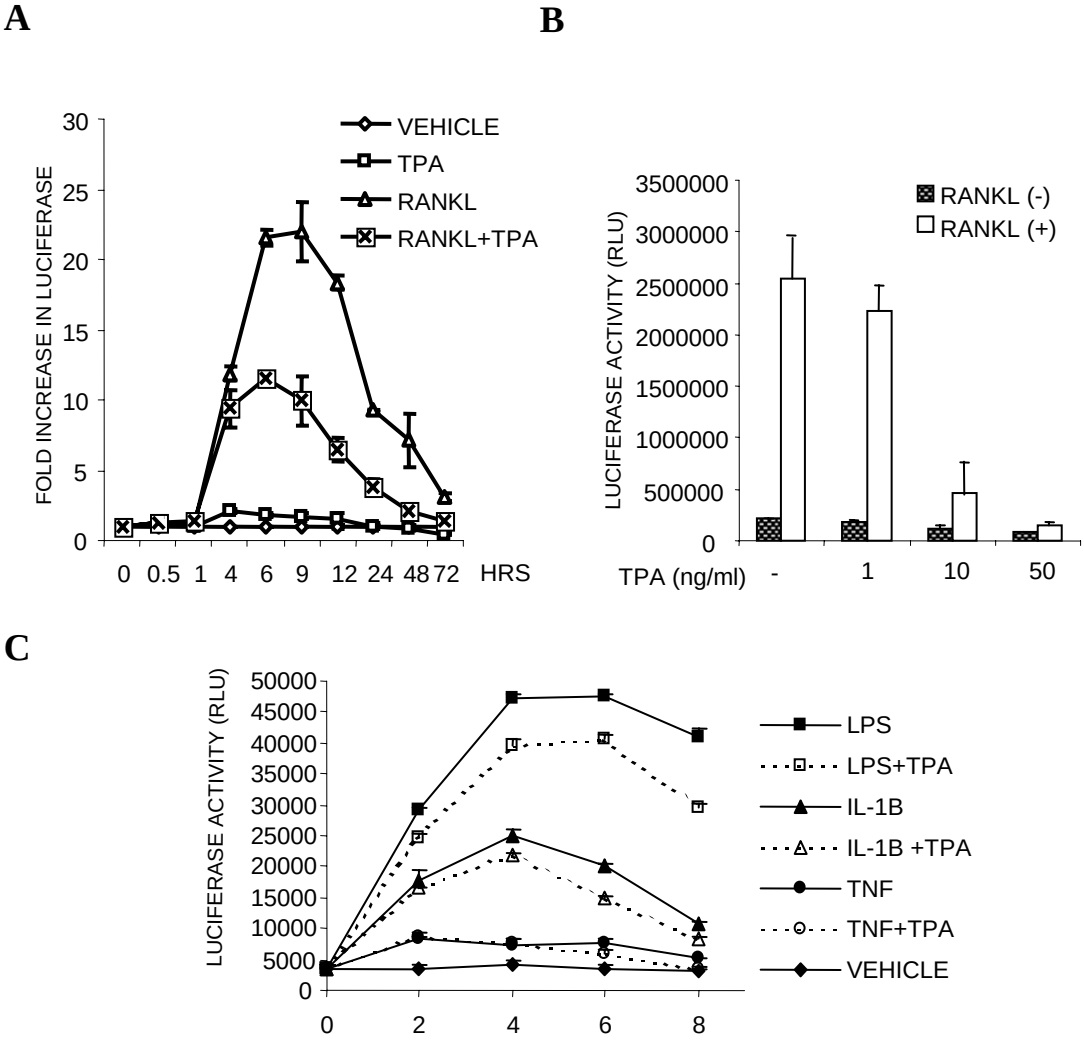

Figure 6.4 TPA inhibits RANKL, LPS, IL-1B and TNF-induced NF-κB-dependent transcription in RAW264.7 cells. (A) RAW264.7 cells, transiently transfected with the *3kB-Luc-SV40* reporter gene, were treated with medium alone (Nil), RANKL (200 ng/ml), TPA (20 ng/ml) or RANKL and TPA and the luciferase activity in lysates determined at various times up to 72 hours. Each point is the mean ± SEM from triplicate wells. (B) TPA suppresses RANKL-induced activation of NF-κB in a dose-dependent fashion. RAW264.7 cells, stably transfected with the *3kB-Luc-SV40* reporter gene, were treated with various doses of TPA (0, 1, 10 and 50 ng/ml) in the presence or absence of RANKL (200 ng/ml). The luciferase activities were measured 24 hours post treatment. Each point is the mean ± SEM from triplicate wells. (C) RAW264.7 cells stably transfected with the *3kB-Luc-SV40* reporter gene were plated into a 24-well culture dish 18 hours before stimulation for 8 hours with TNF α (10ng/ml), LPS (1ug/ml), IL-1β (10ng/ml). Each bar represents the luciferase activity of cells stimulated in the presence or absence of TPA (20ng/ml) (mean ± SEM from triplicate wells).

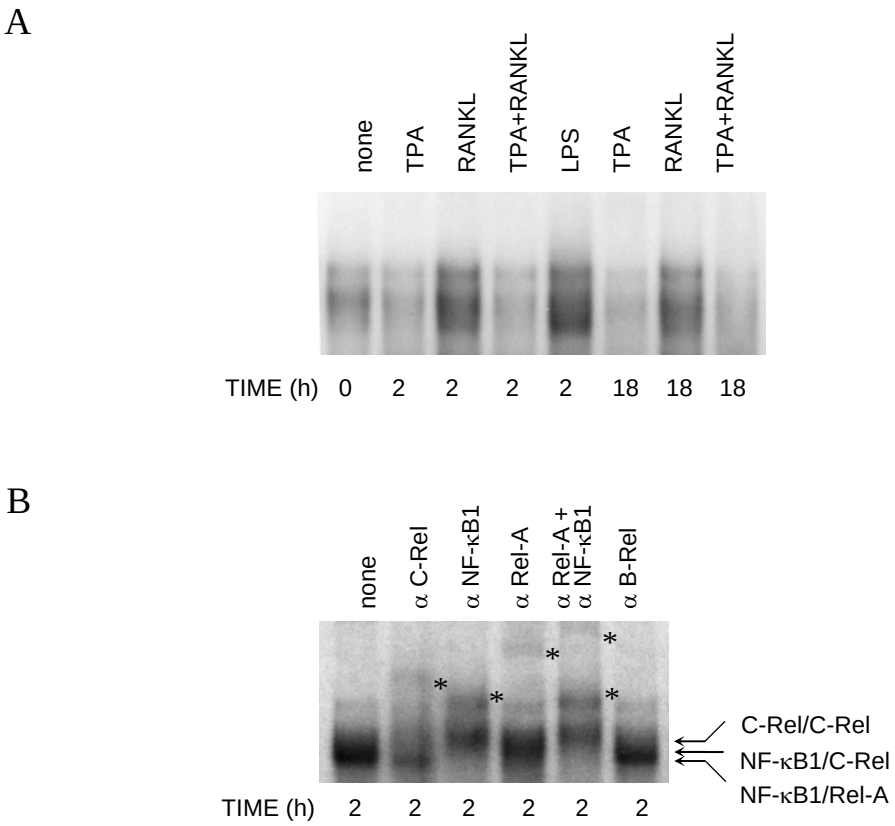

Figure 6.5 TPA inhibits RANKL-induced nuclear translocation of NF-kB in RAW264.7 cells. (A) RAW264.7 cells were treated with medium alone (none), LPS (1mg/ml, positive control), RANKL (200 ng/ml), TPA (20 ng/ml) or RANKL and TPA for 0, 2 or 18 hours. Nuclear extracts were prepared from 1 × 107 cells and EMSA was carried out using [32^{P}] labeled NF-κB oligonucleotide probe. (B) supershift assays using anti-NF-κB1 (p50), Rel-A (p65), c-Rel, and B-Rel antibodies determined that RANKL-induced DNA binding of NF-κB complexes in RAW cells consists of NF-κB1 (p50), Rel-A (p65) and c-Rel but not B-Rel.

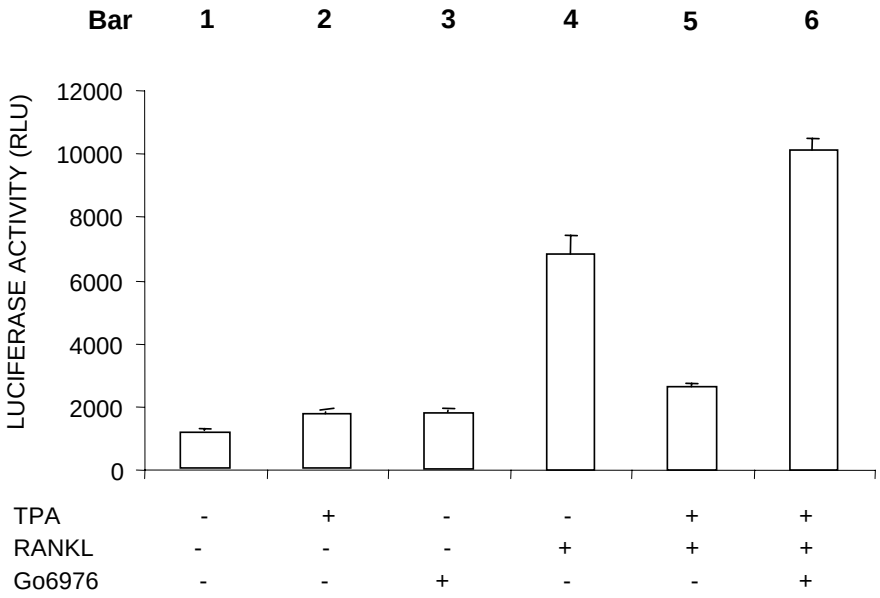

Figure 6.6 Go9676 blocks the inhibitory effect of TPA on RANKL-induced NF-κB-dependent transcription in RAW264.7 cells. RAW264.7 cells stably transfected with the *3kB-Luc-SV40* reporter gene were plated into a 24-well culture dish 18 hours before stimulation for 8 hours with: bar 1 - vehicle, bar 2 - TPA (10ng), bar 3 - vehicle + Go9676 (5μM), bar 4 - RANKL4 (100ng), bar 5 - RANKL (100ng) + TPA (10ng) and bar 6 - RANKL (100ng) + TPA (10ng) + Go9676 (5μM). Each bar is the mean ± SEM from triplicate wells.

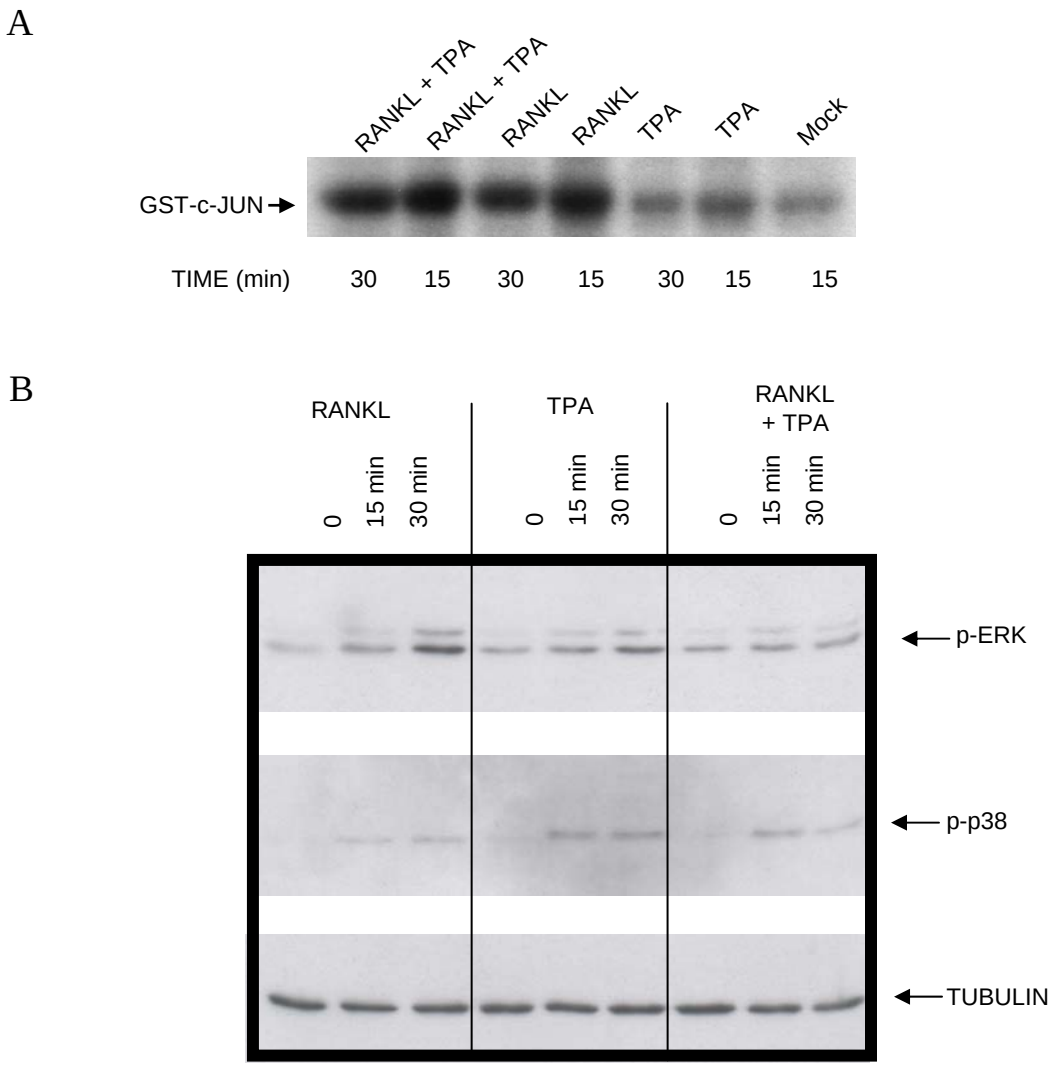

Figure 6.7 TPA has little effect on RANKL-induced phosphorylation of JNK and p-38 but inhibits phosphorylation of ERK. RAW264.7 cells were treated with vehicle alone (mock), RANKL (200 ng/ml), TPA (20 ng/ml) or RANKL and TPA for 0, 15 and 30 min and whole cell extracts analyzed for: A) JNK activity by autoradiography of [32P] phosphorylated GST-c-Jun (1-135) separated on SDS-PAGE gels. B) Phosphorylated forms of ERK and p38 by Western blot analysis. Whole cell extracts were prepared after 0, 15 or 30 minutes of stimulation and proteins separated by SDS PAGE and transferred to PVDF membranes. Membranes were probed sequentially with antibodies to p-ERK, p-p38 and Tubulin (in that order) and bands detected by ECL.

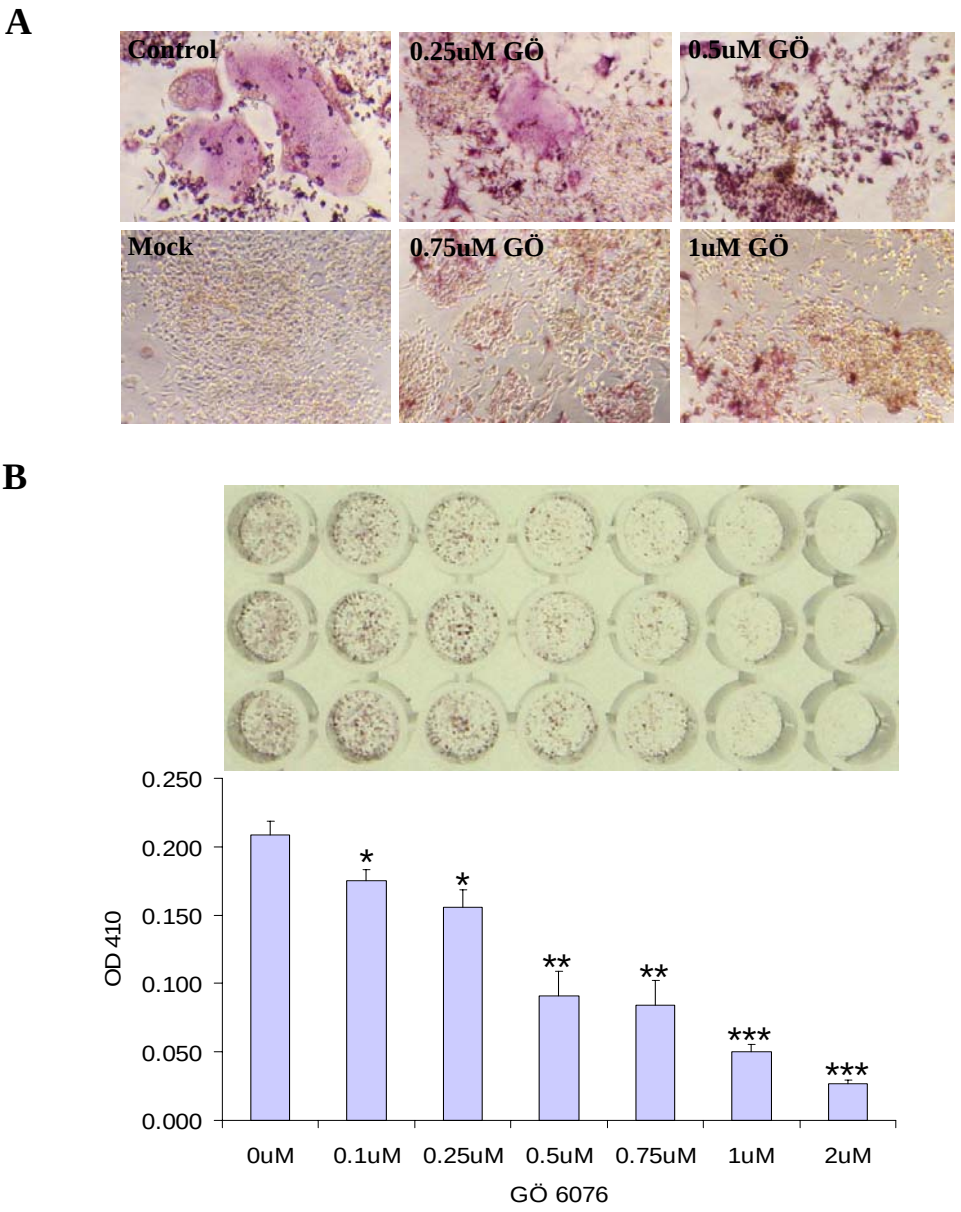

Figure 7.1 GÖ 6976 inhibits RANKL-induced osteoclastogenesis. RAW264.7 cells were cultured in the presence of RANKL and GÖ 6976. After 5 days, the cells were fixed with 4% paraformaldehyde and stained for TRACP activity. (A) Light microscope images showing the effect of GÖ 6976 on RANKL-induced osteoclast formation with morphological changes. Representative images of triplicate wells from one of three experiments are shown. (B) A graph representing the total TRACP activity. The TRACP activities were measured as absorbance at 410nm. The area of each well of the 96-well plate was scanned 3x3mm by the BMG machine and each $1mm^2$ was read 4 times. The average of 36 readings was calculated. (* $p<0.05$, ** $p<0.01$, *** $p<0.001$ compared to control.)

A

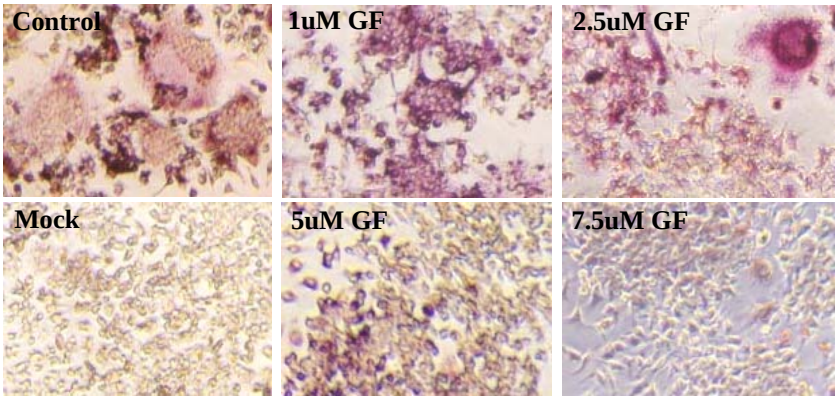

B

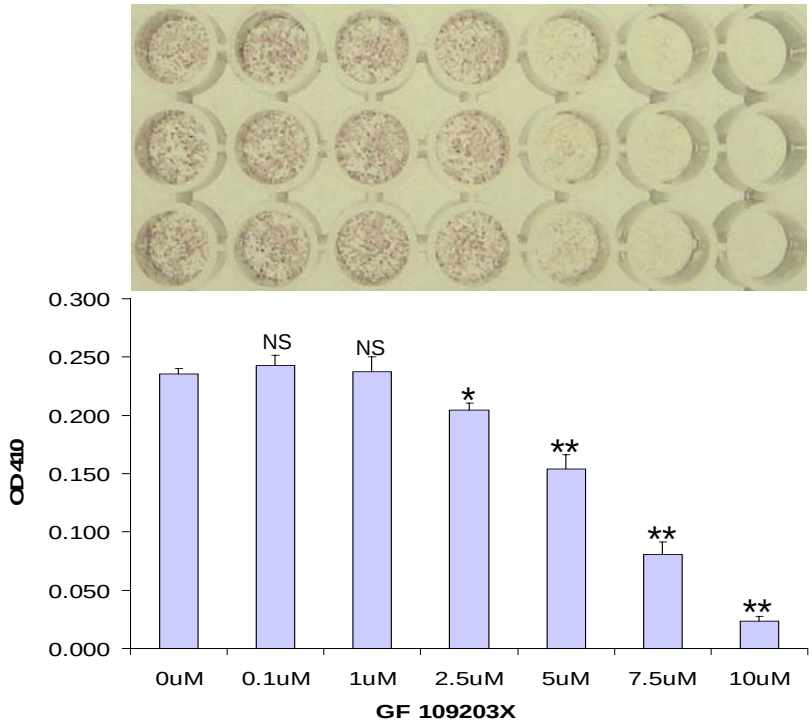

Figure 7.2 GF 109203X inhibits RANKL-induced osteoclastogenesis. RAW264.7 cells were cultured in the presence of RANKL and GF 109203X . After 5 days, the cells were fixed with 4% paraformaldehyde and stained for TRACP activity. (A) Light microscope images showing the effect of GF 109203X on RANKL-induced osteoclast formation with morphological changes. Representative images of triplicate wells from one of three experiments are shown. (B) A graph representing the total TRACP activity. The TRACP activities were measured as absorbance at 410nm. The area of each well of the 96-well plate was scanned 3x3mm by the BMG machine and each 1mm^2 was read 4 times. The average of 36 readings was calculated. (* p value <0.05, ** p value <0.01, NS = No significance compared to control)

A

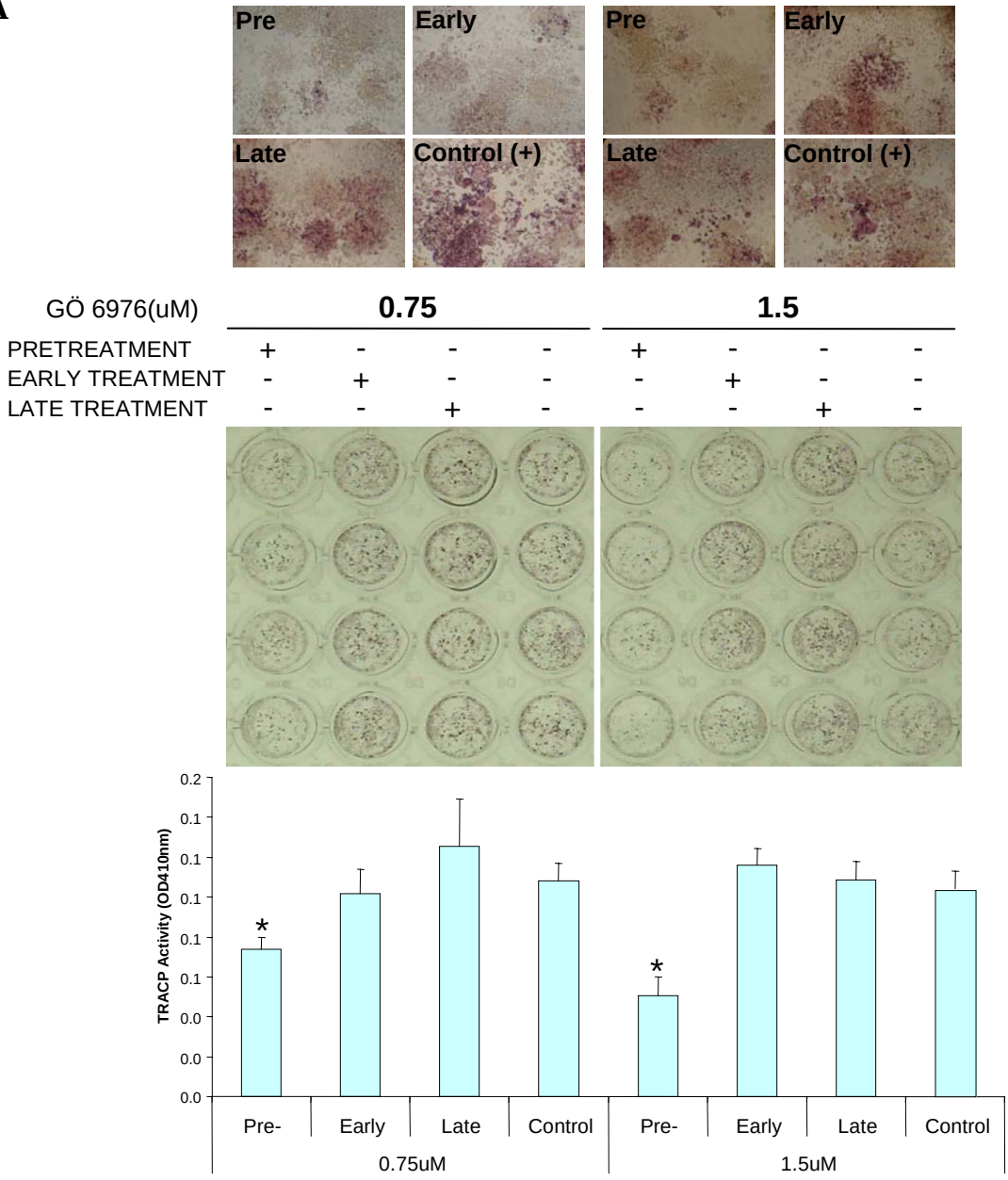
Pre
Early
Pre
Early
Late
Control (+)
Late
Control (+)
GÖ 6976(uM)
0.75
1.5
PRETREATMENT + - - - + - - -
EARLY TREATMENT - + - - - + - -
LATE TREATMENT - - + - - - + -
TRACP Activity (OD410nm)
0.2
0.1
0.1
0.1
0.1
0.0
0.0
0.0
*
*
Pre-
Early
Late
Control
Pre-
Early
Late
Control
0.75uM
1.5uM

B

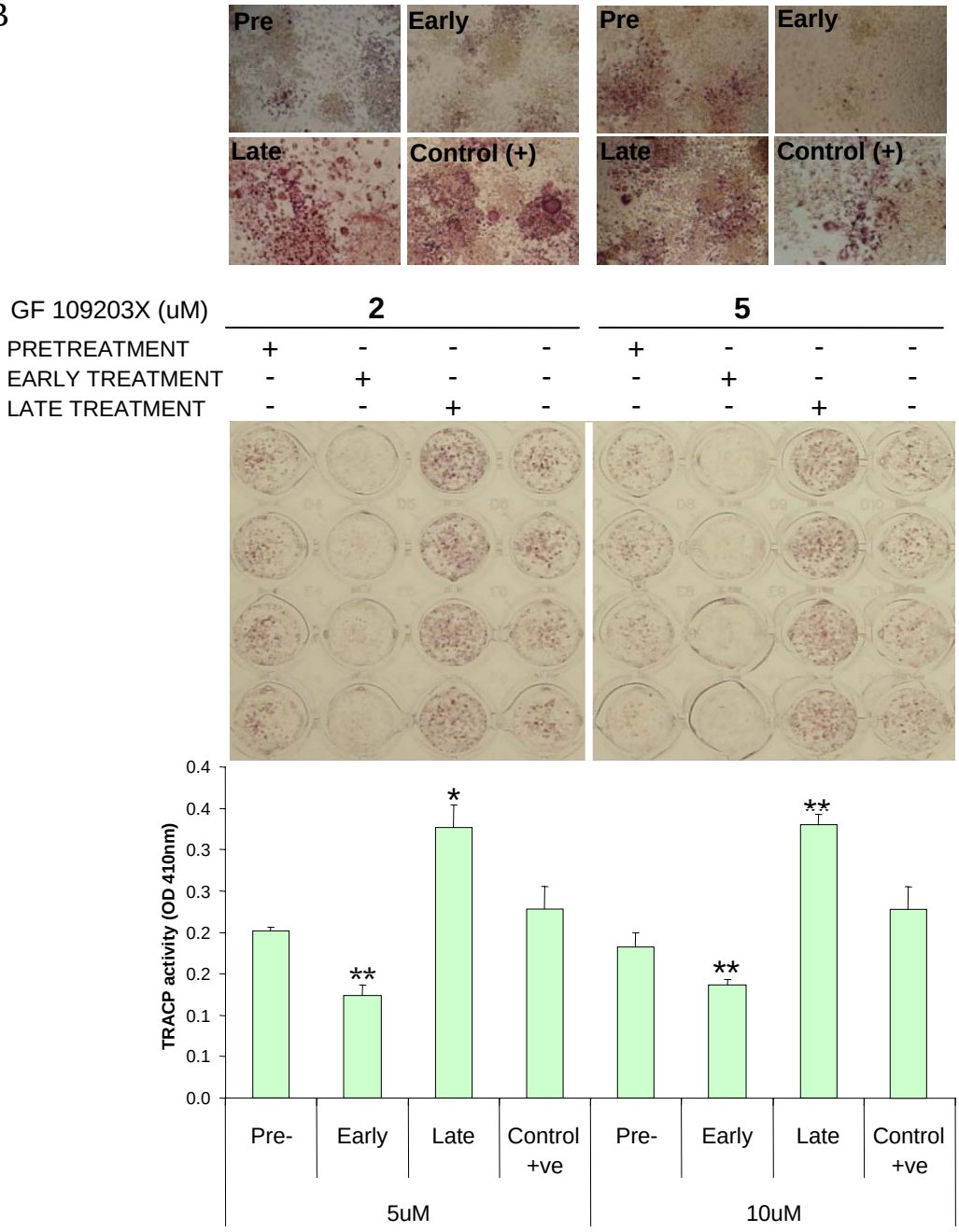

Figure 7.3 GÖ 6976 and GF 109203X modulate RANKL-induced osteoclastogenesis. There are 4 groups: RAW264.7 cells were pre-treated with GÖ 6976 and GF 109203X for 24 hours before the addition of RANKL; treated with GÖ 6976 and GF 109203X at the early time point (at day 1-2) and late time point (at day 3-4); as well as left untreated and cultured in the presence of RANKL for a total of 5 days. The treated cells were fixed with 4% paraformaldehyde and stained for TRACP activity. The graph represents the total TRACP activity which was measured by the BMG machine at OD410nm. (A) Time-course study for GÖ 6976. (B) Time-course study for GF 109203X. (* $p<0.05$, ** $p<0.01$)

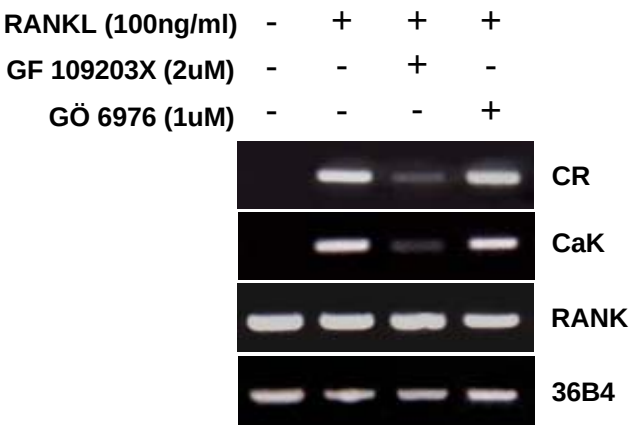

Figure 7.4 GF 109203X reduces RANKL-induced expression of osteoclast genes. RAW264.7 cells were treated GÖ 6976 (1uM) and GF 109203X (2uM) in the presence of RANKL for 5 days. mRNA from cells was subjected to RT-PCR analysis using calcitonin receptor (CR), cathepsin K (CaK), RANK and 36B4.

A

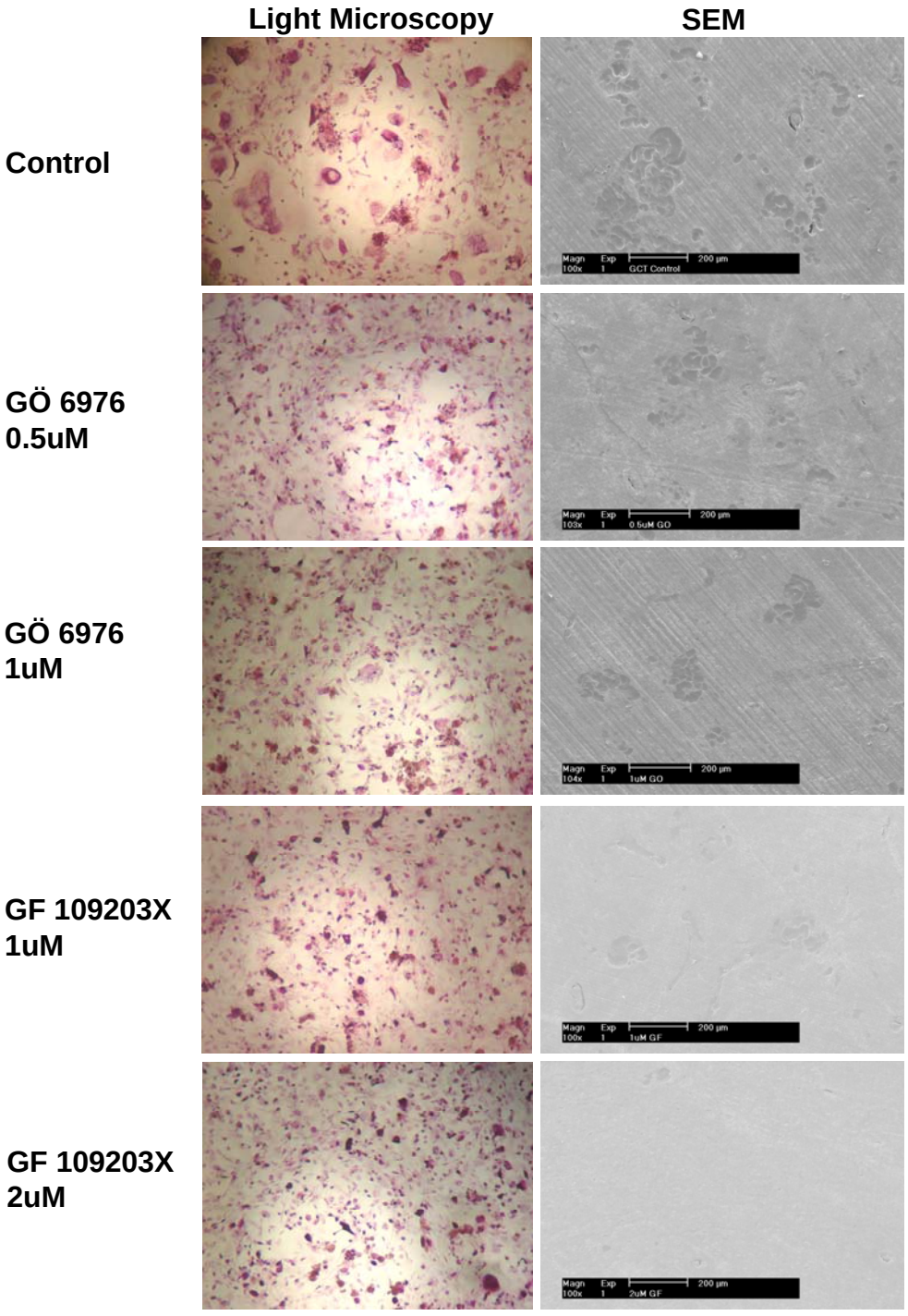
Light Microscopy
SEM
Control
GÖ 6976
0.5uM
GÖ 6976
1uM
GF 109203X
1uM
GF 109203X
2uM

B

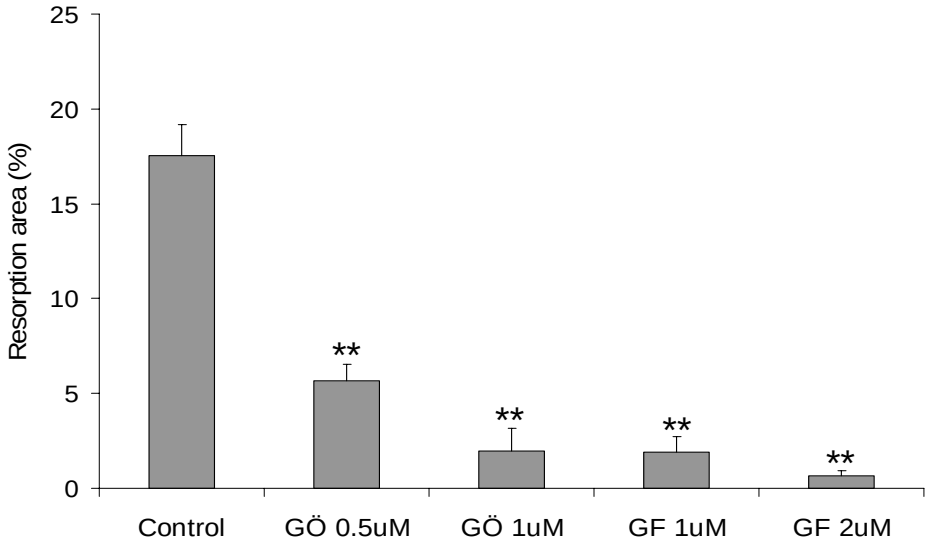

Figure 7.5 GÖ 6976 and GF 109203X inhibit GCT bone resorption. Multinucleated giant cells isolated from patients presenting with Giant cell tumour (GCT) of bone were cultured on the bovine bone slices in the presence and absence of GÖ 6976 and GF 109203X. After 72 hours, the treated cells were fixed with 4% paraformaldehyde and stained for TRACP activity. The cells were then removed, and the resorptive lacunae were assessed by scanning electron microscopy. (A) Light and scanning electron microscopy of OCLs derived from GCT and bone resorptive lacunae, respectively. (B) The percentage of bovine bone slice surface occupied by resorption lacunae. (** $p<0.01$)

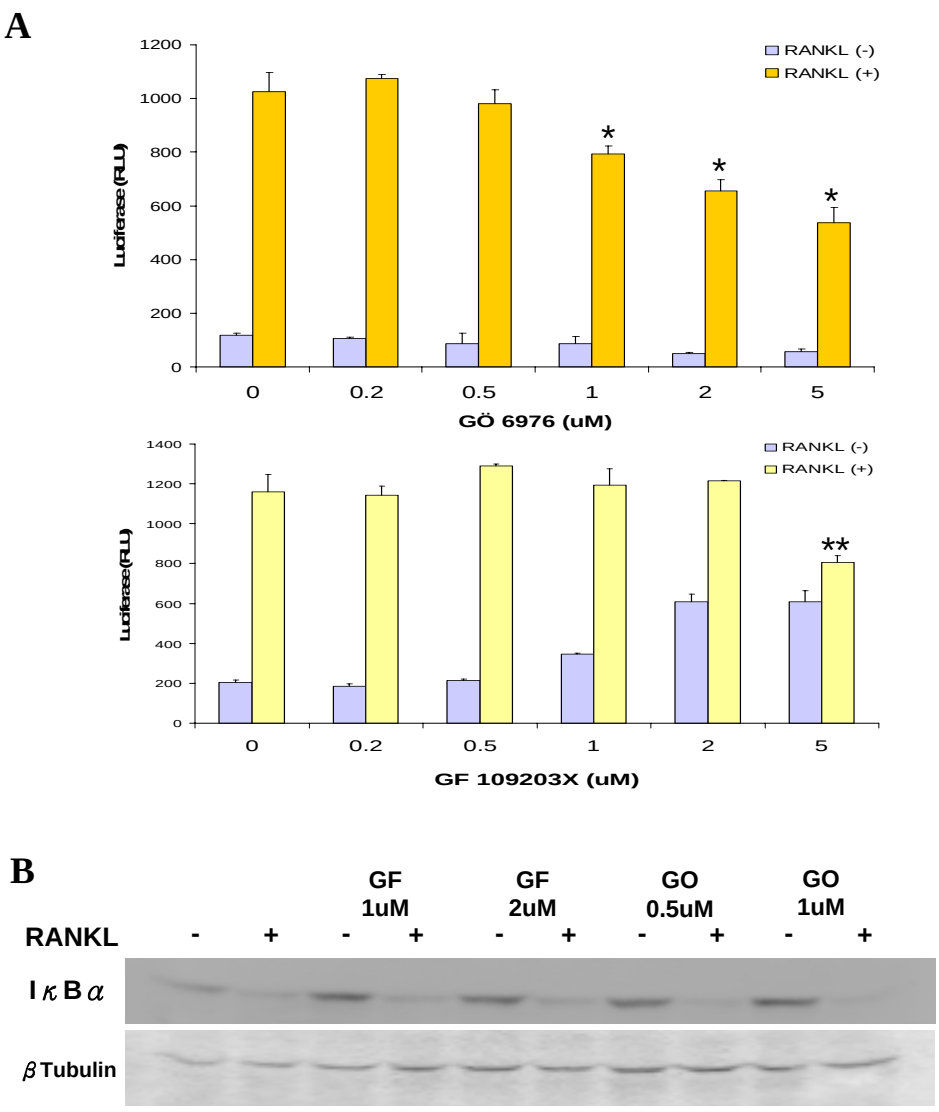

Figure 7.6 GO7976 and GF 109203X modulate RANKL-induced NF-κB activation. (A) RAW264.7 cells were transiently transfected with NF-κB luciferase reporter construct (*3kB-Luc-SV40*) and pre-treated with various doses of GÖ 6976 and GF 109203X ranging from 0.1 to 5uM for 30 minutes before stimulating them with 100ng/ml RANKL for another 8 hours. The firefly luciferase activity was then measured. Results are expressed as means ± SEM of triplicates.(* p value<0.05, ** p value<0.01) (B) RAW264.7 cells were treated for 1 hour with GÖ 6976 (1 and 2uM) and GF 109203X (0.5 and 1uM) prior to stimulation with RANKL (100ng/ml) for 20 min. Whole cell extracts were analyzed for IκBα degradation by Western blotting. Proteins separated by SDS-PAGE and transferred to PVDF membrane. Bands were visualized by ECL.

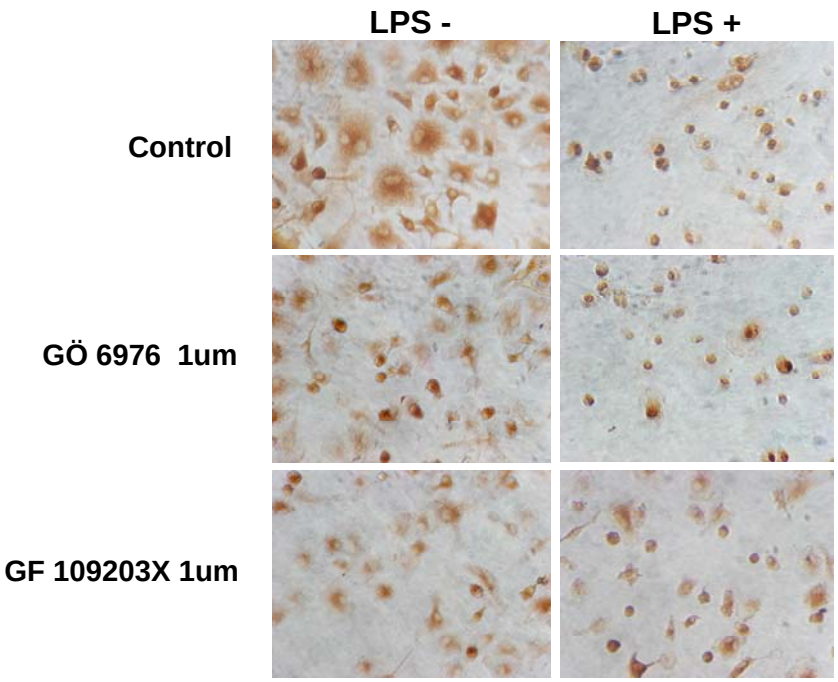

Figure 7.7 GÖ 6976 and GF 109203X inhibit LPS-induced p65 translocation in BMM. Mouse BMM were pre-treated with GÖ 6976 and GF 109203X for 1 hour and then stimulated with LPS for 30 minutes. The cells were then fixed with 4% paraformaldehyde and immunohistochemistry staining was carried out using anti-p65. Light microscopic images show the translocation of p65 from cytoplasm to nucleus upon LPS stimulation.

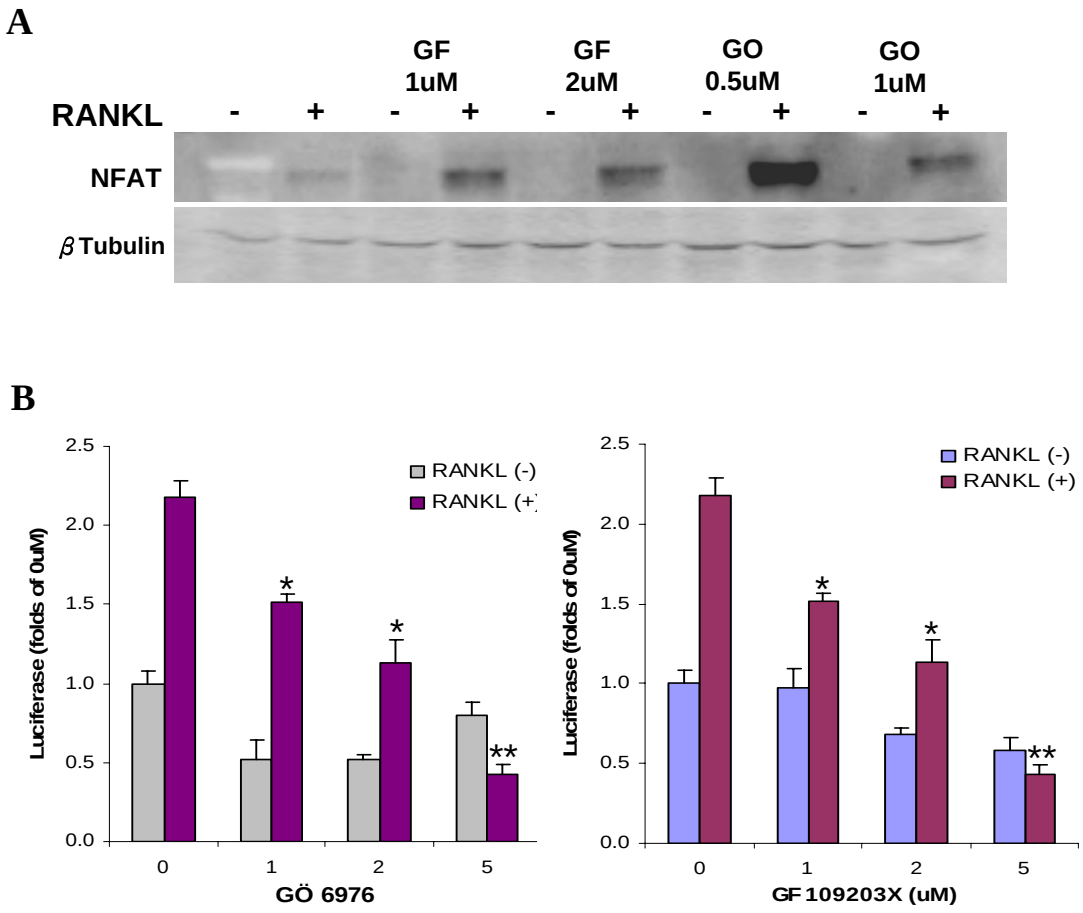

Figure 7.8 GÖ 6976 and GF 109203X modulate RANKL-induced NFAT activity. (A) RAW264.7 cells were pre-treated with two different doses of GÖ 6976 (0.5 and 1uM) and GF 109203X (1 and 2uM) and subsequently cultured for 3 days in the presence and absence of 100ng/ml RANKL. The whole cell extracts were analyzed for NFAT protein expression by Western blotting. The proteins separated by SDS-PAGE and transferred to the PVDF membrane. Bands were visualized by ECL. (B) RAW264.7 cells were transiently transfected with NFAT-luc reporter gene construct, and were treated with GÖ 6976 or GF 109203X (1, 2, and 5uM) in the presence and absence of RANKL for 8 hours. The luciferase activities are the mean $\pm$ SEM of triplicate determinations. (*$p<0.05$, **$p<0.01$)

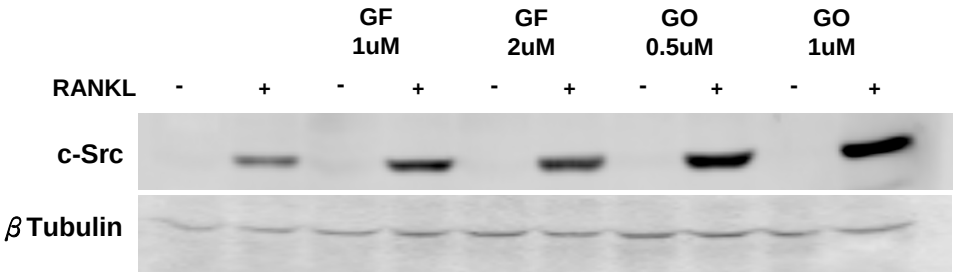

Figure 7.9 GÖ 6976 and GF 109203X increase the total c-Src induced by RANKL. RAW264.7 cells were pre-treated with GÖ 6976 (1 and 2uM) and GF 109203X (0.5 and 1uM) separately and subsequently treated with and without RANKL (100ng/ml) for 3 days The whole cell extracts were analyzed for the total c-Src protein expression by Western Blotting. Proteins were separated by SDS-PAGE and transferred to PVDF membrane. Bands were visualized by ECL.

A

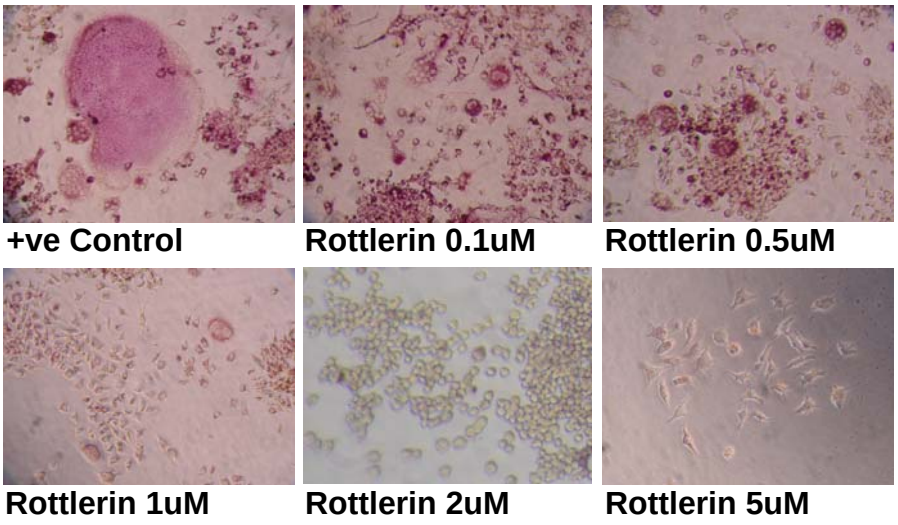

B

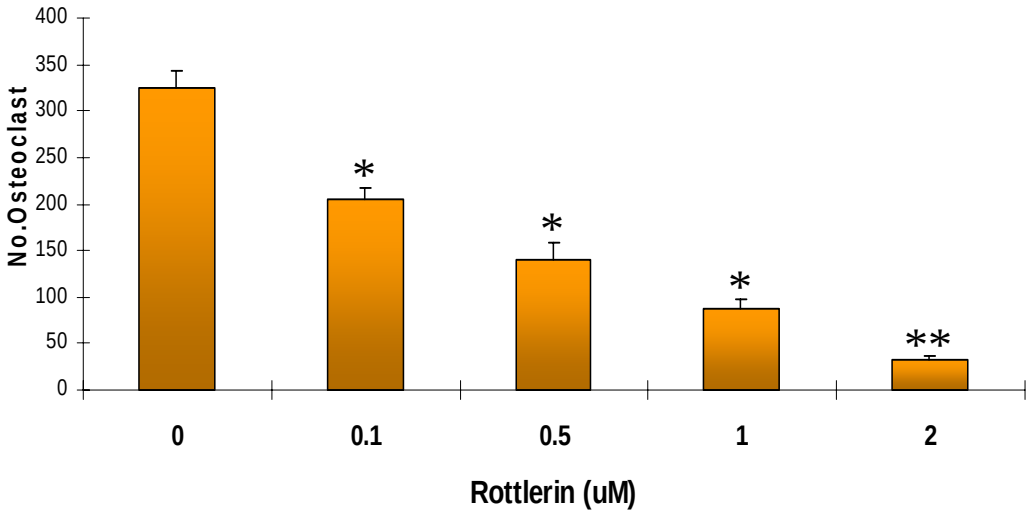

Figure 8.1 Rottlerin inhibits RANKL-induced osteoclast formation. RAW264.7 cells were cultured in the presence of RANKL and Rottlerin (0.1, 0.5, 1, 2 and 5uM). After 5 days, the cells were fixed with 4% paraformaldehyde and stained for TRACP activity. (A) Light microscope images with high magnification showing the effect of Rottlerin on RANKL-induced osteoclast formation with morphological changes. Representative images of triplicate wells from one of three experiments are shown. (B) Effect of Rottlerin on RANKL-induced osteoclastogenesis. The results represent three experiments. TRACP positive cells with more than 5 nuclei are scored (* $p<0.01$, ** $p<0.001$).

A

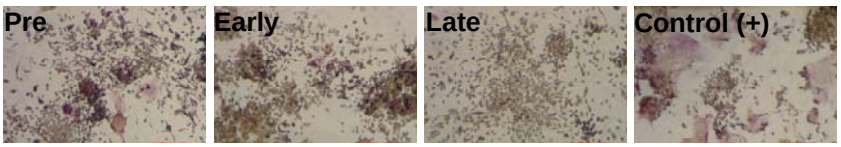
Pre
Early
Late
Control (+)

B

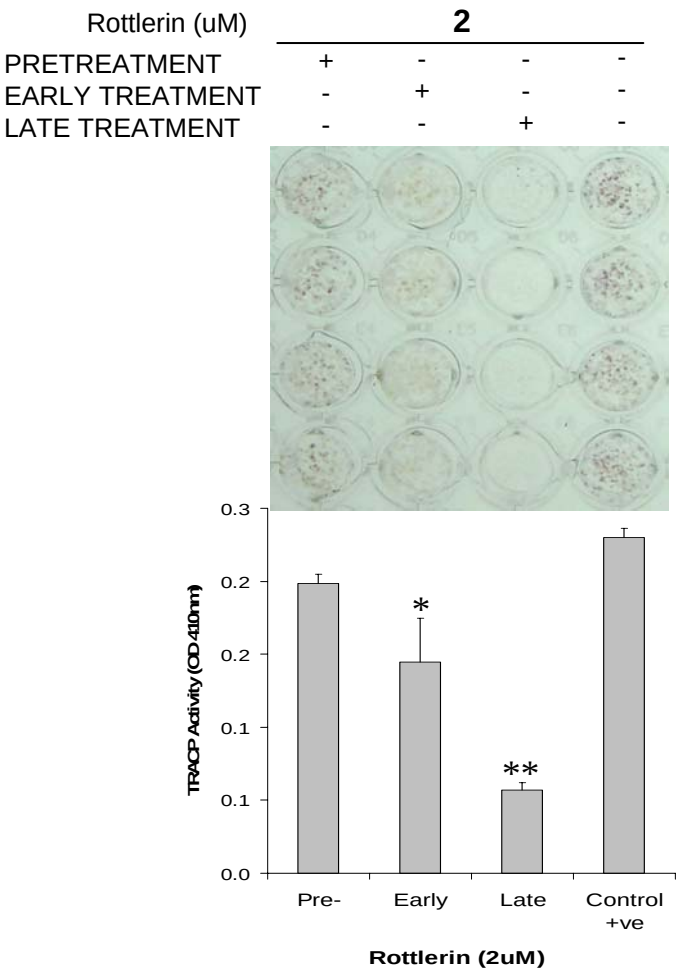
Rottlerin (uM)
2
PRETREATMENT + - - -
EARLY TREATMENT - + - -
LATE TREATMENT - - + -
TRAP Activity (OD 410nm)
0.3
0.2
0.2
0.1
0.1
0.0
*
**
Pre-
Early
Late
Control +ve
Rottlerin (2uM)

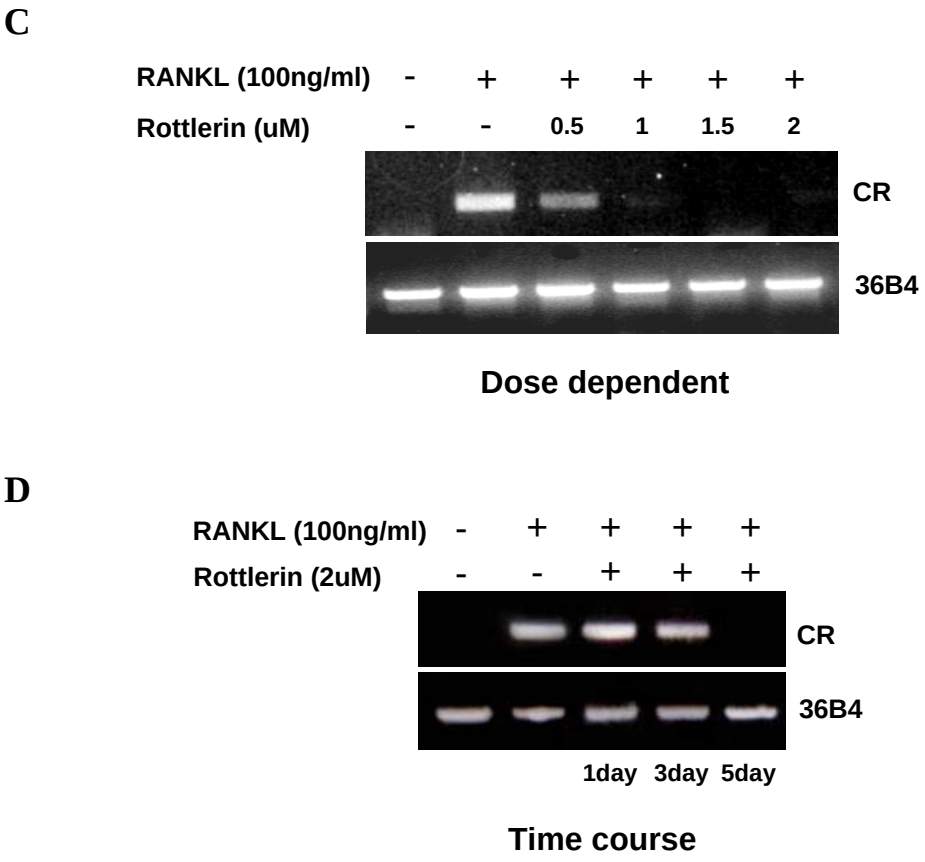

Figure 8.2 Rottlerin inhibited RANKL-induced osteoclastogenesis. There are 4 groups: RAW264.7 cells were pre-treated with Rottlerin (2uM) for 24 hours before the addition of RANKL; treated with Rottlerin at the early time point (at day 1-2) and late time point (at day 3-4); as well as left untreated and cultured in the presence of RANKL for a total of 5 days. The treated cells were fixed with 4% paraformaldehyde and stained for TRACP activity. The graph represents the total TRACP activity which was measured by the BMG machine at OD410nm. (A) Light microscope images showing the effect of Rottlerin on RANKL-induced osteoclast formation with morphological changes. (B) The graph represents the total TRACP activity which was measured by the BMG machine at OD410nm. (* $p<0.05$, ** $p<0.01$) (C) Effect of Rottlerin in different concentration on calcitonin receptor during RANKL-induced osteoclastogenesis. RAW264.7 cells were treated with Rottlerin (0.5, 1, 1.5 and 2uM) in the presence of RANKL for 5 days. mRNA from cells was subjected to RT-PCR analysis using calcitonin receptor (CR). (D) A time course study of effect of Rottlerin on RANKL-induced gene expression (CR).

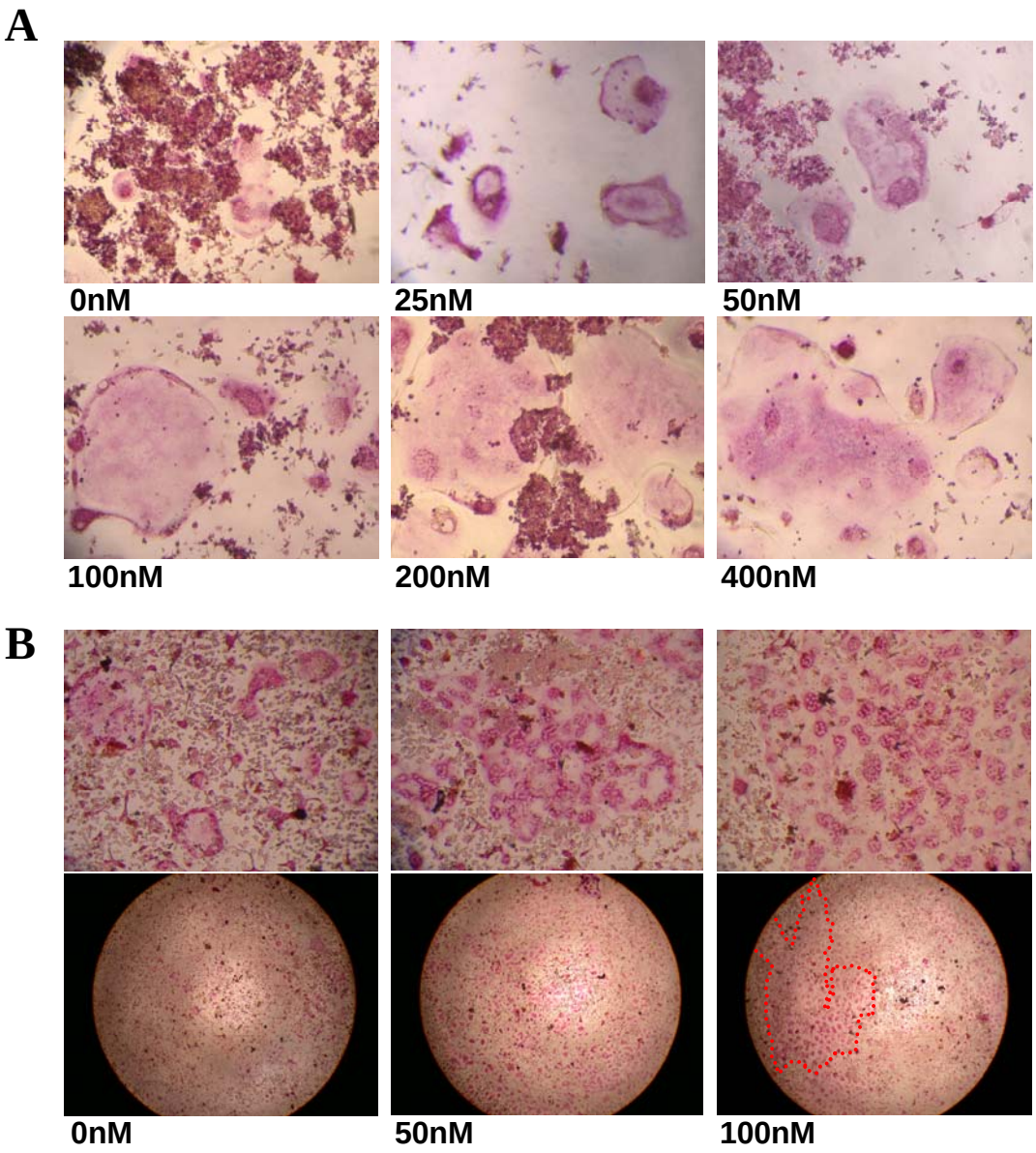

Figure 8.3 Bryostatin1 enhanced the size of OCLs induced by RANKL. (A) RAW264.7 cells were cultured in the presence of RANKL and Bryostatin 1 (25, 50, 100, 200 and 400nM). After 5 days, the cells were fixed with 4% paraformaldehyde and stained for TRACP activity. Light microscope images with high magnification showing the effect of Rottlerin on RANKL-induced osteoclast formation with morphological changes. (B) Mouse BMM cells were cultured in the presence of RANKL m-CSF and Bryostatin 1 (50 and 100nM). After 7 days, the cells were fixed with 4% paraformaldehyde and stained for TRACP activity. Light microscope images with high (top 3 images) and low (bottom 3 images) magnification showing the effect of Bryostatin 1 on RANKL-induced osteoclast formation with morphological changes.

A

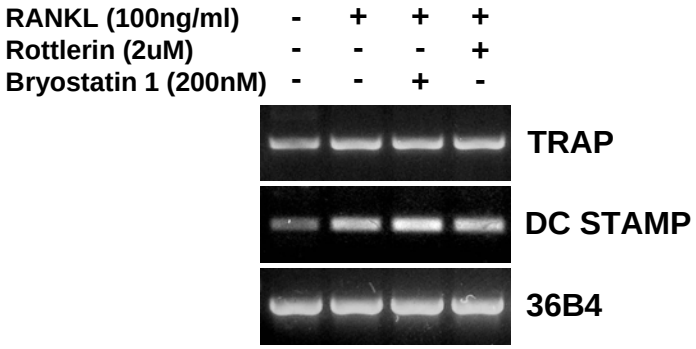

B

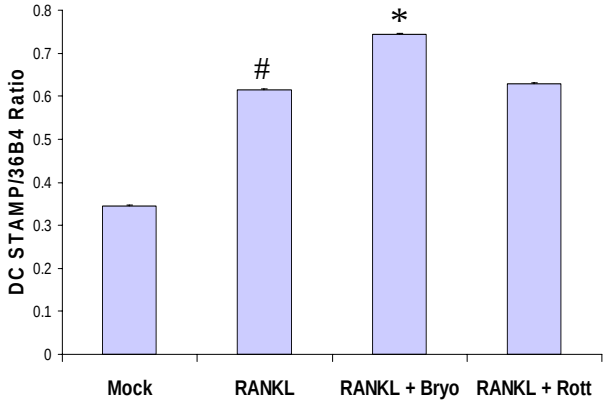

Figure 8.4 Bryostatin 1 enhanced RANKL-induced DC STAMP gene expression. RAW264.7 cells were treated with Bryostatin 1 (Bryo) (200nM) or Rottlerin (Rott) (2uM) in the presence and absence of RANKL for 3 days. mRNA from cells was subjected to RT-PCR analysis using TRAP, DC STAMP and 36B4. (B) Semi-quantitative analysis of DC STAMP gene expression by densitometry. DC STAMP mRNA is shown as the ratio of DC STAMP to 36B4 (# $p<0.01$, comparing RANKL with mock; * $p<0.01$, comparing RANKL+Bryo with RANKL).

A

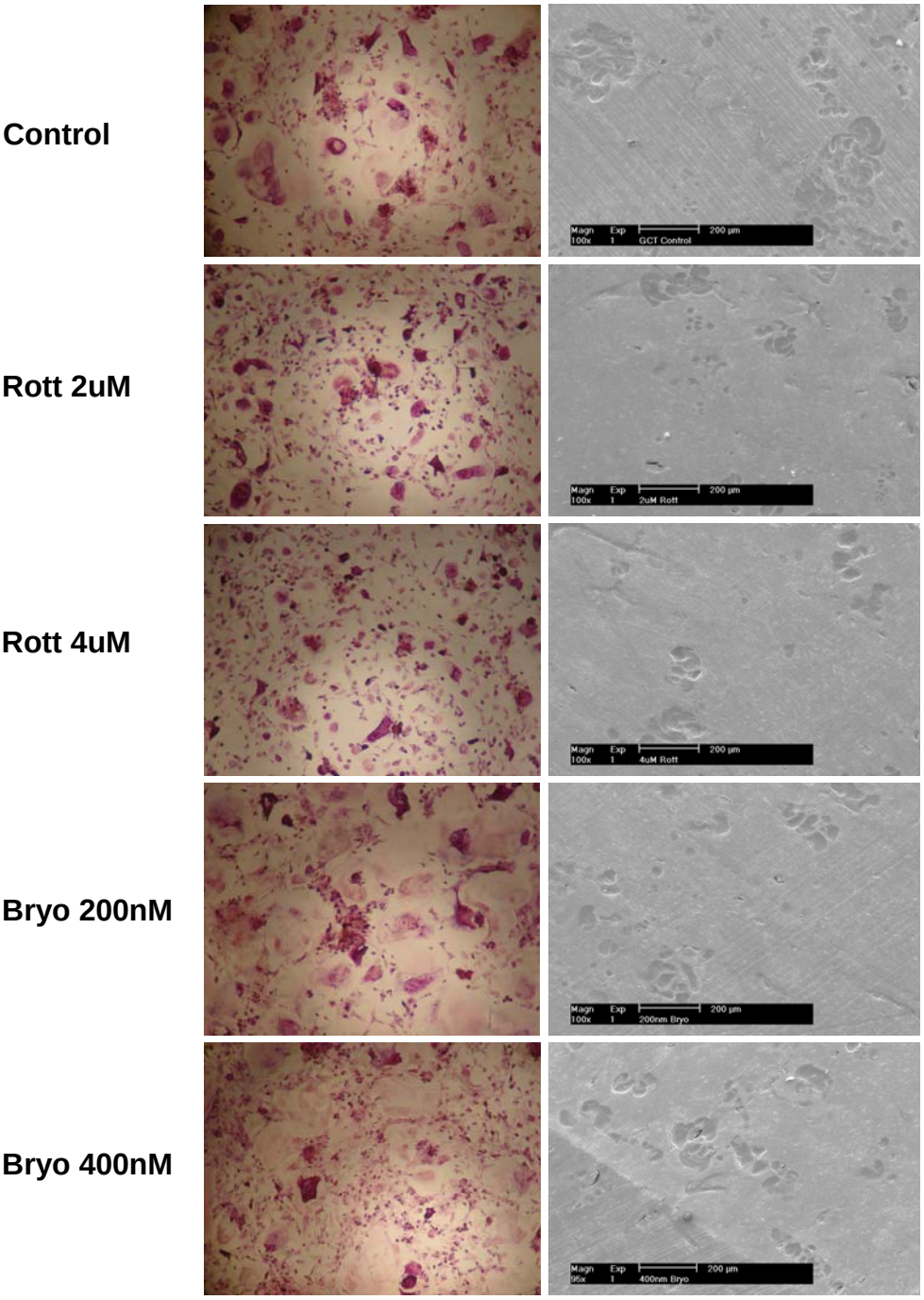
Control
Rott 2uM
Rott 4uM
Bryo 200nM
Bryo 400nM
Magn Exp 200 µm
100x 1 GCT Control
Magn Exp 200 µm
100x 1 2uM Rott
Magn Exp 200 µm
100x 1 4uM Rott
Magn Exp 200 µm
100x 1 200nm Bryo
Magn Exp 200 µm
95x 1 400nm Bryo

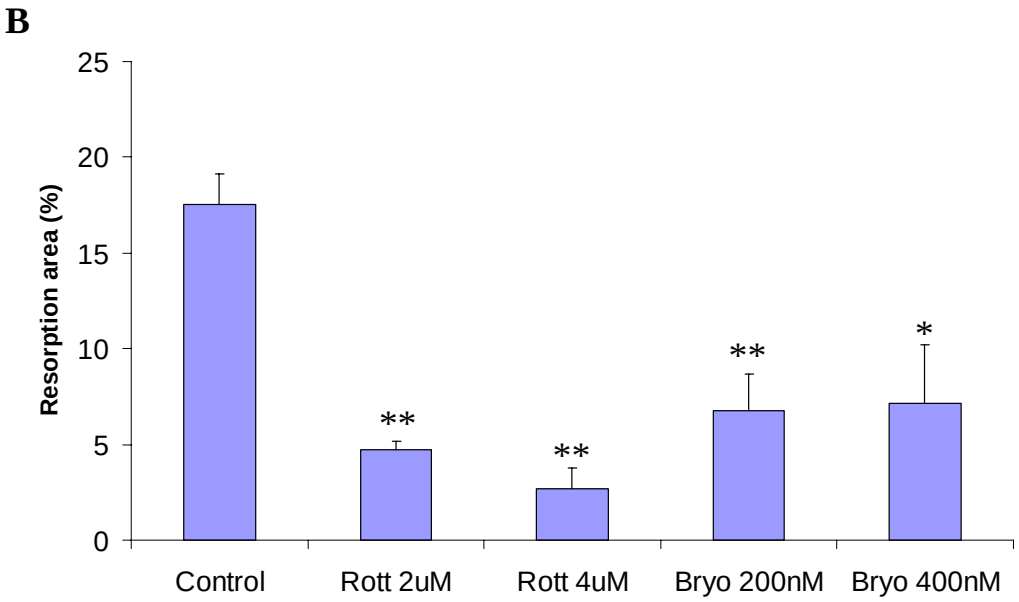

Figure 8.5 Rottlerin and Bryostatin1 inhibit GCT bone resorption. Multinucleated giant cells isolated from patients with Giant cell tumour (GCT) of bone were cultured on the bovine bone slices in the presence and absence of Rottlerin (Rott) and Bryostatin 1 (Bryo). After 72 hours, the treated cells were fixed with 4% paraformaldehyde and stained for TRACP activity. The cells were then removed, and the resorptive lacunae were assessed by scanning electron microscopy. (A) Light and scanning electron microscopy of OCLs derived from GCT and bone resorptive lacunae, respectively. (B) The percentage of bovine bone slice surface occupied by resorption lacunae. (* $p<0.05$, ** $p<0.01$)

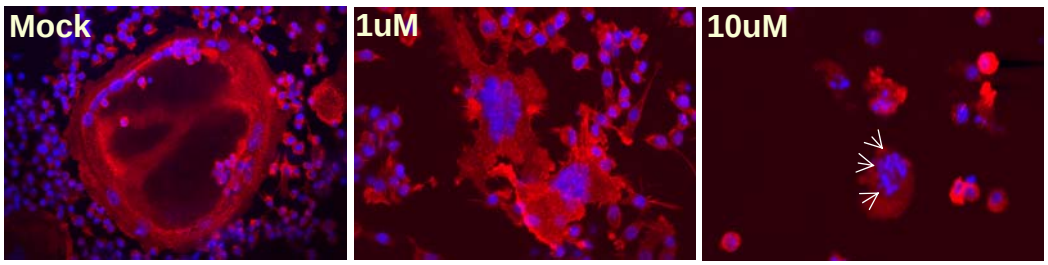

Figure 8.6 Rottlerin induces apoptosis in RAW264.7 cell-derived osteoclast. Mature RAW264.7 cell-derived osteoclasts were seeded on the glass overnight in the presence of RANKL (100ng/ml). The osteoclasts were then treated with Rottlerin (1 and 10uM) for 24 hours before being fixed with 4% paraformaldehyde. The osteoclasts were double stained with Rhodamine-conjugated phalliodin (red) to visualize F-actin and Hoechst (blue) to visualize nuclei. The cells were examined by confocal microscopy. The disrupted cytoskeletal organisation and defragmentation of nuclei represent cellular apoptosis in osteoclasts.

A

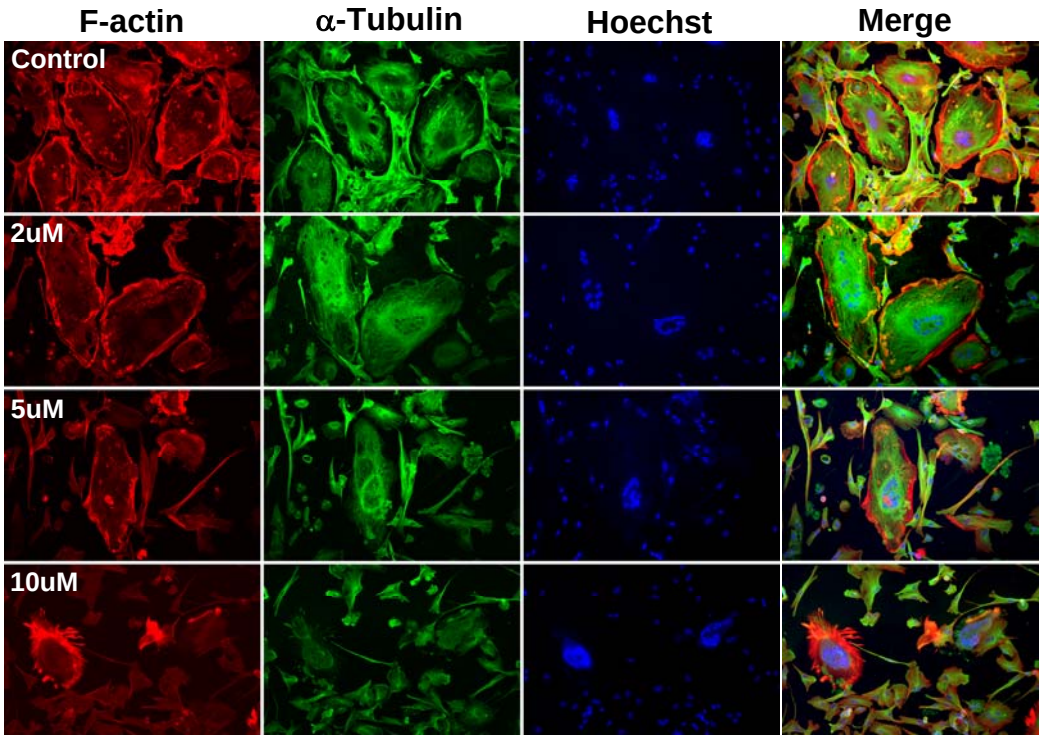

B

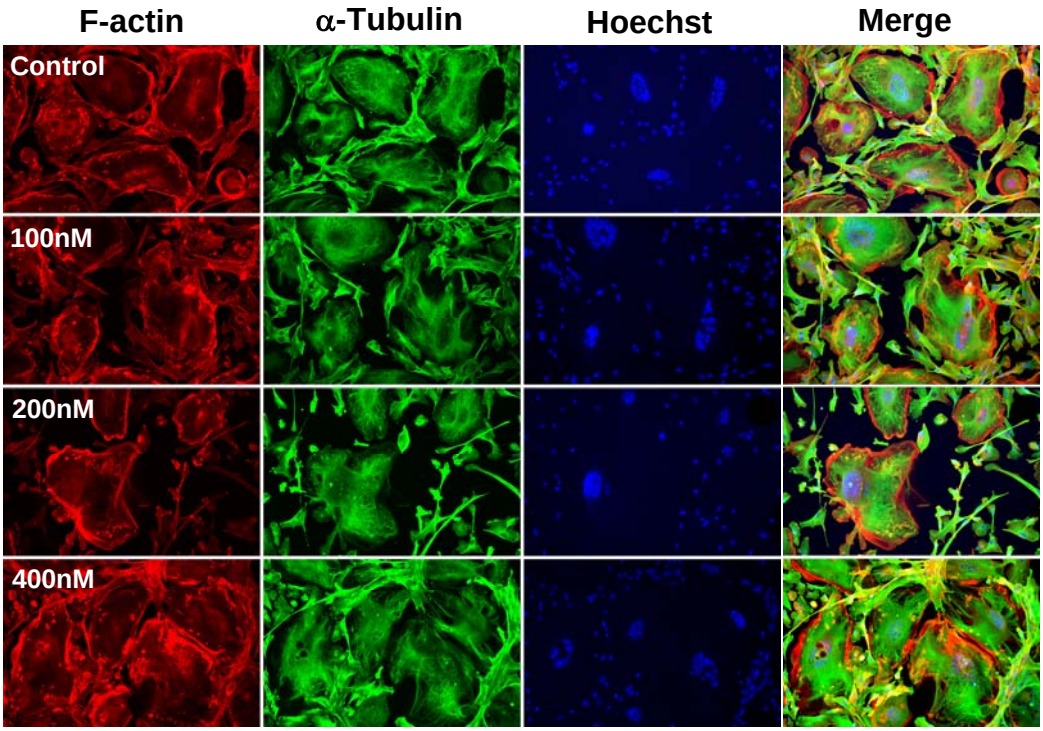

Figure 8.7 Rottlerin induces apoptosis in GCT and Bryostatin 1 has no apoptotic effect on the OCLs derived from GCT. Giant cell tumours (GCT) were seeded onto glass in the presence of Rottlerin (2, 5 and 10uM) or Bryosatatin 1 (100, 200 and 400nM) for 24 hours. The OCLs were fixed and triple-stained with Rhodamine-conjugated Phalloidin (red), α-tubulin (green) and Hoechst 33342 (blue) to visualized microfilaments, microtubules and chromatin, respectively. The cells were examined by confocal microscopy. (A) Effect of Rottlerin on GCT. (B) Effect of Bryostatin 1 on GCT.

A

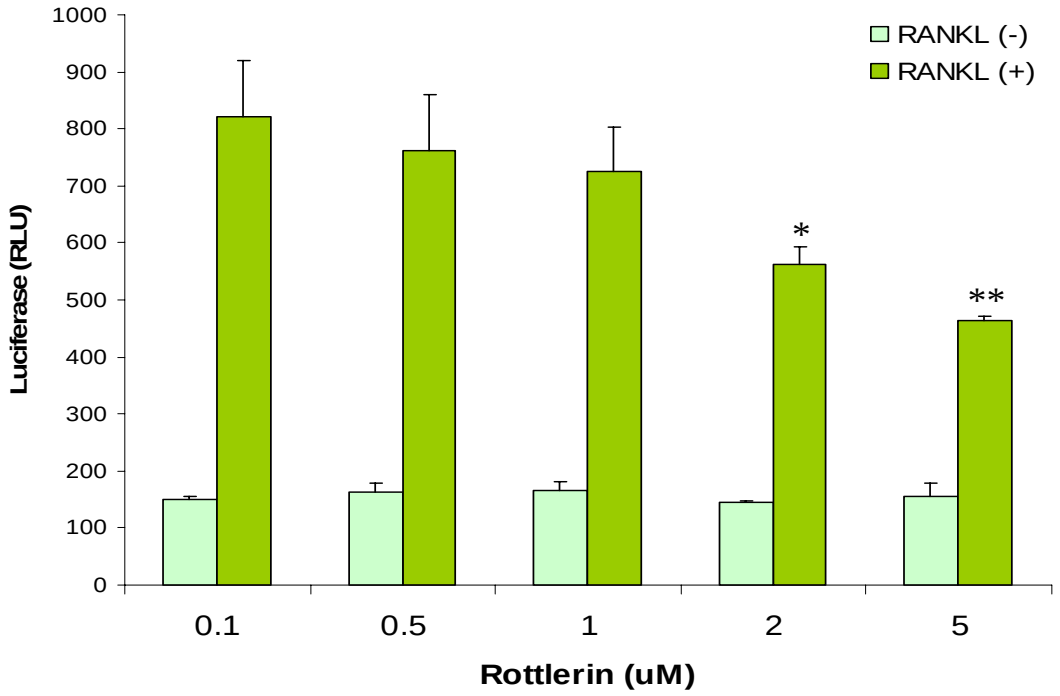
RANKL (-)
RANKL (+)
Luciferase (RLU)
1000
900
800
700
600
500
400
300
200
100
0
*
**
0.1
0.5
1
2
5
Rottlerin (uM)

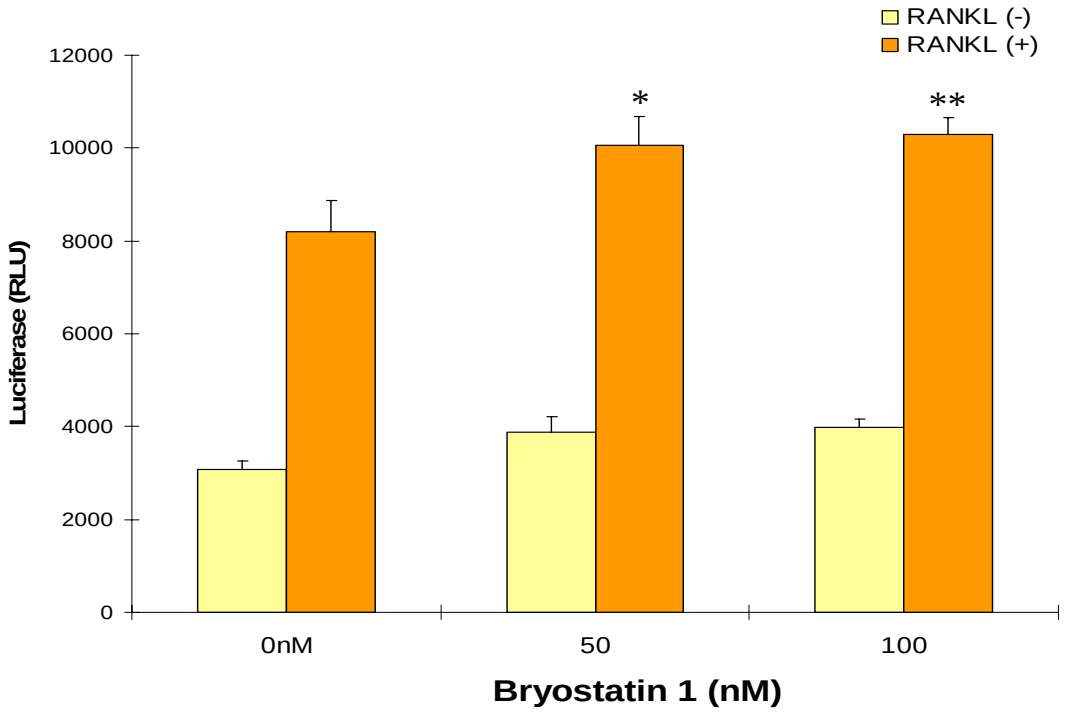
RANKL (-)
RANKL (+)
Luciferase (RLU)
12000
10000
8000
6000
4000
2000
0
*
**
0nM
50
100
Bryostatin 1 (nM)

B

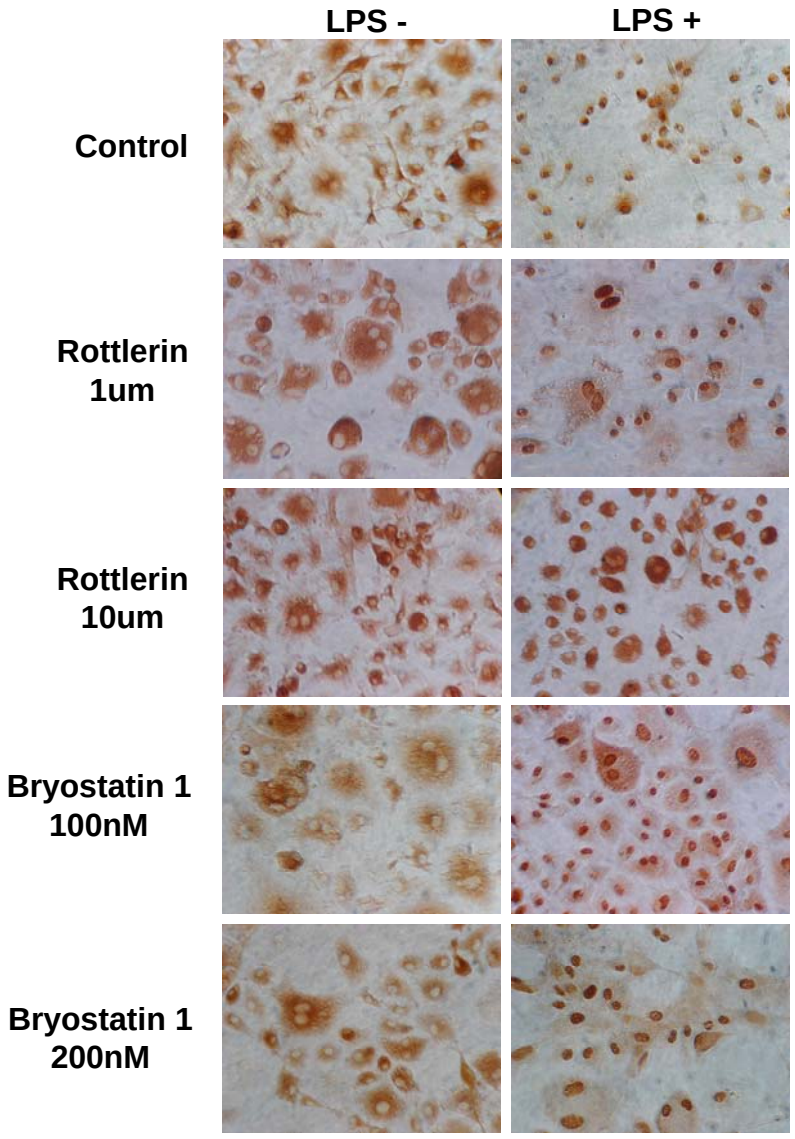
LPS -
LPS +
Control
Rottlerin 1um
Rottlerin 10um
Bryostatin 1 100nM
Bryostatin 1 200nM

C

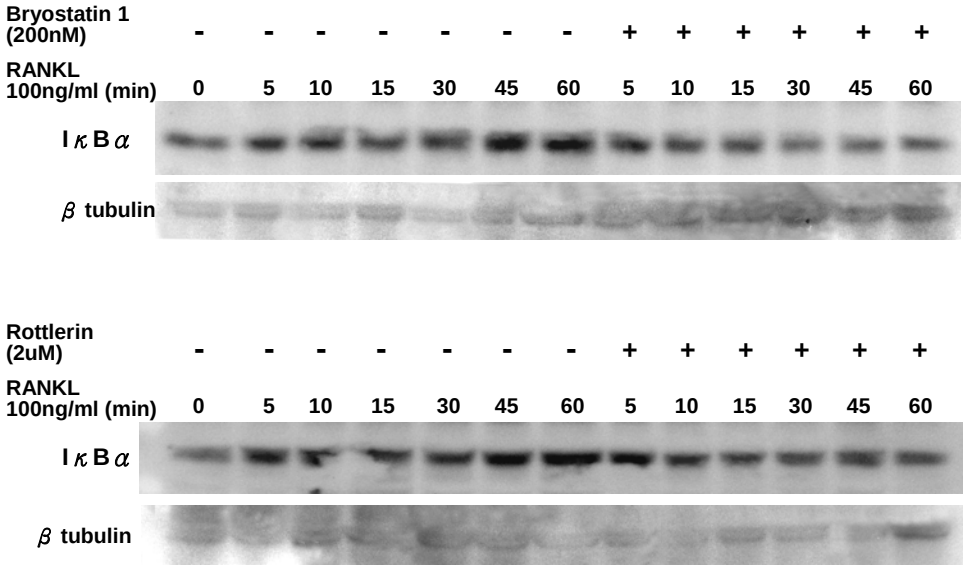

Figure 8.8 Rottlerin suppresses RANKL-induced NF-kB transcription and Bryostatin 1 potentiates RANKL-induced NF-kB transcription. (A) RAW264.7 cells were transiently transfected with NF-κB luciferase reporter construct (*3kB-Luc-SV40*) and pre-treated with various doses of Rottlerin (ranging from 0.1 to 5uM) and Bryostatin 1 (50, 100 and 200nM) for 30 minutes before stimulating them with 100ng/ml RANKL for another 8 hours. The firefly luciferase activity was then measured. Results are expressed as means $\pm$ SEM of triplicates. (* $p<0.05$, ** $p<0.01$) (B) Mouse BMM were pre-treated with Rottlerin (1 and 10uM) and Bryostatin1 (100 and 200nM) for 1 hour and then stimulated with LPS for 30 minutes. The cells were then fixed with 4% paraformaldehyde and immunohistochemistry staining was carried out using anti-p65. Light microscopic images show the translocation of p65 from cytoplasm to nucleus upon LPS stimulation. (C) RAW264.7 cells were treated for 30 minutes with Rottlerin (2uM) and Bryostatin 1 (200nM) prior to stimulation with RANKL (100ng/ml) for 5-60 minutes. The whole cell extracts were analyzed for IκBα degradation by using Western blotting. The proteins were separated by SDS-PAGE and transferred to PVDF membrane. The bands were visualized by ECL.

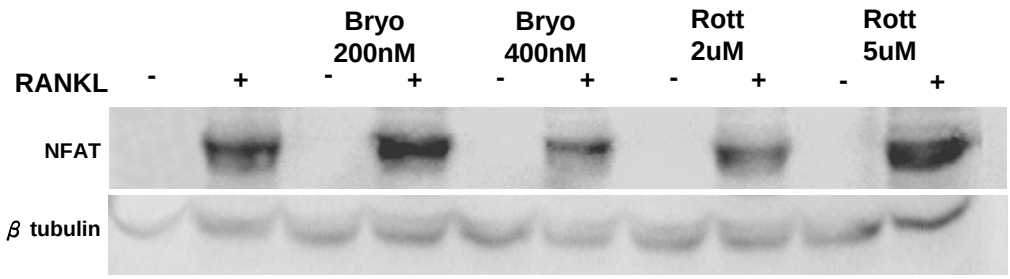

Figure 8.9 Rottlerin reduces RANKL-induced NFAT protein expression. RAW264.7 cells were treated for 1 hour with Rottlerin (2 and 5uM) and Bryostatin 1 (200 and 400nM) prior to stimulation with RANKL (100ng/ml) for 3 days. The whole cell extracts were analyzed for total NFAT protein expression by Western blotting. The proteins were separated by SDS-PAGE and transferred to the PVDF membrane. The bands were visualized by ECL.

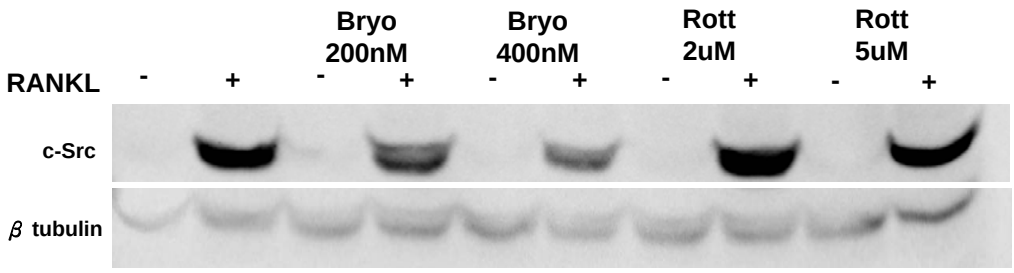

Figure 8.10 Rottlerin enhances RANKL-induced c-Src protein expression, while Bryostatin 1 reduces RANKL-induced total c-Src. RAW264.7 cells were treated for 1 hour with Rottlerin (2 and 5uM) and Bryostatin 1 (200 and 400nM) prior to stimulation with RANKL (100ng/ml) for 3 days. The whole cell extracts were analyzed for total c-Src protein expression by Western blotting. The proteins were separated by SDS-PAGE and transferred to PVDF membrane. The bands were visualized by ECL.